

UNCLASSIFIED

AD NUMBER
ADB157593
NEW LIMITATION CHANGE
TO Approved for public release, distribution unlimited
FROM Distribution authorized to U.S. Gov't. agencies only; Proprietary Information; 20 Dec 1989. Other requests shall be referred to U.S. Army Medical Research and Development Command, Attn: SGRD-RMI-S, Fort Detrick, Frederick, MD 21702-5012.
AUTHORITY
USAMRDC, 8 Jun 1993

THIS PAGE IS UNCLASSIFIED

AD-B157 593



AD _____

20030416036

DINOFLAGELLATE TOXINS RESPONSIBLE FOR CIGUATERA FOOD POISONING

Final Report

Donald M. Miller

March 30, 1991

Supported by

US ARMY MEDICAL RESEARCH AND DEVELOPMENT COMMAND
Fort Detrick, Frederick, Maryland 21702-5012

Contract No. DAMD17-87-C-7002

Department of Physiology, School of Medicine
Southern Illinois University, Carbondale, Illinois 62901-6521

Distribution authorized to U. S. Government agencies only;
Proprietary Information, December 20, 1989. Other requests for this
document shall be referred to Commander, U. S. Army Medical
Research and Development Command, ATTN: SGRD-RMI-S, Fort
Detrick, Frederick, Maryland 21702-5012

The findings in this report are not to be construed as an official
Department of the Army position unless so designated by other
authorized documents.

91-08592

91 8 22 008

REPORT DOCUMENTATION PAGE

Form Approved
OMB No. 0704-0188

1a. REPORT SECURITY CLASSIFICATION Unclassified		1b. RESTRICTIVE MARKINGS	
2a. SECURITY CLASSIFICATION AUTHORITY		3. DISTRIBUTION/AVAILABILITY OF REPORT Distribution authorized to U.S. Government Agencies only, Proprietary Information, December 20, 1989.	
2b. DECLASSIFICATION/DOWNGRADING SCHEDULE		5. MONITORING ORGANIZATION REPORT NUMBER(S)	
4. PERFORMING ORGANIZATION REPORT NUMBER(S)		7a. NAME OF MONITORING ORGANIZATION	
6a. NAME OF PERFORMING ORGANIZATION Southern Illinois University Department of Physiology	6b. OFFICE SYMBOL (If applicable)	7b. ADDRESS (City, State, and ZIP Code)	
6c. ADDRESS (City, State, and ZIP Code) Carbondale, Illinois 62901-6512		9. PROCUREMENT INSTRUMENT IDENTIFICATION NUMBER Contract No. DAMD17-87-C-7002	
8a. NAME OF FUNDING/SPONSORING ORGANIZATION U.S. Army Medical Research & Development Command	8b. OFFICE SYMBOL (If applicable)	10. SOURCE OF FUNDING NUMBERS	
8c. ADDRESS (City, State, and ZIP Code) Fort Detrick Frederick, Maryland 21702-5012		PROGRAM ELEMENT NO.	PROJECT NO.
		TASK NO.	WORK UNIT ACCESSION NO.
11. TITLE (Include Security Classification) DINOFLAGELLATE TOXINS RESPONSIBLE FOR CIGUATERA POISONING			
12. PERSONAL AUTHOR(S) Miller, Donald M.			
13a. TYPE OF REPORT Final Report	13b. TIME COVERED FROM 12/1/86 TO 3/31/91	14. DATE OF REPORT (Year, Month, Day) 1991 March 30	15. PAGE COUNT 225
16. SUPPLEMENTARY NOTATION			
17. COSATI CODES		18. SUBJECT TERMS (Continue on reverse if necessary and identify by block number)	
FIELD	GROUP	SUB-GROUP	
06	03		
06	01		
19. ABSTRACT (Continue on reverse if necessary and identify by block number) During the four years of the contract over 600 grams dry weight of the dinoflagellate Gambierdiscus toxicus was grown in large scale culture. Chemosystematic studies resulted in information which allowed improvements in both culturing and toxin production. Gram levels of cells and toxic extracts were processed in an effort to improve toxin production by G. toxicus. NMR characterization of suspected toxin was completed and partially analyzed. Crude and semi-purified toxins were delivered.			
20. DISTRIBUTION/AVAILABILITY OF ABSTRACT <input type="checkbox"/> UNCLASSIFIED/UNLIMITED <input checked="" type="checkbox"/> SAME AS RPT. <input type="checkbox"/> DTIC USERS		21. ABSTRACT SECURITY CLASSIFICATION Unclassified	
22a. NAME OF RESPONSIBLE INDIVIDUAL Mrs. Virginia M. Miller		22b. TELEPHONE (Include Area Code) (301) 663-7325	22c. OFFICE SYMBOL SGRD-RMI-S

SUMMARY

Ciguatera is a syndrome occurring in humans who have become intoxicated from eating poison fish. Fish sporadically accumulate the toxin through the food chain or directly from eating toxic dinoflagellates. Previous research points to the presence of multiple toxin involvement. In addition to the establishment of facilities, this contract requires the growth of sufficient quantities of three different species of dinoflagellates to allow purification of milligram quantities of toxins for delivery to the U.S. Army Medical Research and Development Command. In the first year of the contract, necessary personnel were acquired and equipment setup to grow the dinoflagellate *Gambierdiscus toxicus* in mass culture.

During the four years of the contract, growth of the dinoflagellate *G. toxicus* in mass culture was successful beyond previous projections and expectations. Gram levels of cells and toxic extracts were processed in an effort to improve existing purification procedures and to develop new procedures for purification and assay. Also numerous physiological (growth) studies were completed in an effort to improve toxin production by *G. toxicus*. Gram quantities of crude and semi-purified toxins were delivered. Purification of the products of one of these toxins, maitotoxin, down to the 0.5 µg/MU level in milligram quantities has been achieved. NMR analysis was completed and partial structure elucidated for one purified product.



Accession For	
NHS 02481	
Date Recd	
Date of Recd	
Justification	
By	
DTIC No 1	
Availability Code	
Dist	Avail for Special
B-3	

FOREWORD

Citations of commercial organizations and trade names in this report do not constitute an official Department of the Army endorsement or approval of the products or services of these organizations.

In conducting the research described in this report, the investigators adhered to the "Guide for the Care and Use of Laboratory Animals" of the Institute of Laboratory Animal Resources, National Research Council (DHEW Publication No. (NIH) 78-23, Revised 1978).

TABLE OF CONTENTS

FRONT COVER.....	i
REVERSE OF FRONT COVER.....	ii
REPORT DOCUMENTATION FORM, DD FORM 1473	iii
SUMMARY	1
FOREWORD	2
TABLE OF CONTENTS	3
TABLE OF FIGURES.....	4
TABLE OF TABLES.....	6
BODY OF THE REPORT.....	9
STATEMENT OF THE PROBLEM.....	9
BACKGROUND.....	9
Ciguatera Poisoning.....	9
The Ciguatera Syndrome	9
Multi-toxin Involvement	10
Dinoflagellate Toxins Affecting Ion Channels.....	10
Dinoflagellate Involvement in Ciguatera.....	12
Strains of Toxin Producing Dinoflagellates	12
Isolation of Dinoflagellate Toxins	13
Fish Toxins.....	13
Significance.....	15
APPROACHES TO THE FOUR YEARS OF THE STUDY.....	16
Methods for Growth of Cells.....	16
Chemosystematic Studies.....	17
Toxin Potencies.....	20
Purification of Toxins from Mass Culture of Dinoflagellates.....	22
Mouse Bioassay.....	22
Ileum Assay Procedures	23
Tests for Purity of Toxins.....	24
NMR Spectroscopy	25
Packaging of Toxins for Shipment.....	25
Overall Objectives for the Four Years.....	26
RESULTS	27
Acquisition and Setup of Equipment.....	27
Culturing and Growth.....	27
<i>Discussion of Culturing Results</i>	31
Acquisition of Toxic Dinoflagellates.....	32
Acclimation & Chemosystematic Studies, <i>G. toxicus</i>	36
<i>Discussion of Acclimation & Chemosystematic Studies</i>	46
Response of <i>G. toxicus</i> Clones to Different Light Intensities.....	49
Maximizing Toxin Production in <i>G. toxicus</i>	60
<i>Discussion of Maximal Toxin Production Studies</i>	70
Acclimation of New Clones of Dinoflagellates.....	73
Physiology & Potency Studies of, <i>P. concavum</i>	76
<i>Discussion of P. concavum Studies</i>	86
Calibration of Ileal Assays.....	86
Brevetoxin Antibody Experiments.....	90
Separation of Toxic Components.....	92
Separation of <i>G. toxicus</i> , clone 175 extracts.....	92
<u>Acetonitrile precipitation</u>	93
<u>C18 fractionation</u>	95
<u>Silicic Acid Chromatography</u>	97

<u>Return to liquid-liquid fractionation</u>	97
<i>Discussion of clone 175 Separations</i>	104
Separation of <i>G. toxicus</i> , clone 350 extracts.....	104
<u>Sep-Pak Separation</u>	104
<u>HPLC separation</u>	114
<i>Discussion of HPLC Separations</i>	126
<u>Solvent extraction of pigments</u>	127
<u>ACN separation</u>	132
<u>Ethyl acetate extraction</u>	136
<u>Purification of large scale cultures</u>	139
<u>Modified solid phase separation</u>	150
<i>Discussion of Separation Attempts for 350</i>	150
Purification of Secondary Components.....	151
<i>Discussion of Chlorophyll Separations</i>	156
NMR of Model Compounds.....	158
NMR of Water Soluble Isolate from GT350.....	182
<u>Spectra of intermediate extracts</u>	183
<u>Spectral correlates from NMR spectra of purified GT-4</u>	184
<i>Discussion of NMR Results</i>	202
PERSONNEL SUPPORTED.....	204
TRAVEL.....	205
PUBLICATIONS.....	206
VISITATIONS TO LABORATORY.....	209
DELIVERIES.....	210
LITERATURE CITED.....	212
GLOSSARY.....	222
DISTRIBUTION LIST.....	223
BACK COVER.....	224

TABLE OF FIGURES

Figure 1.	Estimated mouse units.....	28
Figure 2.	Grams dry weight produced by quarter by clone.....	31
Figure 3.	Plot of estimated cumulative mouse units and grams.....	32
Figure 4.	Acclimation of clone 157.....	36
Figure 5.	Potency vs Days in Culture.....	42
Figure 6.	Potency vs Reproduction Rate.....	44
Figure 7.	Potency vs Days for Clone 350.....	45
Figure 8.	Potency vs Latitude.....	47
Figure 9.	Potency vs Reproduction Rate.....	48
Figure 10.	Potency vs Chlorophyll.....	48
Figure 11.	Potency vs Chlorophyll-c2.....	49
Figure 12.	Reproduction Rate at Four Light Intensities.....	50
Figure 13.	Plot of Biochemical Composition.....	53
Figure 14.	TLC pigment separation.....	54
Figure 15.	Reproduction Rate of Clone 175.....	61
Figure 16.	Protein Content to Clone 175.....	62
Figure 17.	Lipid Content of Clone 175.....	63
Figure 18.	Carbohydrate Content of Clone 175.....	63
Figure 19.	Chlorophyll a Content of Clone 175.....	64
Figure 20.	Chlorophyll-c ₂ Content of Clone 175.....	65
Figure 21.	Peridinin Content of Clone 175.....	65
Figure 22.	Dinoxanthin content of Clone 175.....	66

Figure 23.	Diadinoxanthin Content of Clone 175.....	66
Figure 24.	Culture Potency of Clone 175.....	67
Figure 25.	Population Density vs Potency.....	68
Figure 26.	Ammonium uptake vs Potency.....	68
Figure 27.	Characteristics of growth of Clone 175.....	69
Figure 28.	Cell Densities and pH.....	77
Figure 29.	Depletion of Ammonia.....	78
Figure 30.	Depletion of phosphate from the culture medium.....	79
Figure 31.	Cellular content of protein over the growth cycle.....	79
Figure 32.	Cellular content of carbohydrate.....	80
Figure 33.	Cellular content of lipid.....	81
Figure 34.	Cellular content of the pigment chlorophyll-a.....	82
Figure 35.	Cellular content of the pigment peridinin.....	82
Figure 36.	Cellular content of the pigment chlorophyll-c2.....	83
Figure 37.	Cell potencies of Fast Acting Toxin as determined by mouse bioassay.	84
Figure 38.	Cell potencies of Fast Acting Toxin.	84
Figure 39.	Cellular content of okadiac acid as determined by ELISA as quantity of extractable OA per 100 mg dry cells.....	85
Figure 40.	Cellular content of okadiac acid as determined by ELISA) amount of OA per cell and MU OA per cell.	85
Figure 41.	Records of guinea pig ileum assay (MTX assay)	87
Figure 42.	Records of guinea pig ileum assay	88
Figure 43.	Records of guinea pig ileum assay (CTX assay).....	89
Figure 44.	Records of guinea pig ileum assay (CTX assay)	91
Figure 45.	Results from liquid-liquid partitioning.....	93
Figure 46.	Results from acetonitrile precipitation.....	94
Figure 47.	UV-vis spectra of sep pak separations.....	106
Figure 48.	Analytical HPLC chromatograms of brown fraction.....	106
Figure 49.	Semipreparative chromatogram of the yellow.....	107
Figure 50.	Analytical HPLC chromatograms of the green.....	107
Figure 51.	Comparison of analytical HPLC chromatograms.....	108
Figure 52.	Semipreparative chromatogram (SP-9).....	110
Figure 53.	Semipreparative chromatogram of brown.....	111
Figure 54.	Semipreparative chromatogram of brown xtl.....	111
Figure 55.	Diagrammatic representation of the removal of crystals.....	112
Figure 56.	Semipreparative chromatogram (SP-7).....	113
Figure 57.	Comparison of preparative HPLC chromatograms of WSAP.....	114
Figure 58.	Preparative HPLC chromatogram (P1).....	115
Figure 59.	Preparative HPLC chromatogram (P2).....	116
Figure 60.	Preparative HPLC chromatogram (P3).....	117
Figure 61.	Preparative HPLC chromatogram (P3).....	119
Figure 62.	Preparative HPLC chromatogram (P4).....	120
Figure 63.	Preparative HPLC chromatogram (P5).....	121
Figure 64.	Preparative HPLC chromatogram (P5).....	122
Figure 65.	Semi-preparative HPLC chromatogram (SP3).....	123
Figure 66.	Preparative chromatogram (P-5).....	124
Figure 67.	Preparative chromatogram (P-6).....	125
Figure 68.	Preparative chromatogram (P-6).....	125
Figure 69.	Diagrammatic representation of the components.....	126
Figure 70.	Comparison of analytical HPLC chromatograms.....	128
Figure 71.	Preparative HPLC chromatogram (P2).....	133
Figure 72.	Preparative HPLC chromatograms of WSAP.....	134

Figure 73	Preparative HPLC chromatogram of ACN-soluble.....	134
Figure 74	Preparative HPLC chromatogram of ACN-insoluble.....	135
Figure 75	Schematic diagram for the acetonitrile (ACN) step.....	137
Figure 76	Analytical HPLC.....	138
Figure 77	Semi-preparative HPLC chromatogram	140
Figure 78	Semi-preparative HPLC chromatogram of ACN-insoluble.....	140
Figure 79	Semi-preparative HPLC chromatogram of fraction A.....	141
Figure 80	Semi-preparative HPLC chromatogram of fraction F.....	142
Figure 81	Semi-preparative HPLC chromatogram of the ACN-soluble.....	142
Figure 82	Semi-preparative HPLC chromatogram of fraction C.....	143
Figure 83	Semi-preparative HPLC chromatogram of fraction D.....	143
Figure 84	Semi-preparative HPLC chromatogram of fraction E.....	144
Figure 85	Preparative HPLC chromatogram of ACN-soluble.....	146
Figure 86	Analytical HPLC chromatogram of water soluble extract.....	147
Figure 87	Analytical HPLC chromatogram of "maitotoxin" peak.....	147
Figure 88	Analytical HPLC chromatograms of hexane fraction.....	152
Figure 89	HPLC separation of purified chl _a 666.....	153
Figure 90	Diagram of structure of new chlorophyll.....	155
Figure 91	Proton coupled 500 MHz spectra of atropine.....	158
Figure 92	Proton coupled 500 MHz spectra of atropine.....	160
Figure 93	300 MHz ¹³ C NMR spectra of atropine.....	161
Figure 94	DEPT of atropine.....	161
Figure 95	Proton coupled 500 MHz spectra of quinine.....	162
Figure 96	Proton coupled 500 MHz spectra of quinine.....	163
Figure 97	Proton coupled 500 MHz spectra of quinine.....	163
Figure 98	Proton coupled 500 MHz spectra of quinine.....	164
Figure 99	Proton coupled 500 MHz spectra of quinine.....	165
Figure 100	300 MHz ¹³ C spectrum of quinine.....	165
Figure 101	DEPT of quinine.....	166
Figure 102	Proton coupled 500 MHz spectra of procaine	166
Figure 103	Proton coupled 500 MHz spectra of procaine	167
Figure 104	300 MHz ¹³ C NMR spectrum of procaine.....	168
Figure 105	DEPT plot of procaine.....	168
Figure 106	Proton coupled 500 MHz spectra of xanthosine dihydrate.....	169
Figure 107	Proton coupled 500 MHz spectra of xanthosine dihydrate.....	170
Figure 108	Proton decoupled 500 MHz spectra of xanthosine dihydrate.....	170
Figure 109	Proton decoupled 500 MHz spectra of xanthosine dihydrate.....	171
Figure 110	Proton decoupled 500 MHz spectra of xanthosine dihydrate.....	172
Figure 111	Proton decoupled 500 MHz spectra of xanthosine dihydrate.....	172
Figure 112	Proton decoupled 500 MHz spectra of xanthosine dihydrate.....	173
Figure 113	Proton decoupled 500 MHz spectra of xanthosine dihydrate.....	173
Figure 114	Proton decoupled 500 MHz spectra of xanthosine dihydrate.....	174
Figure 115	¹³ C spectrum of xanthosine dihydrate.....	175
Figure 116	¹³ C proton off-resonance spectrum of xanthosine dihydrate.....	175
Figure 117	Proton coupled 500 MHz spectra of reserpine.....	176
Figure 118	Proton coupled 500 MHz spectra of reserpine.....	177
Figure 119	Proton coupled 500 MHz spectra of reserpine.....	177
Figure 120	Proton coupled 500 MHz spectra of reserpine.....	178
Figure 121	Proton coupled 500 MHz spectra of reserpine.....	179
Figure 122	Proton coupled 500 MHz spectra of reserpine.....	179
Figure 123	Proton decoupled 500 MHz spectra of reserpine.....	180
Figure 124	300 MHz ¹³ C NMR spectrum of reserpine.....	180

Figure 125	DEPT plot of reserpine.....	181
Figure 126	300 MHz Spectrum of Preparative HPLC Purified MTX.....	182
Figure 127	300 MHz Spectrum of Preparative HPLC Purified MTX.....	183
Figure 128	300 MHz Spectrum of Preparative HPLC Purified MTX.....	183
Figure 129	Complete proton spectrum (1-9 PPM) of rust brown fraction..	184
Figure 130	Lowfield region of ^1H spectrum (5.5-8.8 PPM)	185
Figure 131	Lowfield region of ^1H spectrum (5.5-8.8 PPM)	186
Figure 132	Complete ^1H spectrum (1.0-8.0 PPM) of brown ACN soluble.....	187
Figure 133	Lowfield ^1H spectrum of DMSO extraction.....	188
Figure 134	Lowfield region of ^1H spectrum (5.3-8.7 PPM).....	188
Figure 135	Spectrum for maitotoxin published by Yasumoto (1985).....	189
Figure 136	NMR spectra of fraction MTX #2.....	192
Figure 137.	Fragments T through Y determined from ^1H NMR spectrum Projected from ^1H , ^{13}C , and ^1H COSY Spectrum.....	196
Figure 138.	Projected Structure of Terminal Fragment A Determined from ^1H , ^{13}C , and ^1H COSY Spectrum.....	197
Figure 139.	Projected Structure of Terminal Fragment Z Determined from ^1H , ^{13}C , and ^1H COSY Spectrum.....	198
Figure 140.	Coupling of Fragment A to Fragment B-J through ring G.....	202

TABLE OF TABLES

Table 1.	Estimated Production Potential.....	28
Table 2.	Cultures Harvested.....	29
Table 3.	Growth Production Data.....	30
Table 4.	The SIU World Culture Collection of Dinoflagellates.....	34-35
Table 5.	Acclimation of <i>G. toxicus</i> clones	37-39
Table 6.	Acclimation of <i>G. toxicus</i> clones	40
Table 7.	ANOVA of Acclimation Data.....	41
Table 8.	Paired Analysis of Variance	41
Table 9.	Paired Analysis of Variance	42
Table 10.	Extract Potency Differences.....	43
Table 11.	Paired Analysis of Variance.....	43
Table 12.	One Way Analysis of Variance.....	45
Table 13.	Summary of Results for Different Clones.....	46
Table 14.	One Way Analysis of Variance.....	47
Table 15.	Sub-clone Variability of Clone 175.....	47
Table 16.	Growth Pattern of Clone 175.....	50
Table 17.	Biochemical Composition of Clone 175.....	51
Table 18.	Pigment Composition at Five Light Intensities.....	52
Table 19.	Total Chlorophylls and Carotenoids Per Cell.....	52
Table 20.	Summary of Correlation Matrix.....	70
Table 21.	Volume of Media and Cell Production.....	75
Table 22.	A Comparison of Toxicity of Crude Methanol Extracts.....	76
Table 23.	Ileum assays of MTX.....	94
Table 24.	Low Pressure Chromatography of ESMF.....	96
Table 25.	Summary of 8 Grams of Dried Cells.....	99
Table 26.	Products of Extraction and Purification.....	101
Table 27.	Crude Fraction Delivered for Rat Assay.....	102
Table 28.	Results From Liquid-Liquid Separations.....	103
Table 29.	Effects of Toxic Extracts on Ileum at Low Doses.....	105
Table 30.	Quantitation of Crude Toxic Components by Ileum Assay.....	108

Table 31.	Quantitation of CTX Toxic Component.....	113
Table 32.	Quantitation of MTX Toxic Components by Ileum Assay.....	127
Table 33.	Hexane:Methanol Separation.....	129
Table 34.	Acetonitrile.....	129
Table 35.	Ethanol Separation.....	130
Table 36.	Preparative HPLC Separation.....	130
Table 37.	Hexane:Methanol Separation.....	131
Table 38.	Ileum Assays of MTX.....	144
Table 39.	Elution times of chlorophylls.....	153
Table 40.	^1H NMR Resonances of chlorophyll	154
Table 41.	^{13}C Assignments for Chlorophyll.....	156
Table 42.	Relative Concentrations of Chlorophylls-a	157
Table 43.	Specific Concentration of Chlorophylls in the Four Clones.....	157
Table 44.	Table of Projected Groups from Specific ^1H NMR Peaks.....	159
Table 45.	Table of Projected Groups from Specific ^1H NMR Peaks.....	164
Table 46.	Table of Projected Groups from Specific ^1H NMR Peaks.....	181
Table 47.	Assignments from Specific ^1H NMR Peaks.....	181
Table 48.	Partial Peak Assignment to MTX from ^1H NMR Peaks.....	186
Table 49.	Table of Projected Groups from NMR Peaks.....	190
Table 50.	Table of Projected Groups from NMR Peaks.....	194
Table 51.	Table of Projected Groups from NMR Peaks.....	195
Table 52.	MTX from GT-350, Structure groups from ^1H & ^{13}C	195
Table 53.	Tentative Assignments of ^{13}C and ^1H Shifts for Terminal Fragment A.....	197
Table 54.	Tentative Assignments of ^{13}C and ^1H Shifts for Fragments T through Y.....	198
Table 55.	Tentative Assignments for Terminal Fragment A.....	199
Table 56.	Structure and Assignments for part J and I.....	200
Table 57.	Structure and Assignments for part H and G.....	201
Table 58.	Structure and Assignments for part F and E.....	202
Table 59.	Personnel employed on the contract.....	204
Table 60.	Deliverables made to USAMRIID.....	210

BODY OF THE REPORT

STATEMENT OF THE PROBLEM

BACKGROUND INFORMATION

Ciguatera Poisoning

Ciguatera poisoning is a syndrome which occurs following the ingestion of certain tropical marine reef-fishes that sporadically acquire toxicity. It is one of nine known forms of ichthyosarcotoxism: poisoning of humans resulting from eating fishes which contain poison within their musculature, viscera or skin.^[1] Halstead^[2] has reported over 400 species of marine fishes as carriers, most, if not all, of which are an integral part of the food web of coral reefs associated with oceanic islands within a circum-global belt from 35°N to 34°S.^[2,3]

The Ciguatera Syndrome

The symptoms that occur after eating toxic fish typically include both gastrointestinal and neurological manifestations. Typical symptomatology in humans has been reviewed and summarized by several authors.^[4-6] Earliest symptoms of intoxication usually include gastro-intestinal upset, which may last for several hours or days. Moderate to severe intoxications usually produce neurological symptoms which may last weeks to months. Irregularities in nerve conduction parameters in fish,^[7,8] mammals^[9] and humans^[10,11] have been documented. Thus, it is quite clear that intoxication affects the nervous system for extended periods of time. In at least one case of severe intoxication symptoms persisted for 25 years.^[12] death may result and if so, it usually occurs within several days. In an isolated case, death has occurred within ten minutes and the fatality rate has been approximated as 12%^[2] 3%^[5] and 0.5%.^[13] It is suspected that a large number of ciguatera intoxications, some from eating frozen fish, are not recognized as such.^[14]

Multi-toxin Involvement

A few early researchers suggested that the great variety of symptoms displayed by patients suffering from ciguatera and their inconsistent responses to certain clinical treatments indicated that there was more than one primary toxin causing the ciguatera syndrome,^[15,16] while Banner et al.,^[17] argued that ciguatoxin was the principal factor. Nevertheless, later studies coupled with the variability in results from testing of extracted fish tissues on a variety of preparations have emphasized the occurrence and importance of multiple toxins^[18-23] Yasumoto et al.,^[20] provided evidence that ciguatoxin was of exogenous origin and was not a metabolic product of primary consumers. These authors reported that an analysis of gut contents of *Ctenochaetus striatus* (a detrital feeder, exclusively) revealed a portion, designated as unidentified particles, containing a high concentration of "ciguatoxin"(=maitotoxin). A recent report has indicated that ciguatoxin from both fish and dinoflagellate cells are modified forms of, or has a structure similar to, brevetoxin.^[24] A second report has indicated that the toxin detected in ciguatoxic fish (eel) was palytoxin.^[25] Another recent report has indicated that ciguatoxin both from cells and fish is a complex polyether structure.^[26]

Dinoflagellate Toxins Affecting Ion Channels

The use of ion channel toxins has been crucial to uncovering the mechanisms of how ion channels work. It is well documented that two other toxins from dinoflagellates, saxitoxin and gonyautoxins are inhibitors of sodium channels. Brevetoxins have been found to affect sodium ion channels.^[27,28]

Perhaps some of the most interesting recent work on CTX (from fish) is its effect on mammalian and teleost nerve published by Cameron.^[11,29,30] This work indicates that the neural effects of CTX (from fish) are principally upon the small C fibers.

With respect to maitotoxin from cells, earlier reports indicated that it directly activated endogenous Ca^{2+} channels. The evidence for this was circumstantial and our early work indicating that Diltiazem but not other antagonists ameliorated its effect on the ileum preparation, placed doubt on this interpretation. Later work has indicated that MTX may secondarily affect channels by a primary affect upon phospho inositol or protein kinases.

MTX is well known for its positive inotropic response in smooth muscle,^[31-33] contraction of smooth muscle,^[34,35] transmitter release from nerve cells,^[34-36] and hormone release from cultured pituitary cells.^[37] MTX was also found to increase the frequency of miniature end plate potentials^[36] from cardiac diaphragm. Subsequently, MTX was found to increase calcium uptake by synaptosomes,^[38] release GABA from cultured cells,^[39] enhance the formation of phosphate inositol in PC12A cells and increase phosphate inositol metabolism and form pores.^[40] In addition to the concept of pores, Sladeczek^[40] found that there was a Ca^{2+} dependence for the toxin action but not the binding to the membrane. Some of the effects described could be inhibited by organic voltage-sensitive calcium channel blockers.^[37,41,42] In cultured cells MTX was shown to cause a loss of membrane integrity,^[43-45] affect other cells,^[46] increase calcium current^[47] and cause a loss of cellular ATP and an inward leak of calcium.^[48,49] Lee^[50] showed that MTX caused an increase in calcium dependent phospho-inositol in cells. The MTX stimulated inositol phosphate response in rat aortic myocytes was insensitive to organic Ca^{2+} channel blockers.^[51] Finally, another recent article^[52] on MTX indicates that it affects K^{+} transport in a unique manner and not due solely to Ca^{2+}

Nevertheless it should still be emphasized that pure MTX has not been achieved and the structure of MTX has not yet been published. Thus all the above conclusions have been reached with impure toxin. The possibility exists that the effects of MTX may in fact be due to a complex of two or more factors. The fact that toxin approaching the

0.1 µg/MU level produces subtle changes to the ileum response, may point to this or to the modification of the toxin in the purification process.

Dinoflagellate Involvement in Ciguatera

That dinoflagellates are the source of ciguatera-toxins has been well documented. In the Pacific, Yasumoto and others^[53,54] obtained significant quantities of ciguatoxin from samples of detritus collected from dead coral near the Gambier Islands. The most toxic fraction of the detritus contained large numbers of a dinoflagellate, which he tentatively identified as "*Diplopsalis* sp." Subsequently, Adachi and Fukuyo^[55] named the organism *G. toxicus*. Yasumoto et al.,^[19] connected the production of toxin with both the dinoflagellate and toxic effects in mice.^[56] The dinoflagellate, *G. toxicus* has subsequently been isolated from ciguatera prevalent areas near Japan,^[56,57] and Hawaii.^[58,59] McFarren and others^[59] have provided accounts of ciguatera-like poisoning (*G. breve* ?) from shellfish collected from the west coast of Florida. Other investigators have published on *G. toxicus* from Florida.^[60] Tindall and his group^[61] have grown in mass culture and extracted toxins from three dinoflagellate species which were isolated from areas of the Caribbean in which ciguatera intoxication was prevalent. Thus far, four particular dinoflagellates are implicated in the production of ciguatera toxins: *G. toxicus*, *P. concavum*, *P. rathymum*(= *P. mexicanum*) and *Ostreopsis lenticularis*.^[62]

Toxin Producing Dinoflagellate Strains

There is ample evidence to indicate that different strains of the same species of dinoflagellates produce different numbers and amounts of toxin.^[63-65] There are also reports of loss of toxicity of dinoflagellates after culture. Under our conditions we have found that the initiation of mass cultures from unialgal or pure cultures has confirmed the strain differences but our cultures (*G. toxicus*) have produced toxins through continual subculturing since 1979. The same holds true for many of the other species.

Isolation of Dinoflagellate Toxins

Yasumoto^[22] extracted toxic components from *G. toxicus* cells utilizing a boiling methanol extraction prior to doing a water-ether partitioning. The ether extracted portion was further treated with acetone to derive a toxic fraction. Since we have found this fraction to precipitate in very cold acetone we term it the ether soluble acetone precipitate (ESAP) fraction. Most cell isolation procedures used an initial partitioning of the cells with a water-ether mixture. The treatment of the water phase of the cell extracts have been similar by all investigators. After an acetone partitioning the filtrate is chromatographed to yield a water soluble toxic component.

The treatments for the ether phase of the cell extracts have differed. Yasumoto used a technique which involved an acetone extraction of the ether-water phase. Bagnis and others^[66] modified the technique to include a cold acetone treatment that resulted in both ether-soluble acetone precipitates (ESAP) and ether-soluble acetone filtrates (ESAF). Even though he utilized this separation procedure, he then combined the ESAP with the WSAP fraction. Tindall and his group discovered that when the ESAF material was kept in the cold acetone all of the toxic activity eventually precipitated out of the filtrate. Thus, they adopted acetone precipitation as a step in the procedure hoping to further purify the toxic component. The toxic fractions obtained by these procedures differ with the particular dinoflagellate species.

Fish Toxins

The studies of toxins from fish extracts are difficult to draw conclusions from for several reasons. The most critical reason is that, if there are multiple toxins in fish (determined by their diet), and any one toxin may have different effects on a variety of assay systems, then it is possible that the extraction of toxin from the same species of fish by investigators from different locales will produce different symptoms.

From the foregoing we conclude, that if we want to determine if a particular fish is toxic, we must have a test(s) or assay system(s) which is(are) specific at a known level for each of the particular toxins which may be involved in the ciguatera syndrome. For this express reason, we decided at the outset of our experimentation that the utilization of cell cultures would be the most productive approach.

Indeed, the same philosophy argued above for the diagnosis of toxic fish would apply to the treatment of the disease ciguatera. A different treatment would be called for were a person intoxicated with a sodium channel inhibitor rather than a calcium channel activator. Eventually, it would be ideal to have an assay system which would, in fact, reflect the number, kinds and amounts of toxins. The construction of these specific chemical tests is only possible, however, if one has reasonably pure toxin, which is separated from other toxins and identified.

These constraints have dictated our approach to the entire problem since we started our research in 1973, as follows:

1. Identify sources of the toxins.
2. Produce large amounts of toxic organisms.
3. Improve extraction techniques.
4. Find a sensitive bioassay(s) for screening.
5. Use bioassay to assist in purification.
6. Improve purification techniques.
7. Use purified toxins to:
 - a. investigate physiology.
 - b. investigate structure.
 - c. elaborate chemical assay system.

Our preliminary works and the work of others^[61,67-69] have identified several different toxins which may be involved in the ciguatera syndrome:

1. Ciguatoxin
2. Maitotoxin
3. Slow acting toxin (unidentified)

4. Scuritoxin-like toxin
5. Okadiac acid
6. Fast-acting toxin I (unidentified)
7. Fast-acting toxin II (unidentified)
8. Ostreotoxin

Clearly, the understanding of the entire problem of the toxins produced by dinoflagellates requires a definitive test or set of tests which will allow us to discriminate between the toxins and be able to quantify and follow them. Other desirable features of a test procedure would be 1) provide the same baseline for each of the toxins, 2) consume only a small amount of toxin, 3) require a small amount of time for the assay, and 4) be able to detect modifiers of sodium channels in membrane as well as calcium channels.

Significance

"Ciguatera-toxins" are involved in a variety of short term symptoms for which people commonly present themselves to a doctor for treatment (e.g. diarrhea, headache, etc). In addition intoxication can result in prolonged disability or even death. Another aspect of the toxins and one which has yet to be addressed is the long term effects on animals that is: are they cumulative, are there storage sites, what are the affected sites, and how long before excretion? The reoccurrence of neurological symptoms years after intoxication would seem to indicate a retention of the toxin and/or toxic effects in the nervous system.

The toxins affect calcium and sodium channels. In addition, there is the prospect of discovering other new and important ion channel inhibitors. Ion channel inhibitors have been essential to our present understanding of ion channel physiology and structure. Clearly, the identification, isolation and purification of individual toxins involving ion channels will expedite (1) an understanding of their structure, (2) allow the investigation of their physiological actions, (3) expedite the formulation of ameliorative and prophylactic treatments, and (4) allow the elaboration of a specific chemical assay.

APPROACHES TO THE FOUR YEARS OF STUDY

Methods for Growth of Cells

The dinoflagellate cultures which we used for this project are part of the Southern Illinois University Culture Collection, housed in the Department of Plant Biology. At present this collection houses strains representing dinoflagellate species isolated from "ciguatera endemic regions" areas of the world. Our stock cultures are routinely grown in 50 ml volumes in 125 ml Erlenmeyer flasks. The medium is ES Medium^[70] made with natural seawater, with 1.5% soil extract added. These cultures are kept in refrigerator-type culture chambers at 27°C and 300 ft-c. cool white fluorescence illumination (either continuous or on a 16:8 light-dark cycle, depending upon the requirements of the particular species). Stock cultures are transferred every 7-14 days. Two generations of cultures are retained as back-ups to the new transfers. The subculturing and maintenance of triplicate cultures is labor intensive and requires approximately 20 manhours per week by an experienced person. In addition, all cultures are examined periodically by one of us to check for contamination. Currently we maintain stock cultures of over 200+ clones of dinoflagellates. Preparation of the growth medium requires millipore filtration (0.45 or 0.22 μ m) and sterilization of the sea water, sterilization of the flasks, compounding of the growth medium, inoculation and siting in the growth chambers. Conservatively, this requires approximately 20 manhours per week for a total of 18 carboys. Because the growth cycle for both the subcultures and the mass cultures takes four weeks, we initiate a mass culture every two weeks. It is critical for the cultures, to achieve the maximum toxin production, that they be harvested very close to the 30 day period.

The development of mass cultures involves transferring cells from stock cultures to a series of two liter fernbach flasks containing enriched seawater medium. After the late log phase of growth has been reached (approximately 15-20 days) each of these cultures are used to inoculate 18 liters of the same medium in 20 liter carboys. Mass cultures are grown under the same light and temperature

regime as noted above and are aerated continuously in order to prevent CO₂ depletion and to provide moderate agitation. Cells from small cultures are harvested by centrifugation or filtration. Cells from mass cultures are harvested by means of a Pelicon concentrator using 0.45 μ m membranes after cultures reach the early stationary phase of growth (25-30 days). If the culture has excessive amounts of slime it is first sieved before the use of the Pelicon.

Chemosystematic Studies

Systematics is a branch of taxonomy which deals with assessing variation in characters between and within genera from living material.^[71] A systematic study has been incorporated into this project as a means of identifying clones (cultures initiated from individual cells) which are inherently good producers of toxins. Our culture collection now includes more than fifty clones of *G. toxicus* from a variety of locations including Bermuda, the Bahamas, Florida, the Caribbean, Hawaii, Australia, French Polynesia, Mexico, Fiji and other areas. It is this diverse, bank of living material which forms the basis for the systematic studies.

Our first approach in assessing clonal differences was to acclimate the *G. toxicus* clones to the same conditions (light, temperature and medium) in one liter cultures. Once acclimated, the final one liter cultures were harvested and also used to inoculate an additional one liter culture which served as the starter for a 15 liter culture. The toxicities of the crude methanol cell extract from the acclimated one liter cultures were compared in terms of the number of mouse units per milligram of dried cells. This is a quantitative measure of clonal toxicity, and does not consider qualitative differences in toxins. We assert that because of the acclimation process the varying potency of these extracts among clones is due to interclonal genetic differences and not to environmental differences.

Beginning in 1989 the extract potencies of several clones from the first and the last one liter culture were compared in order to assess the significance of the acclimation process. In addition, the potency

of extracts from clone 135 were compared monthly in order to determine when acclimation was achieved and once achieved, how stable a character it is. An additional control experiment was run with the Martinique (Caribbean) clone (175).

Clone 175 has been sub-cloned so that we can assess any toxicity differences which may result from micro-environmental differences in the culture chambers. Only toxicities which exceed the methodological errors were used for "chemosystematic" comparisons ("chemo" referring to the toxins and "systematic" to the clonal comparisons). The material from the 15 liter cultures was used to assess qualitative differences in toxins among the clones.

The genetic comparisons indicated that clone 175 produces more toxin per unit weight than approximately twenty other clones of *G. toxicus* surveyed. Consequently, this clone was selected for physiological experiments designed to enhance toxin production, hopefully including the lipid-soluble toxin. The first phase of this work involves examining the macromolecular components and toxin production of clone 175 when grown under seven different light intensities and at three temperatures. These are 378, 648, 1081, 1999, 3350, 3782 and 4300 lux light intensities and 28°C, 25°C and 22°C temperatures.

The cultures were acclimated to each temperature following the methods of Brand et al.^[72] and Bomber et al.^[73] All cultures are grown in a Percival culture chamber equipped with microprocessor controls. The microprocessor enables us to change temperatures slowly using a constant gradient. The cultures were harvested through a 32 μ m screen and lyophilized for approximately 24 hours until dry.

Kochert^[74] determined protein from cell pellets that were first extracted with chloroform/methanol. Total lipids were then determined from the organic solvent extracts. We determined that as much as 10% of the protein will enter the organic solvents. Thus, we analyzed proteins and lipids separately. The dried cells were

extracted with 1N NaOH with sonication followed by immediately adjusting the pH to approximately 7.5 with distilled, deionized, charcoal filtered water. This method yielded far better protein extraction than SDS (sodium dodecyl sulphate) or the method of boiling the cells in 1N NaOH.^[74] The extract was filtered through a 0.2 μ m screen and analyzed for proteins by the Bio-Rad micro-method. Carbohydrates contents were determined from the same extracts via the sulphuric acid method.^[74,75] Lipids were determined from separate samples following Freeman et al.^[76] and Sperry and Brand.^[77]

The chlorophyll content was determined from the equations of Jeffrey et al.^[78] Carotenoids were determined via the methods of Jensen.^[79] All samples were processed in darkened fume hoods and stored under nitrogen for best preservation. Most samples were analyzed within two weeks of harvest. The potencies were determined as before using the linear interpolation tables of Weil.^[80] Ammonium and phosphate uptake rates were determined from disappearance of the nutrients from the culture medium following the methods of Strickland and Parsons.^[81]

Previous work^[82] has determined that it is not possible to completely identify a systematic "variant clone" or "race" of *G. toxicus* by analyzing only one character, e.g. extract potency. Consequently, this project includes an "acclimated reproduction rate comparison".^[72] In this study the response to light of different intensities by the different clones of *G. toxicus* is being monitored. Four light intensities are being used and include 80, 160, 205 and 250 footcandles of illumination. The reproduction rate (divisions per day) of the clones is plotted against the light intensity and the resulting slope of the line is used as a numerical systematic character. It is critical that the cultures be completely acclimated in this study, as in the toxicity study. The slope of the line is a valid genetic character because the reproduction rate is under enzymatic control and varies with the efficiency of enzymatic transcription (hence chromosomal differences) under different environmental

conditions. These data from these studies will also be useful as a data base in physiological studies which will examine the effect of light on toxin production.

Seventeen clones of the ciguatera-causing dinoflagellate *G. toxicus* were physiologically adapted to the same environment over several months. There were significant variance components detected between non-acclimated and acclimated cells for the cell potencies, yields and reproduction rates of these cultures.

Toxin Potencies

Outbred Harlan Sprague Dawley ICR(BR) mice weighing approximately 20 g were used to assess quantitative differences in the potencies of the methanol extracts. The potencies were then determined as LD₅₀'s for each clone using from 3 to 10 mice at each of 4 dosage levels. The mice were observed for 48 h. The LD₅₀'s were determined from the linear interpolation tables of Weil.^[80] Alternatively, in some cases the LD₅₀ was determined by linear regression.^[83] The final values are expressed as the number of mouse units (LD₅₀ dose for a 20 g mouse) per mg of dried cells, per cell of *G. toxicus* and in terms of number of cells per mouse unit.

The acclimated and non-acclimated cell potencies were compared in the same manner as the growth rate and cell yield statistics. In addition, a one-way Analysis of Variance with Replication^[83] was used to compare selected clones from broad areas. The f_{max} test^[83] was used to assess homogeneity before conducting all ANOVA's. The potencies used in this ANOVA were plotted vs. latitude of collection along with the values for all other clones. The clones used in generating the ANOVA are also plotted with their 95% comparison intervals, calculated from and a-posteriori T-method comparison among means.^[83] Potency and latitude were also tested for correlation by the Pearson test.^[83]

Three clones (177, 350 and 135) were also assayed for potency at 6 to 11 points during the growth cycle and these were plotted vs.

days in culture and compared. The two parameters were then tested for correlation by the Pearson test.^[83] For clone 177, 3 of 11 samples were assayed for potency 4x and compared by one-way ANOVA to test for significance of variation in potency through the acclimation process. The means from this test were also compared by the T-method. The potency and reproduction rate of clone 177 was also monitored after continuous batch culturing was stopped and transfers were made in stationary phase. Potency changes for clone 350 were monitored through acclimation to the vita lite bulbs and then when returned to a cool white light environment at a similar light intensity.

As a control experiment on sub-clone variability, clone 175 was sub-cloned 25x, all isolates survived and 4 were selected randomly to determine the coefficient of variation among fully acclimated sub-clones. As a control experiment on the stability of the acclimated condition, clone 135 is still being monitored for potency data accumulation beyond one year.

Five other relationships were also explored by correlation analysis and include potency vs. cell size and potency vs. reproduction rate for all clones examined. The former test was performed on acclimated potencies only whereas the latter test included all data points. Cell size was determined as the transdiameter and computed from a minimum of 20 cells of each clone collected from a log-phase culture. The potency was also tested for correlation with chlorophyll a, chlorophyll-c₂ and peridinin content (pg cell⁻¹). Pigments were assayed via the methods of Jeffrey et al.^[78] and Indelicato and Watson.^[84] They were subsequently extracted and analyzed for composition of proteins (Bio-Rad method), lipids^[76,77] and carbohydrates.^[74,75]

The initial methods for the extraction of the toxins is very similar to what is currently being utilized by other investigators (especially those attempting to isolate toxin from fish tissues) so that, to some extent, we can compare the toxic fractions which we obtain with what is in the literature. The cells are no longer extracted by

refluxing in boiling aqueous methanol. Instead, extraction is now accomplished by crushing of cell, followed by sonication in methanol at room temperature. The methanol extracts are concentrated and subjected to liquid-liquid partitioning followed by cold acetone precipitation of the toxic components.

Further purification of the toxin was either by thin layer chromatography (TLC), silicic acid chromatography or high pressure liquid chromatography (HPLC). Eluting solvents for column chromatography consist of chloroform-methanol (1:1), and chloroform-methanol-water mixtures (9:1:1). The eluting solvent for HPLC is methanol (100%).

Purification of Toxins from Mass Culture of Dinoflagellates

Separation is achieved using three HPLC instruments associated with a single computer controller system. All three are Waters Company instrumentation and consists of a Delta 3000 Preparative-Semipreparative HPLC and a Model 300 Analytical system all interlinked with SIM modules to an 840 Controller System. While we use C-18 or C-8 columns in each system, the sizes differ, having 15 μ in the Preparative and Semipreparative and 10 μ or 5 μ in the Analytical.

Mouse Bioassay

The mouse bioassay is the officially recognized toxicity assay for ciguatera recommended by the Official Organization of Analytical Chemists and the FDA. In addition, it provides a base line against which we can compare our isolated preparation assays. The carrier for toxic extracts is normal saline containing 0.5 ml of a 1% Tween-60 solution. Toxicity is determined by an intraperitoneal injection of 0.5 ml of a suspension of extract into approximately 20 g mice (Strain CRE:CD:BR:ICR). Toxicity is defined as death of the mouse within 48 hours. LD₅₀ values are calculated according to the method of Weil.^[80] Four dosage levels are used with three repetitions at each

level. The LD₅₀ is calculated from moving average interpolation tables.

Ileum Assay Procedures

We have utilized the terminal portion of the guinea pig ileum to assay dinoflagellate toxins. The overall setup for the ileum assay has been published.^[85]

Guinea Pig Ileum. Female guinea pigs (350-600 g) were sacrificed by a cervical dislocation. A 2-4 cm segment of the terminal ileum was removed and placed in physiological saline solution (PSS) at 37°C. The terminal portion will, however, respond to exogenously applied agonists. Hence its suitability for use in an assay system.

Tissue Bath. The excised terminal ileum is allowed to come to temperature in saline for 15 min then a one cm segment is cut and inserted in an Anderson type tissue chamber^[86] modified as suggested by Bartelstone.

Water Circulating Bath. The guinea pig ileum is extremely temperature sensitive and changes as small as 0.3°C may affect its contractility and therefore your results. For this reason you must have a circulating water bath or some other means of controlling the temperature. The circulating water bath that we presently use is Fisher Model M8000, Isotemp, Constant Temperature Circulator. The ileum is connected to a locally-made device which is a true, isotonic-tension transducer. The counter weight we use is 2 grams. Amplification of the transducer signal is achieved by the use of a DC oscilloscope with a pen output. For storage of records and recording of data for calculations we chose an inexpensive chart recorder (Fisher Recordall Model 5000). Any good DC level recorder can be used, but a ten inch recorder makes the task of measurement much easier. The ileum has been shown to respond to acetylcholine, histamine, substance P, epinephrine, and several other compounds. Indeed, it has varying sensitivity to each of these compounds. We

have found that the toxic fractions will give different inhibitions with different agonists.

Protocol for Reversible Toxins. The first protocol followed is utilized when there is only a reversible toxin in the extract. Initially a control series of acetylcholine or histamine stimulations is performed at different dosages to determine three doses which would give us values between 20 and 80% of maximum contraction of the ileum segment. That particular set of test doses is then utilized throughout the rest of the experiment. All subsequent responses of the ileum to agonist challenge are expressed as a percent of control values.

The toxin containing physiological saline solution is utilized for subsequent washes. Thus when testing for reversible inhibition, the toxin is always present in the PSS at the same concentration.

Non-reversible Assay. The second protocol is utilized when it is suspected that there only a non-reversible toxin in the extract. First a control series of histamine stimulations is performed at different dosages to determine a dose which would give us approximately 80% of maximum contraction of the ileum segment. That particular test dose is then utilized throughout the rest of the experiment. All subsequent responses to histamine are expressed as a percent of that control value.

Tests for Purity of Toxins

The easiest manner to test for purity of the toxin is to run in a recycle mode on the analytical HPLC to determine if after a given number of recycles the single peak remains or resolves into more than one peak. We will use several criteria for testing for purity: first the presence of single peak after recycling on analytical HPLC; second, migration on TLC plates in different solvent systems, and structural data from Nuclear Magnetic Resonance.

NMR Spectroscopy

At the present time Nuclear Magnetic Resonance (NMR) would provide us with the most informative data and yet is non-destructive to the sample analyzed. For these reasons it is the method of choice. Samples of purified toxins will be sealed in special, thin-walled, small-bore, NMR sample tubes from Wilmad Glass Co. Two state of the art NMR instruments are presently available for our use: specifically a 300 MHz Varian VXR-300 and a 500 MHz Varian VXR-500 multinuclear spectrometer system. Both instruments operate in the pulse Fourier Transform mode and are equipped with a liquid helium VXR superconducting magnet and acquisition hardware. Both have H₂ fixed frequency lock system with 5 mm broad band computer switchable probe. Multiple probes to two chambers accepting, 5 mm (narrow bore) and 10 mm (medium-wide bore) tubes for ¹H, ¹³C, ³¹P, ¹⁵N, ¹⁹F and other nuclei. Quadrature detection. Homo- and hetero-nuclear decoupling with spectral limits of 100 to 100,000 Hz. Variable temperature control (-70° to 140°) under computer control for all probes. VXR data station with dual high density disks. The VXR-300 operates at 300 MHz ¹H resonance and is presently used primarily for ¹³C analysis. Automatic performance of standard relaxation experiments, as well as data recording is accomplished by an associated computer. The chemical shifts recorded are then interpreted for structure.

Packaging of Toxins for Delivery

Purified toxins in 100% methanol will be placed into vials, concentrated to almost dryness under nitrogen gas, sealed and labeled for shipment. The vial is then encased in a plastic container with absorbant material. The plastic container is then packed into a metal container and sealed. This is enclosed in packing material and styrafoam box surrounded by a cardboard container. The entire package is shipped by overnight express. Telephone calls are made

before shipment to notify the commanders representative of the shipment and follow up calls are made to ensure delivery.

Overall Objectives for the Four Years.

- (1) Initiate mass culture of *G. toxicus*.
- (2) Continuation of mass culture of *G. toxicus* and initiate culture of *Ostreopsis*.
- (3) Biosystematic studies to improve toxin production.
- (4) Bioassays for each of the isolated toxins.
- (5) Extraction of crude toxins from mass cultures.
- (6) Purification of toxic fractions.
Purification of toxic fractions using preparative HPLC.
Purification of toxic fractions using liquid-liquid separations
- (7) Investigation of factors affecting the stability of stored toxins.
- (8) Examination of toxins by NMR.
- (9) Quantitation of toxins by weight and bioassay.
- (10) Delivery of toxic fractions to U. S. Army Medical Research Institute of Infectious Diseases.
- (11) Continue to search for additional toxic dinoflagellates for addition to the SIU culture collection.
- (12) Continuing investigation of effects of ethanol on toxicity.
- (13) Maintain the SIU culture collection.

RESULTS

Acquisition and Setup of Equipment

While the official starting date of the contract was listed as 1 December 1986, clearance to officially spend funds was not received through administrative channels until 5 Jan 1987.

Approval of positions - The hiring of any new personnel required the submission of requests through the affirmative action channels within the university. These applications were made and approval for the positions were received on 18 February 1987.

Approval of equipment - In the contract proposal we had not anticipated that there would be a 30 to 90 day delay in the "approval to purchase equipment" process. In order to save time we requested (2 Dec 86) and received permission from the contract specialist to initiate the purchasing process with the provision that final purchase would not be made until approval from the contractor was obtained. The last item to be approved was the growth chambers. Final approval for these items was not received until June, 1987.

The large chambers which were due to be operational were held up an additional time period due to construction problems (installation of a cooling tower and recirculating system). Two of the chambers became operational on 15 November 1987.

Culturing and Growth

Notwithstanding the administrative delays experienced, mass culturing of *G. toxicus*, clone 350 on a limited basis began in March 1987. In our initial proposal we had estimated growth based on the figures in Table 1

The amount of clone 350 accumulated at an increasing rate until March 1988. At this time the results of our chemosystematic studies had indicated that we could improve total toxin production by

switching to growing clone 175. Therefore, the decision was made to emphasize the growth of clone 175 over 350.

TABLE 1
ESTIMATED PRODUCTION POTENTIAL

Clone	350	175
LD ₅₀ s based on 20 g mouse		
MU/mg DW	18	120
mg DW/L	116	122
Total MU/L	2,088	14,640
MU/15 L Culture	3.1×10^4	2.2×10^5
LD ₅₀ s based on Kg Mouse	6.3×10^2	4.4×10^3
LD ₅₀ s based on Yasumoto's value of 0.13 ug/Kg		
ug/Carboy	82	572
Monthly production based on 40 carboys per month		
mg/month	3.28	22.88

The significance of the change to clone 175 is appreciated when one examines the total estimated mouse units produced by the two clones in the year that we switched as shown in Figure 1.

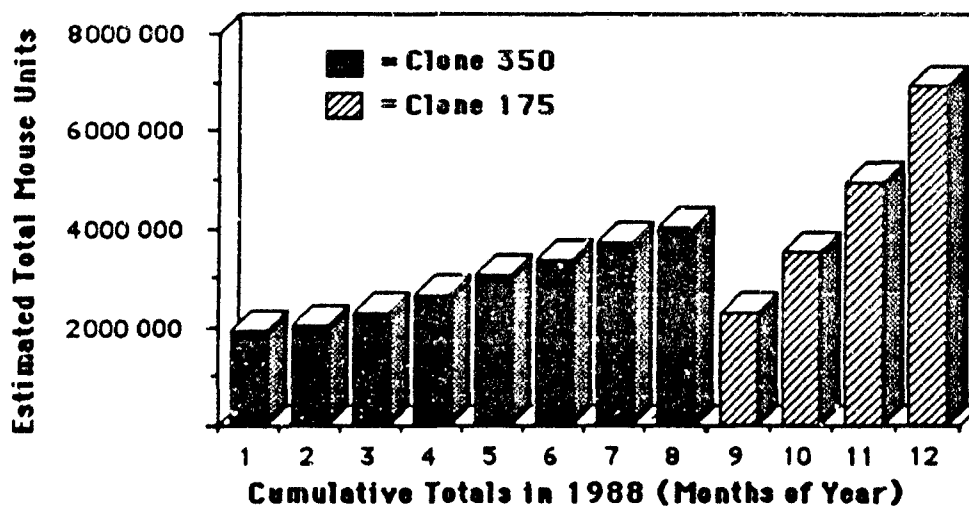


Figure 1. Plot of estimated mouse units contained in cultures of *Gambierdiscus toxicus*, clones 350 and 175 during 1988.

Notice that in just the first three months production of clone 175 we exceeded the total mouse units accumulated from clone 350 for eight months. In the proposal for the contract we had estimated (see Table 1) that the monthly production of mouse units would be approximately 230,000 MU per month. We have more than exceeded that estimate.

Starting in November of 1990, due to the acquisition of clones from French Polynesia and Australia we reduced the growing of clone 175 in mass culture.

TABLE 2
CULTURES HARVESTED

CULTURE DESIG.*	DTE HVST OR RPTD	YIELD	
		Dry Wt	Tot Dry Wt
GT350-4A87D	27Mar	12.2	
GT350-6A87D	13May	13.0	
GT350-7A87D	13May	9.20	
GT350-7B87D	15Jun	2.80	
GT350-8A87D	8Jul	2.60	
GT350-8B87D	8Jul	17.9	
GT350-9A87D	22Aug	2.7*	
GT350-9A-F	22Aug		
GT350-2A88D	25Jan		
GT350-3A88D	12Feb	3.5	
GT350-5A88D	6Apr	12.2	
GT350-7A/88D	8Jun	18.0	
GT350-7B/88D	9Jul	21.1	
GT350-8A/88D	5Aug	16.68	
GT350-10A/88D	9/20	17.7	
GT350-11A/88D	10/25	13.2	30.9
GT175-1A89	Mar-89	31.5	31.5
GT175-1B89	Mar-89	8.57	40.07
GT175-2A89	Mar-89	12.4	52.47
GT175-3A/89D	Jun-89	19.3	71.77
GT175-3B/89D	Jun-89	17.7	89.47
GT175-4A/89D	Jun-89	20.9	110.37
GT175-4B/89D	Jun-89	16.2	126.57
GT175-4B/89D	Jun-89	20.2	146.77
GT175-5A/89D	Sep-89	20.22	166.99
GT175-6A/89D	Sep-89	12.84	179.83
GT175-6B/89D	Sep-89	21.28	201.11
GT175-7A/89D	Sep-89	18.88	219.99
GT175-7B/89D	Sep-89	19.16	239.15
GT175-8A/89D	Sep-89	16.8	255.95
GT175-8B/89D	Sep-89	23.7	279.65

GT175-8B/89D	Sep-89	19.6	299.25
GT175-8B/89D	Dec-89	13.1	312.35
GT175-8B/89D	Dec-89	15.1	327.45
GT175-8B/89D	Dec-89	14.2	341.65
GT175-8B/89D	Dec-89	15.0	356.65
GT175-8C/89D	Mar-90	19.6	376.25
GT175-9A/89D	Mar-90	13.1	389.35
GT175-11A/89D	Mar-90	15.1	404.45
GT175-11B/89D	Mar-90	14.1	418.55
GT175-12A/89D	Mar-90	15.6	434.15
GT175-1A/90D	Mar-90	22.4	456.55
GT175-1B/90D	Jun-90	6.32	462.87
GT175-1C/90D	Jun-90	2.08	464.95
GT175-2A/90D	Jun-90	4.43	469.38
GT175-2B/90D	Jun-90	3.42	472.80
GT175-3A/90D	Jun-90	13.1	485.90
GT175-4A/90D	Jun-90	14.11	500.01
GT175-4B/90D	Jun-90	3.45	503.46
GT175-5A/90D	Sep-90	3.4	506.86
GT175-6A/90D	Sep-90	17.4	524.26
GT175-6B/90D	Sep-90	14.8	539.06

Explanation of numbering system- Because we will be handling a large number of mass cultures we have revised our designating system. The first part of the designation is the initials and strain number of the culture then a dash and a number which represents the month in which the culture was harvested, following this a letter represents the sequence of harvest within that month, followed by a two number designation for the year. Finally, there will be a letter code at the end to designate the stage of processing of the sample. * =estimated **=used to directly inoculate carboys for GT350-9A-F, experimental run to examine faster culture sequence.

At the same time that we started mass culturing the French Polynesian (clone FP100) and Australian clones, we re-started clone 350. Our success in cultivation has continued throughout the four years of the contract during which time we have produced appreciable quantities of dried dinoflagellate cells (Figure 2 & Table 1).

TABLE 3
Growth Production Data

	Produced	Used	On Hand
Grams 350	(105.2)	105.22	0
Grams 175	(567.66)	430.0	137.66
Totals	(672.86)	535.22	137.66

Discussion of Culturing Results. The growth of clone 175 during the third and fourth contract year has produced in excess of 400 grams of *G. toxicus* (dried weight). The record of our production by clone for the entire contract period is shown in Figure 2.

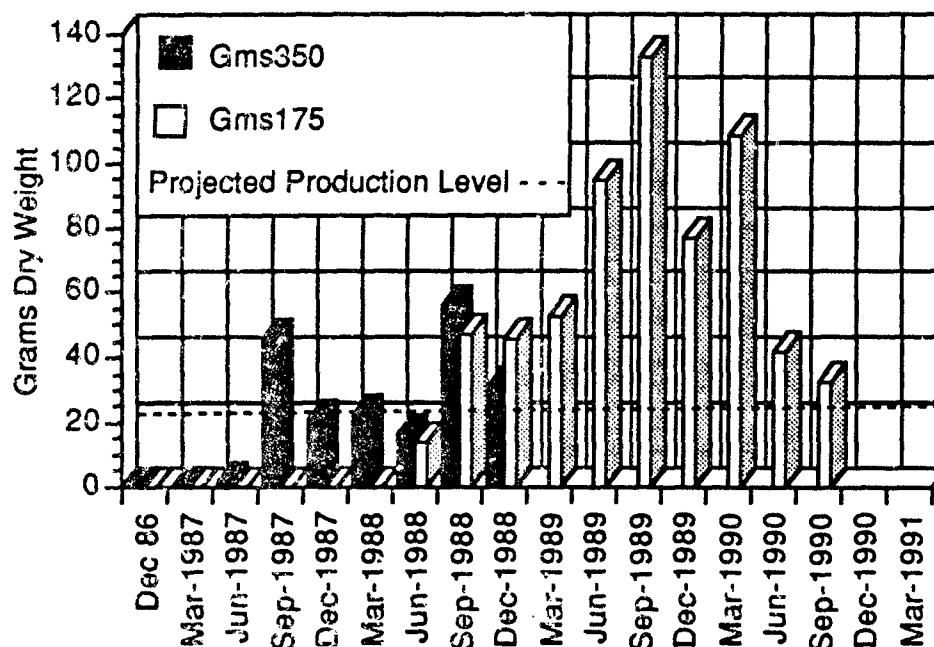


Figure 2. Grams dry weight produced per quarter by clone.

During the entire four years of the contract the production of toxin has exceeded all expectations and projections. This is appreciated when one examines the total estimated mouse units produced as shown in Figure 3. In June of 1990 we began growing newly acquired clones of *G. toxicus* in large scale (e.g. FP100 and A100). Preliminary data on growth and toxicity of these cultures appears in the section on growth. The data for these are not included in Figure 3.

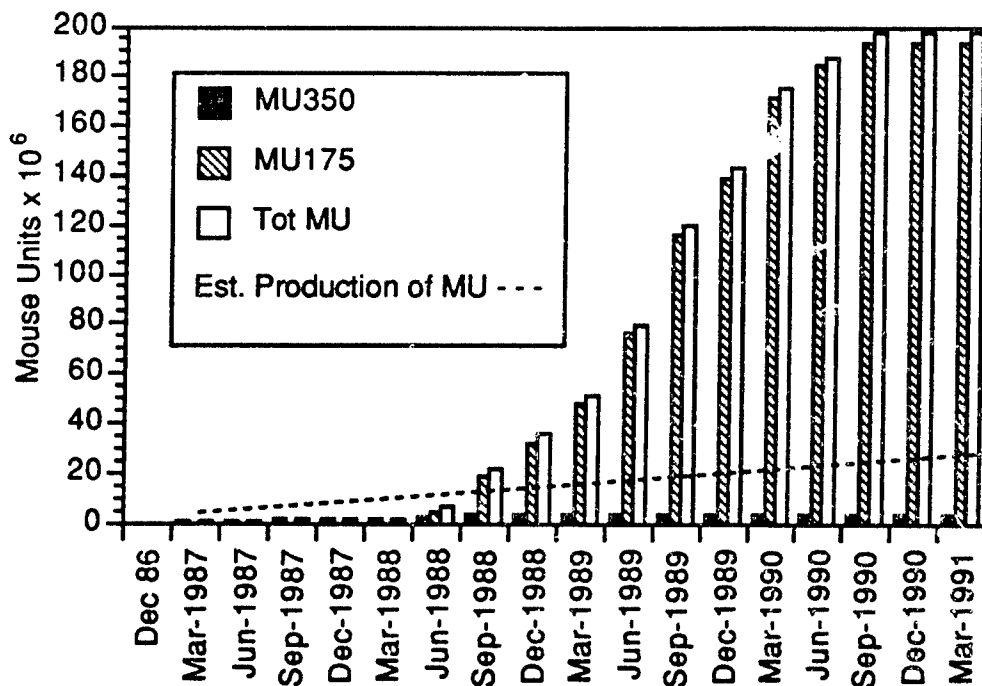


Figure 3. Plot of estimated cumulative mouse units and grams contained in cultures of *Gambierdiscus toxicus*, clones 350 and 175 listed by quarter for entire contract.

Acquisition of Toxic Dinoflagellates

Since the inception of our work on Ciguatera in 1978 we have conducted an extensive survey of ciguatera endemic regions of the British and United States Virgin Islands which resulted in the collection of 46 species of dinoflagellates. Sixty-five strains representing 18 of the most conspicuous epiphytic, benthic and planktonic species were isolated and brought into unialgal culture, harvested, and subjected to our standard extraction procedures. We proposed to continue our yearly survey for toxic dinoflagellates.

In the first year of the contract we acquired over thirty two clones of dinoflagellates from Florida Institute of Technology. The acquisition of these clones extended the range of the culture collection outside the Caribbean area. In 1988 we acquired additional clones from Florida and Mexico. At the end of 1989 we acquired the French Polynesian and Australian clones and have been

cultivating them through the acclimation process with a great deal of success. At the end 1990, we acquired approximately fifty more Australian and Fijian clones. These are now in the acclimation process.

The culture collection has been greatly enhanced and instead of covering the Caribbean it is now truly a "World Collection" (perhaps with the exception of representation from the Mediterranean and Africa). The present culture collection is summarized in Table 4 on the next two pages.

TABLE 4.
THE SOUTHERN ILLINOIS UNIVERSITY (SIU) WORLD CULTURE COLLECTION
OF DINOFLAGELLATES.

Species	SIU Strain or Clone Number	Origin
<i>Amphidinium asymmetricum</i>	831	British Columbia, Canada
<i>Amphidinium carterae</i>	239	South Sound, Virgin Gorda
<i>Amphidinium carterae</i>	810	R. R. L. Guillard
<i>Amphidinium elegans</i>	547	Virgin Gorda
<i>Amphidinium sp.</i>	MB005	Florida Keys
<i>Amphidinium klebsii</i>	83, 101, 104, 126, 145	Knight Key, Florida
<i>Amphidinium sp.</i>	54, 59, 60, 61	Knight Key, Florida
<i>Cochlodinium polykrikoides</i>	208, 489	South Sound, Virgin Gorda
<i>Coolia monotis</i>	263	Hurricane Hole, St. John
<i>Coolia monotis</i>	390	South Sound, Virgin Gorda
<i>Coolia monotis</i>	838	Virgin Gorda
<i>Coolia monotis</i>	602	Grosse Caye, Haiti
<i>Coolia monotis</i>	106, 140, 147, 150, 180, 188	Knight Key, Florida
<i>Ensiculifera carinata</i>	415	South Sound, Virgin Gorda
<i>Gambierdiscus toxicus</i>	350, 467, 850	South Sound, Virgin Gorda
<i>Gambierdiscus toxicus</i>	842	Virgin Gorda
<i>Gambierdiscus toxicus</i>	900, 901, 902	Biras Creek, Virgin Gorda
<i>Gambierdiscus toxicus</i>	851, 852	Greater Lameshur Bay, St. John
<i>Gambierdiscus toxicus</i>	853	Little Lameshur Bay, St. John
<i>Gambierdiscus toxicus</i>	619	St. Thomas Lagoon, St. Thomas
<i>Gambierdiscus toxicus</i>	117, 130, 131, 136, 195, 196, 198, 199	Knight Key, Florida
<i>Gambierdiscus toxicus</i>	135, 190, 192	Bermuda
<i>Gambierdiscus toxicus</i>	157, 158, 160, 164, 165, 191	Bahamian Drift Algae
<i>Gambierdiscus toxicus</i>	196	Northeast Rock, Bahama Drift
<i>Gambierdiscus toxicus</i>	172, 173	Great Isaacs Light, Bahamas
<i>Gambierdiscus toxicus</i>	159, 162, 163, 166, 168, 170, 171, 193	Gingerbreads, Bahamas
<i>Gambierdiscus toxicus</i>	175 (MQ-1), 176 (MQ-2)	Martinique
<i>Gambierdiscus toxicus</i>	177 (T-39)	"Hawaiian Strain"
<i>Gambierdiscus toxicus</i>	AA1, A11, A12	Heron Island, Australia
<i>Gambierdiscus toxicus</i>	H120-126	Heron Island, Australia
<i>Gambierdiscus toxicus</i>	F101-116	Fraser Island, Australia
<i>Gambierdiscus toxicus</i>	FP100	French Pacific
<i>Gambierdiscus toxicus</i>	CM1-4	Cousmel, Mexico
<i>Gambierdiscus toxicus</i>	F104-105	Rakiraki, Fiji
<i>Gambierdiscus toxicus</i>	F106-110	Saweni, Fiji

<i>Gambierdiscus toxicus</i>	F111-113	Tubakula, Fiji
<i>Gambierdiscus toxicus</i>	F114-119	Lautoka, Fiji
<i>Gambierdiscus toxicus</i>	F120-126	Suva Bay, Fiji
<i>Gonyaulax grindleyi</i>	403	Hurricane Hole, St. John
<i>Gonyaulax grindleyi</i>	781	Drake's Channel, St. Thomas
<i>Gymnodinium sanguineum</i>	373, 374, 497	South Sound, Virgin Gorda
<i>Gymnodinium</i> sp.	74, 76, 77, 78, 81, 82	Knight Key, Florida
<i>Gyrodinium fissum</i>	376, 379, 474	South Sound, Virgin Gorda
<i>Ostreopsis lenticularis</i>	702	St. Thomas Lagoon, St. Thomas
<i>Ostreopsis lenticularis</i>	841	Virgin Gorda
<i>Ostreopsis lenticularis</i>	870, 871, 872, 873, 875	South Sound, Virgin Gorda
<i>Ostreopsis lenticularis</i>	874	Biras Creek, Virgin Gorda
<i>Ostreopsis lenticularis</i>	876a, 876b	Little Lameshur Bay, St. John
<i>Ostreopsis heptagonia</i>	200, 201, 202, 203, 204, 208, 207, 208, 209, 210, 211, 212, 213, 214, 219	Knight Key, Florida
<i>Prorocentrum concavum</i>	364	Salt Island
<i>Prorocentrum concavum</i>	843	Virgin Gorda
<i>Prorocentrum concavum</i>	881	Anegada
<i>Prorocentrum concavum</i>	862a, 882b	Little Lameshur Bay, St. John
<i>Prorocentrum concavum</i>	883	Greater Lameshur Bay, St. John
<i>Prorocentrum concavum</i>		Heron Island, Australia
<i>Prorocentrum concavum</i>		Fraser Island, Australia
<i>Prorocentrum lima</i>	700	South Sound, Virgin Gorda
<i>Prorocentrum lima</i>	844	Virgin Gorda
<i>Prorocentrum lima</i>	885	Little Lameshur Bay, St. John
<i>Prorocentrum lima</i>	836	Unknown (cold water form)
<i>Prorocentrum lima</i>	62, 105, 142, 178, 185, 186, 187	Knight Key, Florida
<i>Prorocentrum micans</i>	825	British Columbia, Canada
<i>Prorocentrum</i> sp.	MB130, MB134, MB157	Florida Keys
<i>Prorocentrum</i> sp. nov.	MB136	Florida Keys
<i>Prorocentrum mexicanum</i>	262, 273, 276	Salt Island
<i>Prorocentrum mexicanum</i>	722	Hurricane Hole, St. John
<i>Prorocentrum mexicanum</i>	840	Virgin Gorda
<i>Prorocentrum mexicanum</i>	880	Biras Creek, Virgin Gorda
<i>Prorocentrum mexicanum</i>	884	Greater Lameshur Bay, St. John
<i>Prorocentrum mexicanum</i>	69, 84, 86, 181, 182, 183, 184	Knight Key, Florida
<i>Scrippsiella subsalsa</i>	86, 404, 724,	Hurricane Hole, St. John
<i>Scrippsiella subsalsa</i>	344	Biras Creek, Virgin Gorda
<i>Scrippsiella trochoidea</i>	557, 582, 587	South Sound, Virgin Gorda
<i>Symbiodinium microadriaticum</i>	151, 152	Florida Keys

Acclimation & Chemosystematic Studies of *G. toxicus*

Seventeen clones of *G. toxicus* were acclimated in one liter volumes and taken through the 15 liter culture phase (Tables 5 & 6). The clones varied in their acclimation periods ranging from 60 days for clone 175 to nearly a year for other isolates. An example of the acclimation process (clone 157) is shown in Figure 4 and Table 5.

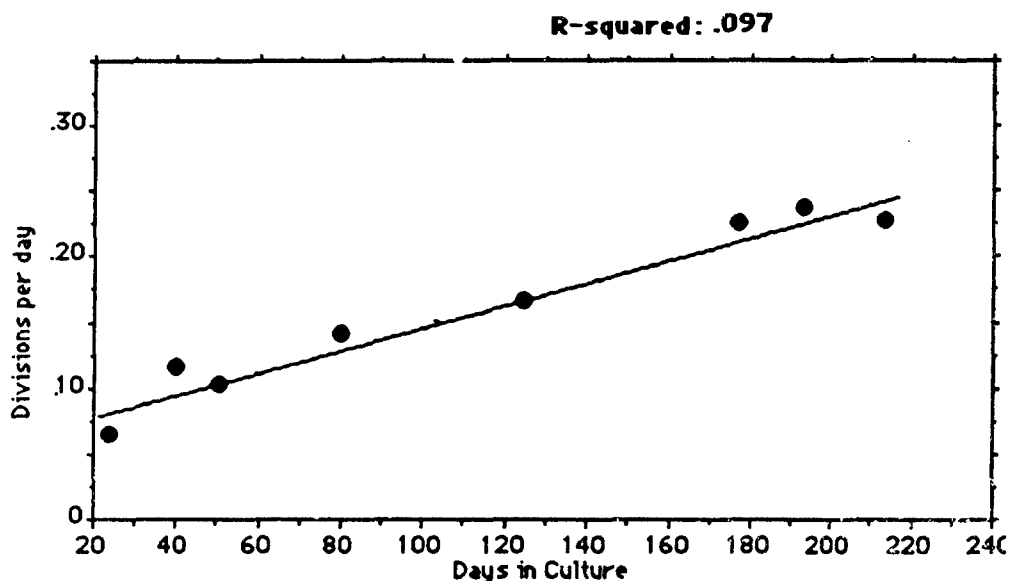


Figure 4. Acclimation of clone 157.

The acclimation process is also important in terms of stabilizing growth rates as is evidenced in Table 7, a two-way ANOVA without replication examining variation in growth rates for 9 clones with similar growth rates through seven culture periods. This ANOVA revealed that the acclimation process was highly significant and indicated that the physiological status of the cultures changes significantly through time.

TABLE 5
ACCLIMATION DATA OF *GAMBIERDISCUS TOXICUS* CLONES IN ONE LITER
VOLUMES
(160 FOOT-CANDLES OF LIGHT)

Clone 175	Interval From:	8/5	9/2	9/18			
	To:	-9/2	-9/30	-10/19			
	Div/Day	.20	.24	.27			
	Yield mg/L	(1)	93	269			
	Yield cells/ml	(1)	2166	3085	COMPLETED		
Clone 350	Interval From:	8/5	9/2	9/28	10/21	11/9	12/3
	To:	-9/2	-10/9	-11/12	-12/7	-12/22	-2/1
	Div/Day	.10	.11	.10	.13	.14	.15
	Yield mg/L	(1)	269	103	184	192	(1)
	Yield cells/ml	(1)	809	1333	989	989	(1)
	COMPLETED						
Clone 135	Interval From:	8/5	9/3	9/25	10/15	11/5	
	To:	-9/4	-10/9	-11/5	-12/3		
	Div/Day	.12	.11	.17	.17	.16	
	Yield mg/L	107	319	259	171	(1)	
	Yield cells/ml	949	2059	1330	2818	(1)	COMPLETED
Clone 135 continued as time control	Interval From:	1/21	2/11	2/25	3/10	3/25	4/11 4/25
	To:	-2/22	-3/7	-3/28	-4/18	-4/25	-4/20 -5.23
	Div/Day	.15	.16	.18	.15	.19	.19 .19
	Yield mg/L	131	164	150	163	105	169
	Yield cells/ml	2022	2439	2628	2249	1870	2249
Clone 177	Interval From:	8/24	9/18	10/20	11/12	12/3	1/21 2/4
	To:	-9/21	-11/5	-12/3	-12/22	-1/5	-2/22 -3/7
	Div/Day	.15	.11	.09	.13	.17	.21 .23
	Yield mg/L	118	184	135	227	(1)	130 135
	Yield cells/ml	800	2275	1128	1059	(1)	857
Clone 177 continued from above	Interval From:	3/14					
	To:	-4/14					
	Div/Day	.18					
	Yield mg/L	(1)					
	Yield cells/ml	(1)	COMPLETED				
Clone 163	Interval From:	8/8	9/2	9/10	10/20	11/9	12/3
	To:	-9/9	-10/7	-9/25	-12/3	-12/22	-1/5
	Div/Day	.17	.12	.12	.18	.14	.14
	Yield mg/L	147	192	207	257	269	(1)
	Yield cells/ml	1040	1166	1655	1912	1014	(1)
	COMPLETED						

TABLE 5. CONTINUED
 Acclimation Data of *Gambierdiscus toxicus* Clones in One Liter
 Volumes
 (160 foot-candles of light)

Clone 158							
Interval From:	8/5	9/2	9/28	10/19	11/12	12/10	1/14
To:	-9/9	-10/9	-11/5	-12/14	-12/22	-2/4	-2/22
Div/Day	.07	.12	.12	.15	.16	.11	.20
Yield mg/L	134	373	191	234	195	141	
Yield cells/ml	1130	1701	1695	2409	1330	1331	
Clone 158 Continued from above							
Interval From:	2/8	2/25	3/17				
To:	-3/7	-3/28	-4/4				
Div/Day	.21	.20	.20				
Yield mg/L	133	175	(1)				
Yield cells/ml	1331	1485	(1)	COMPLETED			
Clone 157							
Interval From:	8/5	9/2	9/28	10/21	11/12	12/7	
To:	-9/9	-10/19	-11/5	-12/3	-12/22	-1/5	
Div/Day	.08	.08	.10	.14	.16	.16	
Yield mg/L	140	268	176	129	189	(1)	
Yield cells/ml	1260	1970	2240	3003	2791	(1)	
COMPLETED							
Clone 199							
Interval From:	8/8	9/4	9/25	10/23	11/17	12/10	
To:	-9/4	-10/19	-11/5	-12/3	-12/22	-1/5	
Div/Day	.12	.12	.12	.16	.15	.15	
Yield mg/L	99	216	117	113	255	(1)	
Yield cells/ml	949	1400	1730	1896	1503	(1)	
COMPLETED							
Clone 169							
Interval From:	8/5	9/4	9/25	10/20	11/12	12/10	
To:	-9/9	-10/7	-11/12	-12/3	-12/22	-1/5	
Div/Day	.11	.10	.10	.12	.13	.12	
Yield mg/L	162	197	195	142	203	(1)	
Yield cells/ml	1000	844	1320	1165	1000	(1)	
COMPLETED							
Clone 196							
Interval From:	1/25	2/11	2/25	3/10			
To:	-2/22	-3/15	-3/28	-3/25			
Div/Day	.19	.20	.23	.23			
Yield mg/L	178	238	206	(1)			
Yield cells/ml				(1)	COMPLETED		
Clone 165							
Interval From:	2/1	2/11	2/25	3/14	3/24		
To:	-2/22	-3/7	-3/18	-4/8	-4/8		
Div/Day	.15	.19	.24	.22	.21		
Yield mg/L	140	101	222	141	(1)		
Yield cells/ml					(1)		

TABLE 5. CONTINUED
 Acclimation Data of *Gambierdiscus toxicus* Clones in One Liter
 Volumes
 (160 foot-candles of light)

Clone GT200					
Interval From:	2/15	3/3	3/17		
To:	-3/15	-4/8	-4/8		
Div/Day	.15	.14	.18		
Yield mg/L	196	114	(1)		
Yield cells/ml			(1)	COMPLETED	
Clone 172					
Interval From:	1/21	2/8	2/25	3/10	3/24
To:	-2/22	-3/7	-3/28	-4/14	-4/15
Div/Day	.13	.17	.21	.22	.22
Yield mg/L	157	153	136	178	(1)
Yield cells/ml					(1)
Clone GT300					
Interval From:	2/8	3/3	3/17	4/4	
To:	-3/15	-3/28	-4/14	-4/20	
Div/Day	.19	.20	.20	.20	
Yield mg/L	122	151	200	(1)	
Yield cells/ml				(1)	COMPLETED
Clone 171					
Interval From:	2/15	3/3	3/17	3/31	
To:	-3/14	-3/28	-4/25	-4/20	
Div/Day	.2	.22	.22	.22	
Yield mg/L	71	122	204	(1)	
Yield cells/ml				(1)	COMPLETED
Clone 170					
Interval From:	2/18	3/3	3/21	4/7	
To:	-3/7	-4/8	-4/25	-4/25	
Div/Day	.17	.17	.17	.17	
Yield mg/L	89	184	186	(1)	
Yield cells/ml				(1)	COMPLETED

Subsequent to completion of the one liter acclimation series the same procedure was followed with cultures in fifteen liter volumes (Table 6). The products of these acclimated larger-volume cultures were utilized to study cellular components in chemosystematic studies.

TABLE 6
Acclimation of *Gambierdiscus toxicus* in 15 liter volumes

ACCLIMATED RATE	YIELD	UPTAKE RATE	TOXICITY		
Div/Day		NH ₄	NO ₃	Initial	Final
MU/mg	cells/ml	pg/cell/hr	pg/cell/hr	MU/mg	MU/mg
Clone 175 Axenic Culture, Caribbean					
ip					
Clone 175-1 Subclone (not Axenic) Caribbean					
.26	2,618				112.29
Clone 175-2 Subclone (not Axenic) Caribbean					
.25	2,700				110.41
Clone 175-3 Subclone (not Axenic) Caribbean					
.27	2,700				128.69
Clone 175-4 Subclone (not Axenic) Caribbean					
.25	2,618				127.64
Clone 175 (Standard) Caribbean					
.27	2,760	18.8	35.56	55.06	120
Clone 350 Caribbean					
.16	1,095	7.3	63.4	6.90	18
Clone 135 Bermuda					
.17	1,190	9.3	50.74	3.72	5.39
Clone 177 Hawaii					
.21	1,250	10.0	42.1	4.6	30
Clone 199 Florida Keys					
.17	1,109	6.9	60.38	4.22	17.5
Clone 300 Florida Keys					
.20	1,200	8.0	47		7.3
Clone 200 Florida Keys					
.18	723				3.88
Clone 196 Florida Keys					
.23	1,108	9.2	41.6		4.0
Clone 163 Bahamas Gingerbread					
.14	860	13.5	31.46	4.52	9.85
Clone 171 Bahamas Gingerbread					
.22	2,208	5.1	27.4		3.0
Clone 170 Bahamas Gingerbread					
.17	800	12.8	32.4		5.1
Clone 157 Bahamas Drift Clones					
.25	1,890	19.3	16.43		2.07
Clone 158 Bahamas Drift Clones					
.20	848	12.7	22.7		5.60
Clone 165 Bahamas Drift Clones					
.21	2,100	6.0	33.9		12.79
Clone 169 Bahamas Drift Clones					
.14	660	6.5	39.3	4.09	4.40
Clone 172 Bahamas Great Isaacs					
.22	2443	7.8	71.7		2.2

TABLE 7.
Two-way ANOVA without replication examining variation in
growth rates for 9 clones with similar growth rates through 7
culture periods.

Source of Variation	df	SS	MS	Fs
Among clones	7	0.010	0.00143	2.38
Among culture periods	6	0.0390	0.00650	10.83
Error	42	0.025	0.00060	
	55			

= P < 0.01

An additional ANOVA examining variation in reproduction rates between acclimated and non-acclimated cells (Table 8) also indicates that the variation is significant ($P < 0.01$).

TABLE 8.
PAIRED ANALYSIS OF VARIANCE EXAMINING VARIATION
BETWEEN NON-ACCLIMATED AND ACCLIMATED REPRODUCTION RATES.

Source of Variation	Degrees of freedom	Sum of squares	Mean squares	F value ^a
Culture stage	1	0.6241		1365.3
Clones	14	0.0025714		5.6
Remainder	14	0.0004571		
Total	29			

^a Significant at 0.01 level.

There was also significant variation among clones detected in this test. The mean reproduction rate for the non-acclimated cultures was 0.138 and 0.195 for acclimated cultures. Cell yields also improved from 115 mg L⁻¹ to 183 mg L⁻¹. The variation between cell yields in the non-acclimated vs. acclimated condition was also significant ($P < 0.01$, Table 9).

TABLE 9.
PAIRED ANALYSIS OF VARIANCE EXAMINING
VARIATION BETWEEN NON-ACCLIMATED AND ACCLIMATED CELL YIELDS.

Source of Variation	Degrees of freedom	Sum of squares	Mean squares	F value ^a
Culture stage	1	38964.73	38964.73	19.8194
Clones	16	22,563.53	1410.22	0.7173
Remainder	16	31455.77	1965.99	
Total	33			

^a Significant at 0.01 level.

Mean cell potencies also improved along with reproduction rates and cell yields through the acclimation process. The number of days in culture and the potency were positively correlated ($P < 0.60$, Figure 5) for clones 177, 135 and 350.

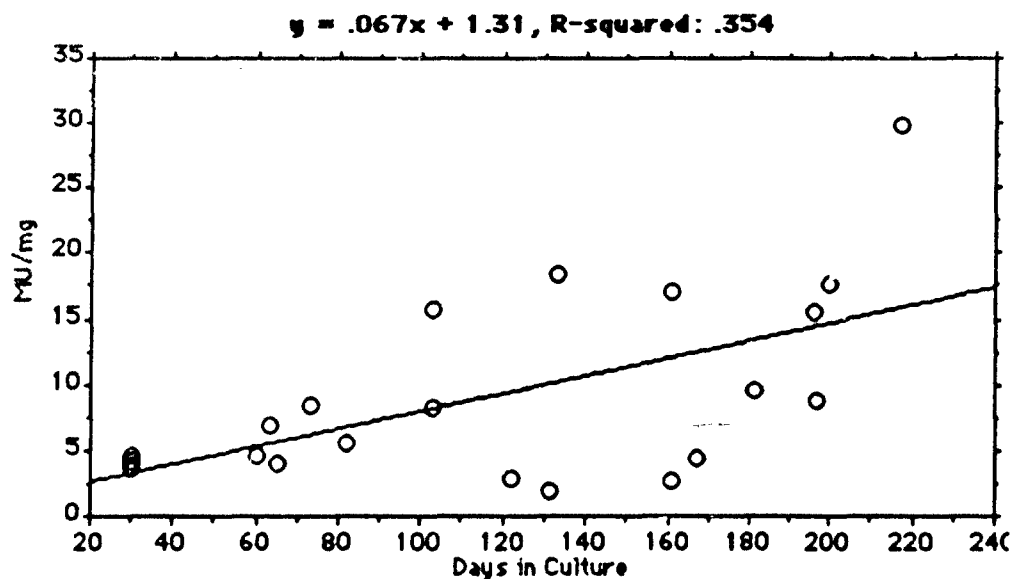


Figure 5. Potency (MU mg^{-1}) vs. days in culture for clones 177, 350, 135, 199, 169 and 163.

Table 10 gives data comparing non-acclimated to acclimated potencies for six clones. The initial mean cell potency for clones 175,

350, 177, 199, 169, 163 and 135 was 13.01 MU mg⁻¹ compared to the acclimated value for these clones of 25.95 MU mg⁻¹.

A paired ANOVA examining variation between non-acclimated and acclimated cell potencies indicates that there are significant differences between the phases (Table 11).

TABLE 10.
EXTRACT POTENCY DIFFERENCES IN THE NON ACCLIMATED VS.
ACCLIMATED PHYSIOLOGICAL STATE.

CLONE	INITIAL POTENCY (MU/mg)	ACCLIMATED POTENCY (MU/mg)
175	55.06	102.25
350	6.90	18.33
135	3.72	5.55
19	3.92	15.30
163	4.52	9.85
169	4.09	4.40
Mean	13.04	25.95

TABLE 11
Paired Analysis of Variance examining
variation between non-acclimated and acclimated cell potencies.

Source of Variation	Degrees of freedom	Sum of squares	Mean squares	F value ^a
Culture stage	1	886.11	886.11	7.48
Clones	6	8230.32	1371.72	11.57
Remainder	6	711.16	118.53	
Total	13			

^a Significant at 0.01 level.

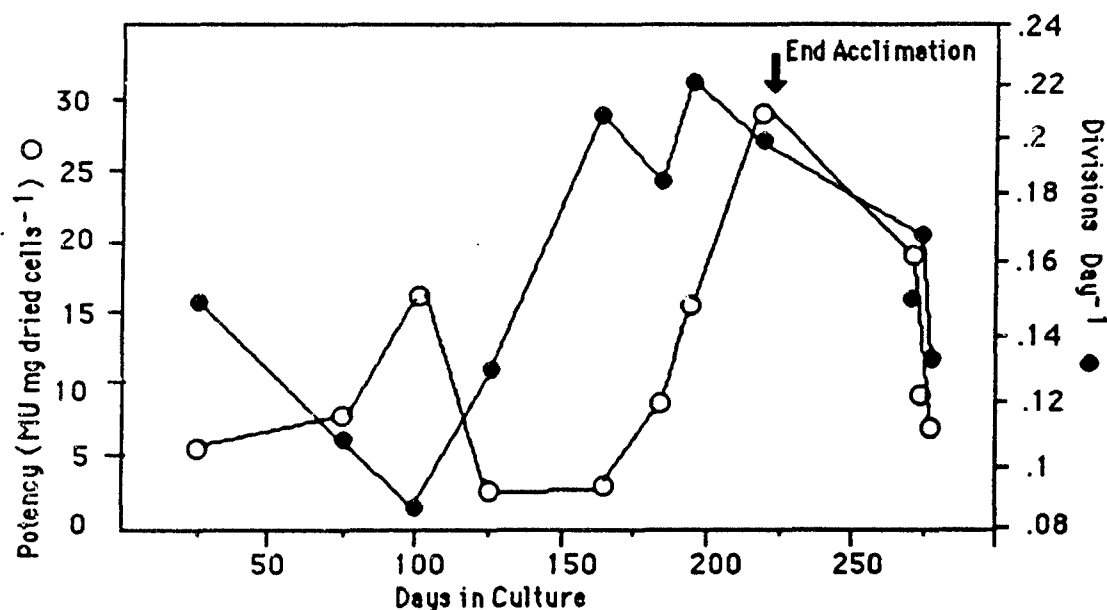


Figure 6. Potency (MU mg^{-1}) and reproduction rate (Div. day^{-1}) vs. number of days in culture for clone 177. The arrow denotes the end of the acclimation process. Three potency determinations are shown with their 95% comparison intervals generated by the T-method. Intervals which do not overlap are significantly different.

An examination of the acclimation process in more detail for clone 177 indicates that potency shows a slow improvement with time (Figure 6). The potency appears to be sensitive to environmental changes and the acclimated cell potency could easily be lost as was shown in Figure 6 when successive transferring begin in stationary instead of log phase. The potency appears to follow reproduction rate closely but improvements in the potency lag behind those in growth rate. The variation among potencies over time for clone 177 was significantly different ($P < 0.0001$, Table 12) and the means are compared by the T-method (Figure 7). The T-method indicates that the potencies calculated at less than 200 days are significantly different from the one calculated at greater than 200 days.

TABLE 12.
One-way Analysis of Variance with replication examining
variation among potencies on three occasions during acclimation
for clone 177.

Source of Variation	Degrees of freedom	Sum of squares	Mean squares	F value ^a
Among culture stages	2	1129.612	564.806	31.562
Within stages	9	161.055	17.895	
Total	11	1290.667		

^a Significant at 0.0001 level.

Figure 7 shows the potency changes for clone 350 which indicates that the acclimated potency was lost when the clone was transferred to a new light environment. We did not monitor the potency past 140 days in the acclimated state for this clone. However, we did continue to monitor reproduction rate and this did not improve past 140 days.

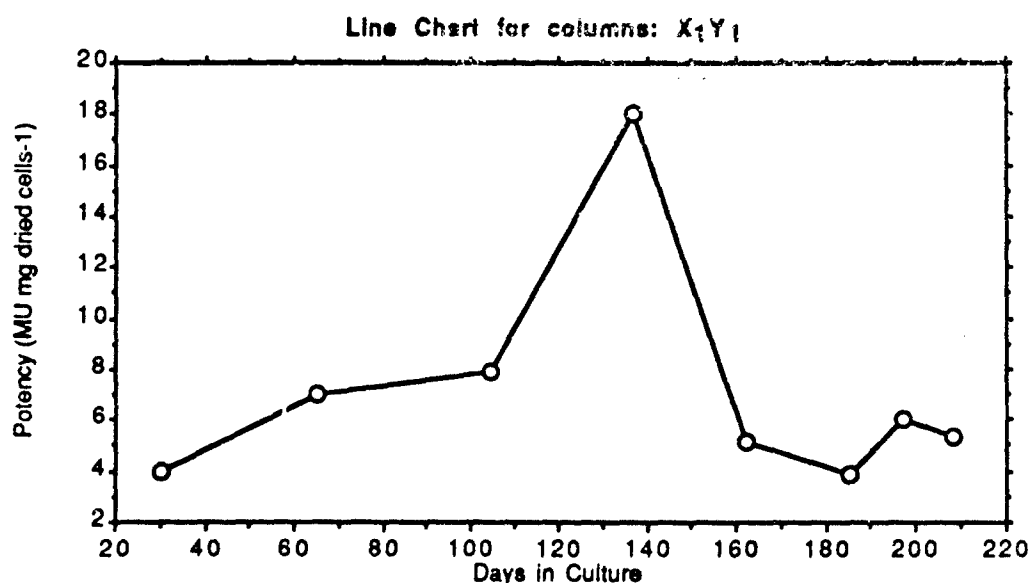


Figure 7. Potency (MU mg-1 dried cells) vs. number of days in culture for clone 350. The first four potencies were determined under Vita-lite bulbs and the last four under cool-white bulbs.

Discussion of the acclimation studies. A summary of the data compiled on the seventeen clones examined is given in Table 13. A one-way ANOVA with replication examining variation in potencies among six clones indicates that the variation in cell potencies is significant (Table 15). An a-posteriori T-method (Figure 8) indicates that two clones collected from Marathon Key (199 and 200) are significantly different from one another. In addition there are larger differences among clones collected from different areas (Figure 8).

TABLE 13.
Summary of results for the different clones in the genetic study.

Clone MU ⁻¹	Cells mL ⁻¹	Mg L ⁻¹	Div. day ⁻¹	MU Mg ⁻¹	MU Cell ⁻¹	Cells
<u>Caribbean</u>						
175	2659	122	0.26	120	55	183
350	781	116	0.16	18	27	368
<u>Hawaii</u>						
177	1488	134	0.21	30	27	372
<u>Florida Keys</u>						
196	1317	254	0.23	4.1	8.0	1263
199	2158	205	0.16	17.5	16.7	601
200	762	116	0.14	2.6	3.9	2537
300	811	200	0.20	7.3	18.0	555
<u>Bahamas</u>						
162	1300	109	0.13	5.5	4.6	2170
163	938	212	0.15	8.8	19.8	504
170	556	187	0.14	5.1	19.2	522
171	430	79	0.19	3.0	5.5	1804
172	1019	178	0.22	2.2	3.8	2605
<u>Drift Algae</u>						
157	2369	148	0.14	2.9	1.8	5512
158	1485	175	0.20	5.6	6.6	1511
165	1301	176	0.22	12.8	17.3	577
169	860	203	0.11	4.4	10.4	963
<u>Bermuda</u>						
135	2249	109	0.19	11.1	5.4	1861

There is a general trend of decreasing potency among the clones with increasing latitude (Figure 8). Latitude and the acclimated potencies are negatively correlated ($r = -0.819$, $P < 0.01$).

TABLE 14
One-way Analysis of Variance with replication examining variation among the acclimated potencies of clones 175, 177, 199, 200, 157, 163 and 135.

Source of Variation	Degrees of freedom	Sum of squares	Mean squares	F value ^a
Among clones	6	43.703	7.284	123.182
Within stages	21	1.242	0.059	
Total	27	44.945		

^a Significant at 0.0001 level.

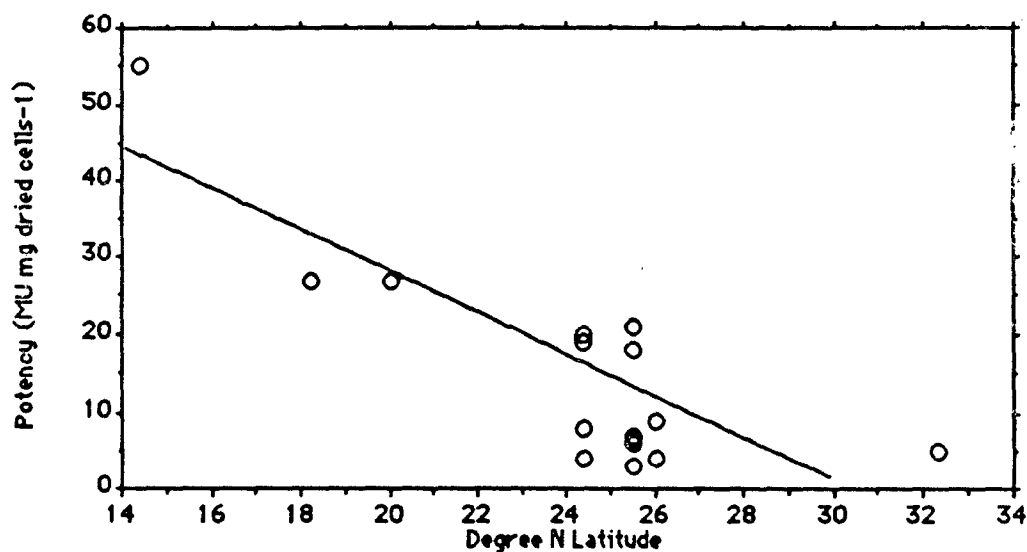


Figure 8. Potency (MU cell^{-1}) vs. latitude for all clones examined in the genetic study. Seven clones are shown with their 95% comparison intervals generated by the T-method and based upon the ANOVA in Table 14. Intervals which do not overlap are significantly different.

TABLE 15.
Sub-clone variability of clone 175.

Sub-clone	Div. day^{-1}	Final cell Yield (cells/ml-1)	MU/mg ⁻¹
8	0.27	2,700	128.69
13	0.26	2,618	112.29
16	0.25	2,600	127.64

22	0.25	2,710	110.41
Mean	0.26	2,657	119.73
Stan. dev.	0.01	56	9.74
coeff. of variation	4.09%	2.24%	8.64%

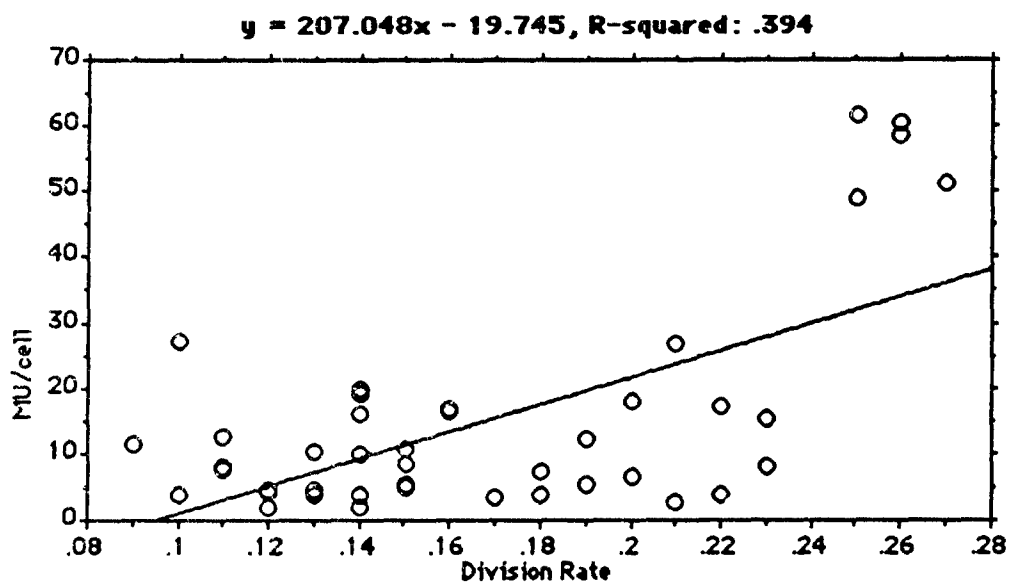


Figure 9. Potency (MU cell^{-1}) vs. reproduction rate (Div. day^{-1}) for all clones examined in the genetic study.

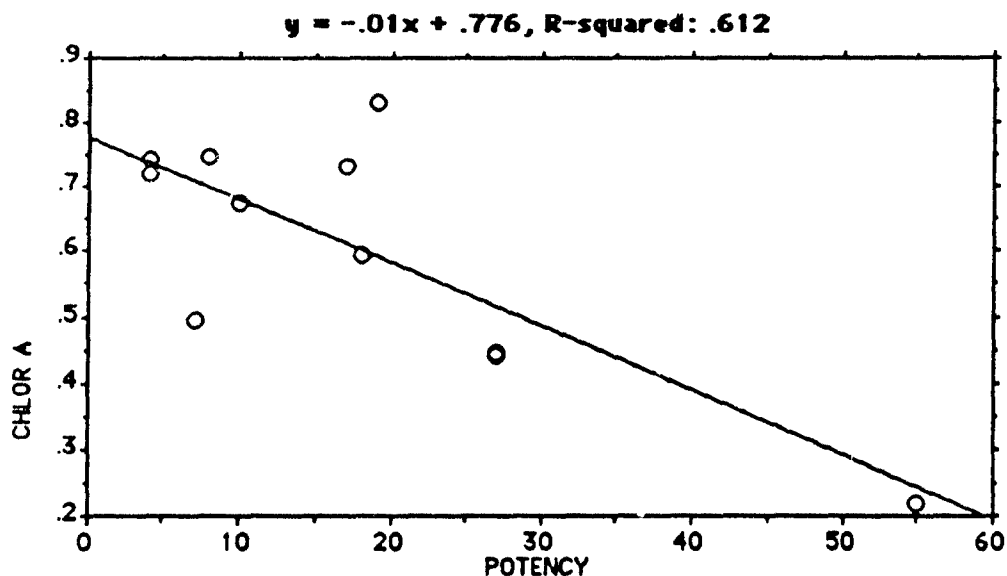


Figure 10. Potency (MU cell^{-1}) vs. chlorophyll a concentration (pg cell^{-1}) of twelve clones.

Reproduction rates vs. acclimated cell potencies for all clones examined were positively correlated (Figure 9, $r = 0.628$, $P < 0.01$). However, the correlation between cell size and potency was not significant. There were negative correlations between acclimated clonal potencies and acclimated pigment content, chlorophyll a (Figure 10, $r = -0.782$, $P < 0.01$) and chlorophyll- c_2 ($r = -0.713$, $P < 0.01$, Figure 11). There was no significant relationship between peridinin content and potency.

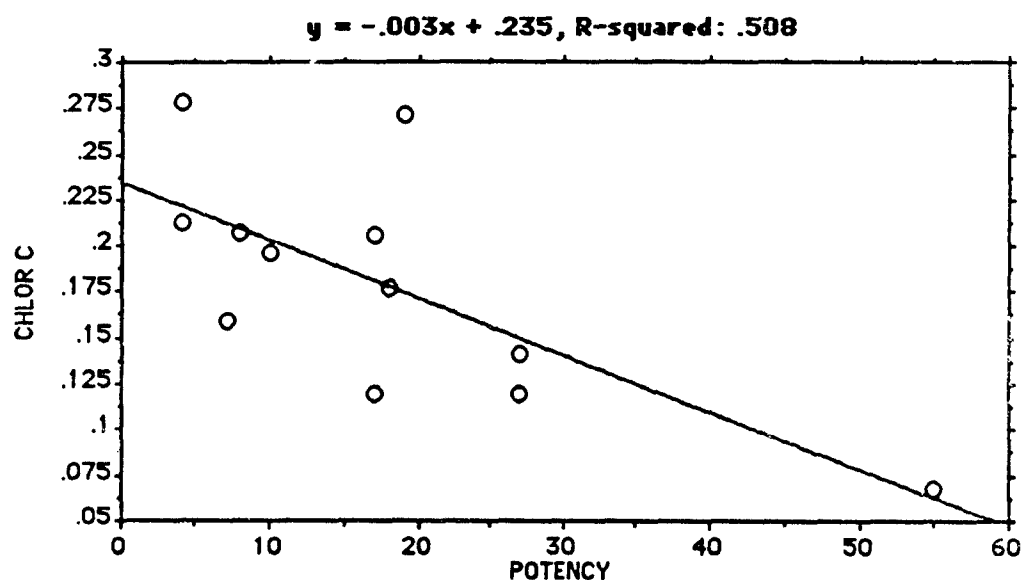


Figure 11. Potency (MU cell^{-1}) vs. chlorophyll- c_2 concentration (pg cell^{-1}) of twelve clones.

Response of *G. toxicus* Clones to Different Light Intensities

Clones have been grown at four light intensities: 40, 80, 160 and 250 footcandles illumination. The toxicity of these clones is currently being compared. In terms of growth rate the clones show significant differences in their light/growth response (Figure 12). These results were generated from tube cultures. In a more detailed examination of the light/growth response for clone 175, there are obvious differences among light intensities (Table 16).

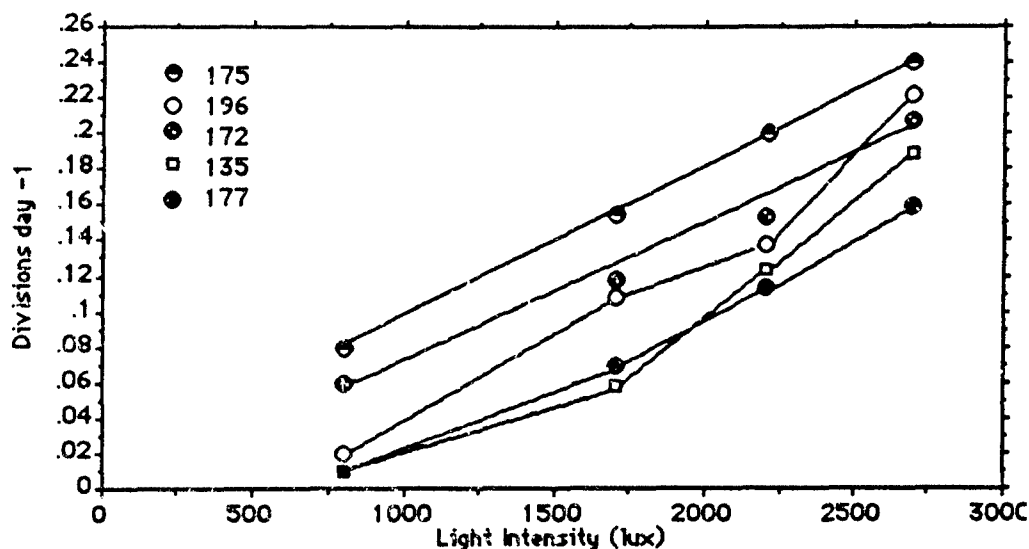


Figure 12. Reproduction rates at four light intensities for five of the clones examined in the acclimated reproduction rate study.

TABLE 16.
GROWTH PATTERNS OF CLONE 175 AT 28°C AND AT FIVE DIFFERENT
LIGHT INTENSITIES IN APPROXIMATELY ONE LITER CULTURES.

Culture Number	Light Intensity lux	Interval	Reproduction Rate	Cells per ml	Number of cells per mg	Total yield in mg (x 10 ⁴)
20	3350	8/29-9/8	0.23	1096	1.12	87
26	3350		0.28	1178	1.65	70
37	1999	9/22-10/4	0.18	1013	1.26	76
38	1999	9/19-10/4	0.18	931	1.56	55
24	1081	8/18-9/8	0.14	1301	2.06	58
36	1081	9/6-10/4	0.13	1178	2.13	47
16	648	7/25-8/22	0.10	1301	2.88	33
32	648	8/22-9/30	0.07	808	0.61	112
33	378	8/5-10/4	0.02	520	0.94	49
34	378	8/5-10/4	0.02	602	0.52	107

These cultures were subsequently extracted and analyzed (Table 17) for composition of proteins, lipids, and carbohydrates. The data for the pigment composition, appears in Table 18. The samples for toxicity comparisons are weighed and await the availability of mice for bioassay in our program. One of the major problems that we

encountered in the experiment was that the cultures in the lowest light intensity (378 lux) would not produce cell numbers above 700 cells/ml in a reasonable time period (< 2 months). In order to avoid cellular degradation by bacteria we harvested these cultures at lower densities.

TABLE 17.
Biochemical composition of clone 175 at five different light intensities.

Culture Number	Light Intensity	Protein (pg per cell) lux	Carbohydrates (pg per cell)	Lipid (pg per cell)
20	3350	364	--	818
26	3350	667	156	--
38	1999	324	--	1,324
37	1999	400	101	--
36	1081	123	--	470
24	1081	189	463	--
32	648	30	--	269
16	648	307	460	--
34	378	371	--	477
33	378	307	460	--

Thus to an extent, it is difficult to compare data from these cultures directly with data from the others. Consequently, instead of using cell numbers we have used growth pattern as our criterion for determining the point of harvest. Thus, all cultures have been harvested in what we determined to be mid log phase based on linear growth/time plots. By this method we insure that although cell numbers and external nutrient conditions may vary at the point of harvest, the relative kinetics of growth are the same and differ only in their magnitude. Also, keep in mind, that the cells at 378 lux are teratogenous and may have leaked cellular components. Therefore, they may not be truly representative of the average cellular condition when grown at low light intensities.

Pigmentation also varies with light intensity. More pigment is produced per cell at higher light intensities (Table 18 & 19). This is

to be expected in that more light is available for harvesting and consequently more pigment can be produced. However, the chlorophyll to carotenoid ratio (Table 19) decreased at both the lowest and highest light intensity.

TABLE 18.

Pigment composition at the five different light intensities at 28°C.
All values are in picograms per cell.

Pigment	Light Intensity (lux)				
	3350	1999	1081	648 ¹	378 ¹
Chlorophyll a	336	204	105	33	2
chlorophyll-c ₂	97	12	15	5	--
Peridinin	395	204	62	22	--
xanthophyll 1	91	26	14	11	--
xanthophyll 2	106	32	17	13	--
β-Carotene	26	8	1	--	--

¹The dashed lines indicate the quantity was too low to be quantified accurately (< 1 picogram per cell).

TABLE 19.

TOTAL CHLOROPHYLLS AND CAROTENOIDS PER CELL, RATIOS OF TOTAL CHLOROPHYLLS TO CAROTENOIDS AND TOTAL LIPID TO TOTAL PROTEIN OF THE CULTURES GROWN AT 5 LIGHT INTENSITIES. VALUES GIVEN AS THE TOTALS ARE IN PICOGRAMS PER CELL.

Parameter	Light Intensity (lux)				
	3350	1999	1081	648	378 ¹
Total Chlorophylls	433	216	120	38	2
Total Carotenoids	618	270	94	46	--
Chlor./Carot. Ratio	0.70	0.80	1.28	0.83	--
Lipid/Protein Ratio	2.24	4.09	3.82	8.97	1.29

¹The dashed lines indicate the quantity was too low to be quantified accurately (< 1 picogram per cell).

The plot of the macromolecular data (Figure 13) indicates that the cell weight decreases with increasing light intensity, with the most cells per mg dry weight occurring at 1999 lux. This is to be expected, with a more favorable environment microalgae tend to partition

photosynthates into a larger population.^[87] The protein per cell follows closely with the cell weight plot. This is also to be expected given that more efficient conversion of photosynthate into more offspring requires high enzymatic efficiency. We believe that the increase in protein with increasing light intensity reflects the increase in intracellular enzymes. Conversely, microalgae tend to produce more lipid and carbohydrates per cell than protein in unfavorable environments.^[88-90] This is thought to be due to the cells preparing storage products for probable dormancy (e.g., encystment) periods.^[91] The increase in lipid and carbohydrate at low light intensities reflects this trend. These data could imply that we should expect more "lipid soluble" toxins (e.g., "ciguatoxin") to occur at lower light intensities. The data so far indicate that we might expect different partitioning of the toxin components with respect to light intensity.

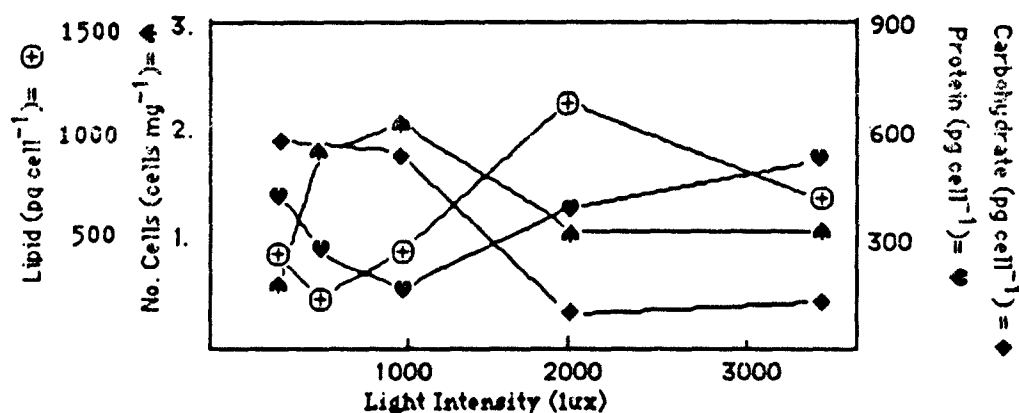


Figure 13. Plot of the biochemical composition (proteins, lipids carbohydrates) and number of cells/mg dry weight of cultures of *Gambierdiscus toxicus* grown at 5 different light intensities. TM=mean of 2; f= 1 est; ⊕=mean of 2.

This implies that at the high light intensity used (3350 lux) saturation is occurring. Saturation is always suspect when more accessory pigments are made per cell relative to chlorophyll^[92] as the accessory pigments (or other photosynthetic modulators) are produced to protect chlorophyll against photooxidation. However,

general lipid metabolism and pigment metabolism do not necessarily coincide. The lipid to protein ratio at 3350 lux is 2.24 where the pigment per cell is highest. Lipid relative to protein is higher at 648 lux (8.97 ratio). Consequently, we may be able to tell from the toxicity data whether toxin synthesis is linked with pigment production or if it is instead linked with general lipid production.

Figure 14 shows an example thin layer chromatogram of the pigments from clone 175. We achieved excellent separation of these pigments which allowed for their identification via scanning spectrophotometry.








Band No.		Rf	λ_{max} Abs	Pigment
7		.92	479.0	β carotene
6		.75	402.6	Chlorophyll a
5		.66	402.6	Chlorophyll a
4		.51	422.3	2 xanthins
3		.30	452.2	peredinin
2		.18	427.6	chlorophyll c ₂
		0	472	chlorophyll-protein

Figure 14. TLC pigment separation of acetone extract of clone 175 of *Gambierdiscus toxicus*. Solvent system was acetone:hexane (50:50).

In Figure 14 is that the non-reversible toxin (MTX-like) occurs only in one band (#1). This band contained several major contaminants in addition to the toxin. Further analysis indicated that all the bands consisted of multiple components.

Discussion of Acclimation & Chemosystematic Studies The acclimation period for the clones studied took from 60 days to one year. During the acclimation period the growth rates changed from and average of 0.195 to and average of 0.138. Cell yields improved from 115 to 183 mg/L. In addition the apparent cell potency increased. Maintenance of the acclimated state is dependent upon a constant environment and transfer of cells in log phase of growth. There is ample evidence that the acclimation process is essential to comparisons of reproduction rates, cell yields and potencies for *G. toxicus*. These results have serious implications for past studies in this area which based results on material acclimated for short time periods. Even broad, relative comparisons made without a genetic basis in mind must be made in the acclimated condition. For example, had clone 177 been compared at its initial potency (5.4×10^{-4} MU cell⁻¹) it would have been grouped along with clones from the Bahamas, the Florida Keys and Bermuda. In fact, it has a much higher potency of 26.9×10^{-4} MU cell⁻¹, when completely acclimated.

The continuous batch culture method of Brand et al.^[72] with concomitant monitoring of reproduction rates appears to be an excellent method of measuring the total fitness of clones of *Gambierdiscus*. For example, the cell potencies and cell yields improved along with reproduction rates. The pattern of changes in reproduction rates and potencies was particularly striking when the data for clone 177 was compared over time. Despite the lag time between reproduction rate increases and potency increases, the two characters appear to be closely associated.

We believe that we eliminated environmental and developmental processes from genetic differences by comparing clones only in the acclimated cell condition. The results corroborate previous results closely. For example, Babinchak et al.^[93] found a value of 250 cells MU⁻¹ for acclimated cultures of clone 175. whereas we calculate an acclimated cell potency for 175 of 183 cells MU⁻¹. The relative differences among clones are clear and highly significant by statistical analyses. In addition, sub-clone variability^[94] does not

appear to be a problem for *G. toxicus*. Durand^[95, 96] also did not find sub-clone potency variability in *G. toxicus* to be significant. Consequently, we conclude that the differences in cell potencies are perhaps genetic in origin.

Laurie-Ahlberg et al.^[97] and Salzman^[98] point out that quantitative characters can be used genetically. Simple analysis of variance have been successfully used with phytoplankton.^[72,99] However, the cell potency differences for a clone of *G. toxicus* in the two phases, acclimated vs. non-acclimated, can be greater than the genetic differences between clones and this stresses the need for a rigorous acclimation process. We were able to investigate environment-genotype interaction by terminating the transferring of clone 177 in log phase and by placing clone 350 back into the cool white lite environment. In both cases the acclimated cell potency was lost. These results suggest that the environment does influence the cell potency in the same way it affects total fitness, i.e. reproduction rates, which also decrease initially when the environment is changed.

Alternatively, there may not be genetic differences in the amounts of toxin produced, rather, there may be quantitative differences in the enzymes necessary for deactivation of the toxins. Previous work^[82,95,96] suggests that *G. toxicus* produces toxins for allelopathic use. If this is true, than *G. toxicus* could have the deactivation enzymes typical of other unicellular organisms that produce bioactive ectocrines.^[100] This would prevent *G. toxicus* from being auto-inhibited. However, this too is unlikely as we would expect the clone with the lowest production of deactivation enzymes to have the slowest growth rate and in fact the opposite is true (clone 175, most toxic, fastest growing).

Most MTX extracts produced identical symptomology in the mice used in the bioassay indicating that we have compared differences among clones in the same toxin. However, clone 135 from Bermuda was an exception in that mice inoculated with material from this clone consistently underwent lumbar contractions. Lumbar

contractions have heretofore not been reported for extracts from *G. toxicus*. Consequently, we realize that this matter will need to someday be resolved at the molecular level as it is possible that different forms of maitotoxin will be found much like were derivatives of saxitoxin. Regardless, this does not exclude the use of the cell potency as a chemosystematic tool. The potency differences either reflect the amount or composition of toxins, both of which appear to be inheritable traits that can be compared once the environmental and developmental processes have been removed.

The potency apparently has a fundamental role in the fitness of the genotype and this is supported by two related pieces of evidence. First, the potency begins increasing in early log phase, implying a direct relationship to primary metabolism. Secondly, the maximum cell potency also improves over time along with increased reproduction rate. This suggests possible pleiotropic interactions among potency and other systems related to the reproduction rate.

It is interesting to speculate upon what metabolic events are occurring in the clones as they slowly adapt to the new environment. Meeson and Faust^[101] speculate that as another dinoflagellate, *Prorocentrum minimum*, adapted to new light quality environments, it may have increased its efficiency in converting photosynthetic products into new cells. The apparent increased efficiency in growth rate was correlated with increasing potency in *G. toxicus* and may reflect a similar trend, with the clones differing in the ability to convert and partition the products, some of which may be toxins. The correlation between increasing growth rate and potency and the pattern of toxin production, coupled with the apparent effect of light bulb type on potency, all strongly suggest that the process of photosynthesis and toxin production are linked. The selective forces modifying photosynthetic response may also effect the potency from South Latitude to North Latitude. Light intensity could be the major selective force leading to the formation of new genotypes, with clone 175 being the most fit for higher light intensities.

We have conducted studies with light to address this hypothesis further. Apparently potency and the gross amount of chlorophylls a and c_2 per cell are negatively correlated. Because clone 175 had the lowest level of chlorophylls per cell, but the highest amount of toxin per cell, studies with light and potency could yield exciting information in determining what metabolic role maitotoxin has in *G. toxicus*. Clone 175 is small and perhaps the small size may account for the reduced amount of pigments. All evidence to date supports the contention that maitotoxin has a role in photosynthesis, including our recent work with chromatography which pinpoints most of the toxic activity from *G. toxicus* into areas closely associated with chlorophyll.

When comparing the potencies with latitude, we found a general decrease in potency with increasing latitude. This is strikingly reminiscent of results found for the potency of *Protogonyaulax* over a latitudinal gradient,^[102] except that in their case potency increased with increasing latitude. We realize that more clones need to be examined to investigate this pattern completely and within site variation first needs to be more thoroughly analyzed. In this study, there was a high level of variation within a collection site (4 to 10x) and as evidenced by the T-method analysis but this was not as large as that between sites (up to 30x). This within site variation was highest (10x) for clones from drift algae.^[72] Watson and Loeblich^[103] and Hayhome, et al.,^[104] also found that there could be genetic variation within a site, but far greater variation existed with increasing geographic distance between two source populations. Nevertheless, appreciable supporting evidence was found when a clone from a different Ocean, Hawaiian clone 177, fit into the latitudinal cline where it would be expected to fall based on its acclimated potency.

The variation among drift algae clones could be analogous to that found in the Gulf of Maine for *Prorocentrum micans* by Brand.^[105,106] In this region the genetic diversity was high, whereas over Georges Bank the variability was low. This was

thought to reflect the relative "stability" of the environments which regulated the mode of reproduction with asexual reproduction being characteristic of the nutrient rich Georges Bank area and sexual reproduction characterizing the Gulf of Maine. We suggest that the drift algal habitat is similar to the Gulf of Maine and sexual reproduction will predominate owing to the poor nutrient levels generally associated with surface waters.

It should be pointed out that there are bound to be exceptions in this overall model. Tosteson et al.^[107] found that a clone of *G. toxicus* from Puerto Rico was not toxic. Considering the influence of drift algal communities on genetic variation within a site and the possible presence of non-acclimated populations, such results are to be expected. The results of the character survey in this study indicate that *G. toxicus* is genetically polymorphic for certain characters. Additional work using clustering procedures indicated that clones from the same patch of drift algae can have the same level of genetic difference as clones from the Florida Keys and Hawaii. These latitudinal patterns suggest that some percent of the polymorphism of certain characters results from selection, the selective forces probably being light and/or temperature in accordance with the potency differences over the latitudinal gradient.

It could be argued that this study suffered in that potency was only examined in one light environment. Brand^[106] and Lewontin^[108] argue convincingly that a character should be examined in more than one environment. As we understand it, this is generally required to allow full expression of the genome regulating the quality or quantity of the character under examination. Because of the large expense and the current dependence on animal bioassay needed to conduct a study such as this, we decided to conclude the study based on the results from one environment. Consequently, we may not be visualizing all possible differences. Nevertheless we believe that we obtained maximum expression of the toxin potency regulating genes in this environment

and detected several races of *G. toxicus*, but again, we cannot argue that all possible races were detected.

When all of the character data are examined by principal components analysis what is interesting are in fact not the differences among clones but the similarities. There may of course be underlying differences in the multiple genes affecting the characters assayed, as each mutation would be of relative small effect. We cannot be sure that the characters assayed arise from isozymes which have different electrophoretic mobilities, although overall the clones examined appear to be closely related. However, it was not the intent of this study to detect such differences and this is left for later work. Still, based upon the overall similarities we conclude that this work resembles what was found by Brand et al^[105] who concluded that clones of *Thalassiosira pseudonana* isolated from different neritic areas of the world were genetically similar. He concluded that this was due to these populations experiencing similar selective forces by living in a similar environment. This could also be the case for *Gambierdiscus* as all of the clones that we examined were isolated from highly similar environments although they arise from areas thousands of miles apart.

This work represents the first exhaustive study dealing with the character analysis of *G. toxicus*. We approached the question of variation by anticipating a large number of phenotypic differences. In short, we assessed the character variation in this species much like a taxonomist explores phenotypic differences among congeneric species.

Maximizing Toxin Production in *G. toxicus*.

Cultures were grown at five light intensities at 28°C, at six light intensities at 25°C, and limited growth occurred at 22°C. We initiated two new light intensities at 25°C (3782 and 4800 lux) because growth did still not appear to be light-saturated at 28°C at 3350 lux (Figure 15). The 3782 lux light intensity also failed to foster

complete saturation. Thus, an even brighter light intensity was used when we moved to 22°C, but cultures only continued at maintenance levels at this temperature. This light/growth pattern is unusual for *G. toxicus* as most clones of this species cannot grow beyond 3,000 lux. Growth could not be sustained at 22°C at the two lowest or two highest light intensities used. We conclude that clone 175 is more light tolerant and less temperature tolerant than other clones of *G. toxicus* based on comparisons to clones used in previous work.^[109]

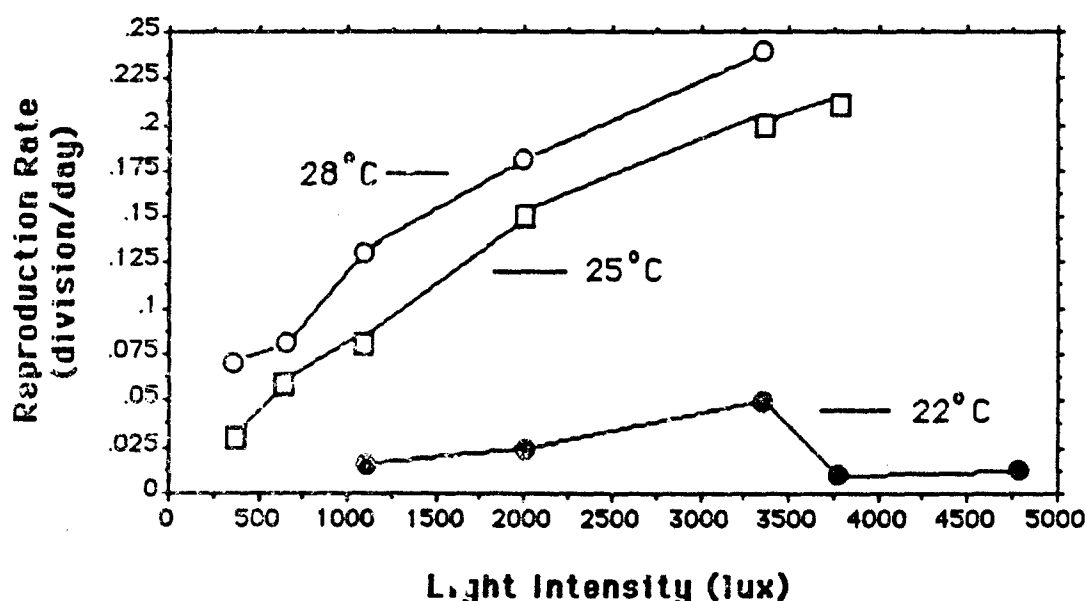


Figure 15. Reproduction rate (divisions/day) of clone 175 vs. light intensity. The pattern is shown for growth at 22, 25 and 28°C.

All cultures grown at 25 and 28°C were extracted and analyzed for protein content in duplicate (Figure 16). Protein content, like most of the other molecular components examined, appears to follow a "normal" or bell-shaped distribution over the range of light intensities used (Figure 16).

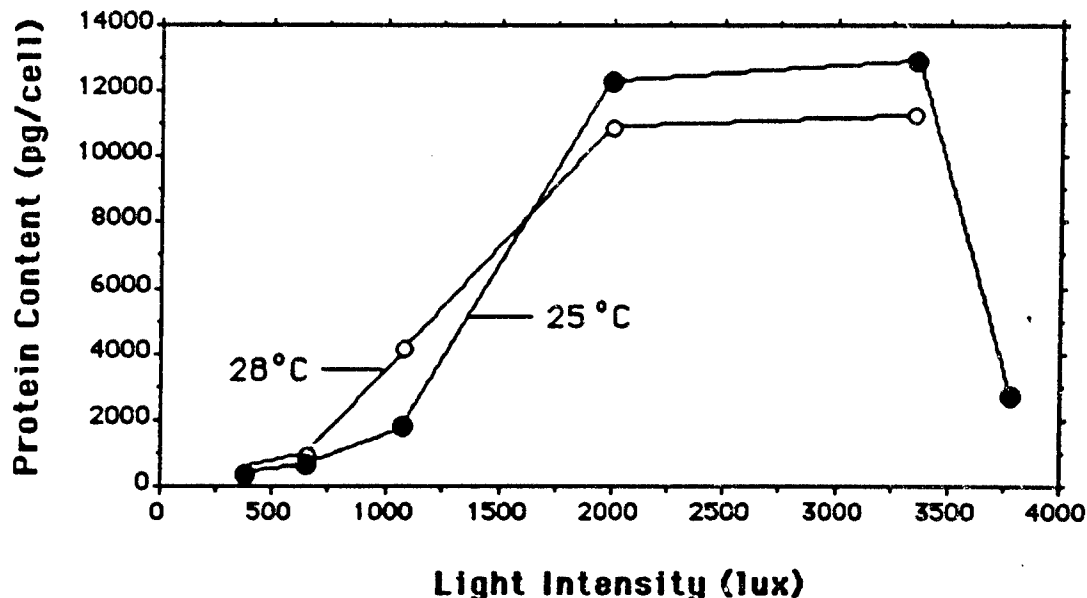


Figure 16. Protein content (pg/cell) of clone 175 vs light intensity. The pattern is shown for growth at 25 and 28°C.

Carbohydrate contents from 28°C are given in Figure 18. Lipid content has also been examined at 28°C (Figure 17). Carbohydrate production was greater in low light than in high light (Figure 18). Lipid content closely paralleled chlorophyll production. The chlorophyll also shows increases with brighter light and then declines at the highest light intensities used (Figures 18 to 20). This pattern is of interest considering that growth rates continue to climb (Figure 15) despite the obvious decay in the light-harvesting apparatus (decreased pigment contents). Chlorophyll production among the three temperatures was similar, again, showing the bell-shaped distributions. Cultures in the lower temperature produced less pigment (Figures 19 to 23).

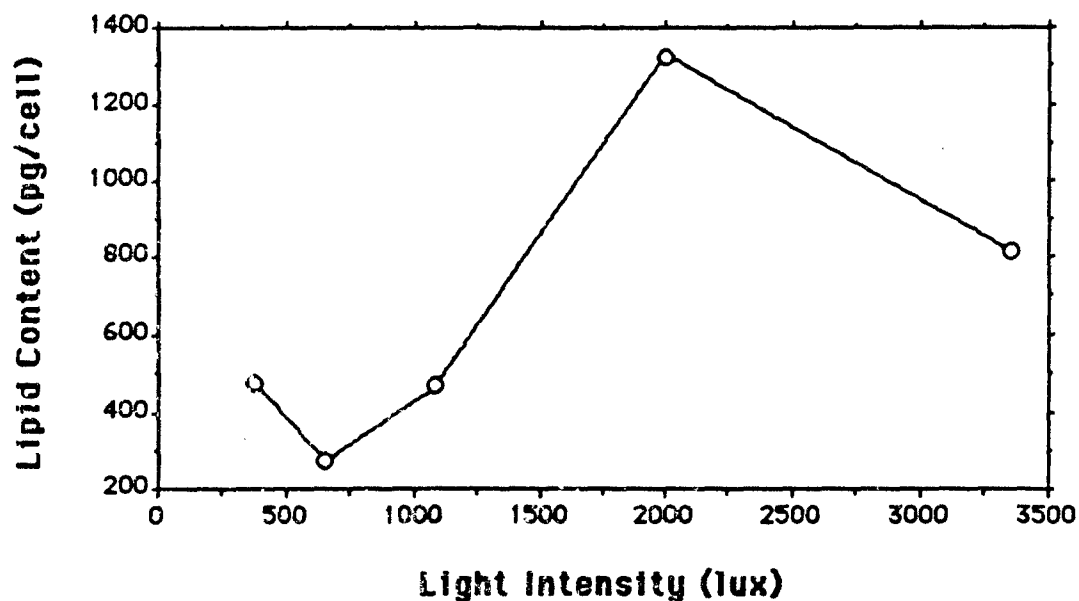


Figure 17. Lipid content (pg/cell) of clone 175 vs light intensity. The pattern is shown for growth at 28°C.

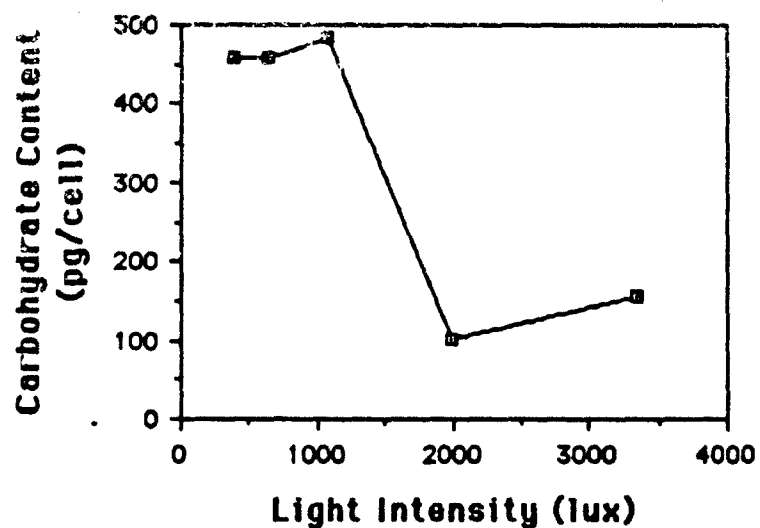


Figure 18. Carbohydrate content (pg/cell) of clone 175 vs light intensity. The pattern is shown for growth at 28°C.

The accessory carotenoids increased linearly with brighter light at the highest temperatures, and the carotenoids indicate that the cultures are obviously in decline at 25°C and only in maintenance at 22°C (Figures 20 to 22).

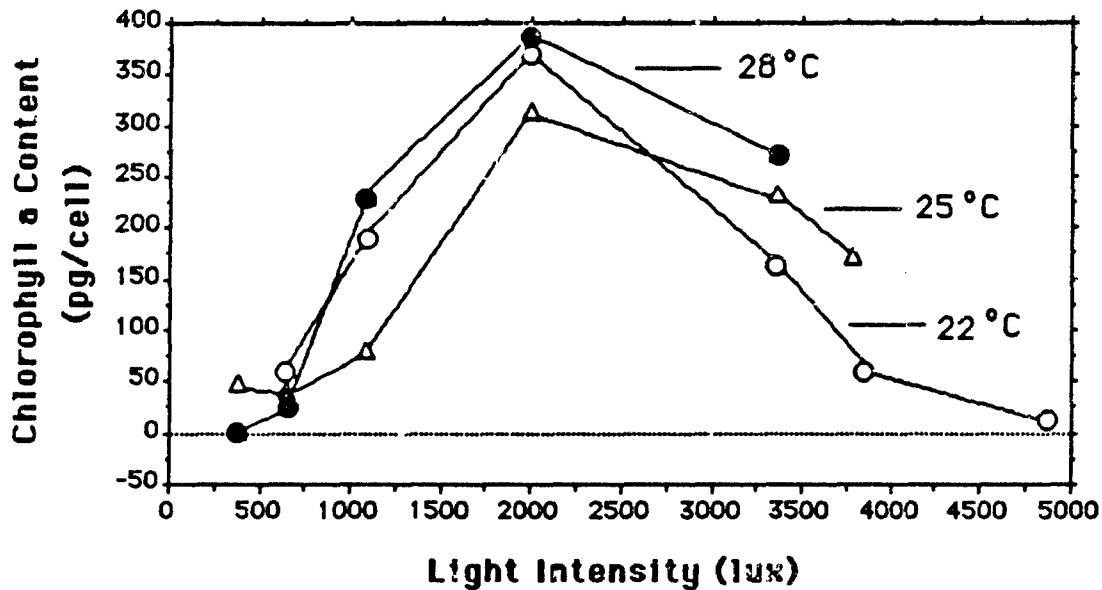


Figure 19. Chlorophyll a content (pg/cell) of clone 175 vs light intensity. The pattern is shown for growth at 22, 25 and 28°C..

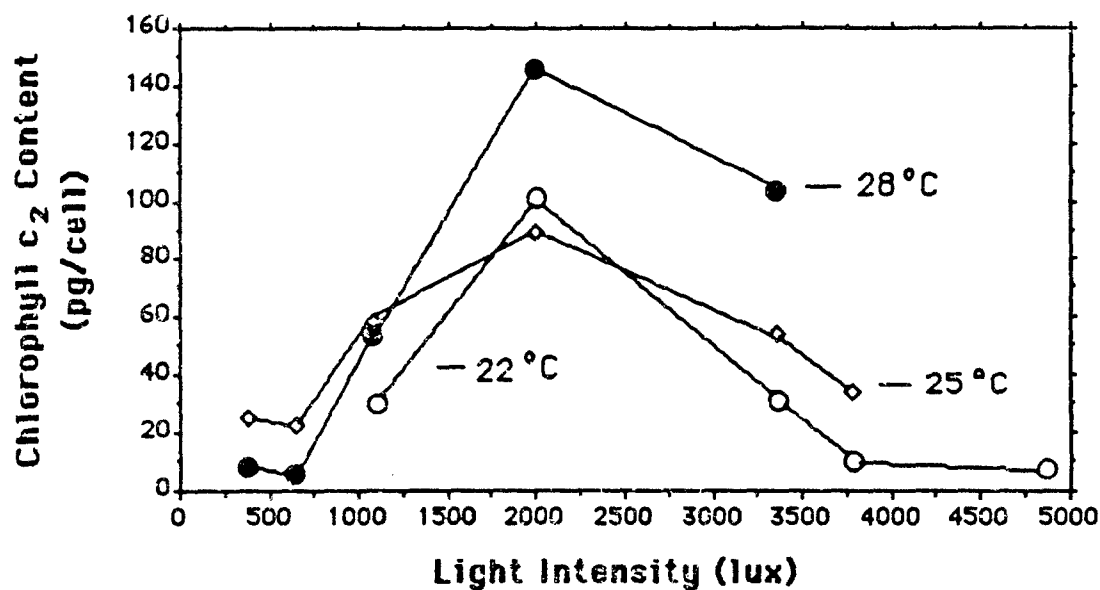


Figure 20. Chlorophyll- c_2 content (pg/cell) of clone 175 vs light intensity. The pattern is shown for growth at 22, 25 and 28°C.

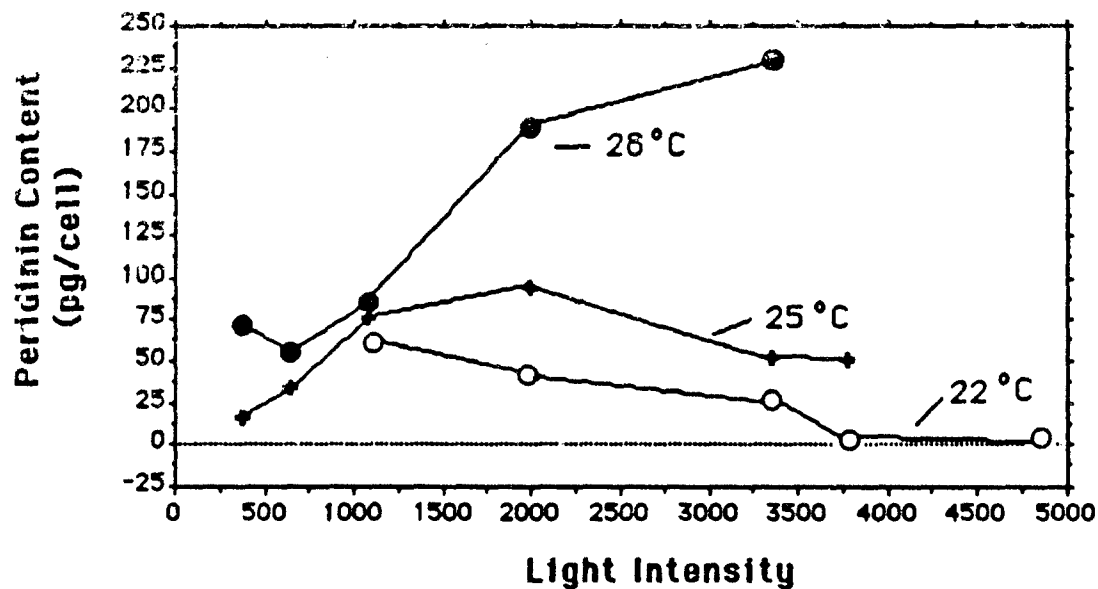


Figure 21. Peridinin content (pg/cell) of clone 175 vs light intensity. The pattern is shown for growth at 22, 25 and 28°C.

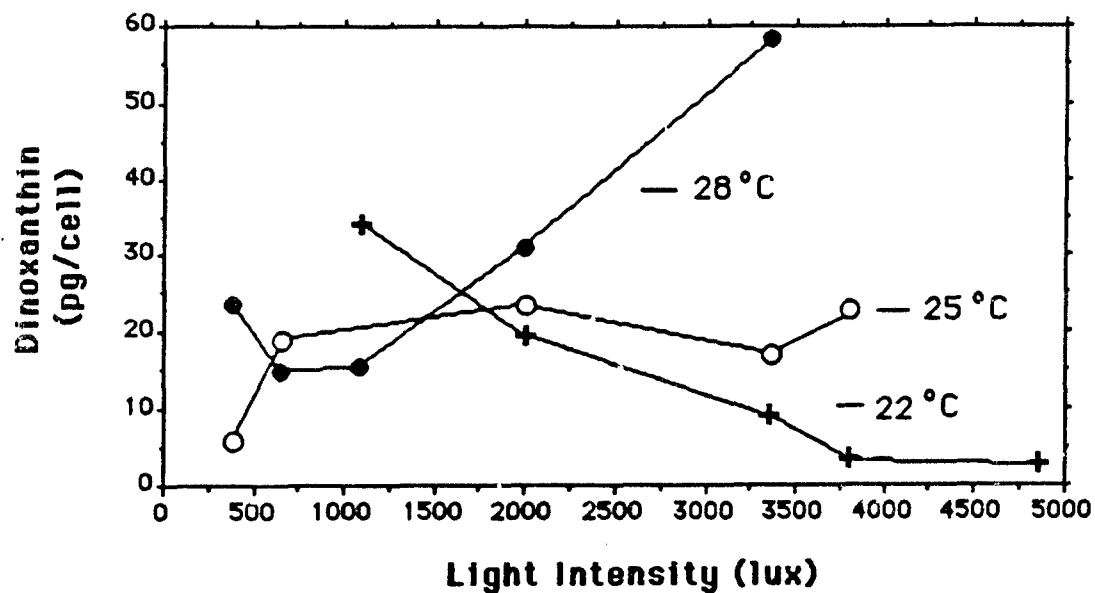


Figure 22. Dinoxanthin content (pg/cell) of clone 175 vs light intensity. The pattern is shown for growth at 22, 25 and 28°C.

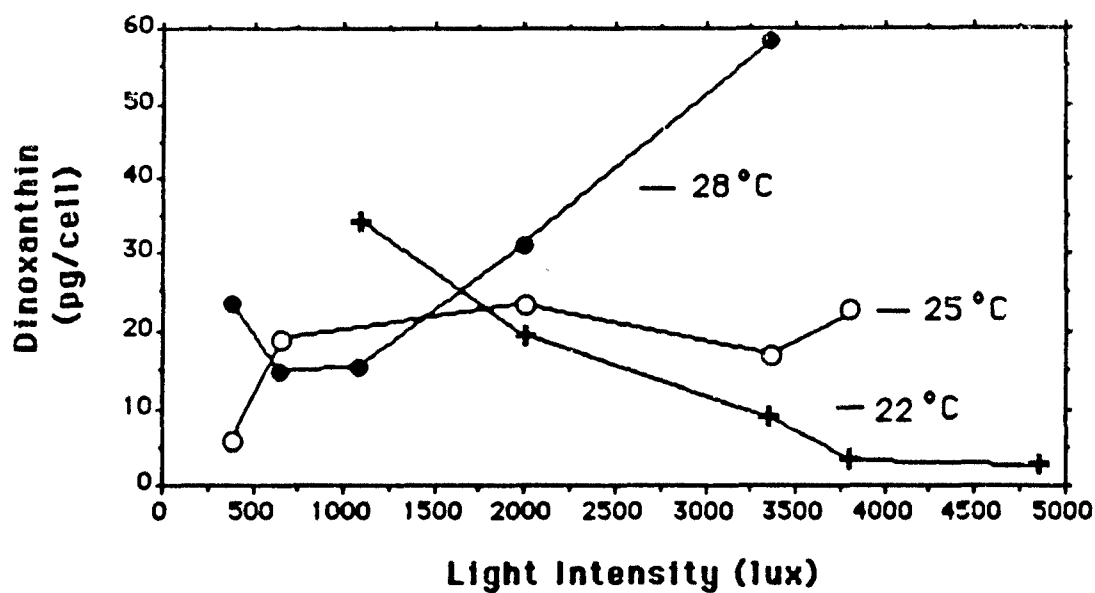


Figure 23. Diadinoxanthin content (pg/cell) of clone 175 vs light intensity. The pattern is shown for growth at 28°C.

Total toxin production has a normal, bell-shaped distribution over the range of light used at 22, 25 and 28°C (Figure 24). It was exciting to learn that decreased temperatures improve toxin production substantially (x10).

Toxin production was not well correlated with the production of any macromolecular components. There were slightly negative correlations between potencies and carotenoid production. However, the most interesting relationships were found between the culture potencies, population densities and ammonium uptake rates. The potencies are significantly and positively correlated with both of these parameters (Figures 26 and 27).

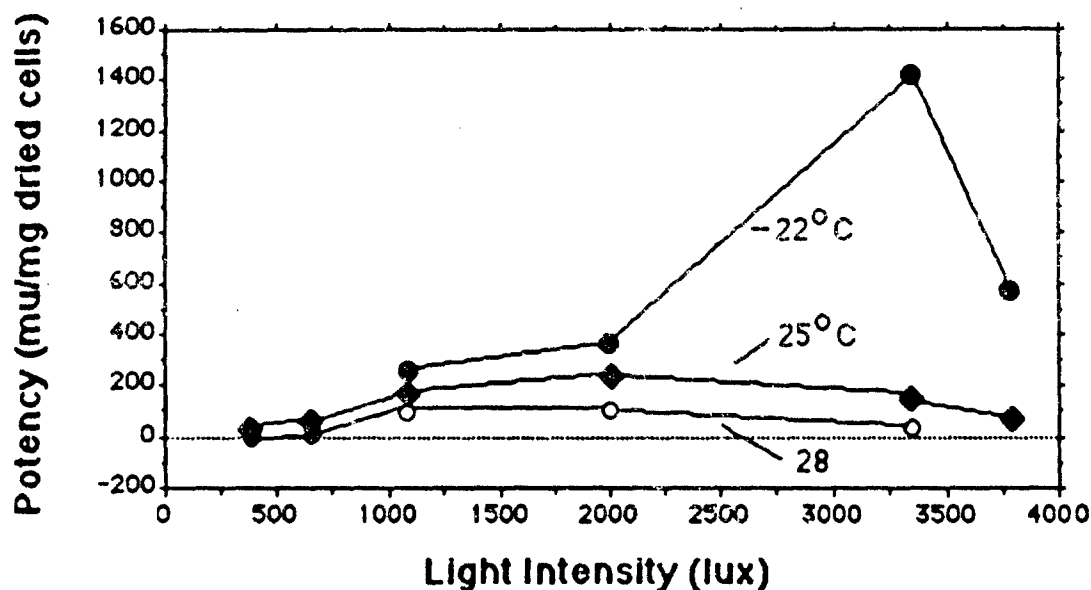


Figure 24. Culture potency (mu/mg dried cells) of clone 175 vs light intensity. The pattern is shown for growth at 22, 25 and 28°C.

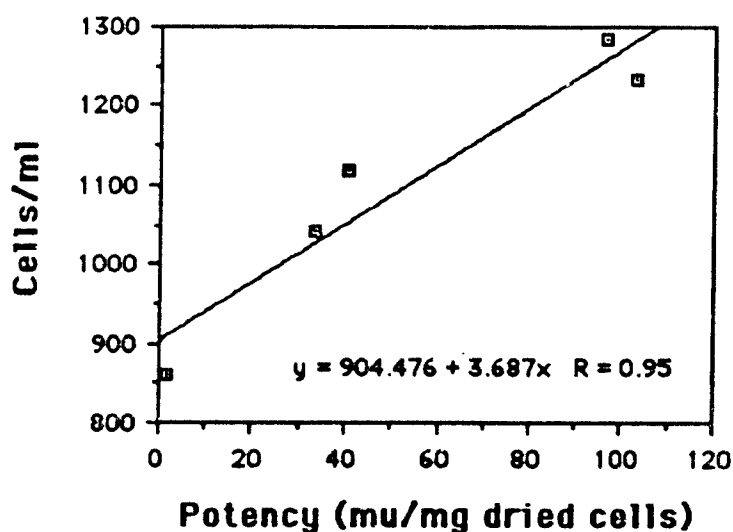


Figure 25. Culture population density (cells/ml) vs. the potency (mu/mg dried cells) of clone 175 (grown at 28°C).

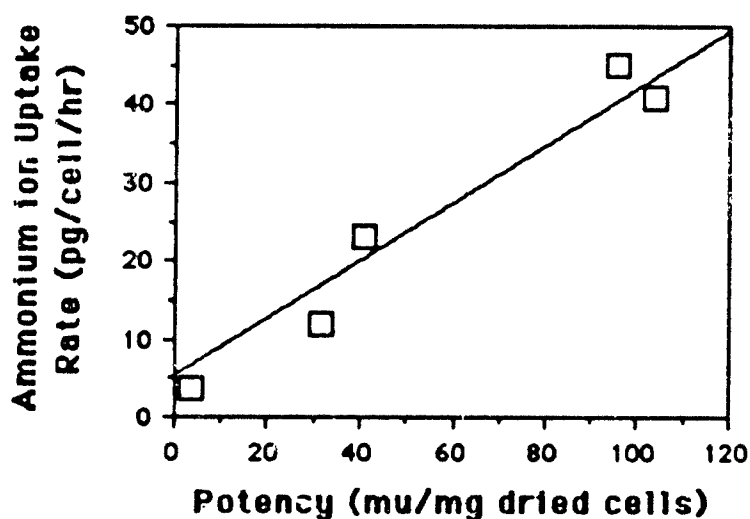


Figure 26. Ammonium uptake take rate (pg/cell/hr) vs. the potency (mu/mg dried cells) of clone 175 (grown at 28°C).

A correlation matrix has been generated on the data acquired thus far. That is, each component analyzed has been tested for association with all other components. The most significant relationships detected are given in Table 20. As expected, light and reproduction

rate are well correlated. Light intensity appears to have far greater effects on most parameters compared to temperature. However, the effects of a temperature on toxicity is the major exception. Protein content was positively correlated with the three major pigments ($r = 0.92$ to 0.97).

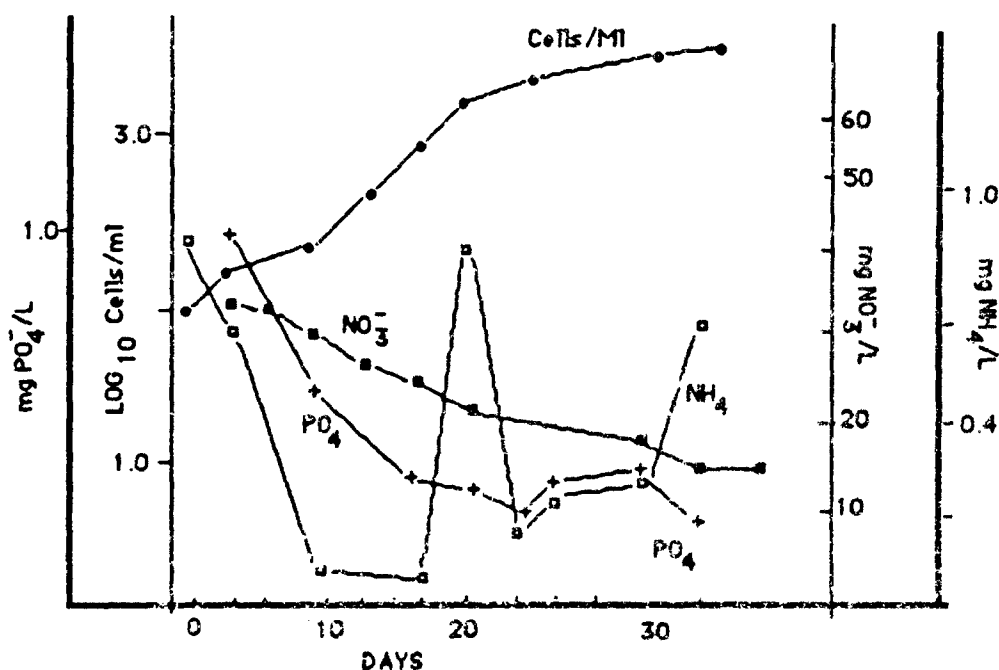


Figure 27. Characteristics of growth of *Gambierdiscus toxicus* (clone 175). Four parameters, cells per ml, nitrate, phosphate and ammonia are plotted as a function of time.

Phosphate-ammonia-nitrate utilization. Studies completed on *G. toxicus*, clone 175, indicate that both phosphate and ammonia are readily taken up by the rapidly dividing cells (see Figure 27). The pulse of ammonia at 19 days of culture is apparently real, having shown up in four separate cultures to date. The cultures begin to foam at this point, indicating a general increase in the production of extracellular metabolites.

TABLE 20.
SUMMARY OF THE CORRELATION MATRIX PERFORMED ON DEPENDENT DATA
FROM *G. TOXICUS* GROWTH EXPERIMENTS.

Variable 1	Variable 2	Correlation Coefficient
Light Intensity	Reproduction Rate	0.99
Protein	Chlorophyll c	0.96
Protein	Peridinin	0.96
Potency	Ammonia	0.96
Potency	Cells/ml	0.95

Discussion of maximal toxin production. One of the major problems that we have encountered in this experiment is that the cultures in the lowest light intensity (378 lux) did not produce cell numbers above 700 cells/ml in a reasonable time period at 28°C and 25°C (< 2 months). In addition, 378 and 678 lux cultures could not support any growth at 22°C. Therefore, in order to avoid cellular degradation by bacteria we harvested these cultures at lower densities. For this reason it is difficult to compare these cultures directly with the others which are harvested at $1,100 \pm 200$ cells/ml. Consequently, we used growth pattern as much as population density as our criterion for determining the point of harvest. Thus, all cultures were harvested in what we determined to be mid log phase based on linear growth/time plots. By this method we insure that although cell numbers and external nutrient conditions may vary at the point of harvest, the relative kinetics of growth are the same and differ only in their magnitude.

Microalgae tend to produce more lipid and carbohydrates per cell than protein in unfavorable environments.^[88-90] This is thought to be due to the cells preparing storage products for probable dormancy (e.g., encystment) periods.^[91] The increase in carbohydrate at low light intensities may reflect this trend. However, lipids are most concentrated at 1,999 lux. This is partially explained by the large increase in pigments at this light intensity.

The decrease in chlorophyll production under bright light is consistent with previous studies.^[92] Interestingly, the growth rate data do not clearly indicate the beginning of growth saturation

whereas the pigment data do. The chlorophyll to carotenoid ratio decreased at the highest light intensity at 28°C. This implies that at the high light intensity used (3350 lux), more carotenoids are produced, presumably to protect the chlorophyll. Saturation is always suspect when more accessory pigments are made per cell relative to chlorophyll^[92] as the accessory pigments (or other photosynthetic modulators) are produced to protect chlorophyll against photooxidation.

The cooler temperatures are obviously stressful for clone 175, given the decline in pigment production. The increase in toxin production with decreasing temperature (or other stress) is a pattern consistent with the production of allelopathic polyethers in bacteria^[110,111] and other bioactive metabolites in dinoflagellates.^[94] The fact that clone 175 is physiologically light tolerant would explain why light has relatively unexciting impacts on its toxin production. However, because it is greatly susceptible to decreasing temperature, from the evolutionary standpoint improved toxin production at this point is highly advantageous. That is, assuming that toxins produced by clone 175 affect other algae. In fact, there is good evidence to suggest that there are allelopathic roles for extracts from *G. toxicus*.^[82,112] The observed pattern of toxin production would enable *G. toxicus* to maintain its ecological position in the benthos under temperature stress, despite the presence of other faster-growing, more temperature-tolerant algae. The hypothesis regarding allelopathy is worthy of further testing and is exciting basic research.

Putting allelopathic considerations aside, the reader should also keep in mind that the biochemical pathways of polyether and carotenoid production probably begin with the same carboxylic acid precursors, e.g., acetate. Therefore, an increase in maitotoxin production during decreased carotenoid production may indicate the existence of an acetate shunt. Carotenoid and toxin contents are negatively correlated. If possible, we will explore the relationships between acetate, toxin and carotenoids in more detail.

It appears that we have in fact almost eliminated production of maitotoxin at some light intensities. We have injected mice with low light intensity samples at 128 times the usual LD₅₀ dose for this clone without adverse effects (512 µg). Perhaps there is more of the less potent, lipid-soluble toxin ("ciguatoxin") present on the ends of the bell shaped toxigenesis curve (Figure 24). Future ileum and HPLC runs may help us determine this. In addition, some of the toxin may be leached. Bomber^[82] was able to detect toxin in the medium of some cultures of *G. toxicus*. We also reported on the poor condition of the cells grown under low light. However, as all cultures are harvested in log phase, leaching is probably not that great a problem. Actively growing cells tend to conserve photosynthates for growth. In contrast, it is the stationary phase cultures which tend to leach a variety of compounds, often for ecological purposes.^[87]

The next important question is, what aspect of the light intensity effect is causing the potency differences? Toxin production was not closely associated with the production of lipids. Therefore, toxin production is probably driven by other processes, such as temperature stress. Toxigenesis could also be linked with the population density of a culture (Figure 25) which in turn may regulate ammonium uptake (Figure 26). This link also supports the hypothesis regarding allelopathy. An increase in the population of any competing cells would provide both physical and chemical stimuli to *G. toxicus*. These stimuli would probably begin with ammonium deficiency because it is perhaps the most ephemeral nutrient. Improved toxin production in response to this stimulus may lead to the death of competing algae as maitotoxin is leached from *G. toxicus*. In order for this hypothesis to be valid the stimulus-response time would have to be rapid because ammonium depletion and the termination of toxigenesis coincide.

Ammonium uptake rates and cell density are both, of course, light dependent. Suppose that maitotoxin facilitates the transport of cations like NH₄⁺ across the cell membrane. If true, then more toxin would need to be produced by a cell when the population increases

in order for it to preserve its fast uptake of ammonium and remain competitive with other cells. This would then explain the strong association. Or, the process may respond to environmental cues. For example, ammonium uptake decreased in the brightest light used because there was simply little ammonium left in the medium. Interestingly, this is precisely the same point at which toxin production decreased.

Perhaps the most valuable information gathered is that we now know that maitotoxin production can be manipulated. An earlier, less detailed report stated that it could not.^[112] We can now further improve toxin production by adjusting the light intensity of our mass cultures to the preferred intensity. A light intensity between 1000 and 2000 lux will foster the greatest toxin production (Figure 24). In addition, if kept below 2000 lux the culture will still be at less than maximum lipid production (Figure 17). Also, if harvesting is maintained in log phase, interfering lipids will be produced at their nominal levels and these features will greatly improve toxin purification. Again, we also now know that a reduced temperature appears to improve toxin production. It will be most interesting to learn if this lower temperature is stimulating an increase in maitotoxin production or perhaps an initiation or an increase in ciguatoxin synthesis.

If the data continue to support the toxigenesis/ammonium relationship then we could improve toxin production by controlling the concentration of this nutrient.

Acclimation of New Clones of Dinoflagellates.

A series of large-scale acclimations including 5 clones from Australia (GT-A9, A11, A12, A14, A16), 1 clone from the Virgin Islands (GT-350) and 1 clone from the French Polynesian Islands (GT-FP100) was initiated in June 1990. Three clones from Cosumel, Mexico (GT-CM, CM1, CM2), 1 clone from Martinique (GT-175), 1 clone from Bermuda (GT-135), and an additional clone from Australia (GT-AA1) were added to the acclimation series in

September 1990. Results of production in this series through September 10 are shown in Table 21. Growth rates will be determined for all cultures in this series. Once acclimated growth rates are achieved, the series will be terminated and potency of methanol extracts from each culture will be determined. Results from these experiments will be compared with results on 17 clones of *G. toxicus* presented by Bomber.^[73] Also methanol extracts will be subjected to our standard purification procedures. Results on types and potencies of toxins from the various clones will be compared with our previous findings and those reported by other laboratories.

TABLE 21
VOLUME OF MEDIA AND CELL PRODUCTION IN CONTINUOUS ACCLIMATION
CULTURES OF 7 CLONES OF *GAMBIERDISCUS TOXICUS*.

Clone	Dates of Initiation - Harvest	6/20-7/17	7/17-8/4	8/4-8/21	8/21-9/10
GT-A9	Vol (L)	10.00	8.20	19.30	19.05
	Cell Mass (mg)	1604	563	1027	1211
	mg/L	160.4	62.2	53.21	63.57
GT-A11	Vol (L)	10.00	7.25	19.50	19.00
	Cell Mass (mg)	395	317	981	1095
	mg/L	39.5	40.28	50.31	57.63
GT-A12	Vol (L)	19.5	8.00	19.6	18.10
	Cell Mass (mg)	834	309	638	852
	mg/L	42.8	35.25	35.41	47.07
GT-A14	Vol (L)	40.50	8.00	20.10	19.55
	Cell Mass (mg)	1604	436	910	1078
	mg/L	39.6	49.25	48.06	55.14
GT-A16	Vol (L)	19.70	7.75	19.80	18.65
	Cell Mass (mg)	561	232	607	846
	mg/L	28.5	27.48	30.66	45.36
GT-350	Vol (L)	10.00	7.50	18.60	18.85
	Cell Mass (mg)	306	251	603	559
	mg/L	31.0	31.2	33.27	29.66
GT-FP100	Vol (L)	19.50	7.50	19.5	19.60
	Cell Mass (mg)	560	215	641	696
	mg/L	28.7	26.13	34.97	35.51
TOTALS	Vol (L)	160.2	54.2	136.4	132.8
	Cell Mass (mg)	6186	2323	5407	6337
	mg/L				

TABLE 22
A COMPARISON OF TOXICITY (LD₅₀) OF CRUDE METHANOL EXTRACTS
OF GEOGRAPHICALLY SEPARATED CLONES OF *GAMBIERDISCUS TOXICUS*

STRAIN (CLONE)	CELLS DW mg	METHANOL EXTRACT mg	LD ₅₀ mg per Kg-Mouse	MOUSE UNITS	TOTAL M.U. mg	M.U. per mg/cells
GT-175	641	364	1.00	0.020	18200	28.39
GT-350 4A	5000	1908	5.75	0.115	16591	3.32
GT-350 6A	5000	1896	5.75	0.115	15878	3.18
GT-350 7A	5000	1800	6.25	0.125	14400	2.88
GT-350 7B	2800	900	5.00	0.100	9000	3.21
GT-350 Cb	25460	8280	5.00	0.100	82800	3.25
GT-135	127	63	14.73	0.295	213	1.68
GT-851	1542	563	54.75	1.095	517	0.34

Add new clones

Physiology and Potency of the Dinoflagellate, *Prorocentrum concavum* During One Complete Growth Cycle.

Studies on growth physiology and acclimation of *P. concavum* (SIU clone 364) were completed.^[113] This clone was cultured in h/2 medium at 25°C under five light regimes (312 lux to 2690 lux). Determination of biochemical differences were made on each culture in a series leading to acclimated growth rates under each light regime. Growth rates of *P. concavum* during the acclimation process increased initially and eventually leveled off to a constant rate (i.e. 0.36 div/day after 4-5 transfers at 2690 lux). Growth rates diminished with decreasing light intensities (0.36 at 2690 lux to 0.04 at 312 lux). During the two month acclimation period (at 2690 lux) total protein increased from 2930 pg/cell to 4130 pg/cell and total carbohydrates increased from 745 pg/cell to 1080 pg/cell. Pigment compositions of acclimated cultures over the five light regimes expressed as a carotenoid to chlorophyll ratio, exhibited a bell-shaped curve. The data indicated that both light intensity and acclimation have a profound affect upon the growth and physiology of *P. concavum*.

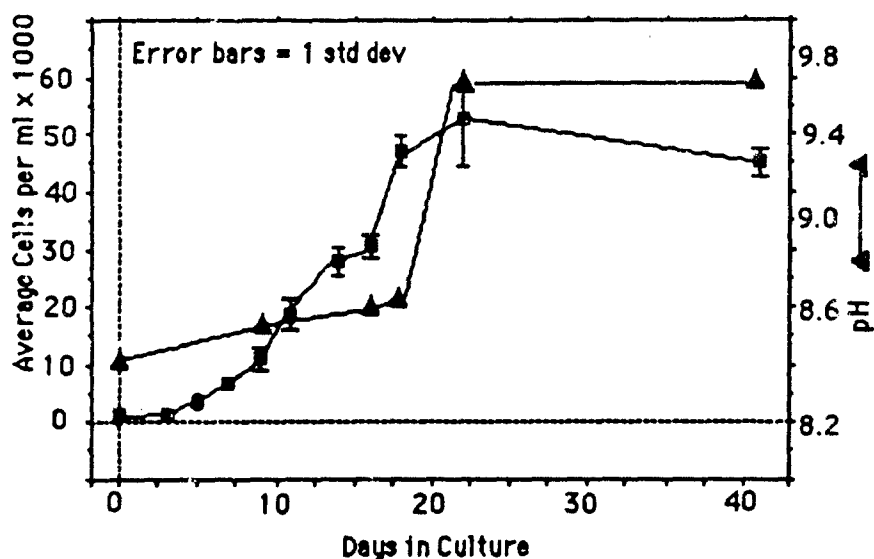


Figure 28. Cell densities and pH measurements of the complete growth cycle of *Prorocentrum concavum* (SIU clone 882a) grown in large-scale batch cultures (16 x 10L) containing h/2 enriched natural seawater medium under 16:8 light/dark cycle (1800 lux) at 28°C.

The present study was initiated in order to achieve the following objectives: (1) to determine changes in physiology of cells during one complete growth cycle; (2) to compare synthesis of FAT and OA with that of other biochemical constituents; (3) to enhance our ability to manipulate production of toxins; and (4) to determine the significance of *P. concavum* as a possible contributor of toxins to the ciguatera syndrome in humans.

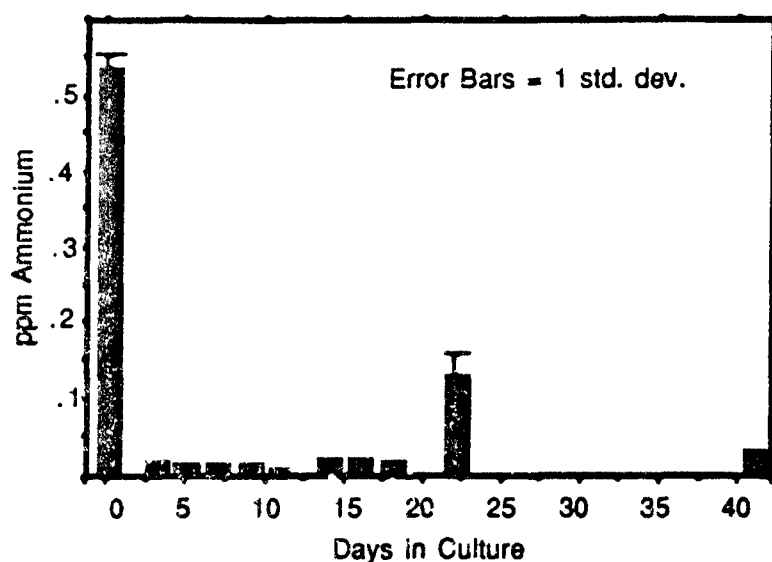


Figure 29. Depletion of Ammonium from the culture medium (h/2) over the growth cycle of *Prorocentrum concavum* (SIU clone 882a).

Results and Discussion. The cell densities obtained from triplicate counts over the entire growth cycle of *P. concavum* ranged from 500 to 55,000 cells/mL (Figure 28). Large-scale cultures displayed a sigmoid growth curve with a short lag-phase, followed by an active log-phase (0.35 div/day) and stationary phase. Concurrent measurements of pH in the culture media showed a significant increase at the end of log-phase (pH 9.6) which was not controllable with bubbling of sterile air (Figure 28).

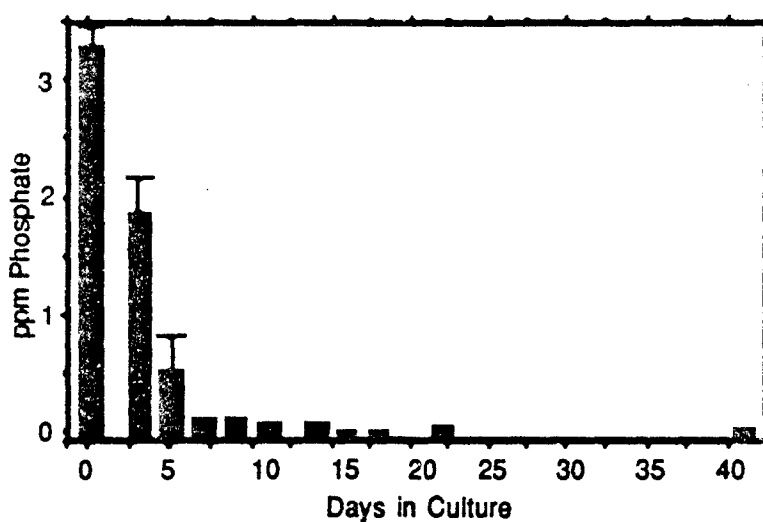


Figure 30. Depletion of phosphate from the culture medium (h/2) over the growth cycle of *Prorocentrum concavum* (SIU clone 882a).

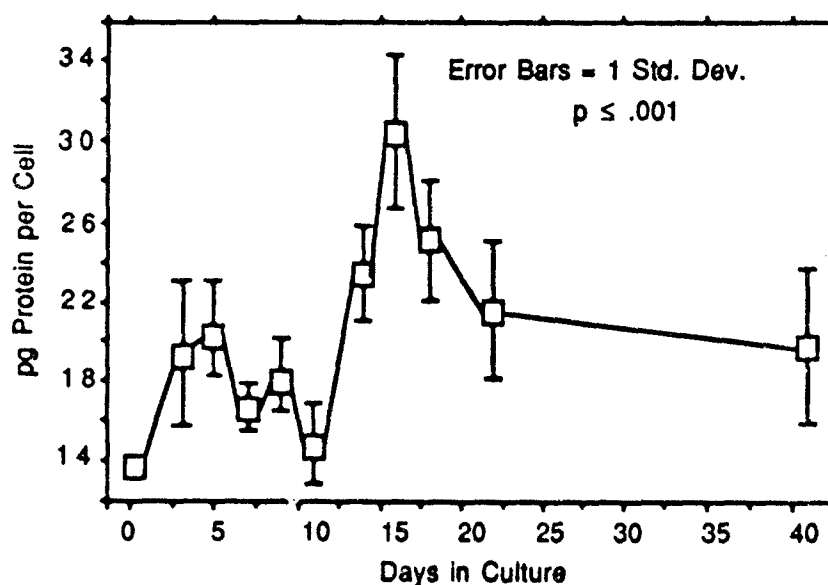


Figure 31. Cellular content of protein over the growth cycle of *Prorocentrum concavum* (SIU clone 882a).

Systematic measurements of nutrient depletion in the culture medium revealed that the levels of nitrogen (NH_4) and phosphate in the culture medium were significantly reduced by early log-phase (Figures 29 & 30). However, nutrients were not deplete or limiting,

since logarithmic growth continued long after measurable amounts of these nutrients had been extracted from the growth medium.

Several biochemical parameters were measured to assess the physiological condition of the cells over this complete growth cycle. These parameters included total soluble proteins, lipids, reducible sugars (carbohydrates), pigments and toxicity. Figure 28-31 show the relationships between protein, lipid and carbohydrate content during culture development. Protein content increased initially from 1400 pg/cell to 2000 pg/cell but returned to the initial level around 1400 pg/cell after 12 days of growth. This suggests that during the log-phase, proteins are subjected to rapid turn-over rates.

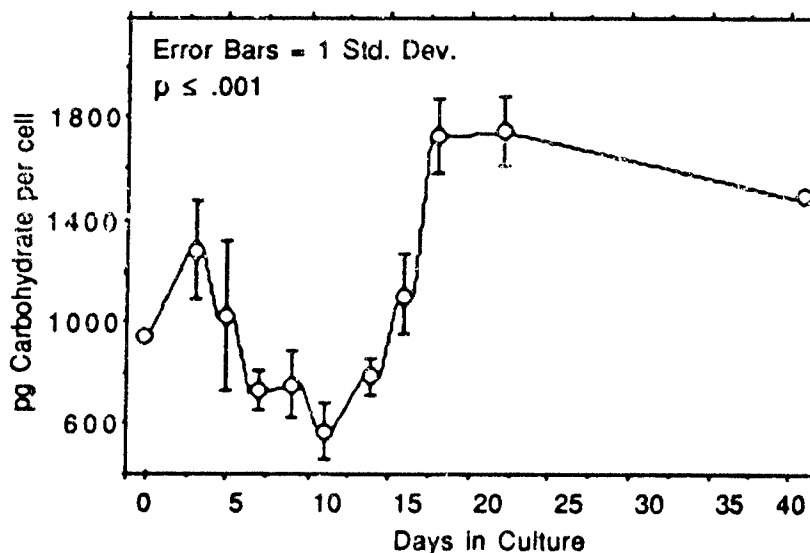


Figure 32. Cellular content of carbohydrate over the growth cycle of *Prorocentrum concavum* (SIU clone 882a).

As the protein level increases during the mid-log phase to around 3100 pg/cell (possibly due to slower turnover rates), total carbohydrates and lipids follow closely behind, reaching their maximum levels of 1800 and 1900 pg/cell respectively near late-log to early stationary phase.

However, protein content then decreases to early log-phase levels (2200 pg/cell) at the onset of stationary phase, indicating their degradation to near basal levels.

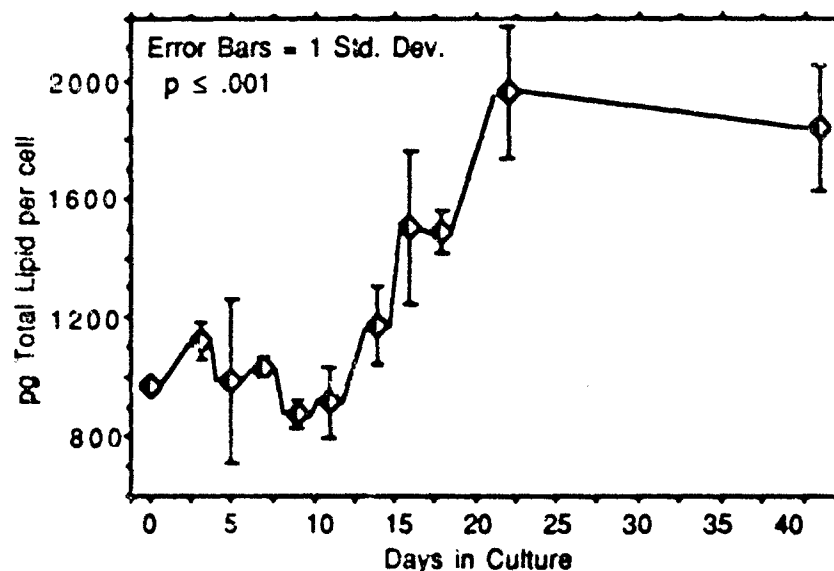


Figure 33. Cellular content of lipid over the growth cycle of *Prorocentrum concavum* (SIU clone 882a).

The cellular content of chlorophyll-*a* and peridinin follow the same developmental pattern as protein, with maximal cell content of 65 and 40 pg/cell respectively during mid-log phase followed by a transient drop in early stationary-phase (Figure 33 & 34). Nevertheless, chlorophyll-*c*₂ content was maintained at mid log-phase levels until late stationary-phase. This suggests that either the metabolic machinery for the production of chlorophyll-*c*₂ is functional for a longer time period or the degradation of this pigment is slow. The indestructible nature of chlorophyll-*c*₂ is also observed in the laboratory. It is relatively insoluble in most organic solvents, it is difficult to separate from toxic fractions of *G. toxicus*, and it persists in extracts long after the degradation of chlorophyll-*a*.

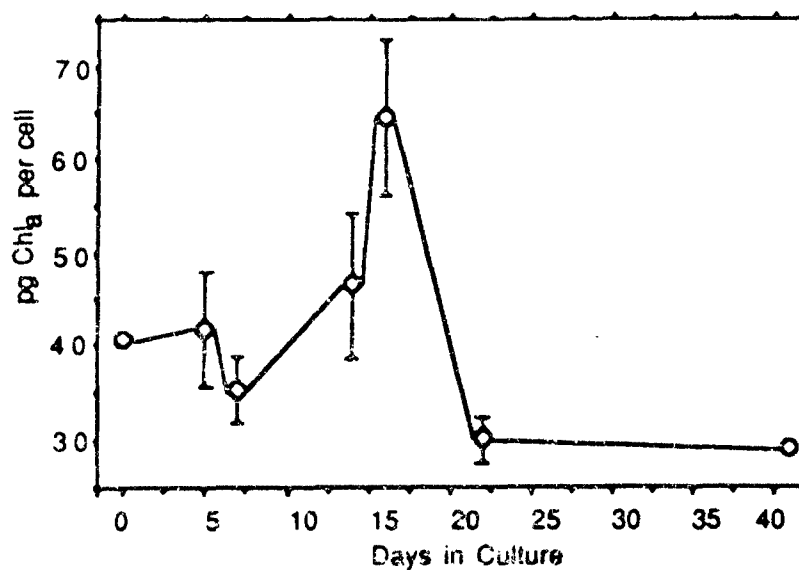


Figure 34. Cellular content of the pigment chlorophyll-a over the growth cycle of *Prorocentrum concavum* (SIU clone 882a).

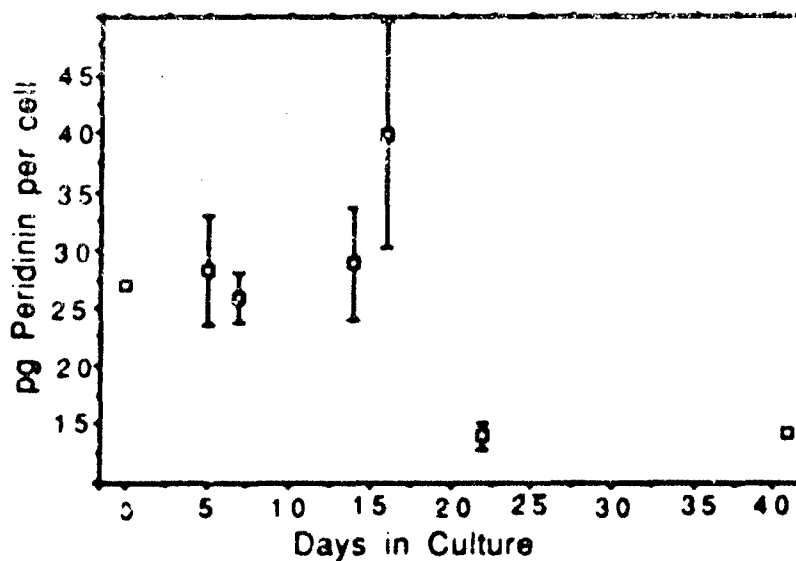


Figure 35. Cellular content of the pigment peridinin over the growth cycle of *Prorocentrum concavum* (SIU clone 882a).

However, this persistence may explain the more or less basal levels of protein maintained in the latter phases of growth, indicating

a possible role of chlorophyll- c_2 in the survival or protection of *P. concavum* cells under unfavorable conditions (i.e. low nutrients, high pH, high light and shading).

Measurements of the potency of the FAT were accomplished using the mouse bioassay. Okadaic acid (OA) was determined using an enzyme-linked immunosorbent assay (ELISA; UBE Industries, Japan). Although these toxins appear to be chemically heterogeneous (FAT is water-soluble and causes similar antagonistic effects on the guinea pig ileum much like maitotoxin from *G. toxicus*; whereas OA is lipid-soluble and causes gastrointestinal distress and appears to inhibit specific phosphatase enzymes), the pattern of *de novo* synthesis was strikingly similar (Figs 10-13).

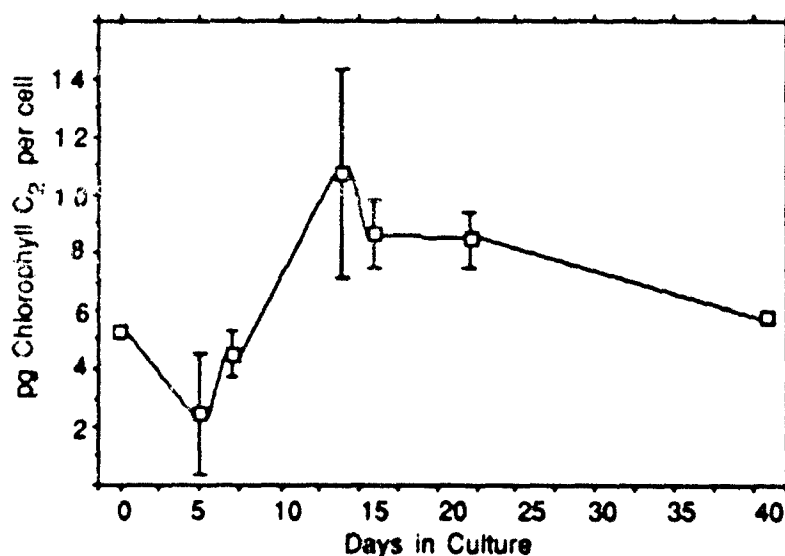


Figure 36. Cellular content of the pigment chlorophyll- c_2 over the growth cycle of *Prorocentrum concavum* (SIU clone 882a).

Interestingly, the plots of toxin content were consistent with plots of biochemical constituents, although the highest correlation existed between toxin content and lipid content per cell ($r = 0.975$ for FAT vs lipid). This relationship is especially interesting since both compounds may have common acetate precursors.^[114]

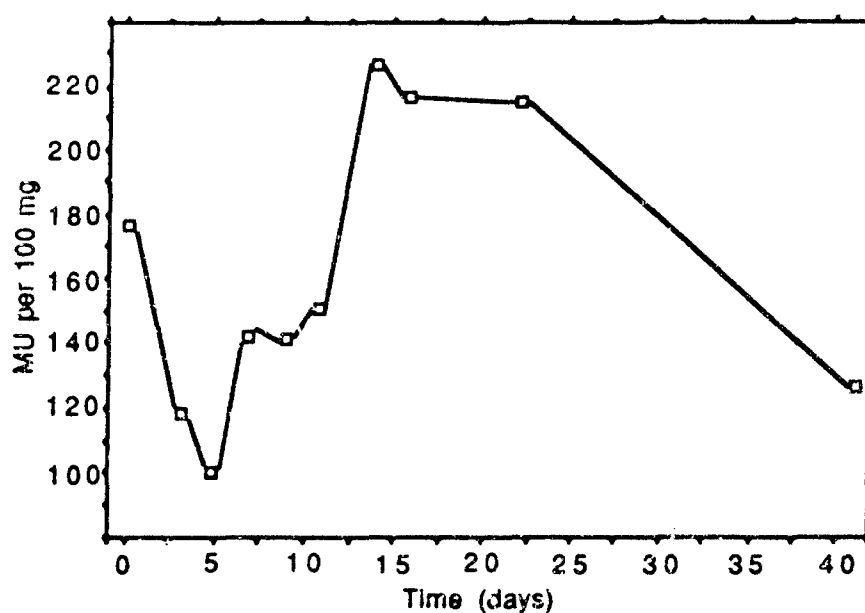


Figure 37. Cell potencies of Fast Acting Toxin as determined by mouse bioassay. Total extractable mouse units (1MU=LD50 dose) per 100 mg dry cells.

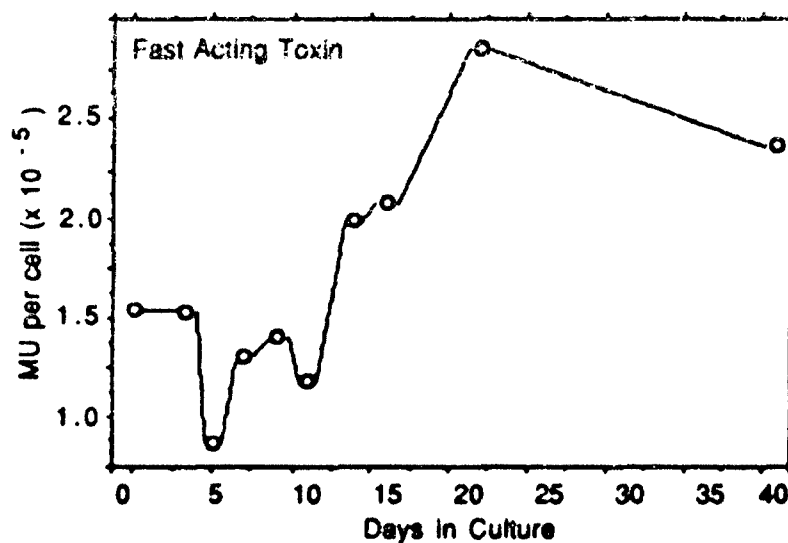


Figure 38. Cell potencies of Fast Acting Toxin as determined by mouse bioassay. Total MU of Fast Acting Toxin per cell, inset gives correlation between MU FAT/cell and total lipid content per cell.

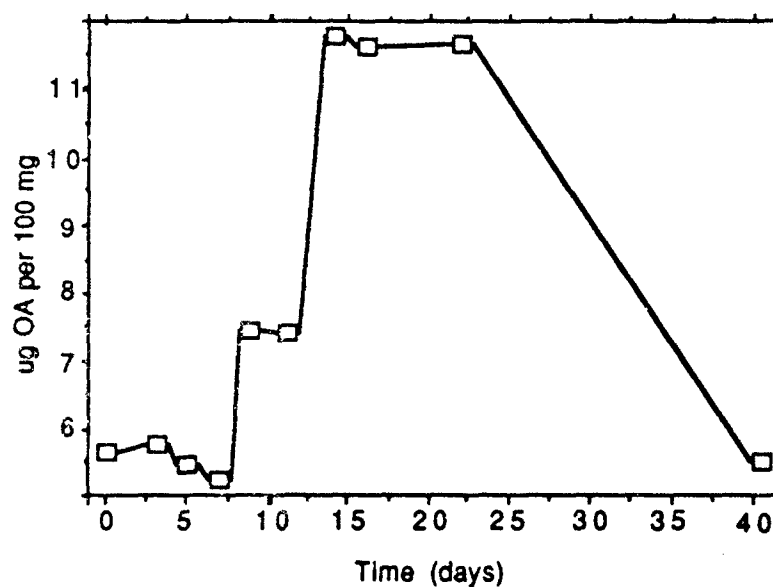


Figure 39. Cellular content of okadiac acid as determined by enzyme linked immunosorbent assay (ELISA) as quantity of extractable OA per 100 mg dry cells.

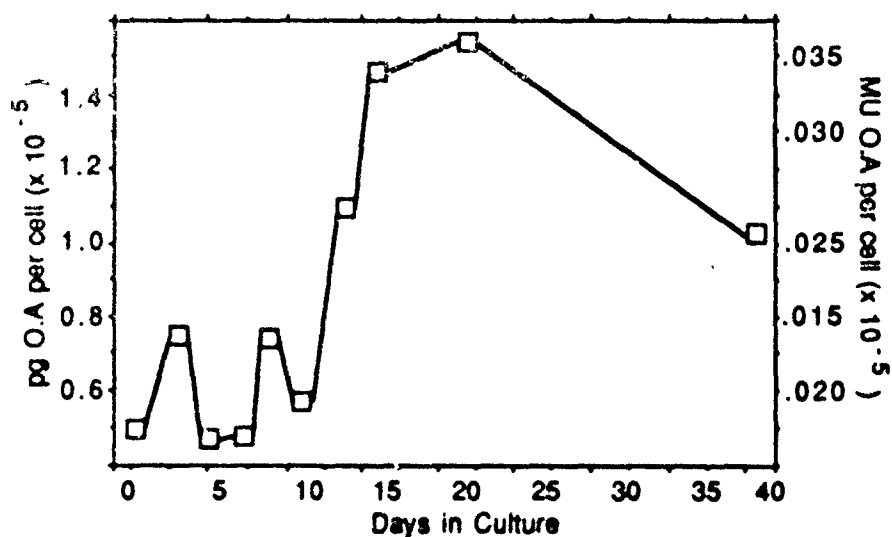


Figure 40. Cellular content of okadiac acid as determined by enzyme linked immunosorbent assay (ELISA) amount of OA per cell and MU OA per cell, this estimation is based on previously reported LD50's of 4 $\mu\text{g}/\text{MU}$. The inset gives the correlation coefficient for pg OA/cell vs total pg lipid/cell.

It is interesting to note the similarities in the ratios of water soluble toxin to lipid-soluble toxin between the two toxic dinoflagellates *P. concavum* (SIU 882a) and *G. toxicus* (SIU 175). The ratio of FAT:OA for *P. concavum* 882a from this study was 74:1, which is not unlike ratios of maitotoxin to ciguatoxin in cultured *G. toxicus* 175. Another important point to note is the inverse relationship between toxin production and the uptake of phosphate ($r = -0.96$). This suggests that the phosphate assimilation mechanism may cause a negative-feedback on *de novo* toxin synthesis. However, low toxicity may be a result of increased rates of division in early log-phase which is the result of the same amount of toxin, being distributed amongst more cells giving the illusion of decreased toxicity. If this were the case one would expect to observe a rise and fall of toxin levels throughout the log-phase. So, this hypothesis should be tested using synchronous cultures.

Conclusions. The changes in physiology over the complete growth cycle of *P. concavum* (SIU clone 882a) were significant and consistent between each measured parameter. Curves for cellular content of protein, carbohydrates, lipids, pigments and toxins were very comparable. Nevertheless, toxin content per cell and total lipid content per cell displayed the highest correlation. These results suggest maximal cellular fitness and toxicity occur at mid-log phase growth. During this phase of the growth cycle the cells were shown to contain the highest cellular content of protein, pigments and toxin. These results also reveal the overwhelming production of water-soluble toxins vs lipid-soluble toxins (74:1) per cell grown in culture. This relationship appears similar to the cellular content of maitotoxin to ciguatoxin in cultured *G. toxicus*. Also, the findings of this study confirm the report of OA in *P. concavum* cells by Dickey *et al.*,^[115] and further supports the conclusion that *P. concavum* may contribute to the disease ciguatera.

Calibration of ileal assays

Concomitantly with our separation work, we began attempting to quantitate the ileum assay with each of the three components that

we isolated from the crude extract. Toxicity to the whole ileum does not imply the same toxicity to the whole mouse. We simply established reproducible end points for the ileum assays, defined these as an "Ileum Equivalent Unit" and then attempted to correlate these with mouse bioassays. For instance, using the 50% inhibition at 90 minutes after a 15 minute incubation as the end point for one MTX ileum unit (MIU), the ratio for crude *G. toxicus* extract is approximately 2000 ileum units equals 1 mouse unit.

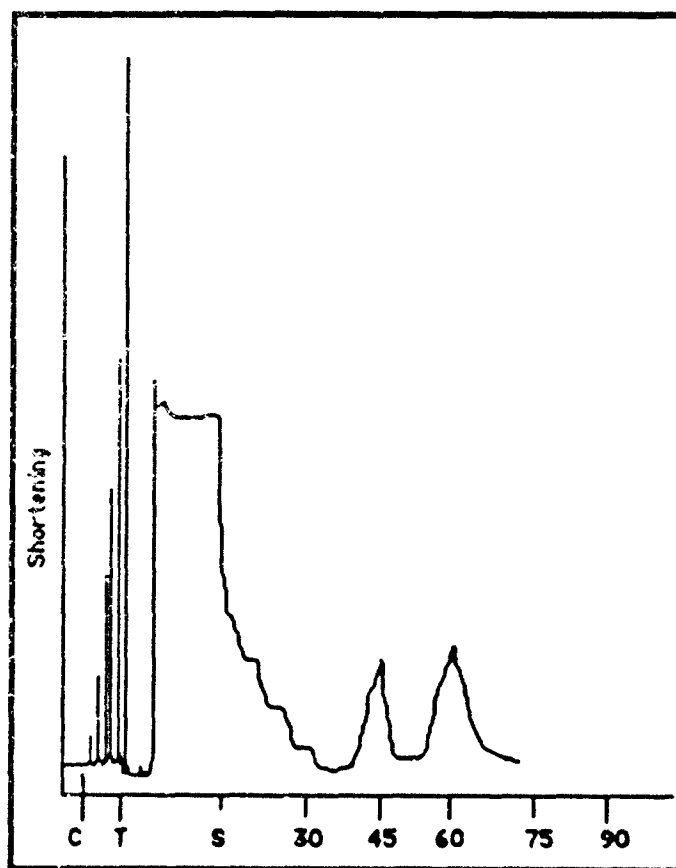


Figure 41. Records of guinea pig ileum assay (MTX assay) of the brown fraction from the sep-pak separation (SK-1 br) of crude methanol extract of *Gambierdiscus toxicus*. C=control stimulations, T=application of toxin, and S=start of experiment. 4 μ l of extract was added to 10 bath of PSS and incubated for 15 min.

Simply stated then:

$$\text{MTX Ileum Equivalent Unit} = \frac{\text{MTX Mouse Unit}}{2000}$$

and

$$\text{CTX Ileum Equivalent Unit} = \frac{\text{CTX Mouse Unit}}{10000}$$

These equivalents are invaluable in allowing us to determine which clean up steps are worth incorporating into our purification technique.

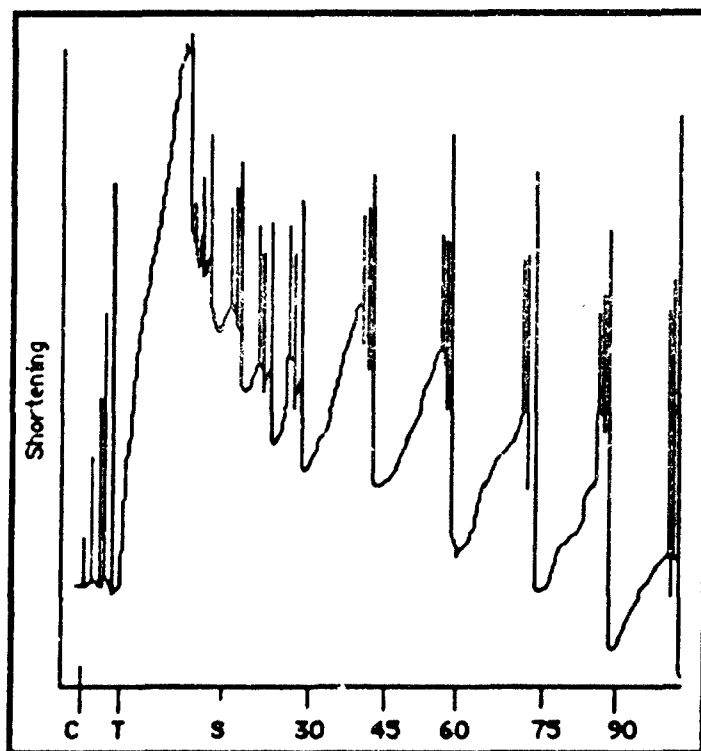


Figure 42. Records of guinea pig ileum assay (MTX assay) of the yellow fraction from the sep-pak separation (SK-1 yel) of crude methanol extract of *Gambierdiscus toxicus*. 1 μ l of extract was added to 10 bath of PSS and incubated for 15 min.

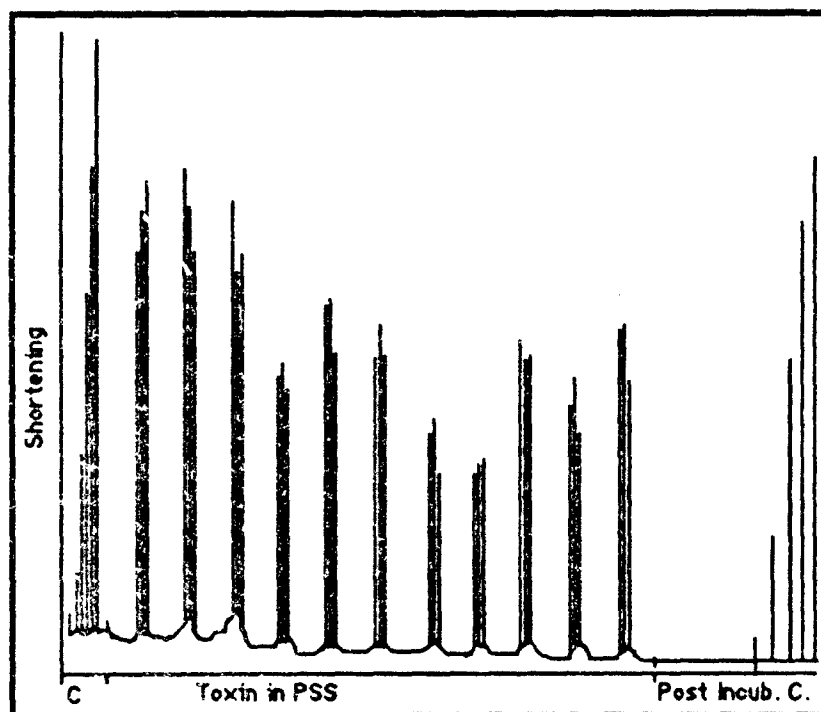


Figure 43. Records of guinea pig ileum assay (CTX assay) of the green fraction from the sep-pak separation (SK-1 gr) of crude methanol extract of *Gambierdiscus toxicus*. 50 μ l of extract in 500 ml of PSS.

During the four years of this contract over 4,000 ileum assays were conducted. Review of the ileum assays indicates that certain solvent and reagents have a distinctive effect upon the type of result that one sees on the ileum. Some tend to change the response seen from an irreversible to a reversible effect (e.g. ACN soluble, acetone). Acetone also causes an erratic response of the base line of the preparation. Still other solvents cause a decided change in the inotropic response of the ileum.

In order to examine these factors which affect the loss of toxin in storage and to determine which solvent would be best for separation of the toxin, we previously setup experiments with the water soluble extract. The procedure was to aliquot the same amount of water soluble extract into different vials, blow the toxin dry with dry nitrogen gas, and then take it up into the solvent being tested. The test-solvent was pipetted out into a separate vial to be blown dry

again. Both vials then received the original amount of methanol solvent. A control vial served to establish a killing dose for the ileum. At time intervals after the initial aliquoting, ileum assays were conducted on the samples. The solvents examined were methanol, ethanol, acetonitrile, methanol plus water and acetone. In addition to solvents, two other factors were examined in the experiments. These were acid versus basic conditions and light versus dark. All samples except the light vial (stored at room temperature) were stored in the freezer and aliquoted at intervals for testing on the ileum preparation.

Brevetoxin Antibody Competition Experiments:

Antibodies to brevetoxin were received from Dr. Mark Poli, USAMRIID and immediately put them to use. The procedure was to take a dose of toxin which we had calculated from previous runs would produce a 50% inhibition on the ileum. This sample of toxin would be combined with an aliquot of brevetoxin antibodies, allowed to incubate for 10-15 minutes and then applied to the ileum. The toxin + antibody was allowed to incubate for the regular 15 minute period and then the preparation was rinsed and challenged with the same control doses of agonist. To calculate the percent inhibition we add the heights of all the dose responses and divide by the number of doses for both the control and the experimentals - then calculate the percentage inhibition versus the pre-incubation control.

We started with a 100 fold dilution of antibody material added to GT-4 extract. No effect was seen so we used a 10 fold dilution. No effect was seen at this concentration so we utilized a 1 to 1 concentration. The results are shown in the Figure 44.

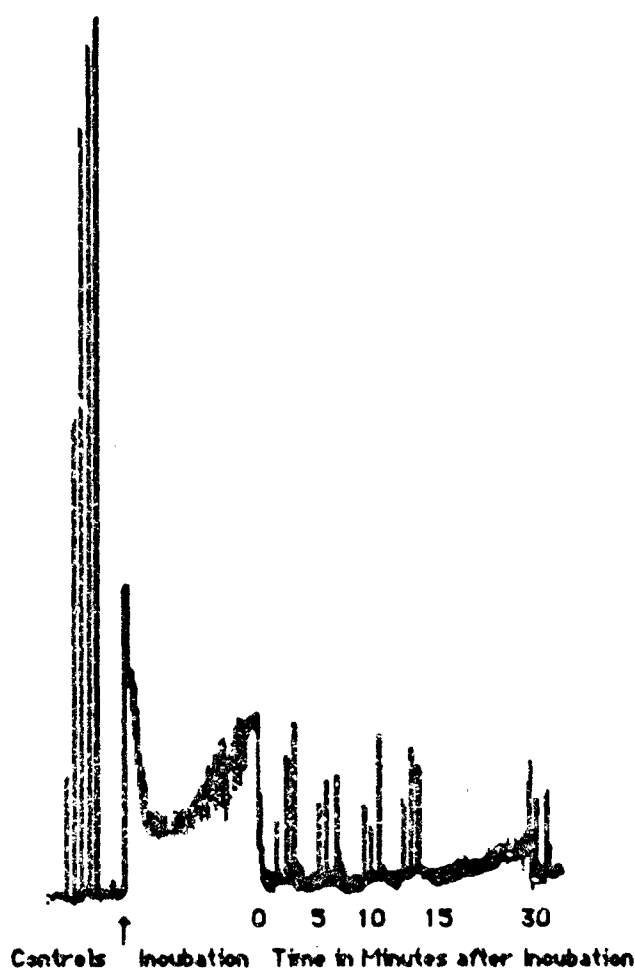


Figure 44. Controls were acetylcholine (1×10^{-6} , 3×10^{-6} , 5×10^{-6} , 7×10^{-6} , and 9×10^{-6}) A $5 \mu\text{l}$ aliquot of a 1:10,000 dilution of GT-4 was added to $1 \mu\text{l}$ of anti-brevetoxin preparation, incubated for 10 minutes and applied to ileum preparation at arrow. After a 15 minute incubation the preparation was inhibited 87%.

It is quite apparent that the antibodies had no effect on the efficacy of GT-4 ("MTX") on the ileum preparation. Next, inasmuch as we had some fish toxin in storage that was provided by Dr. Michael Capra (Queensland Institute of Technology) we utilized the same procedure to test the efficacy of the anti-brevetoxin preparation against it.

Again the conclusion was that the antibodies had no protective effect for the ileum when toxic fish extracts were applied. Finally, we utilized an aliquot of GT-1 ("CTX") prepared from *G. toxicus* to see if in fact it would react.

We have repeated these experiments several times without results. I think that the conclusions right now are that, at least with the ileum preparation, brevetoxin antibodies provide no protection from either GT-4, GT-1 nor toxin isolated from toxic Australian fish. We have provided Dr. Poli with samples of the same toxins we utilized (GT350 GT-1; GT350 GT-4; GT175 GT-1; and GT175 GT-4) to see if they work better on his system.

Separation of Toxic Components.

In the separation of the toxic components, clone 350 and clone 175 are treated separately. This is because crude methanolic extracts of clone 175 are ten times as pure with respect to toxin as opposed to clone 350. Clone 175 has an approximate concentration of 120 MU per milligram whereas clone 350 extracts have only 18 or so. The difference between the two is essentially lipids. Clone 350, then, represents much more of a challenge in the separation process than clone 175.

Separation of Clone 175 Extracts.

After comparing the results from several "first-step" treatments of crude methanol extracts from clone 175 we have concluded that small-scale liquid-liquid partitioning would yield the highest quantity and quality of toxic products. An example of such a separation and results thereof are shown in Figure 45. Without consideration of the weakly toxic ESAF fraction, we consistently recovered over 80% of the total MU's in the more potent ESMF and WSMF fractions. Other methods utilized for large-scale purification of ESMF and WSMF (from clone 175) developed include: (1) acetonitrile precipitation and (2) low pressure semi-preparative C-18 reverse phase chromatography.

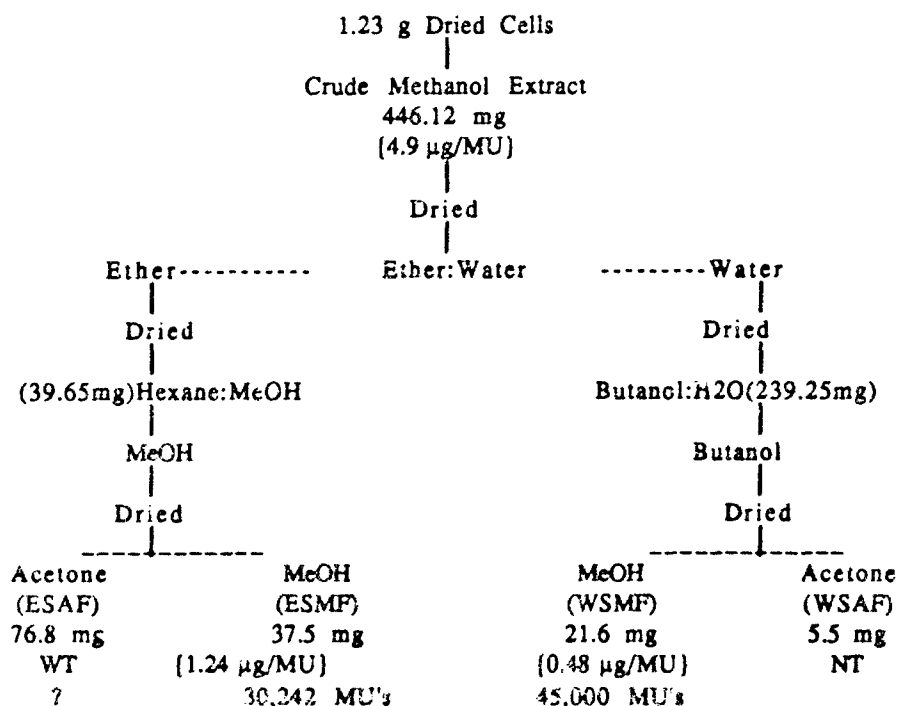


Figure 45. Results from liquid-liquid partitioning of a crude methanol extract from *G. toxicus* (clone 175).

Acetonitrile precipitation

WSMF in methanol was slowly added to acetonitrile to a final volume ratio of 2:8. The solution was allowed to stand at room temperature for 72 hours. During this period the solution was centrifuged at approximately 12 hour intervals. After 72 hours the precipitate was removed and assayed for potency using 20 g mice (some were assayed using the guinea pig ileum preparation). Five such treatments were completed. All supernatants displayed some degree of toxicity. These were consolidated and stored for future purification and assay. One sample of ESMF was subjected to the same treatment. Results from this purification step is shown in Figure 46.

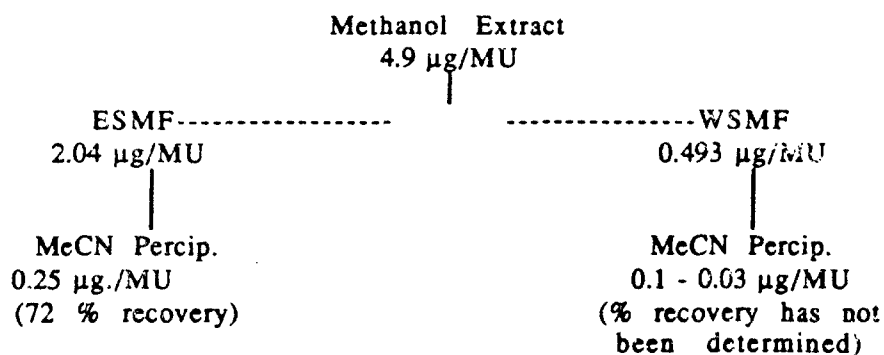


Figure 46. Results from one acetonitrile precipitation treatment.

Note that the acetonitrile treatment resulted in a 816.0% improvement in potency of ESMF and up to a 1643.3% improvement in potency of WSMF. Although this method currently yields somewhat variable results, one treatment yielded "MTX" with a potency of 0.03 $\mu\text{g}/\text{MU}$ (10% pure based upon Yasumoto's estimated MU of .003 μg). The LD₅₀ of our most potent fraction is 1.5 $\mu\text{g}/\text{Kg}$ mouse. This is the best purification of MTX reported from *G. toxicus* except for that of Yasumoto and co-workers. Results of assays of this toxin on the guinea pig ileum preparation are shown in Table 23

Table 23.
Ileum assays of "MTX" (LD₅₀ 1.5 Mg/Kg mouse)

Toxin in bath solution pg/ml	% Inhibition of ACH response	
	15 min.	90 min.
1.5	0.0	5.54
15.0	64.5	72.15
150.0	100.0	100.00

This is the most potent "MTX" fraction which we have assayed with the ileum preparation. The irreversible nature of this toxic fraction is consistent with previous reports for MTX. Also, these results confirm our previously reported ratio of 2000 ileum units to one mouse unit (0.015 ng (ileum unit) X 2000 = 30 ng (mouse unit)).

We continued to investigate the acetonitrile (ACN) extraction of the WSAP extract of *G. toxicus*. Five hundred μ l of the water soluble extract was dried down and submitted to acetonitrile extraction. The acetonitrile was decanted off leaving an ACN-insoluble residue. The result was an ACN-insoluble and an ACN-soluble division of the original water soluble extract each of which was dried down and diluted up to 500 μ l with dry methanol.

When tested on the ileum both fractions were toxic, but produced subtle differences. Subsequent second and third extractions of the original water soluble extract with ACN were not toxic to the ileum. These results led us to conclude that there are in fact two or more toxins in the water soluble extract and the ACN-soluble fraction is perhaps less polar than the ACN-insoluble portion.

Further purification of bulk quantities of toxic extracts of clone 175 was accomplished using two other basic approaches. This was predicated on the assumption that the method which yielded the highest recovery of the most potent material would become our standard.

C18 fractionation.

The second method involved low pressure C18 fractionation into three major components (brown {containing polar toxin(s)}, yellow, and green {containing less-abundant less-polar toxin}) followed by preparative HPLC of the brown fraction. This treatment yields 90-100% of the total mouse units (in two fractions) with potency as high as 2.9 μ g/MU. Major impurities in these two fractions are limited to chlorophyll- c_2 , peridinin, and one or a few heavy unknown compounds which absorb at 210 nm. Initial analytical HPLC fractionation of the above fractions yielded products with a potency as high as 1.09 μ g/MU (with nearly 100% recovery). The latter value represents an LD₅₀ of 55 μ g/Kg mouse. Although quantities obtained by analytical HPLC are small, they are quite sufficient for experimentation using nerve-muscle preparations and primary cell cultures.

TABLE 24.
LOW PRESSURE LIQUID CHROMATOGRAPHY OF ESMF

Fraction	Solvent	Volume ml	Weight mg	Potency $\mu\text{g}/\text{MU}$	Total MU
1	Acetone	2.0	.06	NT	
2	Acetone	1.0	.39	NT	
3	Acetone	1.0	.96	.265	3623
4	Acetone	1.8	1.35	.9	1519
5	Acetone	2.0	.24	NT	
6	Acetone	15.0	.69	NT	
7	Acetone+	7.0	.45	NT	
8	Chloroform precip.	14.0	4.14 6.89	6.0 NT	690
9	Chloroform+	5.0	.51	NT	
10	Methanol	2.0	.60	1.5	400
11	Methanol	4.0	.54	.9	600
12	Methanol	5.0	.18	NT	
13	Methanol	15.0	.30	NT	
14	Methanol	10.0	.15	NT	
TOTAL			17.45		6832 (82 %)

Toxic products (ESMF and WSMF) from *G. toxicus* (clone 175) were subjected to low pressure liquid chromatography using a C-18 column (1.5 X 6.5 cm) and successive solvent applications including acetone, 95% chloroform:methanol, and methanol. Results from such a treatment of ESMF are shown in Table 24. The starting sample of ESMF (16.99 mg in 1 ml of methanol) was applied to a C-18 column which was preconditioned with acetone. The potency of the sample was 2.04 $\mu\text{g}/\text{MU}$ (total 8328 MU)

Clearly, this first-step chromatographic treatment accomplishes considerable purification. For example, fraction 3 (.960 mg) displayed a potency of 0.265 $\mu\text{g}/\text{MU}$ which represents a 769.8% increase in purity. More importantly, this procedure appears to have resulted in the separation of the two different toxins expected in the ESMF fraction (fractions 3, 4, and 8 appear to be of the "CTX" type; whereas, fractions 10 and 11 appear to be of the "MTX" type). This procedure was used for separation of several additional ESMF

fractions. Preliminary mouse assays revealed results similar to those shown in Table 24.

Silicic acid chromatography.

The third method for initial bulk purification of methanol extracts tested was standard silicic acid column chromatography. We were successful in processing 200-300 mg levels of crude toxin with yields having potencies approaching 1 $\mu\text{g}/\text{MU}$. However, recovery of material with this potency is at the 40-50% level. The remaining toxin is not lost but recovery requires laborious rechromatography. We are attempting to increase purity of all toxic fractions from the silicic acid column using preparative TLC. Preliminary results are promising. Initial mouse assays of toxin from one TLC treatment revealed potencies at about 0.5 $\mu\text{g}/\text{MU}$ ($\text{LD}_{50} = 25 \text{ mg}/\text{Kg}$).

Return to liquid-liquid fractionation.

After evaluation of all the methods employed we initiated liquid-liquid separation which represents a return to our standard liquid-liquid partitioning procedure. As previously discussed, this method yielded two fractions containing "maitotoxin(s)" (GT3 and GT4) and one fraction containing small quantities of "ciguatoxin(s)" (GT1 and GT2). We had hoped to avoid using this method because it has consistently resulted in the loss of over 50% of the toxic activity present in the initial methanol extract. However, after numerous experiments with varying solvent to toxin ratios, we have achieved nearly 90% recovery of the initial toxic activity in terms of mouse units. The maitotoxin fraction (GT3) which partitions to ether in the initial ether:water partitioning has a potency of 1.5 $\mu\text{g}/\text{MU}$. The bulk of the maitotoxin (GT4) which partitions to water has a potency of about 0.6 $\mu\text{g}/\text{MU}$ (48 hour mouse assay is being conducted at this time). Analytical HPLC of this fraction (GT4) shows it to be quite clean compared to the toxic fractions from single preparative HPLC and silicic acid column treatments. Interestingly, a comparison of results from analytical HPLC of GT3 and GT4 revealed the possibility that these toxic components may differ to some degree.

As a result of discussions during a contractors meeting in November, 1988, we initiated the processing of 60 g of dried cells of *G. toxicus* (clone 175). We have determined that 2 g of dried cells is the ideal sample size for extraction in workable volumes of methanol. Five 2 g samples were extracted (plus one such sample delivered on 11 November 1988 as delivery item number 0001BL). The yields from these extractions ranged from 102,782 to 169,377 mouse units per sample ($LD_{50}/20$ g mouse = 1 MU). Corresponding mouse unit values of these samples ranged from 4.6 to 3.5 μ g.

It was hoped that the quantity and purity of GT4 derived by liquid-liquid partitioning would be such that preparative HPLC or preparative TLC may be used to efficiently process large quantities with a resulting potency of about 0.1 μ g/MU ($LD = 5$ μ g/Kg mouse).

In an additional experiment eight grams of dried cells of *G. toxicus* (clone 175, harvest 9A/88D{2}) were extracted with methanol and yielded 2.56 grams of crude toxic extract. A total of 421.6 mg (100,024 mouse units) of this extract was subjected to liquid-liquid partitioning.

Crude methanol extract and the six products of the partitioning procedure were assayed using mice. The WSMF fraction was dried under nitrogen and redissolved in methanol at which point crystals formed. These were immediately removed (slowly soluble in methanol and insoluble in acetone). Acetone was added to the WSMF solution until a precipitate formed. The mixture was centrifuged to remove the acetone insoluble precipitate. This precipitate was dried under nitrogen and brought up in about 1 ml of methanol and applied to a C18 column in two 0.5 ml lots. The column was developed with acetone under low pressure. The fractions collected and their approximate total volumes were 1A (3.0 ml), 1B (precipitate from 1A), 2 (5.0 ml), and 3 (37 ml). A final fraction, 4 (27 ml) was collected using methanol. Each fraction was assayed using mice. LD-50 determinations were completed using female mice (Harlan Sprague Dawley ICR 'BR') weighing 18-22 g. Doses of toxic fractions were suspended in 0.5 ml of 0.15M NaCl containing 1%

Tween 60 and administered by intraperitoneal injection. Control mice were injected with carrier only. Four mice were injected with each of four doses of geometrically increasing concentrations. All mice were monitored for 48 hours. LD-50's were calculated using moving average interpolation tables provided by Weil.^[80] One mouse unit (MU) is the LD-50 for individual 20 gram mice. Toxic fractions also were assayed using the guinea pig ileum preparation as previously described.

TABLE 25
A SUMMARY OF THE TREATMENT OF 8 GRAMS OF DRIED CELLS OF
GAMBIERDISCUS TOXICUS (CLONE 175, HARVEST 9A/88D[2]) AND RESULTS
AND ACCOUNTING OF TOXIN IN THE VARIOUS PURIFICATION STEPS.

FRACTION RECOVERY	TOTAL WT WT(mg)	POTENCY $\mu\text{g} / \text{M U}$	TOTAL MU	%
CELLS	8000.00			
MEOH EXTRACT	2561.63	4.215	600,232	
↓ MEOH EXTRACT RETAINED				
↓ MEOH EXTRACT LIQUID-LIQUID PARTITIONED				
↓ ESMF	37.50	0.920	40,823	
↓ WSMF	19.00	0.350	54,288	95.1
↓ CRYSTALS (1 & 2)	0.60	0.700	857	
↓ ACETONE SOLUBLE	12.54	4.180	3,000	7.1
↓ ACETONE PRECIPITATE	5.86	0.116	50,431	
↓ C18 COLUMN				
↓ FRACTION 1A	1.14	1.500	760	99.4
↓ FRACTION 1B*	0.69	0.014	48,936	92.3

FRACTION 2	0.60	1.500	400	
↓				
FRACTION 3	0.06	NT	---	
↓				
FRACTION 4	1.	NT	---	

*Delivered to Dr. Judy Pace (621 µg in 3 ml, #0001BR)

A summary of the results of the above treatment is shown in Table 25. Liquid-liquid partitioning yielded two toxic fractions (ESMF and WSMF) which accounted for 95.1% of the total mouse units present in the initial crude methanol extract. Treatment of the WSMF on the C18 column resulted in a single fraction (1B) containing 92.3% of the total mouse units present in the WSMF. A total of 99.4% of the beginning mouse units in the WSMF was accounted for in the various fractions. Fraction 1B contained 0.690 mg of toxin with an LD-50 of 0.7 µg/Kg mouse (0.014 µg/MU). Based upon Yasumoto's estimation of the LD-50 of pure maitotoxin (0.15 µg/Kg mouse), our Fraction 1B is approximately 25% pure.

The effects of this fraction on the ileum have been remarkable. For example, a concentration of 0.023 pg/ml of bathing solution caused 67.31% and 77.9% inhibition of the acetylcholine response in the ileum at 15 and 90 minutes (respectively) after incubation. A concentration of 0.0115 pg/ml caused 36.97% and 28.25% inhibition following the same procedure.

Experience with this method of separation has shown that the most efficient amount to work with in the liquid-liquid extraction process is 2 grams of crude. Amounts larger than this seem to lead to increased loss of toxin. The reason for this is not apparent at this time. Therefore, owing to the fact that the liquid-liquid separation is done 2 grams at a time, separation of large quantities takes longer.

A total of 13 g of dried *G. toxicus* (175, harvests 9A88D, 11A88D, and 3B89D) was extracted for the purpose of purifying GT-4 (MTX). Four g were expended in attempts to improve our purification procedure. We were successful in collecting a significant amount of

relatively pure MTX from the remaining 7 g of cells. Extraction and purification of an additional 2 g has been initiated. A summary of the products of this purification are included in Table 25.

When the total 9 g has been taken through our preliminary purification series, we will have accumulated over 21.24 mg of MTX with a purity of 0.03-0.07 $\mu\text{g}/\text{mouse unit}$. This represents a total of more than 362,904 mouse units. Assuming a mouse unit equivalent for pure MTX to be 0.003 μg (based upon Yasumoto's best estimate), our total collection of 21.24 mg (5.1% pure) contains 1.09 mg of MTX.

You will note in Table 25 that there was a significant amount of toxin which partitioned to ether and ended up in the ESMF fractions. We believe that this fraction contains MTX or a derivative thereof. However, it may contain quantities of ciguatoxin (CTX) as reported by other researchers. We are trying to develop new methodology which will help us determine the presence and quantities of multiple toxins in the ESMF fractions.

TABLE 26.
PRODUCTS OF EXTRACTION AND PURIFICATION OF MAITOTOXIN FROM
GAMBIERDISCUS TOXICUS (175).

HARVEST	FRACTION	TOTAL WEIGHT mg	$\mu\text{g}/\text{MU}$	TOTAL MU's
11A88D 1B	DRIED CELLS	1,000.00		
	MEOH EXTRACT	307.50	2.49	148,795
	HEXANE	48.00	NT	NT
	ESAF	51.50	NT	NT
	ESMF	29.00	0.60	48,333
	WATER	222.60	NT	NT
	WSAF	NA		
	WSMF (MTX)	30.00	0.40	75,000
	C18 2B (MTX)	1.68	0.03	56,000
	C18-3	23.04	1.40	16,457
	C18-4	2.16	NA	NA
3B89D 1AB	DRIED CELLS	2,000.00		
	MEOH EXTRACT	645.00	2.346	274,936
	HEXANE	92.00	NT	NT
	ESAF	119.50	NT	NT

	ESMF	62.00	0.60	103,333
	WATER	317.52	NT	NT
	WSAF	1.56	NT	NT
	WSMF (MTX)	33.75	0.27	125,119
	C18-2B (MTX)	5.06	0.069	73,000
	C18-3B & 4 (MTX)	0.60	0.07	8,571
	C18-3A	17.16	2.86	< 6,000
3B89D 2AB	DRIED CELLS	2,000.00		
	MEOH EXTRACT	667.00	2.30	290,000
	HEXANE	93.25	NT	NT
	ESAF	122.00	NT	NT
	ESMF	72.50	0.70	103,571
	WATER	316.79	NT	NT
	WSAF	2.88	NT	NT
	WSMF (MTX)	35.72	0.236-.365	124,469
	PRECIPITATE (MTX)	4.40	0.063-.069	67,000
	SOLUBLE	12.66	2.00	6,342
3B89D 3AB	DRIED CELLS	2,000.00		
	MEOH EXTRACT	669.00	< 3.33	> 200,900
	HEXANE	89.60	NT	NT
	ESAF	119.50	NT	NT
	ESMF	57.00	0.60	95,000
	WATER	310.69	NT	NT
	WSAF	0.96	NT	NT
	WSMF (MTX)	33.08	0.279-.357	104,569
	IN PROGRESS (EST. MTX)	> 4.50	0.06	> 75,000
3B89D 4AB	DRIED CELLS	2,000.00		
	MEOH EXTRACT	652.50	2.23	292,600
	IN PROGRESS (EST. MTX)	5.00	< 0.06	> 83,333

During 1990, we initiated a series of liquid-liquid separations of the major toxic fractions of *G. toxicus* (175) in order to accumulate quantities sufficient for completion of purification. Representative samples of crude methanol extract and the water soluble and ether soluble toxic fractions were delivered to USAMRIID for assay using rats (Table 27.).

TABLE 27.
CRUDE *GAMBIERDISCUS* TOXIC FRACTIONS DELIVERED TO USAMRIID FOR
RAT ASSAY (HARVEST 3B89D 5(AB).

TOXIC FRACTIONS (in MeOH)	VOL (ml)	TOTAL WT(mg)	MU (-g)	TOTAL MU's	MU/μl
---------------------------	-------------	-----------------	------------	---------------	-------

1 (5AB) Crude MeOH Extract	2.9	2.15	2.23	964	0.332
2 (5B) Water Sol. (Crude MTX)	1.0	0.34	0.30	1133	1.133
3 (5B) Ether Sol. (Crude CTX/MTX)	1.0	0.71	0.806	881	0.881

In processing these separations, some of which are listed in Table 28, we noted that there was some variation in number of mouse units per mg cells harvested (crude MeOH extracts, WST, and EST). These variations appear to have been due to differences in the physiological status of cells at the time of harvest rather than alterations of the extraction and separation procedures. The results from seven separate extractions of harvest 3B89D (1AB-7AB) show the good consistency obtained with our procedure.

TABLE 28.
RESULTS FROM LIQUID-LIQUID SEPARATIONS AND MOUSE ASSAYS
COMPLETED DURING EXTRACTION OF TOXINS FROM *G. TOXICUS* 175. WST=
WATER SOLUBLE TOXIN (CRUDE MTX); EST= ETHER SOLUBLE TOXIN (CRUDE
CTX+MTX); MU= MOUSE UNIT (ONE MU= LD50/20G MOUSE, IP INJECTION)

HARVEST	CELLS (mg)	MEOH EXT.		WST		EST	
		(mg)	(MU)	(mg)	(MU)	(mg)	(MU)
5A88D1AB	2000	537	111991	63.8	45425	20.0	3641
5A88D2AB	2000	522	101754	68.0	38558	14.0	2064
11A88D2AB	2000	690	298314	39.0	83459	65.0	49815
3B89D1AB	2000	645	274936	33.8	125000	62.0	94804
3B89D2AB	2000	667	263116	35.7	124468	72.0	99042
3B89D3AB	2000	669	232292	33.1	104564	57.0	98038
3B89D4AB	2000	653	292600	29.9	104444	69.0	83334
3B89D5AB	2000	648	292583	32.0	107172	69.0	86812
3B89D6AB	2000	666	288312	35.0	128621	77.5	66601
3B89D7AB	2000	642	277922	35.0	116723	76.5	90823
4A89D1AB	2000	603	154615	27.0	105556	57.5	69445
5B89D1AB	2000	591	115205	24.0	65615	86.0	61209
6A89D1AB	2000	594	118021	31.0	48613	58.0	44753
6C89D1AB	2000	666	271837	37.5	94444	44.5	69694
7A89D1AB	2000	663	162580	26.0	60496	47.5	50174
8A89D1AB	2000	591	144287	40.5	92857	60.0	44444
9A89D1AB	2000	681	207306	39.0	166981	52.0	69418
11B89D1AB	2000	744	154846	30.0	42231	51.0	51052
1A90D1AB	2000	672	254545	32.0	132129	42.0	55642

TOTAL MU (WST + EST) = 2, 978, 161 or 74.1% No significant mouse units were found in other products of liquid-liquid separation.

A total of 1772.8 mg (2,928,995 MU's) of semipurified toxins have been accumulated. This amount represents 8.79 mg of pure MTX (equivalents). We anticipated producing approximately 70 mg of toxin with an equivalent potency of about 2,300,000 MU's (estimated MU = 0.03 mg or 10% pure). Several WST fractions have been purified to a level of 6% purity (MTX equivalent).

Discussion of clone 175 separation procedures. Much as we reported for separation of clone 350 we experience a loss of toxicity (ca. 25%) as we progress from crude extracts to the two toxic endproducts. We have no proven explanation for this loss; however, we speculate that the loss may be due to: alteration of the toxic compounds, loss of toxins in the rather heavy "non-toxic" end products (H₂O, hexane and ESAF), and/or there is a positive synergistic effect of two or more toxins present in the crude methanol extract.

Separation of Clone 350 Extracts.

Sep-pak separation.

It was at first thought that sep-pak processing would help immensely in the extraction of excess lipids from clone 350 extracts. When processing samples through Sep Pak C18 the color sequence is the same as that seen from HPLC. Experimentation revealed that if the sample was loaded on the sep-pak column and then eluted slowly, the methanol extract of crude was split into three different colored fractions based upon the time of elution.

The procedure for this is as follows: A sep-pak is first wetted with 2 ml of methanol. Then approximately 1.5 ml of crude methanol extract is applied to the sep-pak. This is followed by a 0.25 ml. wash to rinse the syringe. Following this one ml of methanol is flushed through the column and the initial eluent is clear but at the end of the flush is muddy brown in color. A second flush of 0.5 ml. of methanol produces a yellowish-green eluent. Following this a 1.0 ml wash produces a bright green fraction and finally, a 2.0 ml

wash produces a more viscous light green fraction. For our purposes we combine the two final washes into a green fraction.

Five ml of GT-350 Combo (=methanol crude) (9.2 mg/ml) was processed by the sep-pak procedure described above and labeled SK-1 br, SK-1 yel, and SK-1 gr. When these fractions were tested on the ileum, the results suggested that the toxic moieties in the three fractions are different. The initial brown fraction produces the typical GT-4 (maitotoxin) effect on the acetylcholine response of the ileum.

The yellow intermediate produces the effects we have seen previously with GT-2, but at this point it is hard to judge. It may simply be a combination of small amounts of GT-1 and GT-4. It is interesting to note, that this fraction has a very pronounced inotropic effect upon the ileal preparation. Nevertheless, the ileum preparation, with successive washes, recovers from the effects of the toxin and at the end of the run is stimulated. The amount of total toxin in this fraction was too small to justify retention. Thus 99% of the toxicity occurs in the brown and green fraction from sep-pak separation with the majority occurring in the brown.

The green fraction produces the reversible GT-1 (or ciguatoxin effects) that we have reported before. We conducted an experiment to assess the relative scale up factor between ileum units and mouse units for ciguatoxin. Our ileal results were summarized as follows.

TABLE 29.
EFFECTS OF TOXIC EXTRACTS ON ILEUM AT LOW DOSES

Fraction from		Assay	Inotropic	Onset of	Recovery
Chrom.	Sep Pak	type	response	inhibition	%
GT-1	Green	CIX	0	gradual	100%
GT-2	Yellow	MTX	+++	immediate	100%+
GT-3	Brown	MTX	++	gradual	Partial
GT-4	Brown	MTX	+	gradual	none

The same fractions were examined on UV-Vis spectrophotometer and the results are shown in Figure 47.

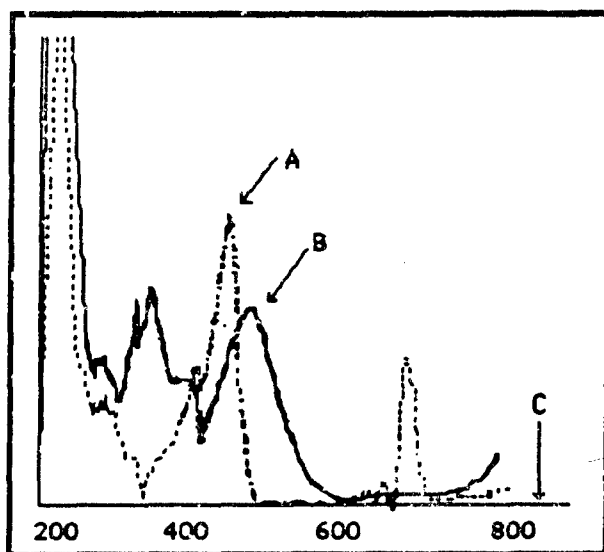


Figure 47. UV-vis spectra of the yellow (A), brown (B) and green (C) fractions (SK-1) from the sep-pak separation of crude methanol extract of *Gambierdiscus toxicus*.

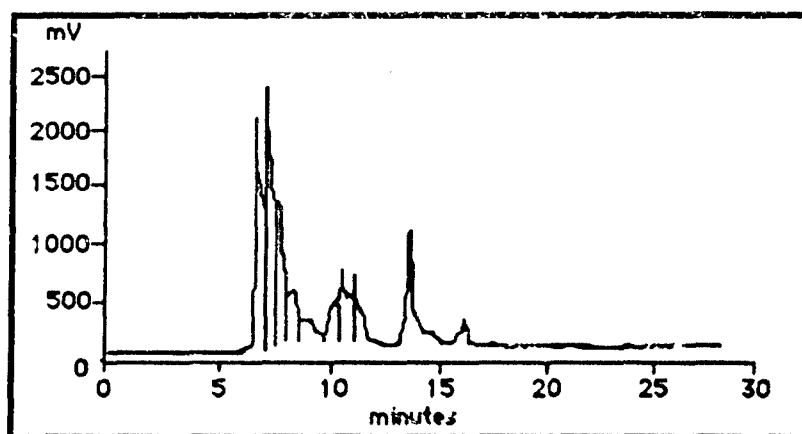


Figure 48. Analytical HPLC chromatograms of the brown fraction (SK-1) from the sep-pak separation of crude methanol extract of *Gambierdiscus toxicus*.

The UV-Vis scans indicate that both the brown and the yellow fraction have maxima at 209-10, 267 and 314. The brown fraction has distinct maxima at 388 and 510, and the yellow has a distinct

maxima at 450. The green did not have a distinct maxima, perhaps due to an insufficient concentration.

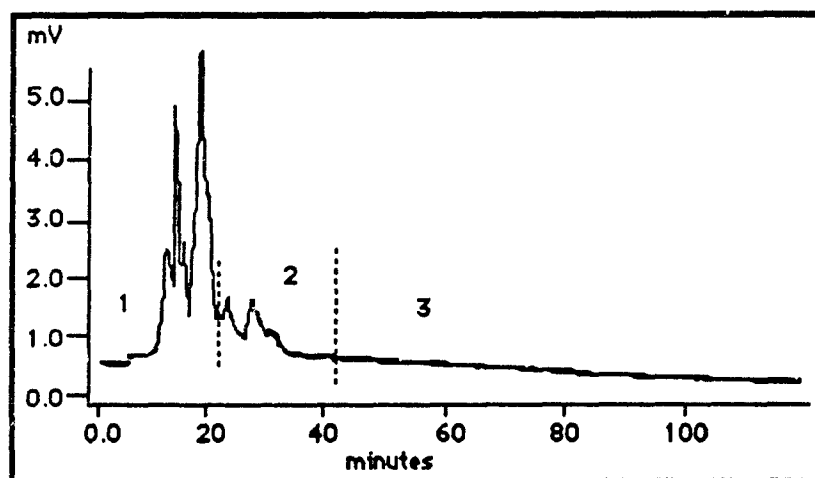


Figure 49. Semipreparative chromatogram of the yellow fraction from (SK-1) the sep-pak separation of crude methanol extract of *Gambierdiscus toxicus*.

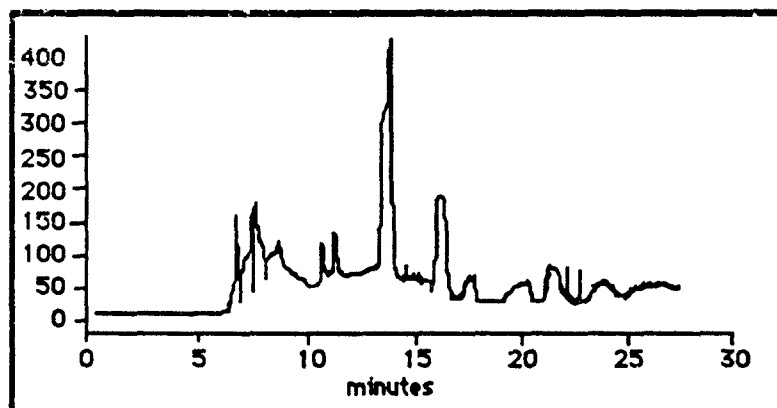


Figure 50. Analytical HPLC chromatograms of the green fraction (SK-1) from the sep-pak separation of crude methanol extract of *Gambierdiscus toxicus*.

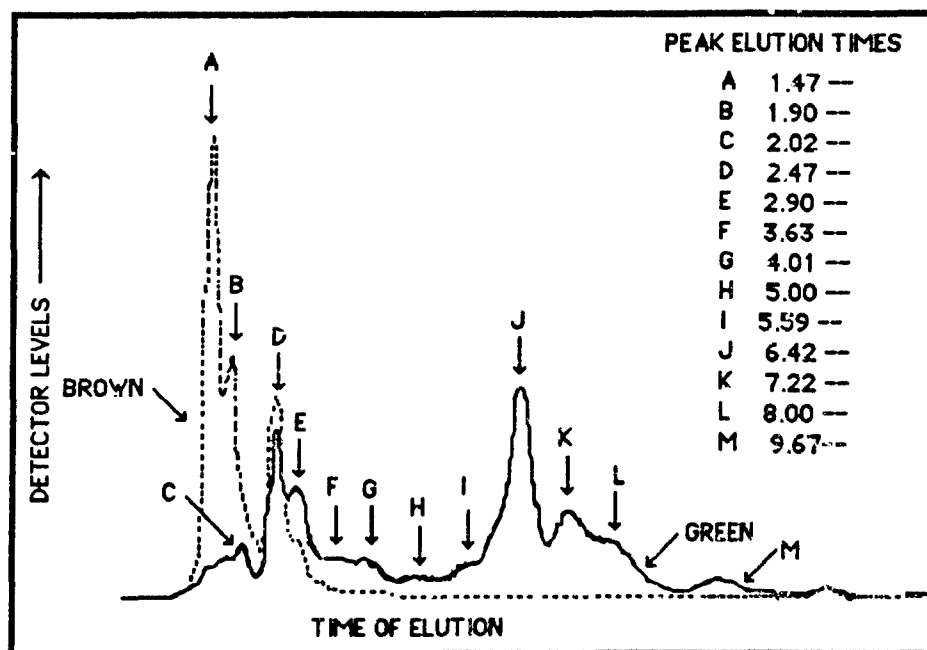


Figure 51. Comparison of analytical HPLC chromatograms of Sep Pak brown and green. Running conditions were: Novapak 5 micron C-18 silica gel, 3.9 mm X 7.5 cm column, and 100% methanol as solvent, run time 20 min.

Aliquots of the sep-pak separation were then run on HPLC and the results are shown in Figures 46-49.

In the Sep Pak C-18 separation process, the brown portion, When examined at 210 nm using HPLC chromatography, shows four major composite peaks (A, B, D, and E in Figure 51). Only two of these, D and to a small extent E, are common to the green fraction. The green fraction has the major portion (i. e. 11 major composite peaks) of the 210 scan.

TABLE 30.
QUANTITATION OF CRUDE TOXIC COMPONENTS BY ILEUM ASSAY
SEP-PAK SEPARATION OF ONE ML OF CRUDE G. TOXICUS EXTRACT (9.2 MG/ML)

FRACTION OF CRUDE	COLOR OF FRACT	% OF FRACT	TOTAL ACTIVITY *MU-MTX	SPEC ACTIVITY MU/μg	WEIGHT ACTIVITY μg/MU	% PURITY (note 1)	% YIELD
Crude Ext	Dk Br	100.	300	.0326	30.6	.0098	100
Void	Clr	0	0	0	0		

Brown	Brown	83.16	210	.0236	42.3	.0070	70%
Yellow	Yellow	2.71	0.16	.0006	1558	.0001	.05%
Green	Green	7.48	*1.8	.4048	.00247	*	.6%
Straw	Cream	2.89	>>1	n d			
Flush	Cream	3.74	0	n d			

Note 1. To calculate % purity by weight we tentatively accepted Yasumoto's value for a mouse unit being 0.003 μ g/. Therefore the % purity is calculated as:

$$\% \text{ purity} = \frac{\text{weight of pure or .003 } \mu\text{g}}{\text{weight of impure } \mu\text{g}} * 100$$

Note 2. MTX ileum equivalent unit (MIEU) is 50% inhibition at 90 minutes following a 15 minute incubation with toxin. CTX ileum equivalent unit (CIEU) is 50% inhibition with toxin continually present in the physiological saline for at least thirty minutes and full recovery after a wash of saline contain no toxin.

Note 3. The LD₅₀ values used in this table are estimates based upon preliminary mouse data and the actual graph and LD₅₀ value will be reported in the next quarterly.

* indicates a CTX assay rather than an MTX assay on the guinea pig ileum

In the initial Sep-Pak separation, we achieved a virtually complete separation of GT-1 & 2 and GT-3 & 4, we have only doubled the sample volume and achieved a ten fold increase in purity but lost 30% of the toxicity. Indeed, this may only be an apparent loss, inasmuch as we have no immediate way to assess the contribution of the GT-1,2, and GT-3 toxins in relatively high concentration in the crude to the toxicity seen in the ileum assay for MTX.

Further processing of the brown sep-pak fraction from SK-1. The brown fraction was run on the semipreparative as SP-9 and tested on the ileum - the results are shown in Figure 52.

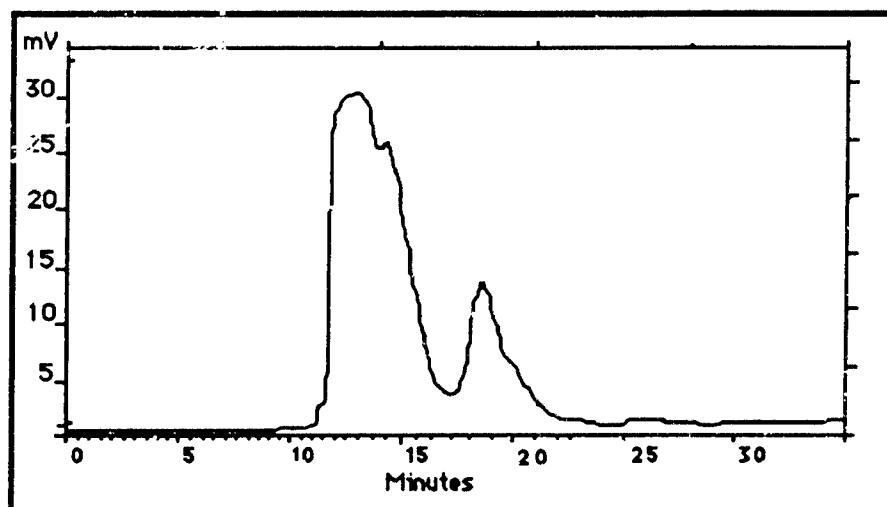


Figure 52. Semipreparative chromatogram (SP-9) of the brown fraction from the sep-pak treatment (SK-1) of crude methanol extract.

Because fraction SP9F4 showed most of the MTX activity it was reprocessed on the semipreparative HPLC as SP10. The area which demonstrated the most MTX activity on the ileum preparation was SP10F4. Concomitantly we began experiencing blockage of the HPLC systems due to fine precipitates. It was at this point that we experimented with the formation of crystals.

Introduction of the crystallization step in purification. Both the crystals and the supernatant of SP10F4 were assayed on the ileum preparation.

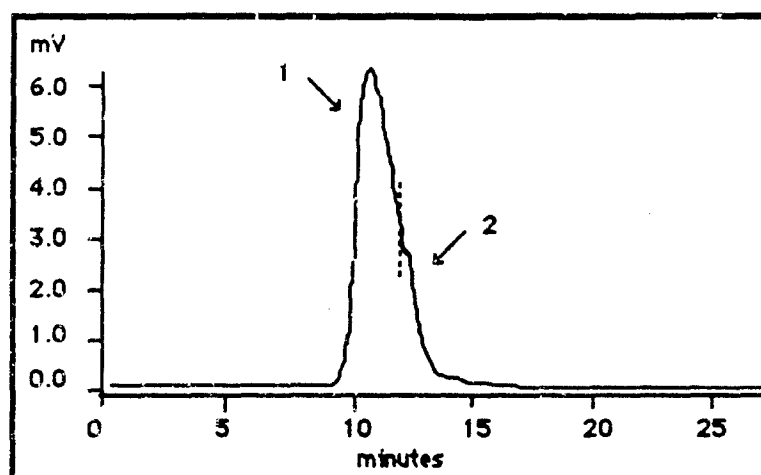


Figure 53. Semipreparative chromatogram of brown supernatant fraction from sep pak treated SK-1, crude methanol extract.

The supernatant from the crystallization step (XTL-1) contained the majority of the MTX activity (approximately 93% by ileal assay).

NMR scans were performed on fraction SP10F4 supernatant. The complete results of this and other NMR data are discussed in the section on NMR. At this point it was decided to incorporate the crystallization as a step in the purification process.

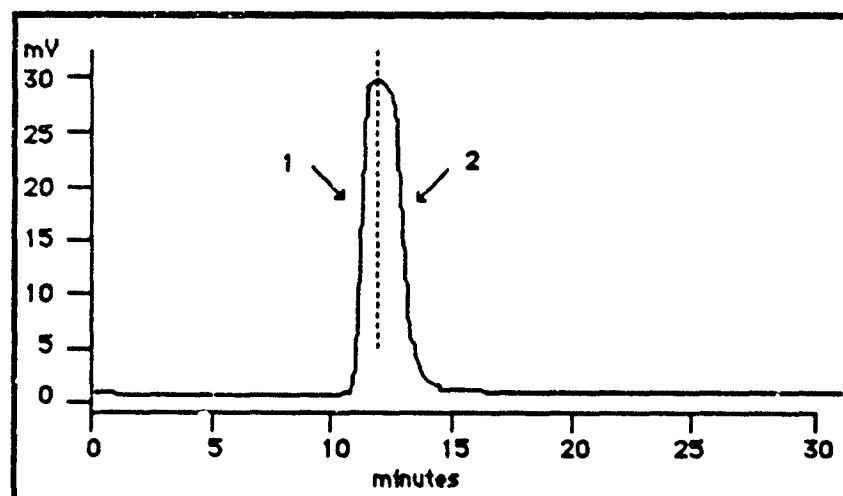


Figure 54. Semipreparative chromatogram of brown xtl fraction from sep pak treated SK-1, crude methanol extract.

Once the brown fraction is separated by means of the sep-pak treatment, the fraction is taken to complete dryness. Then small amounts of methanol are added until the crystals form. They are allowed time to settle and the supernatant decanted. These crystals have been resuspended in methanol and tested on the ileum. The toxicity level of the crystals is very low (approximately 7% of what is in the sample as determined by ileal assay) and we believe it is due to toxin trapped within the crystals when they are formed. The advantages of this step are obvious in removing a large percentage of the contaminants.

Prior to further processing of the brown fraction, it was taken to complete dryness under dry nitrogen gas and then slowly taken up in small amounts of methanol, at which time a crystalline precipitate forms. The supernatant which contains the toxicity was then decanted off.

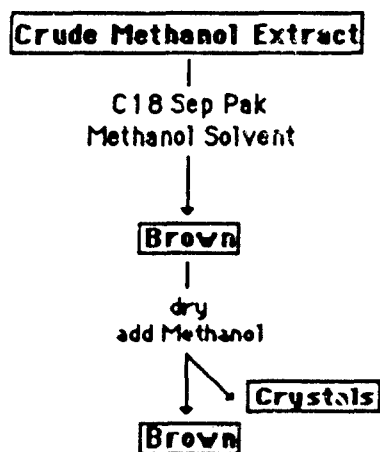


Figure 55 Diagrammatic representation of the removal of crystals from MTX brown.

The green fraction from SK-1 gr was applied to semipreparative HPLC and the resulting chromatogram is shown as Figure 54.

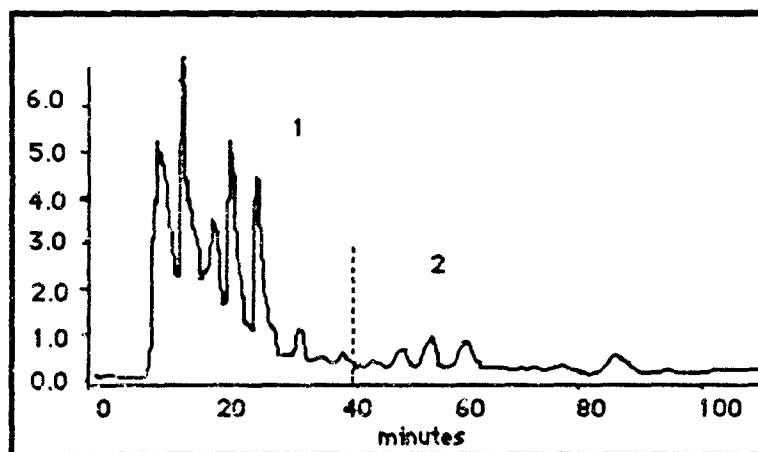


Figure 56. Semipreparative chromatogram (SP-7) of the green fraction from the sep-pak separation of crude methanol extract of *Gambierdiscus toxicus*.

The chromatogram from SP-7 shows some contamination but the significant item was the increase in the more lipid components in relation to the more polar ones. Fractions SP7F4 and SP7F5 were combined and rerun on the semipreparative as SP-8. Table 31 lists the tentative results from these experiments.

TABLE 31.
QUANTITATION OF CTX TOXIC COMPONENTS BY ILEUM ASSAY

FRACTION	COLOR	PERCENT		TOTAL	SPEC	WEIGHT	PERCENT
OF	PERCENT		ACTIVITY		ACTIVITY		
CRUDE	OF	PURITY	YIELD				
	ACTIVITY	mg%	MU-MTX	MU/ug	ug/MU	(note 1)	
CRUDE	FRACT						
Crude Ext	Dk Br	100.	300	.0326	30.6	.0098	100
Green	Green	7.48	*1.8	.4048	.00247	.7411	.6%

Note. The LD₅₀ values used in this table are estimates based upon preliminary mouse data and the actual graph and LD₅₀ value will be reported in the next quarterly.

The data we accumulated indicated that the percent of CTX in the cell extracts is small being less than 0.6% in toxicity. If we assume .009 µg/MU and there is 1.8 MU/9.2mg crude, this means that there is .0162 mg of CTX per gram of dried extract. Then there was 3.24

mg of material in the 200 grams of dried material that we had accumulated. Preliminary preparative HPLC of the green fraction indicated that toxicity eluted in a broad band within the central portion of the chromatograph.

Preparative HPLC separation of crude extracts of clone 350.

Our preliminary results with direct preparative separation of crude extract can best be understood when the results are scaled to actual detector settings and presented as a stereogram as shown in Figure 57.

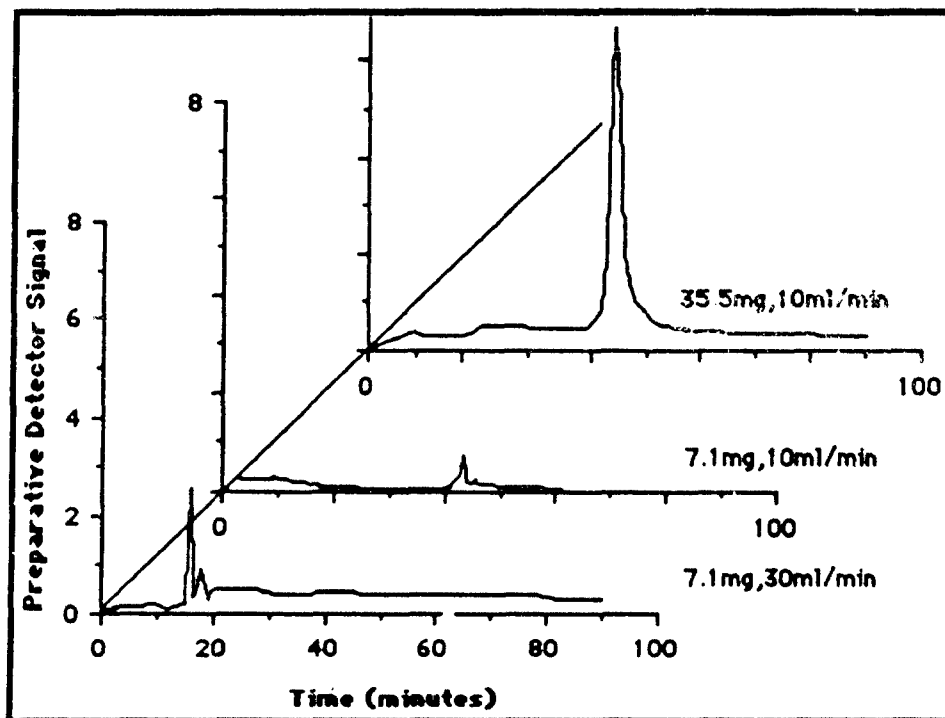


Figure 57. Comparison of preparative HPLC chromatograms of WSAP at different flow rates and quantities. Sample application and flow condition are shown on diagram. Other running conditions were: 15 micron C-18 silica gel, 5 cm X 28 cm column, and 100% methanol as solvent, run time 55+ min.

Essentially when amounts less than 10 mg of WSAP are applied to the column there is some separation of peaks, but when over 10 mg

are applied the peaks fuse into a single broad complex of peaks. Running the column at flow rates slower than 20 ml/min results in the elution of the first large 209 nm peak at 40 minutes (with increased base width of the peak), whereas flow rates greater than 20 ml/min make the 209 nm and other peaks elute earlier, but accuracy in the collection of the separate peaks is sacrificed. A flow rate of 20 ml/min was therefore instituted in later experiments.

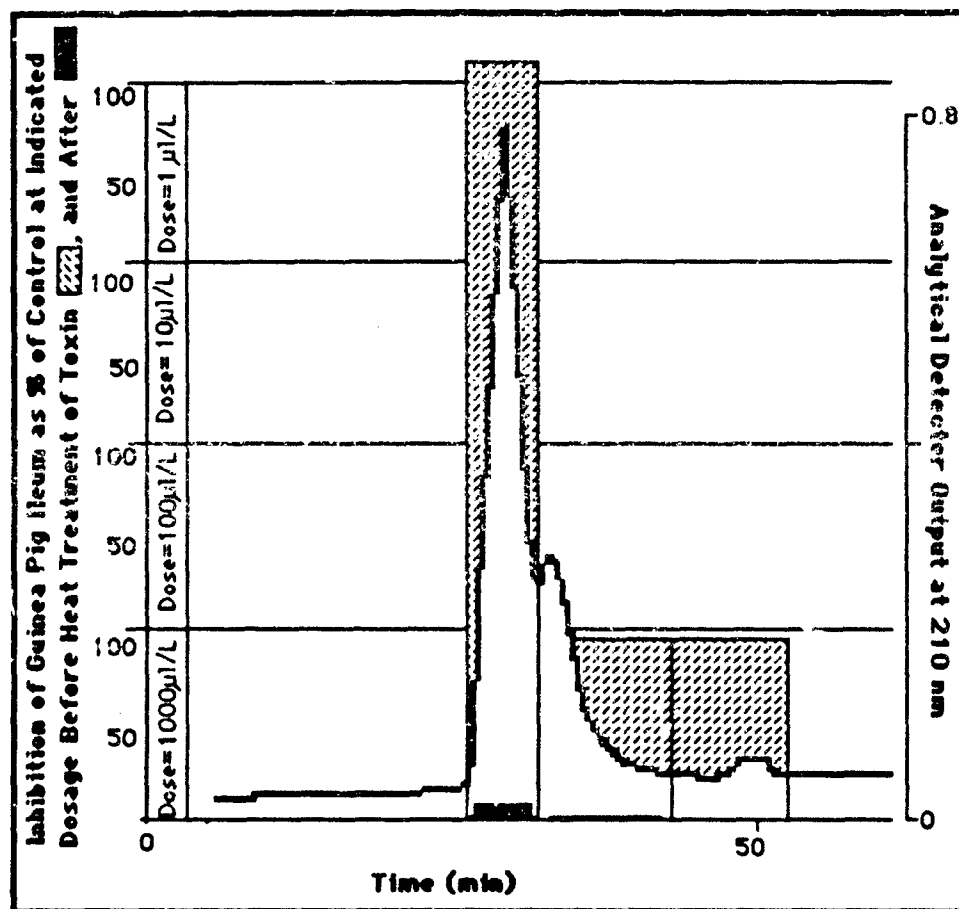


Figure 58. Preparative: HPLC chromatogram (P1) of 1 ml of WSAP (7 mg/ml). Running conditions were: 15 micron C-18 silica gel, 5 cm X 28 cm column, flow rate 10 ml/min, and 100% methanol as solvent, run time 70 min. Detector set at 210 nm.

Figure 58 is a summary of our first preparative run (P1). Three fractions were collected from this run of one ml (7 mg/ml) and

labeled fraction P1F1, fraction P1F2 and fraction P1F3. When tested on the ileum preparation most of the toxicity appeared in fraction P1F1 which contained the area of the first large 209 nm peak. Some toxicity appeared in fractions P1F2 and P1F3, but it should be noted that these two fractions had levels of toxicity that were two orders of magnitude less than the P1F1 fraction. Once the ileum assays were completed, the fractions were dried down for weighing on the Cahn microbalance. In order to speed the process of weighing them, the fractions were dried on a warm heater. However, after weighing, when the samples were put back into methanol and tested for toxicity, they had lost all their toxicity to the ileum. Our major conclusion from this experimental run was that, once the toxin is purified (or separated from the lipid) it becomes unstable to heat or it loses its potency to the ileum preparation

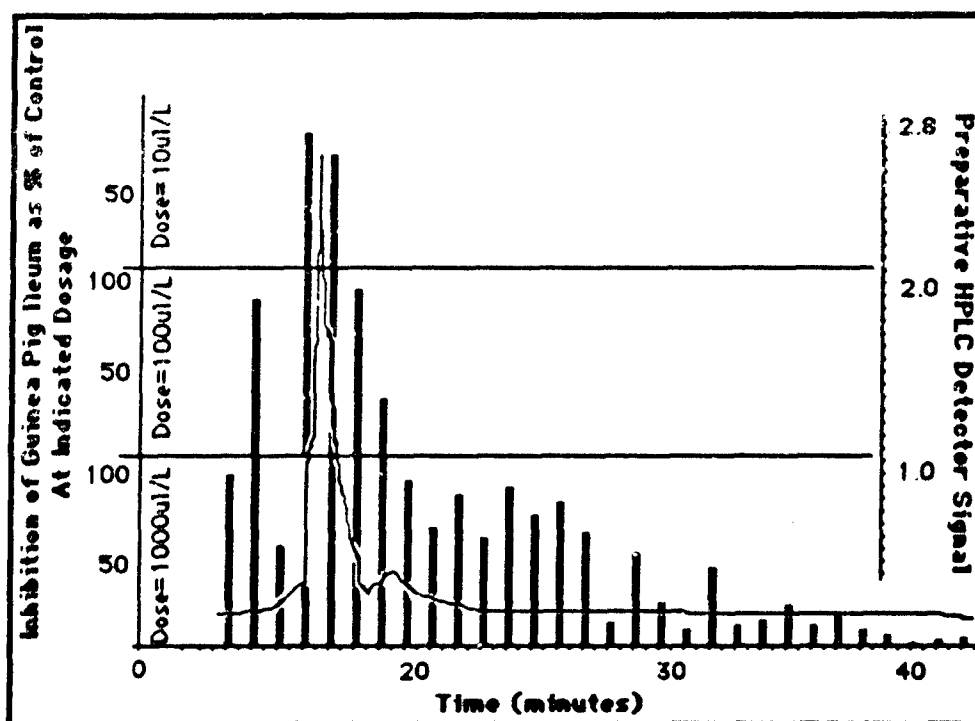


Figure 59. Preparative HPLC chromatogram (P2) of 1 ml of WSAP (7 mg/ml). Running conditions were: 15 micron C-18 silica gel, 5 cm X 28 cm column, flow rate 30 ml/min, and 100% methanol as solvent, run time 55 min. Detector set at 210 nm.

Figure 59 above is a summary of preparative run (P2) which was actually run as a control for the acetonitrile experiments that will be discussed later on in the report. In this experiment, we collected some 50 fractions (P2F1 through P2F50) from a preparative HPLC run of 1 ml of WSAP (7 mg/ml). Each of these 50 fractions were evaporated to dryness and re-solubilized in 1 ml of methanol. As in the previous experiment, the largest amount of toxicity was found to be associated with the first large 209 nm peak. Some levels of toxicity are found after the first large 209 nm peak and we surmised, at the time, that this is a smearing of the toxin in the HPLC system which comes out after adequate flushing (we now think that it was just the problem of limited solubility).

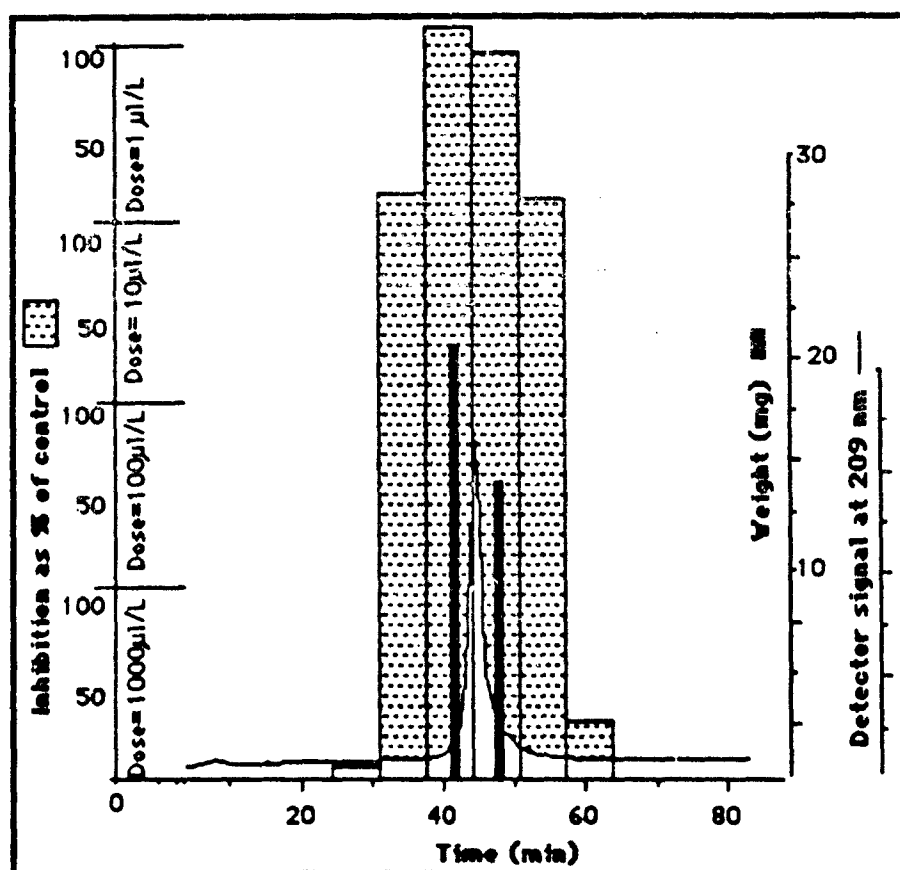


Figure 60. Preparative HPLC chromatogram (P3) of 5 ml of WSAP (a total of 35.7 mg). Running conditions were: 15 micron C-18 silica gel, 5

cm X 28 cm column, flow rate 10 ml/min, and 100% methanol as solvent, run time 65 min. Detector set at 210 nm.

Figure 60 above is a plot of the third preparative run (P3) in which five ml or 35.7 mg of WSAP was applied to the column. In this run six fractions (F1 through F6) were collected around the first large 209 nm peak. These fractions were evaporated down to 1 ml volume and aliquots taken for weighing (100 μ l) and guinea pig ileum assay (10 μ l).

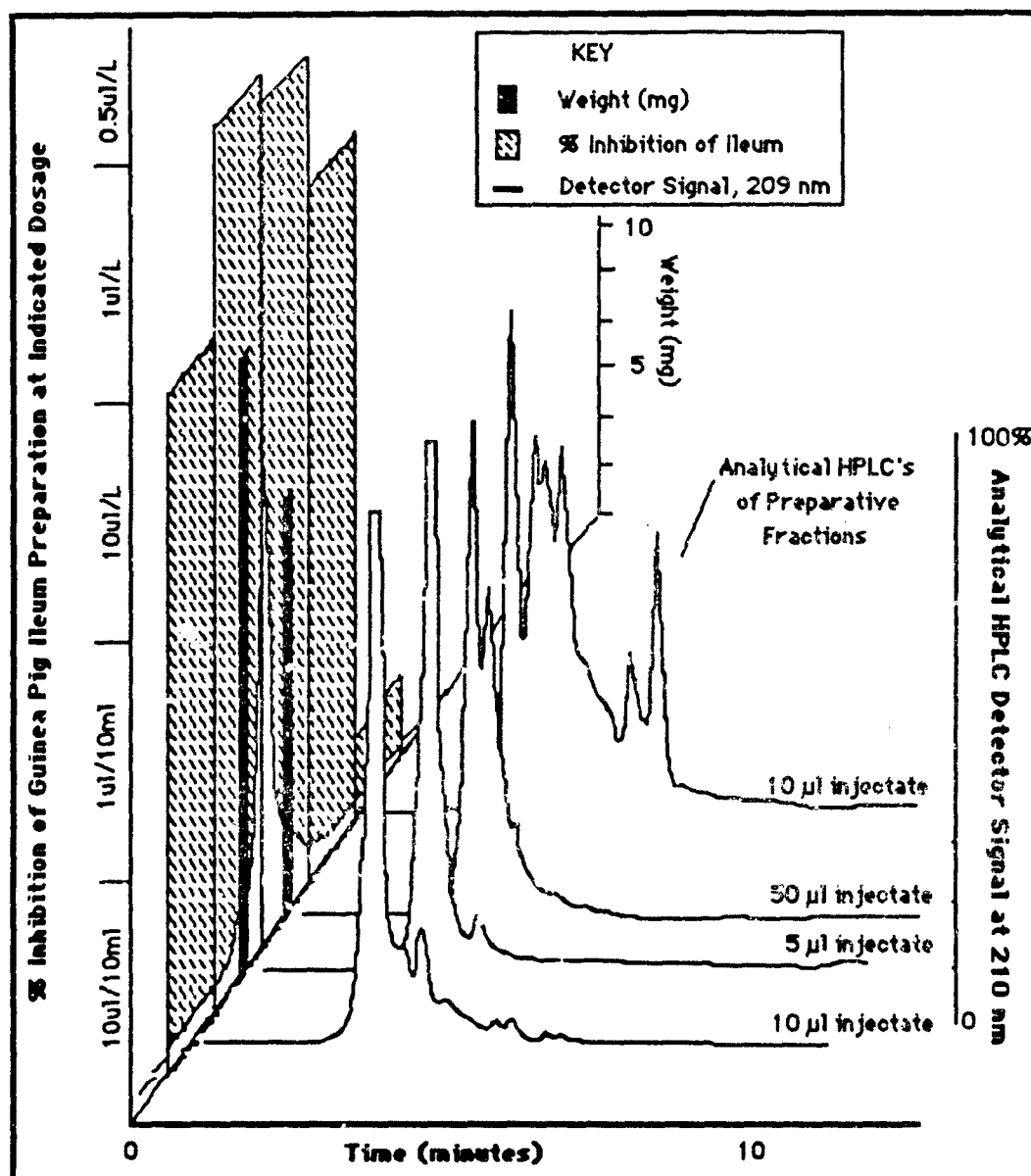


Figure 61. Preparative HPLC chromatogram (P3) of 5 ml of WSAP (35.7 mg total) compared with analytical chromatograms of the fractions collected. Running conditions were: 15 micron C-18 silica gel, 5 cm X 28 cm column, flow rate 10 ml/min, and 100% methanol as solvent, run time 65 min. Detector set at 210 nm. Other running conditions were 10 micron C-18 RCM column. Flow rate 0.5 ml/min and 100% methanol as solvent.

After weighing the 100 µl aliquot was returned to the sample. Fractions P3F3 and P3F4 associated, with the first large 209 nm peak

were the most toxic. The fractions on either side of these, P3F2 and P3F5 were an order of magnitude less toxic to the ileum. This experiment also demonstrated that the most of the weight of the sample was recovered in fractions P3F3 and P3F4. Fractions P3F5 and P3F6 were combined into one fraction.

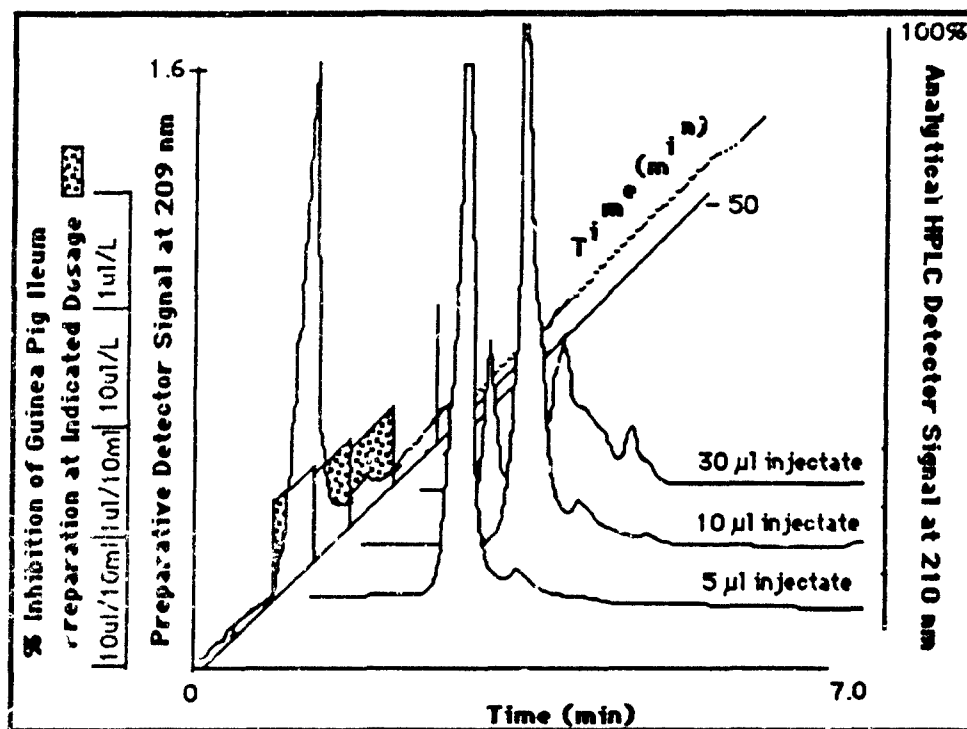


Figure 62. Preparative HPLC chromatogram (P4) of fraction P3F2 dried down to 1 ml. Running conditions were: 15 micron C-18 silica gel, 5 cm X 28 cm column, flow rate 20 ml/min, and 100% methanol as solvent, run time 65 min. Detector set at 210 nm. Other running conditions were 10 micron C-18 RCM column. Flow rate 0.2 ml/min and 100% methanol as solvent.

The fractions from the previous preparative run (P3F1 through P3F4+5) were aliquoted for analytical HPLC. Figure 62 above summarizes these results. First of all, note that different amounts of injectate were utilized for the analytical runs. Fractions P3F1A and P3F2A have the cleanest first large 209 nm peak and the narrowest base width. For each successive two fractions P3F3A and P3F4+5A, higher amounts were applied to the analytical column (implying a

lesser amount of material in the fraction), the chromatogram becomes more complex and the relative height of the first large 209 nm peak decreases.

Once the analytical chromatograms were completed for the fractions from preparative run P3, the two fractions around the first large 209 nm peak, P3F2 and P3F3, were re-chromatographed on the preparative HPLC resulting in preparative runs P4 and P5 respectively. Figure 62 above is a summary of the preparative run P4 plotted on the Y-Z plane. Three fractions were collected (P4F1, P4F2 and P4F3)

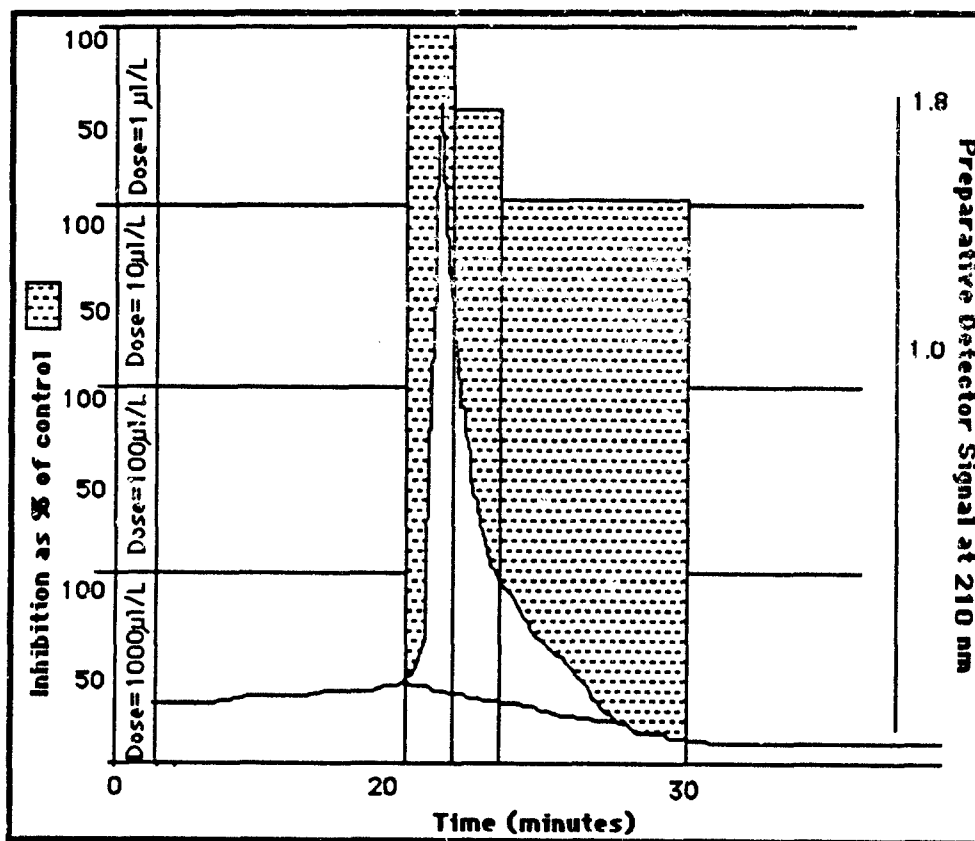


Figure 63. Preparative HPLC chromatogram (P5) of fraction P3F3 dried down to 1 ml (14.03 mg). Running conditions were: 15 micron C-18 silica gel, 5 cm X 28 cm column, flow rate 20 ml/min, and 100% methanol as solvent, run time 55 min. Detector set at 210 nm.

Analytical HPLC chromatograms of these fractions have been completed and the results are plotted on the X-Y plane. As was found in the parent separation (P3), for each successive fraction P4F1A, P4F2A and P4F3A, higher amounts were applied to the column, the chromatogram becomes more complex and the relative height of the first large 209 nm peak decreases.

The results of the re-chromatographing of fraction P3F3 in preparative run P5 are presented in Figure 63. Three fractions were collected (P5F1, P5F2 and P5F3) and aliquots of these tested on the ileum preparation.

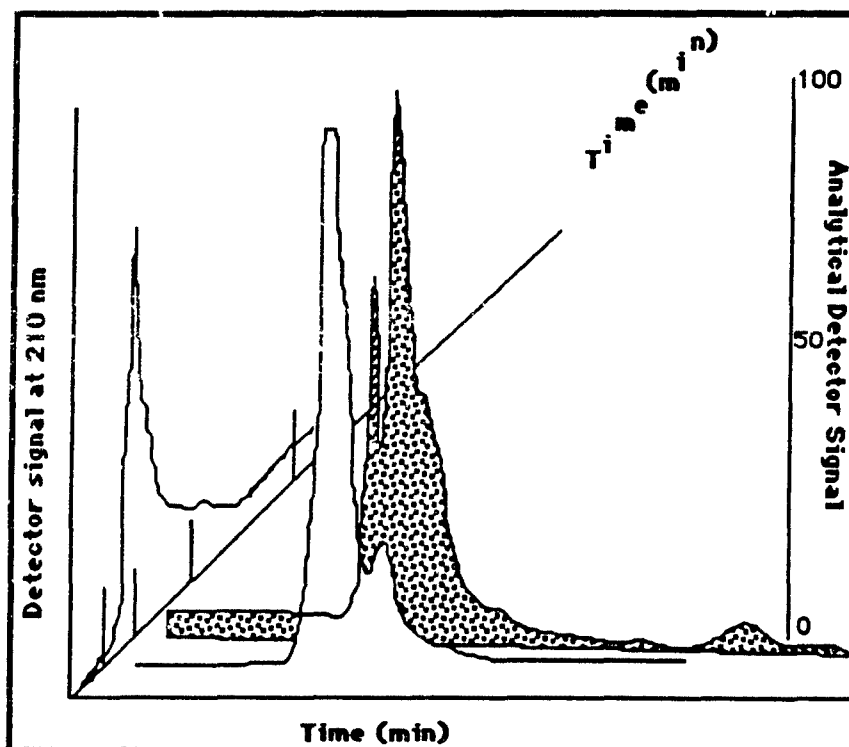


Figure 64. Preparative HPLC chromatogram (P5) of fraction P3F4 on the Y-Z plane and associated analytical chromatograms on the X-Y plane. Running conditions were: 15 micron C-18 silica gel, 5 cm X 28 cm column, flow rate 20 ml/min, and 100% methanol as solvent, run time 55 min. Detector set at 210 nm. Other analytical running conditions were 10 micron C-18 RCM column. Flow rate 0.2 ml/min and 100% methanol as solvent.

As can be seen, smaller amounts of the first large 209 nm peak are in fraction P3F3 and much larger amounts of the later, low contaminating peak are in fractions P5F2 and P5F3. Nevertheless, since we are dealing with larger samples applied to the column, the amount of toxin is significant and worth collecting. Analytical HPLC chromatograms were performed on the fractions from the fourth fraction from P3. The results are presented in Figure 64 and they confirm what we surmised from the previous preparative separation.

In an attempt to shorten the purification process and save toxin we entertained the possibility of separating the crude material from *G. toxicus* on the preparative HPLC into two fractions corresponding to the maitotoxin and ciguatoxin fractions directly. Accordingly, we initiated an experiment wherein 60 μ l of crude material was run on the semi-preparative HPLC.

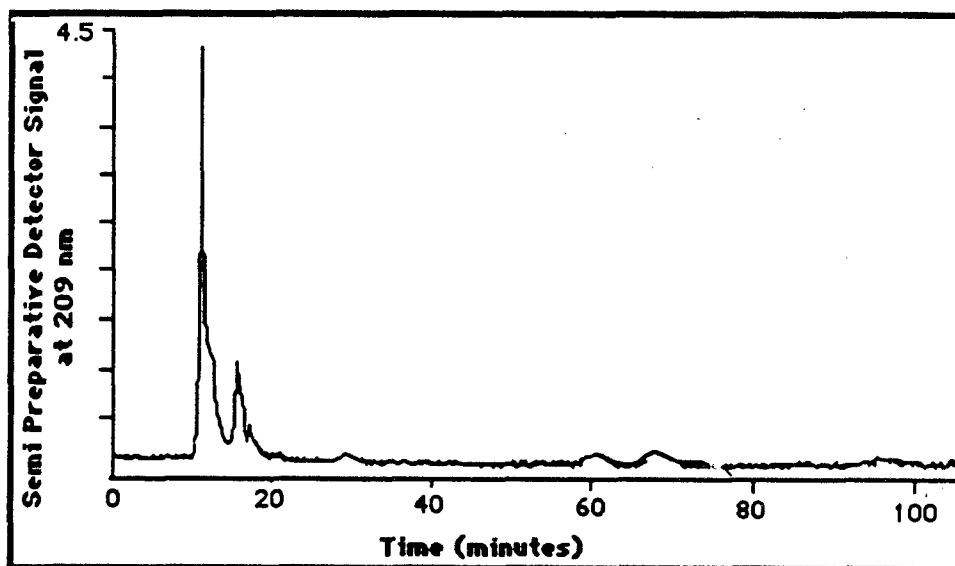


Figure 65. Semi-preparative HPLC chromatogram (SP3) of 60 μ l crude extract of *G. toxicus*. Running conditions were: 15 micron C-18 silica gel, 5 cm X 28 cm column, flow rate 30 ml/min, and 100% methanol as solvent, run time 120 min. Detector set at 209 nm.

The effluent from the semi preparative chromatography (SP3) of 60 μ l of crude *G. toxicus* extract was collected in nine fractions

(SP3F1 and SP3F9). All fraction were collected for a time period of 10 minutes with the exceptions of SP3F3 and SP3F9 which were 20 minutes in length. In this scheme of collection it is expected that GT-3,4 (maitotoxin) would elute in fraction SP3F2 and that GT-1,2 (ciguatoxin) would elute sometime after fraction SP3F5.

The semipreparative fractions were evaporated down to 200 μ l volume. Because it was expected that the most of the maitotoxin would be in fractions SP3F2 and SP3F3, 5 μ l aliquots of these were utilized for testing on the ileum preparation using the MTX procedure. In the case of the other fractions in which we expected the ciguatoxin activity, the entire fraction was used to assay for ciguatoxin on the ileum preparation.

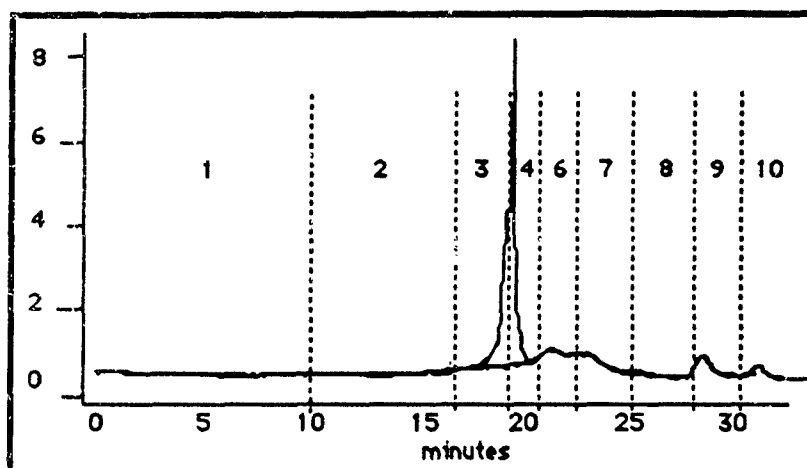


Figure 66. Preparative chromatogram (P-5) of the brown fraction from the sep-pak treatment (SK-3) and subsequent crystallization of ten ml of crude methanol extract (GT-350 Combo).

During the course of the previous preparative run P-4 it was decided that the crystallization step could be performed immediately from the brown sep pak fraction. This made the HPLC run characteristics much better and reduced the chances of fowling the column. Therefore the brown fraction (SK-3 br) was evaporated and crystal formation induced. The supernatant (XTL-1) was decanted off leaving the crystals (XTL-2). Fraction XTL-1 was applied to the

preparative HPLC (P-5) and the chromatogram from this run is shown in Figure 66.

Preparative run P-5 was collected in nine fractions as was done in the previous one ml run. Fractions P5F4 and P5F5 were assayed by ileum procedure and then combined with P4F4 and P4F5 respectively before running on the NMR.

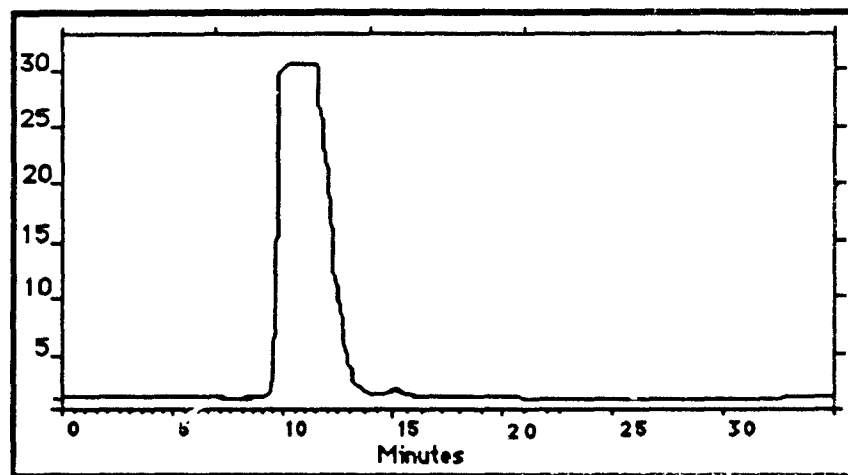


Figure 67. Preparative chromatogram (P-6) of the brown fraction (P5F6) from the preparative run P5.

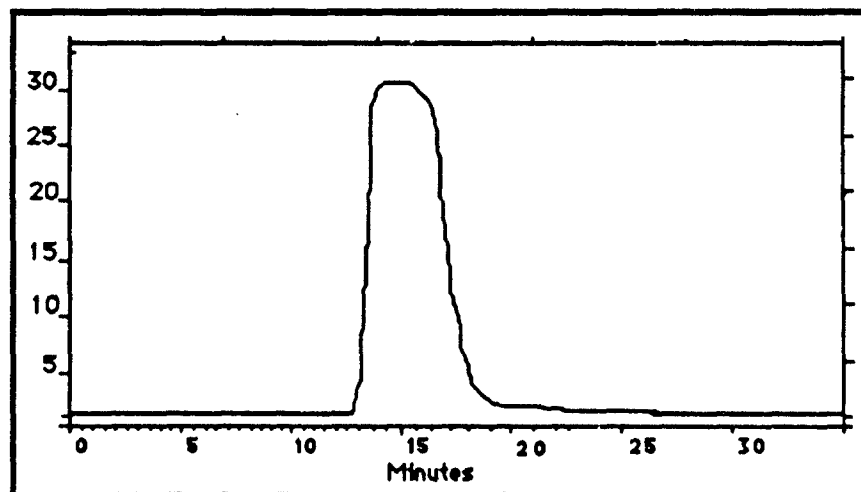


Figure 68. Preparative chromatogram (P-6) of the brown fraction (P5F5) from the preparative run P5.

SK-3br was slowly evaporated until crystals no longer formed and the supernatant decanted. The supernatant was then applied to the preparative HPLC and run as P-6. Nine fractions were collected and MTX activity identified in P6F3. This fraction was then reduced in volume and re-applied to the preparative HPLC as run P-7. Four fractions were collected from this run.

Discussion of HPLC separation attempts. In looking over the data from our ileum assays, HPLC chromatograms and NMR scans we came to several conclusions. The ileum records indicated that each time we split the major 209 nm peak material on the HPLC we split the toxic activity. Even when we split and split again, not only was the toxin was not 100% pure, but there was no gain in purity and we began to lose total toxicity. The conclusions from the NMR data up to this point indicated that several compounds were being scanned. From all of the data then it was surmised that the 209 nm peak seen on the preparative HPLC consisted of seven components (Figure 69).

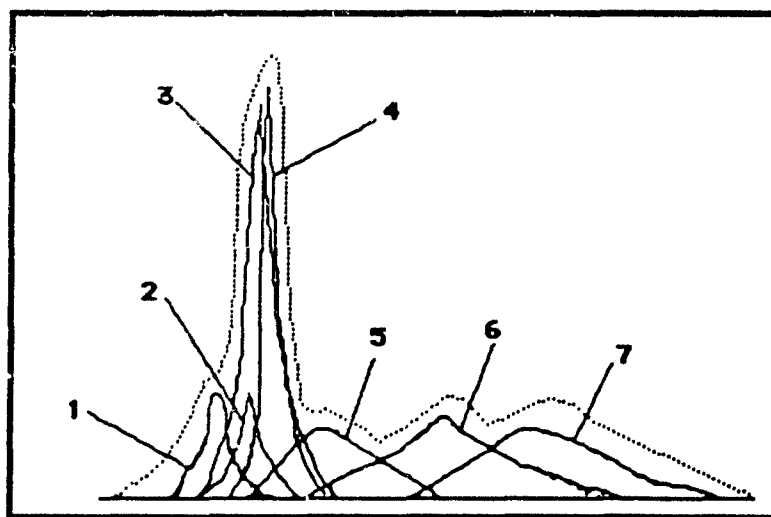


Figure 69. Diagrammatic representation of the components of the major 209 nm peak. Actual peak is dotted line. See text for explanation.

Figure 69 above represents the overall waveform seen in the preparative HPLC of the toxic fraction (dotted line). We have been

able to identify a minimum of seven different components that constitute that waveform and they all overlap. Component 2 is light green when concentrated, #4 is brown in color, #6 is yellow, and #7 is light green.

Some of the solvents which we would like to have utilized in the HPLC either caused continual precipitation within the columns (e.g. acetonitrile) or had an absorption in the range we wanted to monitor (210 nm). We rationalized that we could effect the selective solvent separation prior to HPLC detection and fractionate the similar compounds.

Solvent extraction of pigments.

To continue the separation of the maitotoxin fraction we investigated selective solvent extraction of the solid phase material. To this end we found that extraction of the dried material with ethyl acetate produced an ethyl acetate soluble and an ethyl acetate insoluble fraction. The bulk of the toxicity was found in the insoluble fraction.

TABLE 32.
QUANTITATION OF MTX TOXIC COMPONENTS BY ILEUM ASSAY

FRACTION	COLOR	PERCENT	TOTAL	SPEC	WEIGHT	PERCENT
OF	OF		ACTIVITY	ACTIVITY		ACTIVITY
CRUDE	PURITY	YIELD				
	FRACT	mg %	MU-MTX	MU/ug	ug/MU	(note 1)
Crude Ext	Dk Br	100.	300	.0326	30.6	.0098
Brown	Brown	83.16	210	.0236	42.3	.0070
EtOacIns	Green	40	200	.0530	18.25	.0164
ACN ppt	Green	13	45	.0384	26.57	.0112
						100
						70%
						66
						15

Note. The LD₅₀ values used in this table are estimates based upon preliminary mouse data

The ethyl acetate extraction of the brown fraction is an especially fortuitous step in that, with it, we (1) partially separate the complexes, (2) split off the majority of the peridinin carotenoid from the toxic fraction, (3) achieve an increase in specific activity with a

ten fold increase in purity and (4) retain 66% of our starting material. This is a two and a half fold increase in the cost benefit ratio. HPLC chromatograms of the ethyl acetate fraction is shown in the following Figure 70.

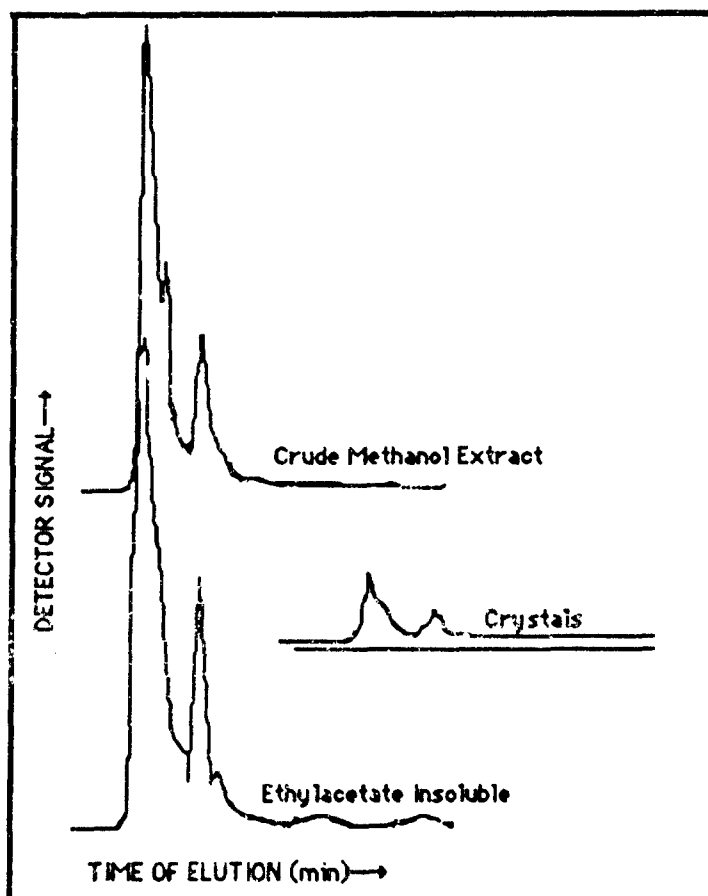


Figure 70. Comparison of analytical HPLC chromatograms of crude brown versus ethylacetate insoluble. Running conditions were: Napak 5 micron C-18 silica gel, 3.9 mm X 7.5 cm column, and 100% methanol as solvent, run time 55 min.

In the processing of GT-350 samples, a radical approach to separation was initiated. Entire cultures were extracted with methanol and subjected to solid phase extraction. Each extraction was monitored by analytical HPLC (230, 330, 440 nm) and toxin level monitored by ileum assay. At each step we have attempted to

selectively extract a pigment or class of compounds and keep the toxin precipitated. Previous experiments have shown that the toxic activity can be retained under these conditions.

Accordingly, 12.21 grams of dried cells (*G. toxicus* 350, culture 5A/88D) identified as 1000 series was processed to a methanol extract by sonication and methanol extraction as previously described. This crude extract was treated with hexane:methanol (1:1). Both the hexane fraction and the methanol fraction were assayed by ileum and the data is as follows:

TABLE 33.
HEXANE:METHANOL SEPARATION OF GT350, 1000 SERIES

Code	Fract.	Color	$\frac{\text{MU}}{\mu\text{g}}$	$\frac{\mu\text{g}}{\text{MU}}$	Total MU	% Rec	
	% Pur						
1000y	Crude	Grn-Brn	.0039	254	48000	100	.0011
1000v	Hex Ext	Green			<5.0	0	-
1000g	Hex Ppt	Choc.Br	.1517	6.59	44000	91.6	.0455

As can be seen the hexane:methanol step was a very successful innovation in that almost all of the mouse units were retained but the weight was reduced such that the μg per MU value went from 254 to 6.59 and at the same time the % purity went up by more than a factor of ten. The second step involving the acetonitrile extraction was instituted on the fraction 1000g and the data is as follows:

TABLE 34.
ACETONITRILE EXTRACTION OF GT350, 1000 SERIES

Code	Fract.	Color	$\frac{\text{MU}}{\mu\text{g}}$	$\frac{\mu\text{g}}{\text{MU}}$	Total MU	% Rec	
	% Pur						
1000g	Hex Ppt	Choc.Br	.1517	6.59	44000	91.6	.0455
1000w	ACN Ext	Red Br	-	-	100	-	-
1000c	ACN Ppt	Pea Gr	0.588	1.70	38000	79.1	.1764

The acetonitrile extraction step has also proven to be very effective in extraction of peridinin and monopolar carotenoids meanwhile retaining toxic activity. With this step we achieve a

purity level of .176% (based upon Yasumoto's figure of .003 $\mu\text{g}/\text{MU}$) and a specific activity of 1.7 $\mu\text{g}/\text{MU}$.

The third step was one in which we attempted to isolate the toxic moieties from the large amount of chlorophyll-c which remained. In this step a simple dilution-precipitation step using ethanol as the diluent for the methanol was instituted. A precipitate was obtained from the solution as follows:

TABLE 35.
ETHANOL PRECIPITATION OF GT350, 1000 SERIES

Code	Fract.	Color	$\frac{\text{MU}}{\mu\text{g}}$	$\frac{\mu\text{g}}{\text{MU}}$	Total MU	% Rec	
	% Pur						
1000c	ACN Ppt	Pea Gm	0.588	1.70	38000	79.1	.1764
1000n	EtOH sol	Green	-	-	200	-	-
1000p	EtOH Ins	Green	0.95	1.05	36000	75.0	.285

This ethanol precipitation step is one which gets us to the 1 $\mu\text{g}/\text{MU}$ range or at about .3% purity. Thus, we were able to achieve the 1 $\mu\text{g}/\text{MU}$ range of purification for GT350 very easily using large samples.

Table 36.
Preparative HPLC Separation of GT350, 1000 Series

Code	Fract.	Color	$\frac{\text{MU}}{\mu\text{g}}$	$\frac{\mu\text{g}}{\text{MU}}$	Total MU	% Rec	
	% Pur						
1000s1	0-3.0m	Clear	-	-	-	-	-
1000s2	-4.0m	Cream	3.93	0.285	20,000	41.6	1.2
1000s3	-6.0m	Clear	-	-	-	-	-

At this point it was decided that the preparative HPLC unit would be used for further separation of the toxin. Because an HPLC pilot study had shown that the composite peak at approximately 3.7 minutes elution time corresponded with toxicity, the entire sample of 36000 MU was applied to the preparative HPLC and the area corresponding the the 3.7 minute peak collected separately. Ileum assay of the fractions indicated that the large peak had 20,000 MU

remaining. Analytical HPLC chromatograms indicated each preparative fraction had multiple peaks and none corresponded to toxin activity.

A different approach was taken on the remaining 20,000 MU's of series 1000 in that an acetonitrile precipitation was attempted to precipitate the toxin. Several subsequent steps were tried after the acetonitrile precipitation. However, these steps were not so successful for the retention of the toxin. Accordingly, a second 18.0 grams of dried cells (*G. toxicus* 350, culture 7A/88D) identified as the 3000 series was processed by the first two steps.

Table 37.
Hexane:Methanol Separation of GT350, 3000 Series

Code	Fract.	Color	$\frac{\text{MU}}{\mu\text{g}}$	$\frac{\mu\text{g}}{\text{MU}}$	Total MU	% Rec	
	% Pur						
3000y	Crude	Grn-Brn	.0526	19	278000	100	.0157
3000g	Hex Pt	Choc.Brn	.0310	16.02	256000	92.0	.0156
3000c	ACN Pt	Pea Grn	0.087	7.8	250000	72.4	.026

Summary of solvent extraction experiments.

From our previous small scale studies it was evident that the large concentrations of pigments and lipids interfered with HPLC separation of the toxic components in GT350. Therefore, we continued adding steps in the extraction scheme designed to eliminate the pigments entirely. To accomplish this, the first extraction was with hexane:methanol (1:1). This previously mentioned extraction step was expected to remove nonpolar carotenes and chlorophyll-a. During this step we discovered an unusual type of chlorophyll-a contained in the dinoflagellate.^[85] Once this step was accomplished a second solid phase extraction was accomplished utilizing acetonitrile. The step with acetonitrile was expected to remove peridinin and other monopolar carotenes. A third step was incorporated to selectively precipitate the toxic components out of solution and leave the remainder of the chlorophyll-c in solution.

The results were impressive in that routine purification of very large quantities down to the level of 1 $\mu\text{g}/\text{MU}$ with retention of 95% of the toxic activity was now routine. The loss of toxic activity now came with solubility and attempts to purify below this level. Separation of this material on a C18 column with methanol and water produced large quantities (60,000 MU) per batch of 10% purity as determined by ileum assay.

The separation of 350 material by solid phase extraction as previously described has allowed purification of material down to the 1% level with retention of 60% of the toxic activity. Inasmuch as the toxin content of 350 is much less and the amount of interfering lipids is higher than that of 175 much more material must be processed to accomplish the same purification.

Acetonitrile separations

Our early experiments with acetonitrile, led us to believe that only a very minor portion of the GT-3,4 toxic components, the GT-3 was soluble in the solvent.^[116,117] This, of course, would have meant that we had found a mechanism for precipitation of the GT-4 fraction (we now know this is not true). Later experiments on solubility, using the ileum as an assay, had shown that part of the problem we faced was that the toxin had a very limited solubility in chloroform, DMSO, acetone and acetonitrile. Interestingly enough, extraction of the toxin into these media each produced subtle differences on the ileum preparation. This indicated to us that each of the solvent system, perhaps in conjunction with dissolved oxygen, etc was modifying the toxin in some way.

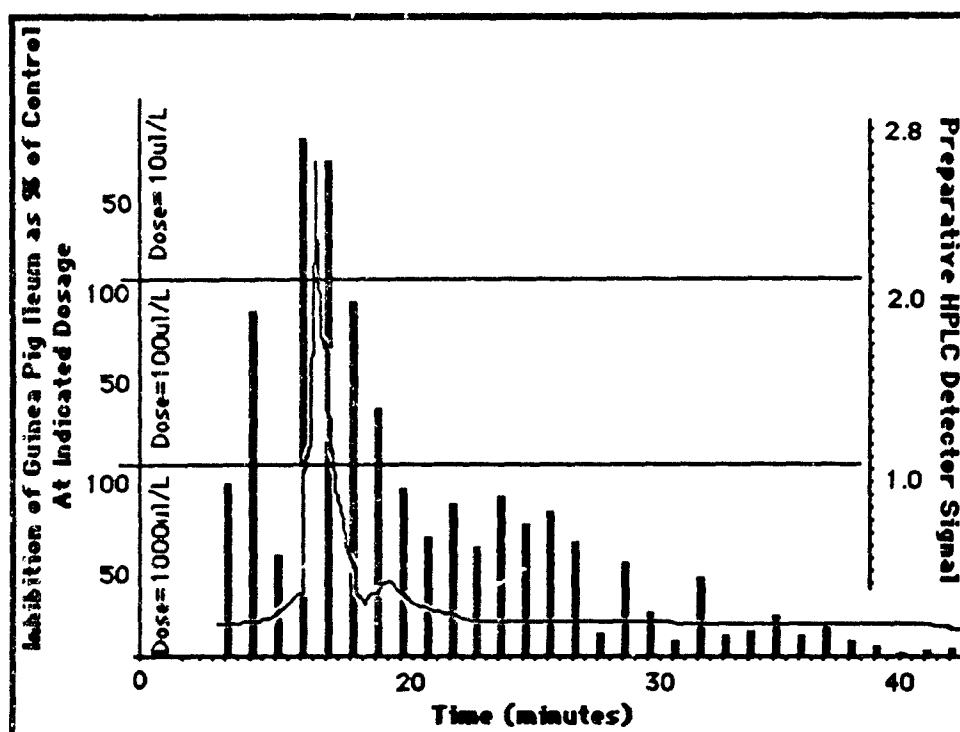


Figure 71. Preparative HPLC chromatogram (P2) of 1 ml of WSAP (7 mg/ml). Running conditions were: 15 micron C-18 silica gel, 5 cm X 28 cm column, flow rate 30 ml/min, and 100% methanol as solvent, run time 55 min. Detector set at 210 nm.

As a preliminary to the ACN experiment, we ran a control chromatogram of the same material we used for the ACN-extraction. The results of this chromatogram is shown here as Figure 71. Notice in the control, that the most of the toxicity is associated with the initial large 209 nm peak. However there is a small peak of toxicity the precedes the large 209 nm peak and a gradual decrease of toxicity that occurs after the large 209 nm peak. In other words, the toxin was distributed in the solvent.

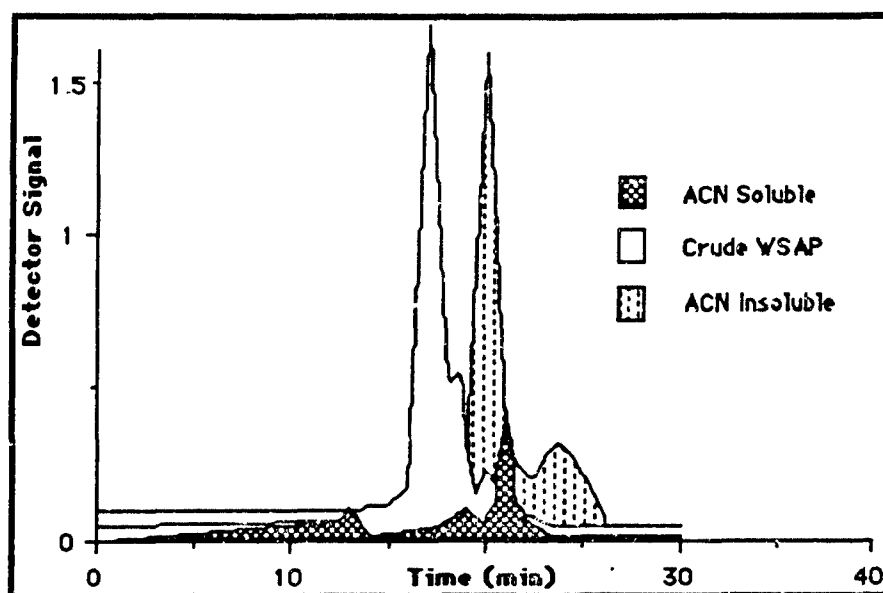


Figure 72. Preparative HPLC chromatograms of WSAP, ACN-soluble and ACN-insoluble. Curves scaled to actual detector levels at 210 nm. Running conditions were: 15 micron C-18 silica gel, 5 cm X 28 cm column, flow rate 30 ml/min, and 100% methanol as solvent, run time 55 min.

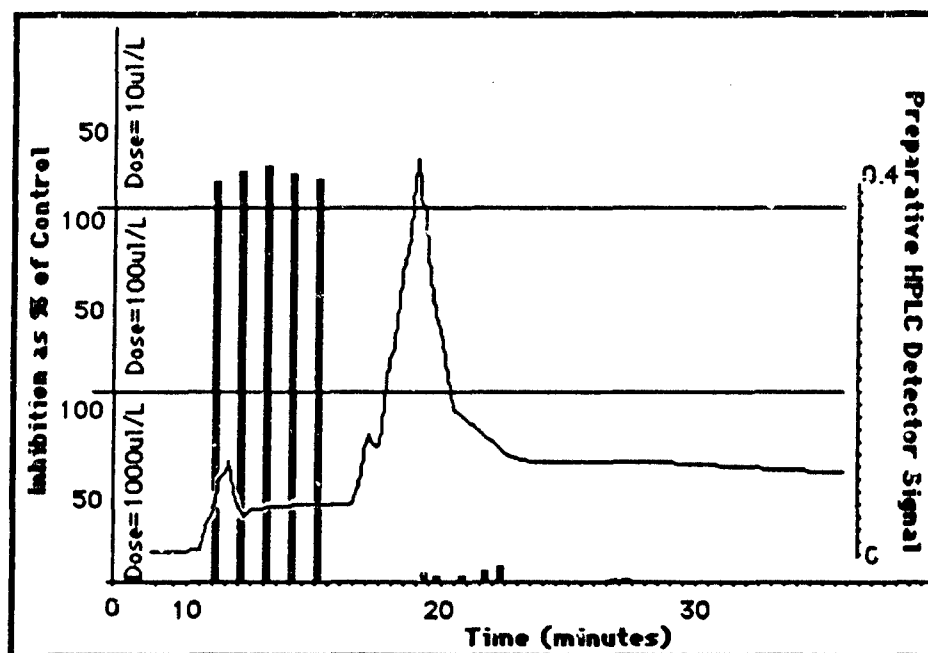


Figure 73. Preparative HPLC chromatogram of ACN-soluble material isolated from WSAP superimposed upon a bar chart of toxicity to guinea pig ileum. Sample application was 1 ml. Running conditions were: 15

micron C-18 silica gel, 5 cm X 28 cm column, flow rate 30 ml/min, and 100% methanol as solvent, run time 55 min. Detector set at 210 nm.

Chromatography of the ACN-soluble and ACN-insoluble fraction is compared with the starting in material in Figure 72. Notice that in terms of the detector output the ACN-soluble is a very small portion of the crude WSAP.

When crude WSAP is extracted with acetonitrile and fraction are collected from preparative chromatography, the results shown in Figure 73 are surprising. All of the toxic activity preceded the normal elution time. In addition, there are two first large 209 nm peaks, albeit at much lower detector levels.

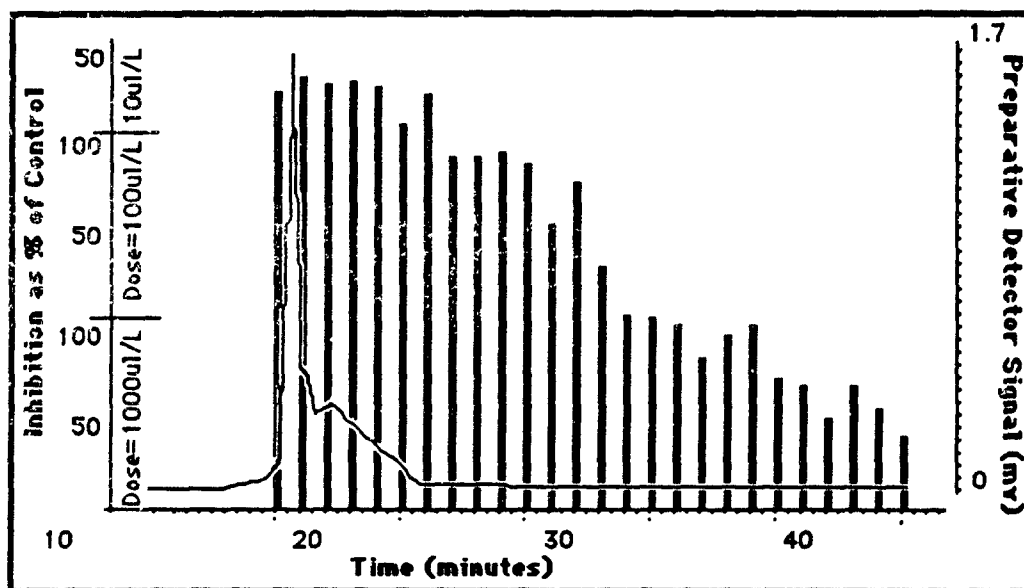


Figure 74. Preparative HPLC chromatogram of ACN-insoluble material isolated from WSAP superimposed upon a bar chart of toxicity to guinea pig ileum. Sample application was 1. Running conditions were: 15 micron C-18 silica gel, 5 cm X 28 cm column, flow rate 30 ml/min, and 100% methanol as solvent, run time 55 min. Detector set at 210 nm.

Preparative chromatography of the ACN insoluble material produced even more surprising results (Figure 74). After extraction, the toxicity in the ACN-insoluble material is still associated with the

first large 209 nm peak at its normal elution time. The gradient of toxicity after the first large 209 nm peak is even higher.

The conclusions we made from this experiment, at the time, were that the acetonitrile treatment separates the toxic material into two fractions. Notice in Figure 73 that all toxic activity precedes the 20 minute elution time and that in Figure 74 the toxic activity follows the 20 minute elution time.

Ethyl acetate extraction compared with acetonitrile.

Extracting with both ethyl acetate and acetonitrile was conducted. When the fractions were examined on the analytical column and the wavelengths scanned, they indicate that the principal brown component extracted by the ethyl acetate is peridinin. Indeed NMR examination of the fractions indicate that the peredinin peaks are present in the crude and almost absent in the ethyl acetate insoluble material. After the ethyl acetate separation, we tried to selectively precipitate the toxic fractions with acetonitrile (see Figure 75 below).

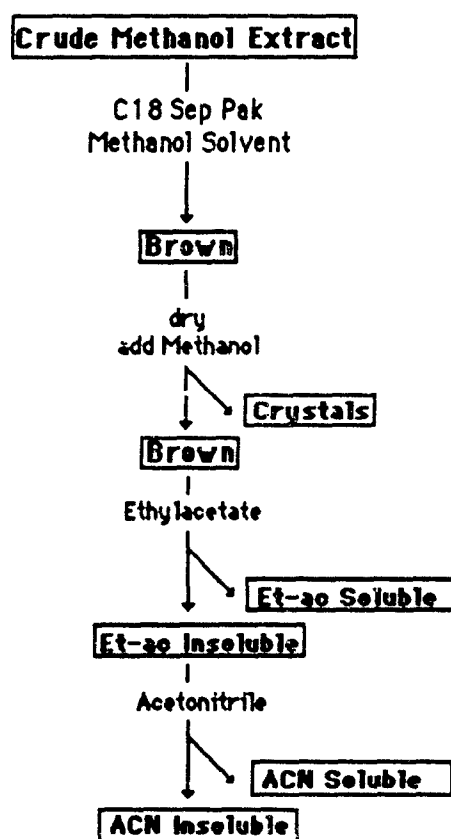


Figure 75. Schematic diagram for the acetonitrile (ACN) step.

When the ACN-soluble and ACN-insoluble material was examined by ileum assay and compared with the starting material it became apparent that ACN extraction reduces the total amount of GT-4 activity and converts it to the GT-3 type (from this we inferred that the toxin moiety was changed). Indeed, there was a decrease rather than an increase in the specific activity.

Because the ACN treatment gave us a decrease in specific activity (due to a degrading of toxin), it was decided this was not a viable step. However, the ethyl acetate step is a valuable step. Examination of the ethyl acetate insoluble material on semipreparative HPLC produced eight peaks which eluted within the first ten minutes. All of these peaks overlap one another and tend to co-migrate. Finally, because the most likely action occurring to degrade the toxin was a

methylation, we conducted an ACN precipitation in ethanol rather than methanol. This procedure had produced the cleanest HPLC chromatogram of yet. This fraction had a reduced toxicity. Nevertheless a major fraction of the toxin was retained and was associated with the sharp peak at 210 nm and the other wavelengths. Once again, there was a decrease in the specific activity.

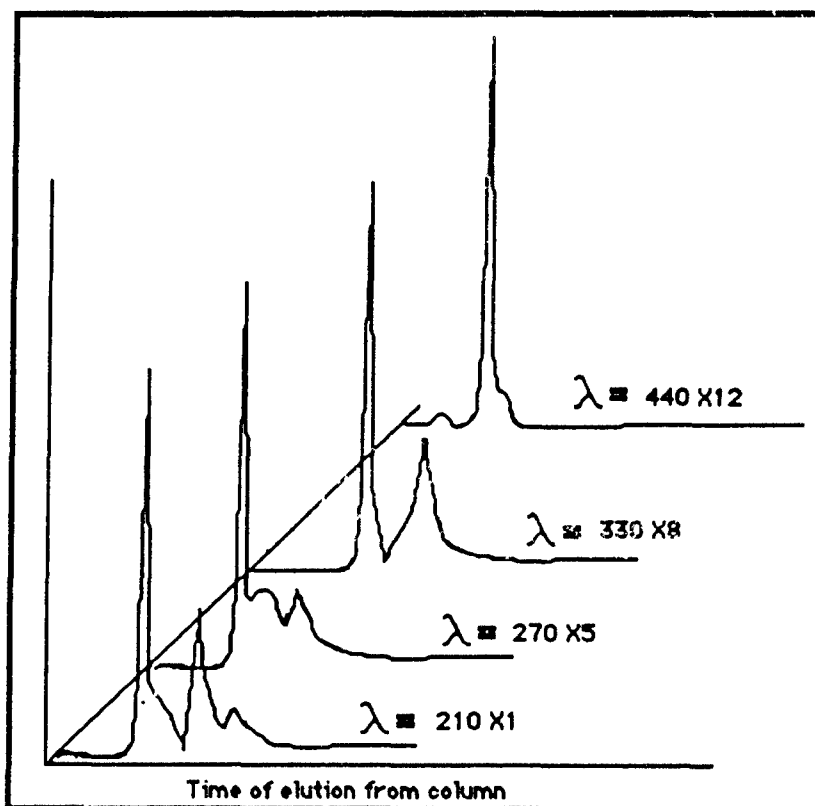


Figure 76. Analytical HPLC aliquot sizes were 5 μ l. Other running conditions were 5 micron C-18 RCM column. Flow rate 0.3 ml/min and 100% methanol as solvent.

Purification of large scale culture products.

Examination of our studies of extraction procedures pointed to a considerable loss of toxin along with a decrease in specific activity or no net increase. Sep-pak, solvent-solvent and extensive HPLC had not been effective in purification of the toxin. We concluded at that time that shortening of the procedures and elimination of water would considerably cut down on toxin loss. Therefore we initiated studies which would allow us to proceed to HPLC as expeditiously as possible. Accordingly we initiated four studies directed at (1) examining the separation of toxins on the semi-preparative system preliminary to application of larger amounts the the preparative system, (2) concomitant separation of peaks on the analytical system, (3) application of trial amounts to the preparative system, and (4) experimentation to eliminate water and shorten the separation process. Preliminary chromatograms indicated that the peaks of the crude toxin distribute differently on the semi-preparative column than they do on the analytical.

This was probably due to the fact that the resin size is different on the semi-preparative unit as opposed to the analytical system (15 versus 10 microns). Attempting to run the toxin on the semi-preparative HPLC with a mixture of methanol and acetonitrile resulted in blocking of the column. Further investigation of this phenomenon indicated that crystallization was occurring within the column.

Further experimentation with acetonitrile. Experimentation with the ratio of water to methanol in the medium demonstrated that crystallization could be induced in the water extract simply by altering the concentration of methanol. Once we learned the mechanism of formation, crystals were easily induced. Figure 77 is a diagram of semi-preparative HPLC recordings of both the crystal supernatant and crystals put into solution. Crystals were separated from the extract and tested on mice and the ileum, with negative results. We concluded that the crystals are products of non-toxic

components. Nevertheless, this procedure was extremely beneficial as a rapid clean-up method for the crude fraction.

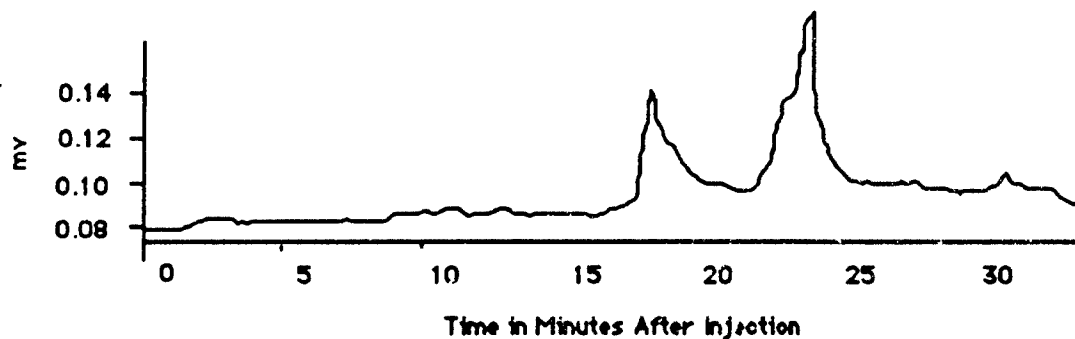


Figure 77. Semi-preparative HPLC chromatogram of water soluble extract. Sample application was 50 μ l of a sample of 7 mg/ml. Running conditions were: 15 micron C-18 silica gel, 4.7 mm X 128 cm column, flow rate 0.2 ml/min, and 100% methanol as solvent. Detector set at 210 nm.

The original water soluble extract when chromatographed on the semi-preparative HPLC indicates a composite of many peaks in two distinct groups (Figure 77 above). Five hundred μ l of this water soluble extract was dried down and submitted to acetonitrile extraction.

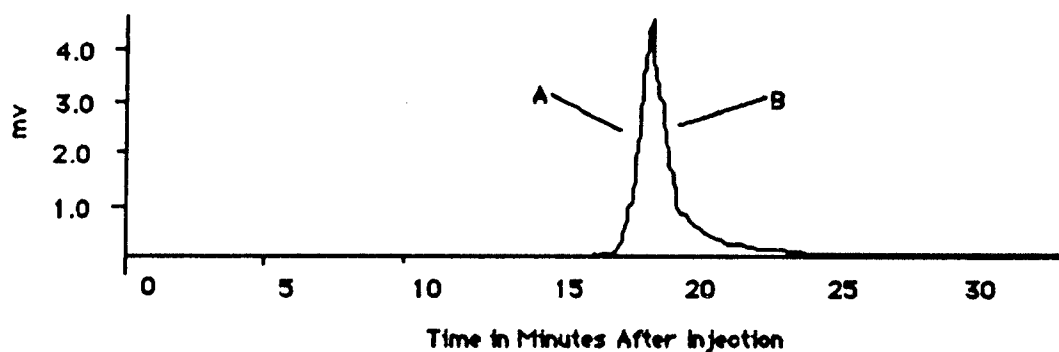


Figure 78. Semi-preparative HPLC chromatogram of ACN-insoluble material. Sample application was 50 μ l of a sample of 7 mg/ml. Running conditions were: 15 micron C-18 silica gel, 4.7 mm X 128 cm column, flow rate 0.2 ml/min, and 100% methanol as solvent. Peak eluant was separated at dotted line as fractions A and B. Detector set at 210 nm.

The result was an ACN-insoluble and an ACN-soluble division of the original water soluble extract each of which was dried down and diluted up to 500 μ l with dry methanol. When tested on the ileum (10 μ l sample directly in the bath of 10 ml of saline) both fractions are toxic, but produce subtle differences.

Chromatography of the ACN-insoluble material revealed a single peak which is a composite of several. These were split exactly at the top of the peak resulting in fractions A and B (Figure 78 above). The collected eluants were dried down and the fractions resuspended in 100 μ l of dry methanol. 10 μ l of these fractions were tested on the ileum preparation. Toxicity to the ileum was 100% for both peaks.

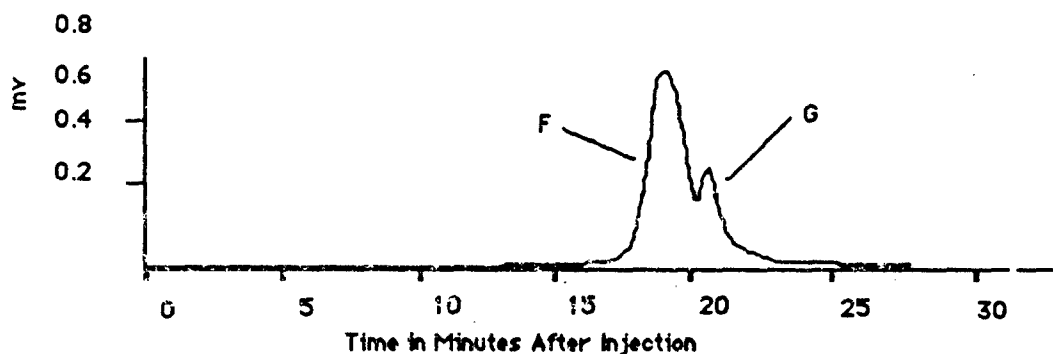


Figure 79. Semi-preparative HPLC chromatogram of fraction A from ACN-insoluble material isolated from water soluble extract. Sample application was 50 μ l of a sample of 7 mg/ml. Running conditions were: 15 micron C-18 silica gel, 4.7 mm X 128 cm column, flow rate 0.2 ml/min, and 100% methanol as solvent. Detector set at 210 nm.

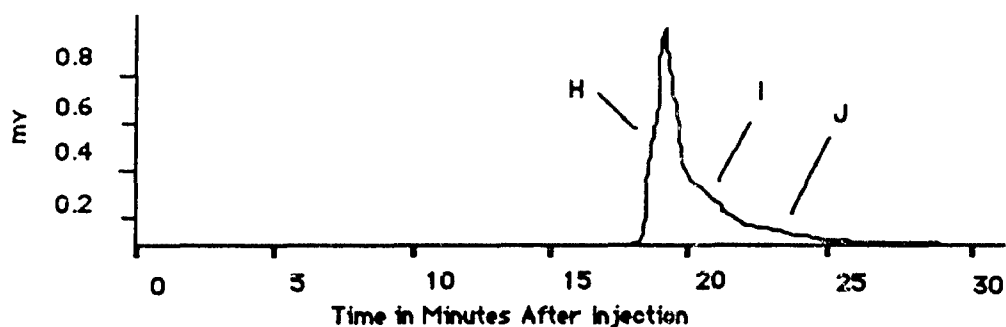


Figure 80. Semi-preparative HPLC chromatogram of fraction F from ACN-insoluble material isolated from water soluble extract. Sample application was 50 μ l of a sample of 7 mg/ml. Running conditions were: 15 micron C-18 silica gel, 4.7 mm X 128 cm column, flow rate 0.2 ml/min, and 100% methanol as solvent. Detector set at 210 nm.

When fraction A was re-run on the semi-preparative HPLC two complexes were resolved, fractions F and G (Figure 79 above). G was relatively non-toxic, but F was toxic to the ileum.

Re-chromatography of complex F resulted in a complex peak and the eluant was collected in three fractions, H, I and J (Figure 80 above). Of these three fractions collected only fraction I, the middle portion showed toxicity.

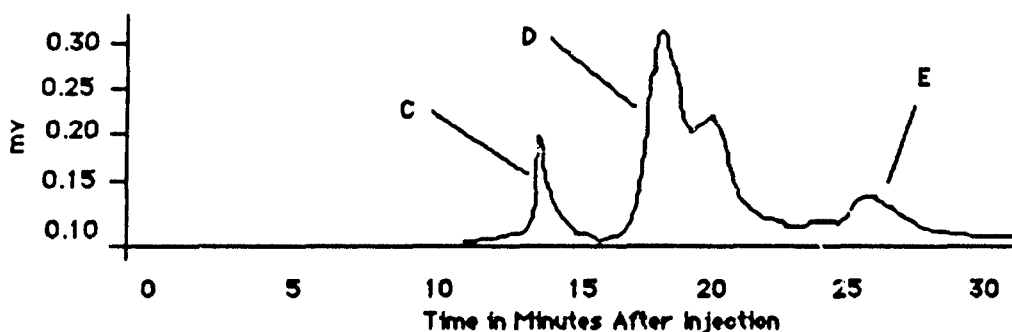


Figure 81. Semi-preparative HPLC chromatogram of the ACN-soluble material isolated from water soluble extract. Sample application was 50 μ l of a sample of 7 mg/ml. Running conditions were: 15 micron C-18 silica gel, 4.7 mm X 128 cm column, flow rate 0.2 ml/min, and 100% methanol as solvent. Detector set at 210 nm.

The ACN-soluble fraction chromatographed into complex peaks C, D and E (Figure 81 above). When tested on the ileum preparation fraction C was toxic, D was slightly toxic and E was not toxic at all.

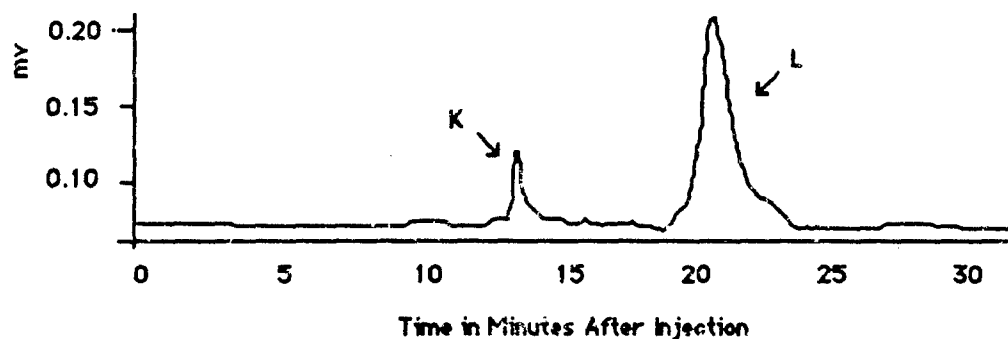


Figure 82. Semi-preparative HPLC chromatogram of fraction C from the ACN-soluble material isolated from water soluble extract. Sample application was 50 μ l of a sample of 7 mg/ml. Running conditions were: 15 micron C-18 silica gel, 4.7 mm X 128 cm column, flow rate 0.2 ml/min, and 100% methanol as solvent. Detector set at 210 nm.

When fraction C was re-chromatographed (Figure 82 above) it resulted in a toxic peak K and a nontoxic peak L.

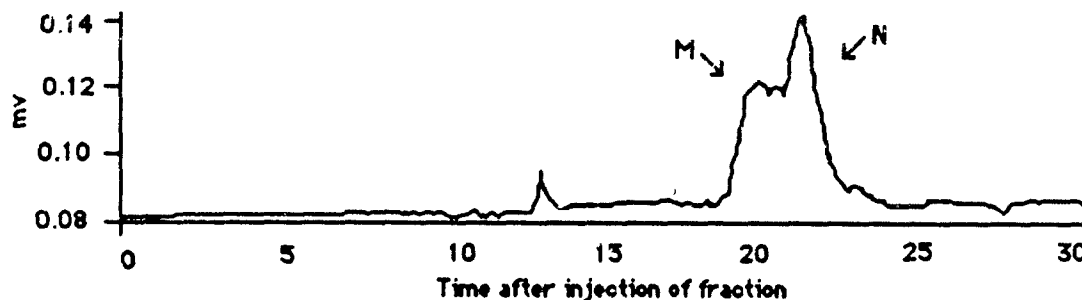


Figure 83. Semi-preparative HPLC chromatogram of fraction D from ACN-soluble material isolated from water soluble extract. Sample application was 50 μ l of a sample of 7 mg/ml. Running conditions were: 15 micron C-18 silica gel, 4.7 mm X 128 cm column, flow rate 0.2 ml/min, and 100% methanol as solvent. Detector set at 210 nm.

When fraction D was re-chromatographed it separated into fractions M and N (Figure 83 above). Neither of these peaks were toxic to the ileum.

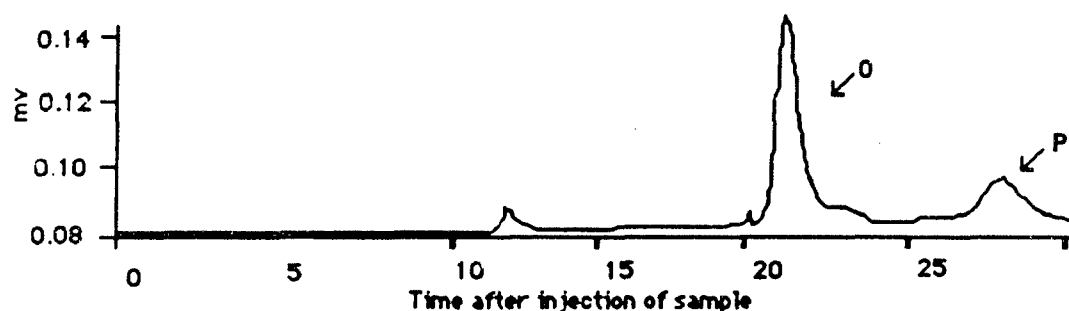


Figure 84. Semi-preparative HPLC chromatogram of fraction E from ACN-soluble material isolated from water soluble extract. Sample application was 50 μ l of a sample of 7 mg/ml. Running conditions were: 15 micron C-18 silica gel, 4.7 mm X 128 cm column, flow rate 0.2 ml/min, and 100% methanol as solvent. Detector set at 210 nm.

TABLE 38
Ileum Results of HPLC Fractions

NO	SAMPLE	% INHIB		RESOLVED
		@ 15 min	@ 90 min	INTO PEAK
1	WS			
2	ACN-INS	100	100	
3	ACN-SOL-1	100	100	
4	ACN-SOL-2	0	0	
5	ACN-SOL-3	0	0	
6	A	100	47	F & G
7	B	100	100	H, I & J
8	C	97	94	K & L
9	D	34	26	M & N
10	E	0	1	O & P
11	F	98	100	
12	G	18	14	
13	H	0	0	
14	I	98	100	
15	J	0	0	
16	K	95	68	
17	L	0	0	
18	M	0	0	
19	N	3	0	
20	O	9	0	
21	P	0	0	

Above test were conducted on ilea by injecting 10 μ l directly into the bath. The % inhibition listed at 15 and 90 min are as % of the acetylcholine control. WS = water soluble extract. ACN-INS = acetylcholine insoluble material. ACN-SOL = acetylcholine soluble material. Letters A through P represent HPLC fractions which were collected and tested for toxicity.

Re-chromatography of fraction E resolved it into peaks O and P (Figure 84 above). Again when tested on the ileum preparation neither of these fractions were toxic.

After these preliminary runs on the semi-preparative system were completed, we then took one ml of water soluble material (7 mg/ml) and subjected it to ACN extraction. The resultant ACN-soluble and ACN-insoluble products were blown dry and resuspended in 1 ml of dry methanol. First the entire one ml of the ACN-insoluble material was separated on the preparative column. The column eluants were collected between 10 and 50 minutes after ACN-insoluble injection in 50 ml samples (Figure 85).

Twenty seven 50 ml samples were collected resulting in a total of 1350 ml. Each of the 27 samples were lyophilized down to a volume of approximately 2 ml and 10 μ l aliquots taken for testing on the guinea pig ileum. Once the ileum aliquoting was completed the samples were blown completely dry and weighed on the Cahn microbalance in a tared vessel. All the samples were then reconstituted to 1 ml with dry methanol and an analytical run completed on ten μ l of material. This procedure was utilized in order not to miss a minor toxic component which may be present in very small sample amounts and be lost in diluting up from small volumes.

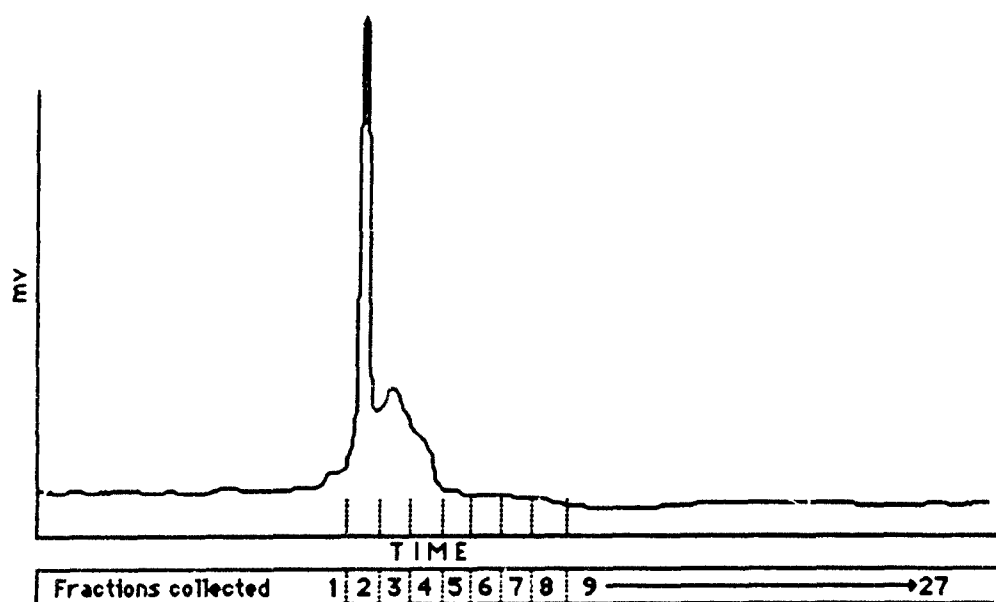


Figure 85. Preparative HPLC chromatogram of ACN-soluble material isolated from water soluble extract. Sample application was 1 ml of a sample of 7 mg/ml. Sample loaded on column in 4 min using flow rate of 10 ml/min. Running conditions were: 15 micron C-18 silica gel, 5 cm X 28 cm column, flow rate 30 ml/min, and 100% methanol as solvent, run time 55 min. Detector set at 210 nm.

This experiment with the preparative column was designed to demonstrate the correspondence of chromatograms when switching from semi-preparative to preparative systems, the precise localization of toxic components coming off the column and as a preliminary to running larger amounts on the preparative column. It is important to note at this point that these three runs (Crude, ACN-soluble and ACN-insoluble) on the preparative HPLC produced over 100, one ml fractions. Each one of these fractions were tested on the ileum preparation for toxicity using only 10 μ l of each fraction. The savings in terms of mice and toxin was a significantly large amount.

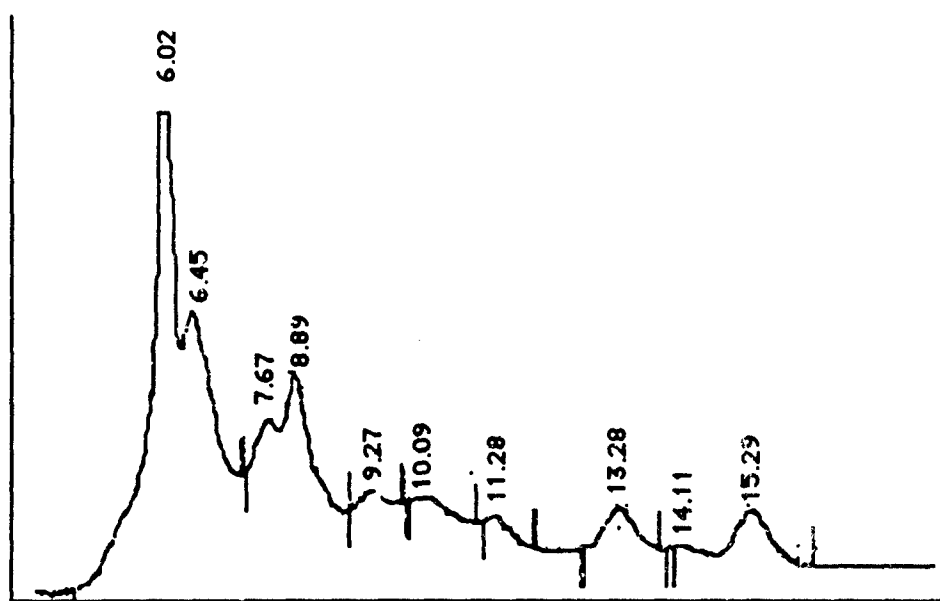


Figure 86. Analytical HPLC chromatogram of water soluble extract. Sample application was 15 μ l of a sample of 3.59 mg/ml. Peak elution times are displayed above the peaks detected. Running conditions were 10 micron C-18 RCM column. Flow rate 0.2 ml/min and 100% methanol as solvent.

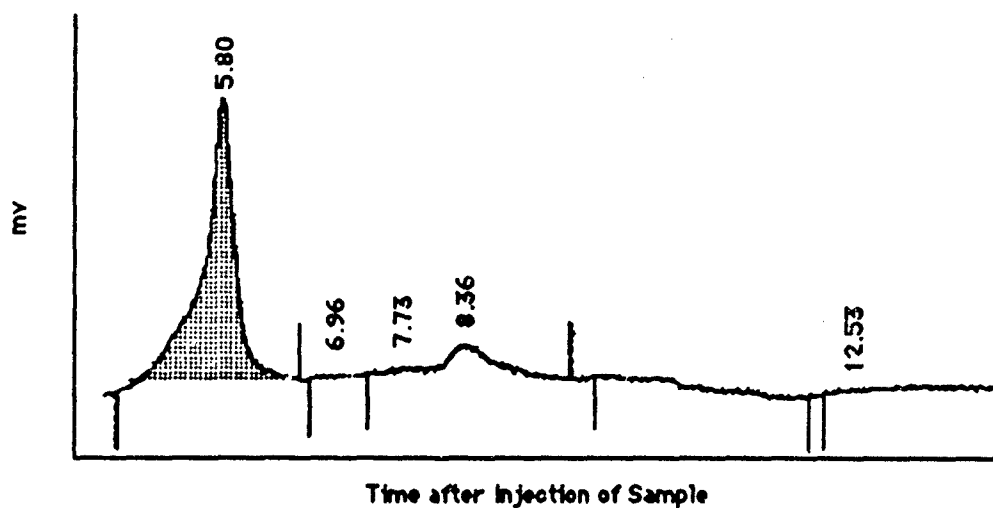


Figure 87. Analytical HPLC chromatogram of "maitotoxin" peak collected directly from repetitive analytical runs.. Sample application was 10 μ l of a sample of 400 μ l. Peak elution times are displayed above the peaks detected. Running conditions were 10 micron C-18 RCM column. Flow rate 0.2 ml/min and 100% methanol as solvent. Shaded area of chromatogram is toxic area.

Our results with acetonitrile led us to conclude that the toxin was changed by the solvent, that the use of acetonitrile subdivided the toxic fractions, reduced total toxicity and decreased specific activity.

Small amounts of toxin can be produced with our previously published method for HPLC purification of "maitotoxin".^[118] The relative purity can be estimated by comparing an HPLC chromatogram of the crude material (Figure 86) with one of the isolated material (Figure 87). Nevertheless, separation of material by analytical HPLC was not considered to be effective for large scale production.

Summary and discussion of clone 350 GT-1 (CTX) separation. GT-1 can be extracted with hexane and in a relatively light-weight fraction ($\approx 0.1\%$). Further purification of the material on C-18 columns and subsequent HPLC revealed that the major contaminant is C-18 lipid, a major component of the 350 cell system. Attempts to further purify this fraction on C-18 continue. The HPLC records confirm what has been previously stated about the initial separation process, showing multiple peaks for each fraction at 209 nm.

With respect to GT-4 (MTX), the ileum and mouse assay confirms that the sep-pak process effects a clear separation into fractions (GT-1, and GT-3,4). Nevertheless, the process does not prevent the loss of toxicity in continued separation and purification efforts.

While we can purify small amounts of toxin by continually splitting peaks on the analytical HPLC, scaling up to purify very large amounts presents problems. As the amount of material processed is increased the separation of peaks decreases and their base width increases. In addition, the peaks represent more than one compound. Therefore, using the preparative HPLC for separation, we began experimenting to see if we could either selectively extract contaminants or further separate peaks.

On the HPLC using reverse phase columns, the GT-3 and GT-4 toxins as defined by ileum assay, always eluted immediately after

the void volume. Toxic components GT-1,2, however, invariably eluted after twenty five minutes or more depending upon the flow rate. In examining, the fractions eluted from the HPLC, we noted that the toxic peaks, as determined by ileum assay, coincide with the pigments. Analysis of the sep-pak fractions by weight indicated that the bulk of the mass was associated with the GT-3,4 or brown component and the GT-1,2 or green component was small. Solid state extraction of the brown fraction with acetonitrile, chloroform, DMSO and acetone proved to indiscriminately separate the toxin complexes, such that there was a continual division of the toxicity.

The separation of *G. toxicus* extracts on HPLC, column and TLC, not only confirmed these conclusions but also indicated that the toxin and the pigments are very large complexes. These complexes have been described in *Glenodinium* sp. and *Gonyaulax polyhedra*.^[119] Indeed our investigations have indicated that GT-4 is closely associated with chlorophyll-c₂ and GT-1 is associated with the chlorophyll-a complex.

Hence we began to think in terms of isolating the pigment complexes to extract the toxins. In this respect, we were hampered by the fact that the HPLC detector we have does not cover the portion of the spectrum from 600-900 nm. Attempts were made at using silicic acid columns. When crude material is applied to silicic acid columns, the majority of the toxicity sticks to the beginning of the column and cannot be eluted. In TLC plates it sticks to the origin, but some - not 100%- can be eluted from the fines. This would be expected of a molecule with a large number of hydroxyl groups. The material eluted in both cases is light green in color when concentrated.

Our analysis of data indicated that GT-4 was contained in material which migrated at the front when methanol was used as the eluent in the HPLC. This is a composite peak, containing several other closely related compound in terms of solubility-solvent characteristics. We then attempted to use an alternate solvent system for extraction.

Modified solid phase separation.

At this point then, the decision was made to reverse the process for purification once the precipitation step was finished. That is, the pigments and associated toxin would be selectively extracted from the maitotoxin fraction while it was in the dried form. Because as previously reported (and had erroneously assumed) only GT-3 was soluble in acetonitrile, it was utilized to force crystallization of the GT-4. Once a pigment complex was isolated it was taken up in methanol and then an equal volume of acetonitrile was added and mixed. The sample was then slowly dried under dry nitrogen gas until precipitation occurred. The supernatant was decanted and the process repeated until no more crystals formed. Each was then dried down and taken up in the original volume of methanol and aliquots taken for ileum assay.

The fractions from the separation of pigments were tested on the ileum preparation. The amount of toxin required to produce 50% inhibition 90 minutes after a 15 minute inhibition has been defined as an ileum equivalent unit (IEU). We knew from experience that approximately 2,000 IEU will equal 1 mouse unit of crude maitotoxin.

This procedure allows us to recapture much more toxin in the process of purification than we had ever been able to do before. Notice that we can recover up to 90% (at the 1 μ g/MU level) of the total toxin assayed in the crude. All but one of the toxic fractions recovered are multi-component systems, having pigments associated with them. Thin layer chromatography of the toxic precipitates (as well as NMR) indicates at least three components.

Summary and discussion of clone 350 separations. Experiments with sep-pak, analytical, semipreparative, preparative, low pressure and solid phase chromatography indicate that several of these methods can be utilized to obtain toxic fractions at the 1.0 to 0.1 μ g/MU level of purity. Attempts to purify the toxin beyond this

level results in division of the toxic fraction, loss of specific activity, and loss of total toxicity. Monitoring of the 1.0 to 0.1 $\mu\text{g}/\text{MU}$ level of purity fractions by NMR spectroscopy indicates that there numerous components in the fractions. Our latest approach to this problem is to purify each of the components from the 1.0 to 0.1 $\mu\text{g}/\text{MU}$ level of purity and obtain NMR spectra on them. Therefore we will have a composite aspect of all of the structures that exist within the toxic fraction. In the NMR section we provide partial structure of the largest of the components.

Purification of Secondary Components.

In the process of extracting toxin from the 350 clone of dinoflagellates we discovered that there was an additional type of chlorophyll-a present which was different from the normal type. Preliminary ^1H NMR data indicated that the new type of chlorophyll differed in having an extra ring structure and information on this pigment was presented at the Dinoflagellate Conference in Sweden.^[120]

Because of its uniqueness, we looked further at the structure and presence of the new pigment. Chlorophyll was extracted from several mass cultures and purified first by hexane extraction. The hexane extract was dried down and taken up in methanol. The methanol solution was applied to the preparative HPLC and monitored at 270 nm.

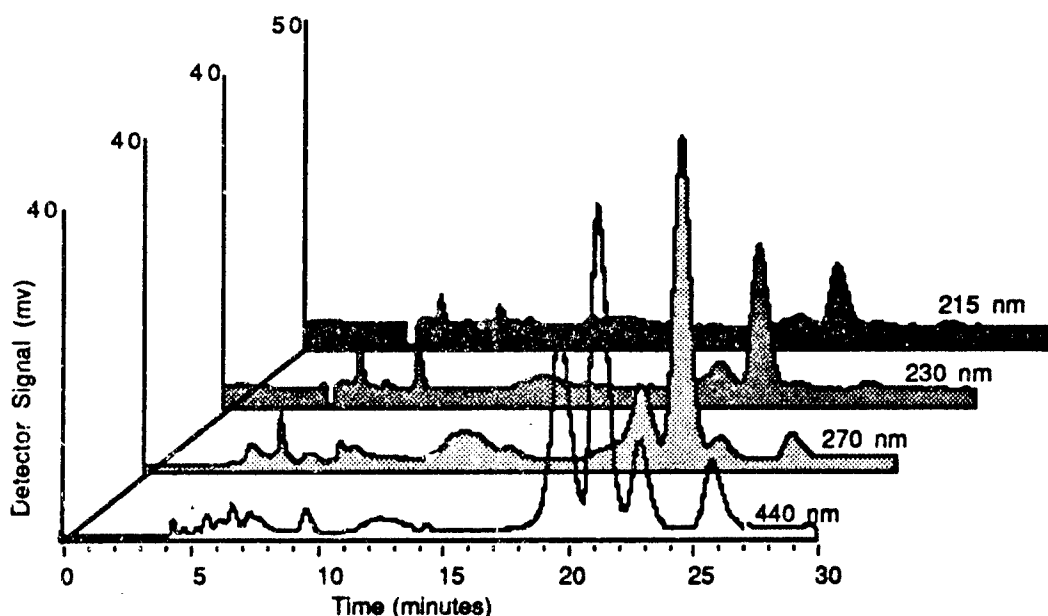


Figure 88. Analytical HPLC chromatograms of hexane fraction of *Gambierdiscus toxicus* (GT-350) run at 0.3 ml/min on Radial Pak μ BONDASPHERE 15 μ C18 300Å column, using a Waters 490 programmable detector set at 215, 230, 270 and 440 nm. Three chlorophyll peaks occur at 19.5, 21.5 and 22.8 min. The peak at 26.1 is β -carotene.

For elution from the column a complex gradient starting with 90% acetonitrile-10% ethyl acetate. This changed to 100% ethyl acetate in 10 minutes, after which the ethyl acetate was replaced by methanol in the next ten minutes. Six distinct peaks appeared in the chromatogram at 9.5, 18.0, 19.5, 21, 22.0, and 26.5 min. The largest at 19.5 minutes proved to be the blue pigment. A second run of that peak using the same gradient conditions produced a peak of 30 mg of blue pigment (which we designated chlorophyll-a666). This was subjected to both ^1H and ^{13}C NMR. On the analytical HPLC the chlorophyll peaks appeared as three distinct peaks. The Chl(s)-a eluted as three distinct peaks, #C-1, #C-2, and #C-3 at 19-26 minutes (Figure 88 and Table 39).

TABLE 39.
ELUTION TIMES OF CHLOROPHYLLS-A FROM DINOFLAGELLATE EXTRACTS
ON ANALYTICAL, SEMI-PREPARATIVE AND PREPARATIVE HPLC

	Peak #C-1	Peak #C-2	Peak #C-3
Analytical	19.5	21.5	22.8
Semipreparative	28.5	29.1	30.1
Preparative	26.0	29.0	33.0
Color of Peak	Pea green	Blue green	Kelly green

Milligram amounts of the pigments were purified by peak selection and rechromatography. Interestingly enough, the initial peaks separated on the HPLC contained lipid plus pigment. The relative colors were as shown in Table 39.

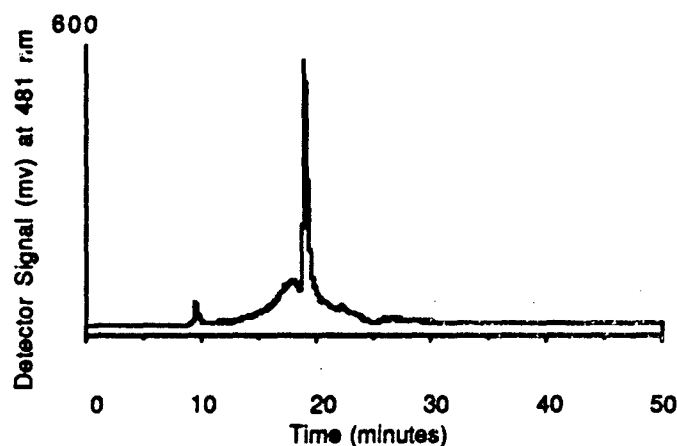


Figure 89. HPLC separation of purified chl_{a666} by selecting single peak at 19.5 minutes on preparative system using acetonitrile/ethyl acetate/methanol (1:1:1) in an isocratic mode. The large peak at 19.5 is chlorophyll-_{a666}.

The lipids are easily removed from the pigment by rechromatographing, using a mixture of acetonitrile/ethyl acetate/methanol (1:1:1) isocratically and selecting peaks (see Figure 89). However, experience has shown that the pigment is more stable and stores better without allomerization when the lipids are present. Upon further purification and elimination of some of the lipids, it was found that the peaks contained varying amounts of two different chlorophylls-a, one appearing deep grass-green having a major

absorption peak at 673 and another, appearing brilliant cobalt-blue, having a major absorption peak at 666. Hence to discriminate the two we have termed them simply chlorophyll-a₆₆₆ (chla₆₆₆) and chlorophyll-a₆₇₃ (chla₆₇₃). After purification, the two chlorophylls were dried, then taken up in deuterated methanol and examined on 500 MHz for ¹H (Table 40) and on the 300 MHz for ¹³C (Table 41).

TABLE 40.
¹H NMR RESONANCES OF GREEN (673) AND BLUE (666) CHLOROPHYLL
ISOLATES FROM *GAMBIERDISCUS TOXICUS* (GT-350)

Proton	Chlorophyll-a ₆₇₃	Chlorophyll-a ₆₆₆
β	9.60s	9.60s
α	9.46s	9.38s
δ	8.61s	8.38s
2	7.98dd	7.97dd
2'	6.29d	6.18d
2''	6.18d	5.99d
10	6.25-5.5s	-
P-2	5.2t	5.0t
8	4.46q	4.32q
P-1a	4.51t	4.12t
P-1b	4.45m	4.08m
7	4.15dd	4.55dd
10 OMe	3.70s	3.68s
4 CH ₂	3.70q	3.74q
5Me	3.60s	3.58s
1Me	3.40s	3.31s
3Me	3.22s	3.28s
7a	2.6, 2.45m	2.26t
7b	2.25, 2.22m	2.26t
8Me	1.78d	1.43d
4Me	1.68t	1.65t
P-3Me	1.58s	1.48s
Phytol Me's	0.84, 0.78	0.84, 0.78

Integration of the ¹H peaks of NMR indicates that fraction C-1 consisted of 38 mg of a linoleic acid derivative and 14.5 mg of green chlorophyll-a₆₇₃ as described in the literature. Peak C-2 consisted of a linoleic acid derivative and blue chlorophyll-a₆₆₆ and peak C-3 consisted of lipid and both chlorophyll-a₆₇₃ and chlorophyll-a₆₆₆

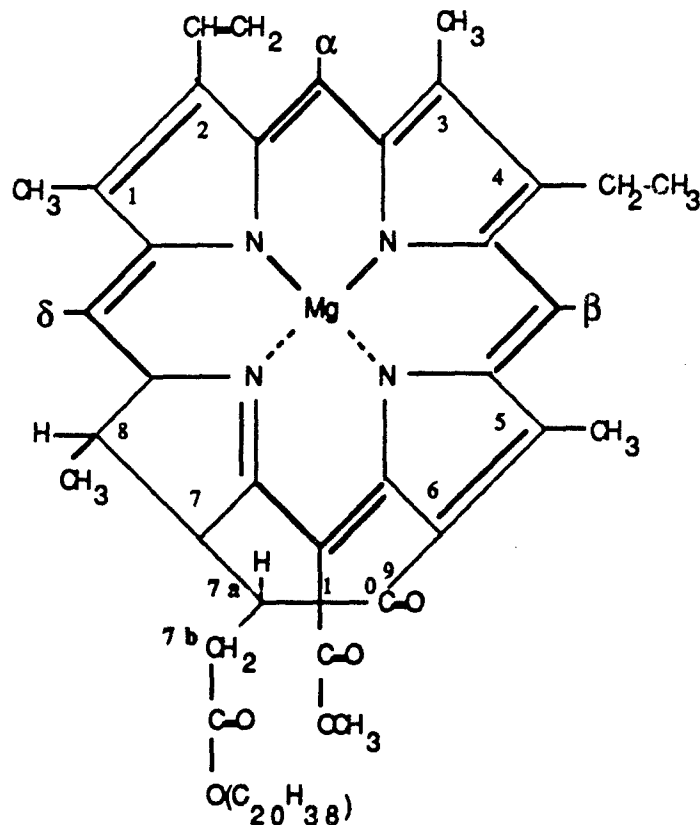


Figure 90. Diagram of structure of new chlorophyll isolated from dinoflagellates.

Upon inspection of the proton data it was observed that the blue pigment did indeed contain the porphyrin ring structure. The ring low field methine signals, the 2 vinyl group and ring methyl groups all match very closely with traces of standard chlorophyll-a₆₇₃. Furthermore, all the distinguishable resonances from the phytyl chain are in place. However several differences can be seen; (1) the 6.25s is completely missing, (2) the 2.6 and 2.45 methylene signals are missing and (3) several resonances in ring IV (H-7, H-8, 8-Me) are significantly shifted. Furthermore in the blue chlorophyll trace, a large resonance at 2.26 is coupled to the 4.55 ppm signal, something not observed in standard chlorophyll-a. With these data we affirm the following structure (Figure 90) for the blue chlorophyll-a₆₆₆.

which amounts to the formation of a new ring with covalent bonding of C-7a with C-10.

TABLE 41
¹³C ASSIGNMENTS FOR STANDARD CHLOROPHYLL-A₆₇₃ AND THE NEW
 BLUE CHLOROPHYLL-A₆₆₆

	Standard Green Chlorophyll-a ₆₇₃	Blue Pigment Chlorophyll-a ₆₆₆
P-3	143.0	143.0
C-2a	130.4	130.24
C-2b	119.9	120.21
P-2	117.7	117.6
C-β	107.8	107.49
C-α	100.1	102.16
C-8	92.6	93.86
C-10	65.3	64.95
P-1	61.5	61.57
C-10b	53.0	52.93
C-7	50.4	52.31
C-8	49.7	48.41
P-4	39.8	39.73
P-14	39.4	39.36
P-10, P-8, P-12	37.4	37.41, 37.36, 37.27
P-6	36.6	36.66
P-11	32.8	32.78
P-7	32.7	32.66
C-7a	30.9	45.18
C-7b	28.0	31.43
P-15	28.0	27.96
P-5	25.0	25.0
P-13	24.8	24.79
P-9	24.4	24.44
C-8a	23.6	22.46
P-15a, P-16	22.7	22.70, 22.60
C-4a, P-7a, P-11a	19.7	19.72, 19.62, 19.49
C-4b	17.5	17.61
P-3a	16.4	16.01
C-1a, C-5a	12.6, 12.3	12.38
C-3a	11.0	11.15

To obtain a ¹³C spectrum of the blue chlorophyll we found it necessary to use a sample of about 30 mg. This gave significant differences between the resonance peaks of the pigment and those of the accompanying lipids. The lipid peaks were predetermined from samples of almost pure lipid, extracted from the pigments. The following is a listing of the peaks of the proton-decoupled ¹³C spectrum of the chlorophyll-a₆₆₆ in CDCl₃ which were clearly

resolved in about 12,000 transients, nearly three hours of accumulation.

In Table 41 the ^{13}C resonances obtained for the chlorophyll-a₆₆₆ are shown along with those for the standard green chlorophyll-a₆₇₃ and clearly show certain peaks which undergo a significant shift.

TABLE 42.
RELATIVE CONCENTRATIONS OF CHLOROPHYLLS-A HPLC PEAKS FROM
EXTRACTS OF A DINOFLAGELLATE *GAMBIERDISCUS TOXICUS* (GT-350)

Color Crude Peak	Peak #C-1 Pea green	Peak #C-2 Blue green	Peak #C-3 Kelly green
Amt of Chl ₆₆₆	0.0 mg	10.5 mg	2.1 mg
Amt of Chl ₆₇₃	14.5 mg	0.0 mg	5.0 mg
Amt of Lipid	38.0 mg	7.3 mg	33.9 mg
The mass cultures examined and the content of chlorophylls-a per unit weight are detailed in Table 43.			

TABLE 43
SPECIFIC CONCENTRATION OF CHLOROPHYLLS-A IN THE FOUR CLONES OF
DINOFLAGELLATES EXAMINED

SPECIES (SIU CLONE NO.)	BLUE mg Chl ₆₆₆ /gm	GREEN mg Chl ₆₇₃ /gm
<i>G. toxicus</i> (350)	0.29	0.40
<i>G. toxicus</i> (175)	19.51	0.01
<i>P. concavum</i> (364)	6.30	1.35
<i>O. lenticularis</i> (874)	0.51	0.01

Discussion and conclusions from chlorophyll-a investigations. This investigation has detailed a new procedure for the quantitative separation of chlorophyll(s)-a from dinoflagellates which can be used on other organisms equally well. The structural characterization of a new type of chlorophyll-a is another outcome of this study that is of considerable import. Our research has shown that is present in several clones of dinoflagellates. In fact, dried cells with larger content of blue chlorophyll pigment were much darker in color than those with less. It would be of interest to know if it is present outside of the dinoflagellates or if like peridinin this is pigment which is more or less specific to this group.

From the small number of clones that we have examined so far, we surmise that both types of chlorophyll are produced but the

concentration may vary depending upon the growth conditions. This aspect needs further examination. Even more intriguing is the role of this new kind of chlorophyll-a in the photosynthetic system in the dinoflagellate.

NMR of Model Compounds

We examined many known model compounds but present data for five. These compounds were chosen for their biomedical interest, because they had structures similar to what we are expecting in our isolated toxins and also to demonstrate our NMR capabilities. The five compounds chosen were: atropine, quinine, procaine, xanthosine dihydrate and reserpine.

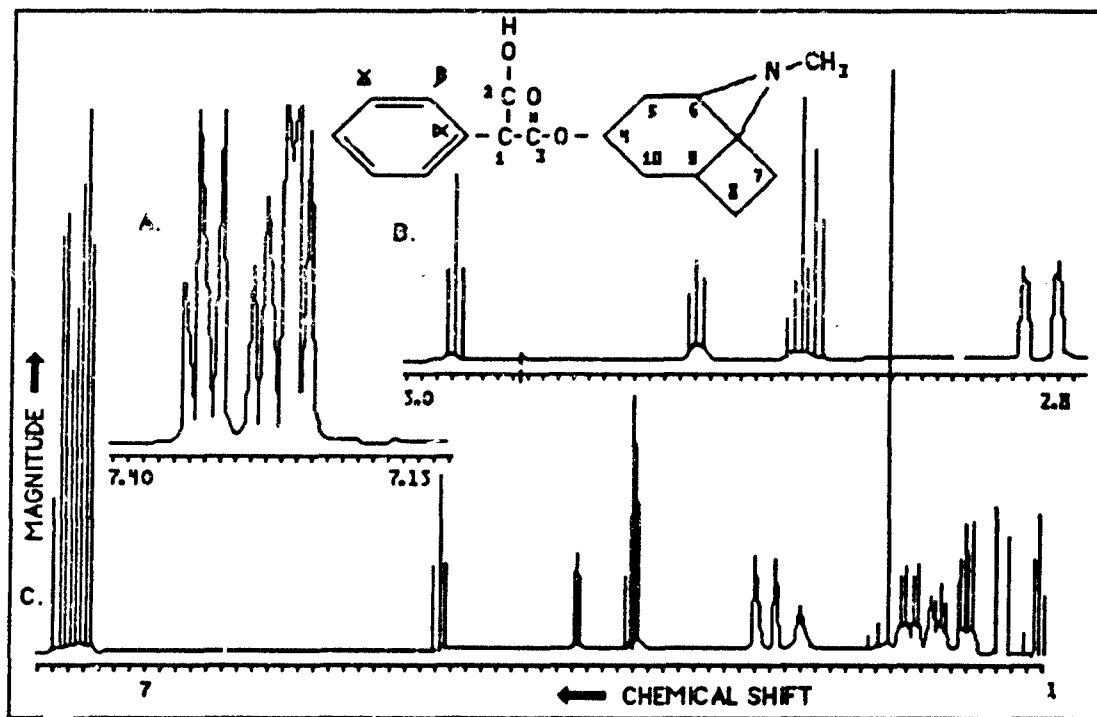


Figure 91. Proton coupled 500 MHz spectra of atropine. Upper insert right shows the 2.8 to 5.0 region.

Atropine.

The F-T high resolution proton spectrum of atropine, $C_{17}H_{23}NO_3$ in deuteriochloroform, $CDCl_3$, is shown in Figure 91. Note the distinct resolution of each peak. The upper insert shows an enlargement of the 2.8-5.0 PPM spectral region. The resonance assignments are made by location in the appropriate chemical shift range and by selective decoupling double resonance experiments. We show here 1H assignments and accompanying coupling constants.

TABLE 44.
 1H PROTON ASSIGNMENTS

RingM	C1H	C2HA	C2HB	C4H	C5HA	C5HB	NH3	C10HA	C10HB	C6H	C7HA
7.3	4.14	3.8	3.75	5.0	1.99	1.42	2.17	2.07	1.63	2.87	1.72
	C7HB	C8HA	C8HB	C9H							
	1.67	1.82	1.15	3.0							

 1H - 1H COUPLING CONSTANTS DETERMINED BY DOUBLE RESONANCE

J1,2A	J1,2B	J2A,2B	J4,5A	J4,5B	J4,10A	J4,10B	J5A,5B	J5A,6
9.0	4.6	3.0	5.0	0	5.1	0	15.0	3.5
J5A,7A	J6,7A	J7A,7B	J8A,8B	J8A,9	J8A,10A	J9,10A	J10A,10B	
1.2	7.0	8.4	7.3	7.0	1.2	3.5	15.0	

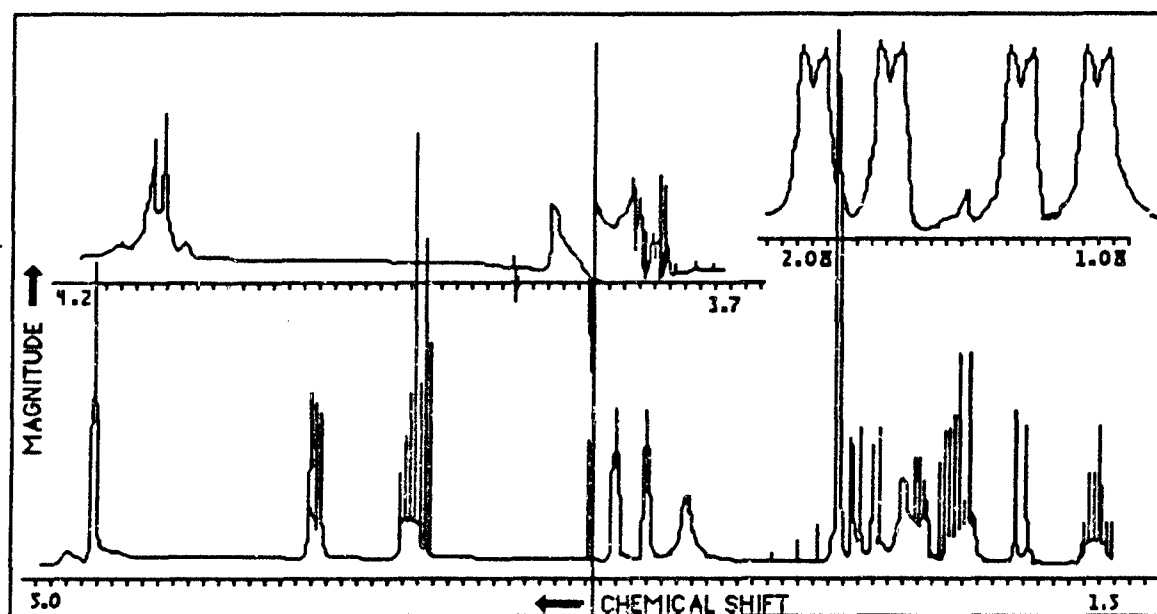


Figure 92. Proton coupled 500 MHz spectra of atropine. 1.4 to 5.2 PPM region of proton spectra with 3.80 (C2HA) decoupled. Upper left region is 3.7 to 4.2 PPM region. Upper right inset shows multiplets at 2.07 (C10HA) and 1.99 (C5HA).

As is characteristic in rigid systems, the methylene protons resolve individually and we designate the low field proton as A and the up field proton as B. Figure 92 shows the decoupling of C2HA (3.80) and the resulting 4.6 Hz doublet at 4.15 (C1H). This 4.6 Hz splitting is the coupling constant between C1H and C2HB. The upper right insert of Figure 92 shows the resulting multiplets at 2.07 (C10HA) and 1.99 (C5HA) after decoupling C4H at 5.0. Here coupling constants of 15.0, 3.7, and 1.2 Hz can be seen. A coupling constant of 5.5 Hz is thereby lost in the decoupling of C4H from both C10HA and C5HA. This further shows the symmetrical nature of the saturated ring structure of this molecule.

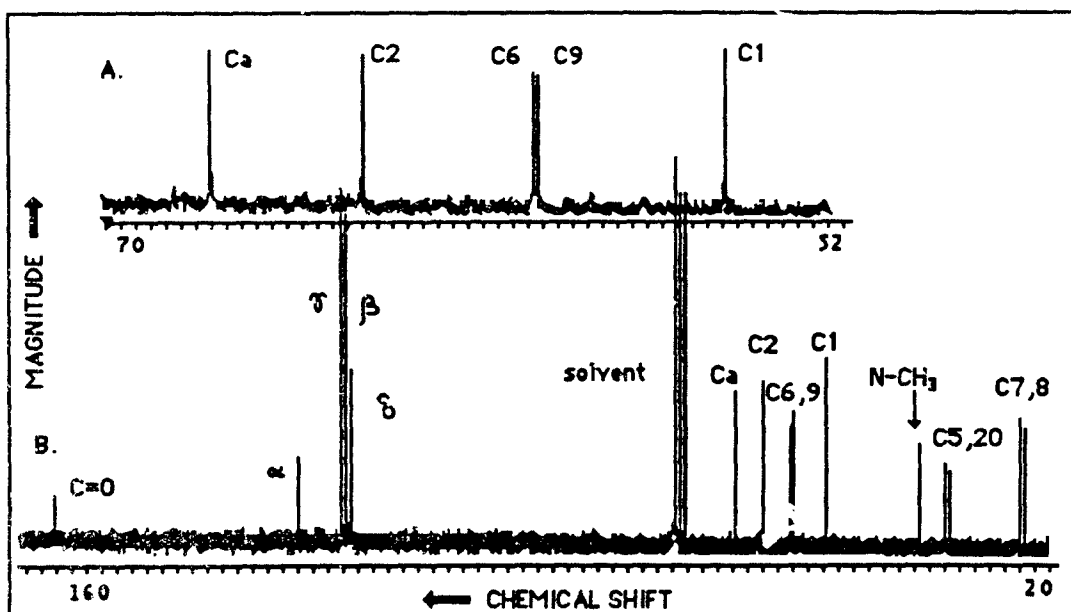


Figure 93. 300 MHz ^{13}C NMR spectra of atropine.

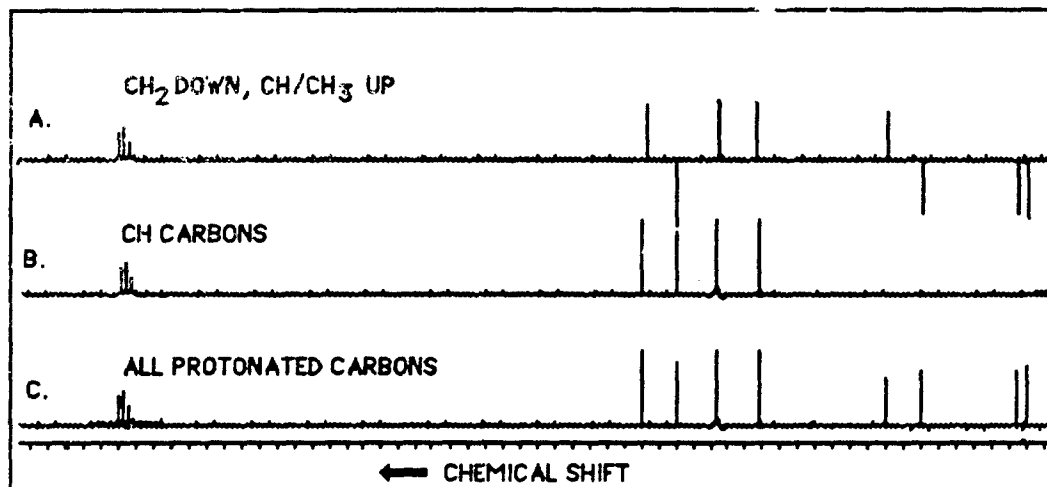


Figure 94. Distortionless, enhancement polarization transfer plot of atropine. This plot differentiates between CH, CH₂ and CH₃ carbons.

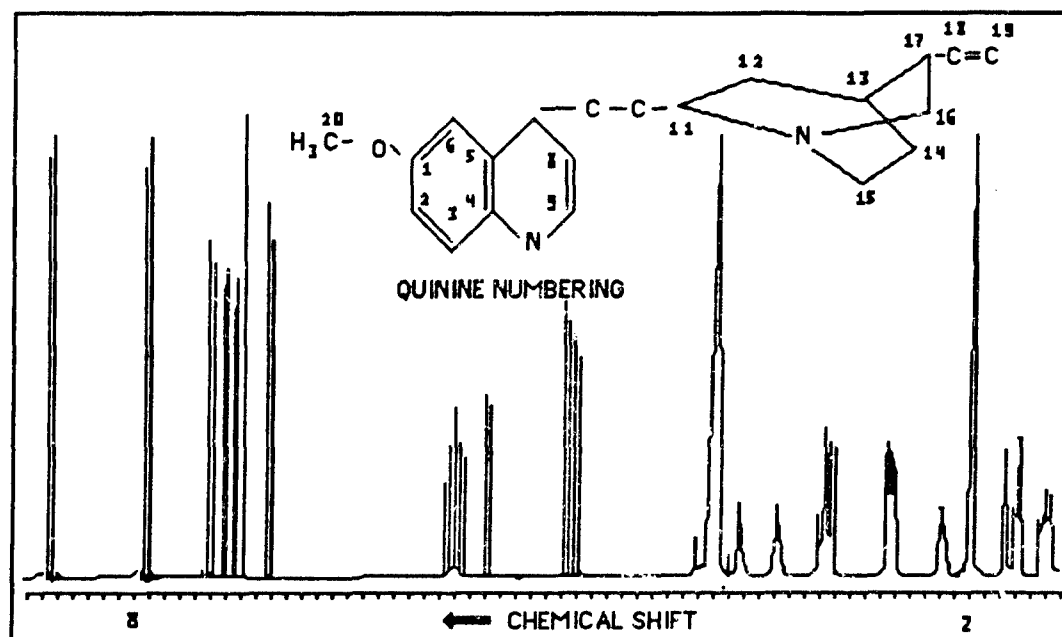


Figure 95. Proton coupled 500 MHz spectra of quinine. 1.3 to 8.6 spectrum with ^1H assignments.

The proton decoupled ^{13}C spectrum is shown in Figure 93. Each carbon resolved separately with the exception of the double resonance of α and β carbons. This situation is easily recognized by the approximate doubling of height of the spectral line. The insert at the top of Figure 93 shows an enlargement of the region from 52 to 70 PPM, thus allowing the two distinct lines at 59.5 to be clearly visible.

Figure 94 is a spectral plot of carbon-proton correlation called a DEPT plot, short for Distortionless Enhancement Polarization Transfer. This plot shows all protonated carbons and distinguishes between CH , CH_2 , and CH_3 carbons. Quarternary carbons do not register on DEPT but can be distinguished from the normal proton decoupled ^{13}C spectra as shown in Figure 93. For atropine here, the carbonyl (172 PPM) and ring alpha carbon (136 PPM) are seen to be quarternary carbons. The resonance line at 64 PPM shows on DEPT as CH_2 and hence must be the hydroxyl carbon, C2, being in the 60-80 PPM range. Assignment of the methyl carbon at 40.2 PPM would be

difficult without DEPT which makes it unambiguous. Hence, the value of this plot is most obvious.

Quinine.

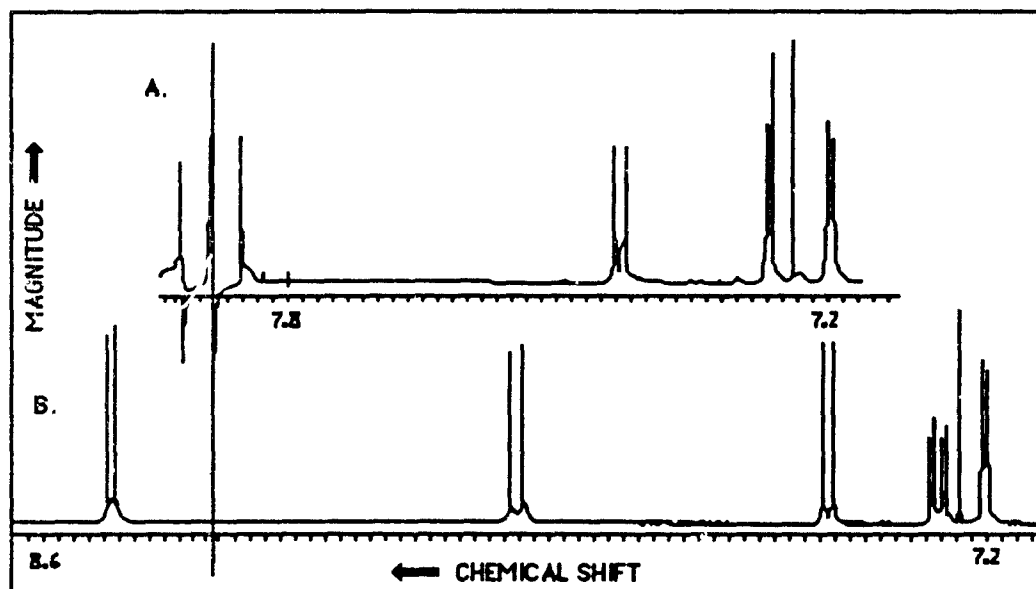


Figure 96. Proton coupled 500 MHz spectra of quinine in the region of 7.0 to 8.6 PPM. Upper insert shows the low field region with decoupling of C3H from C2H.

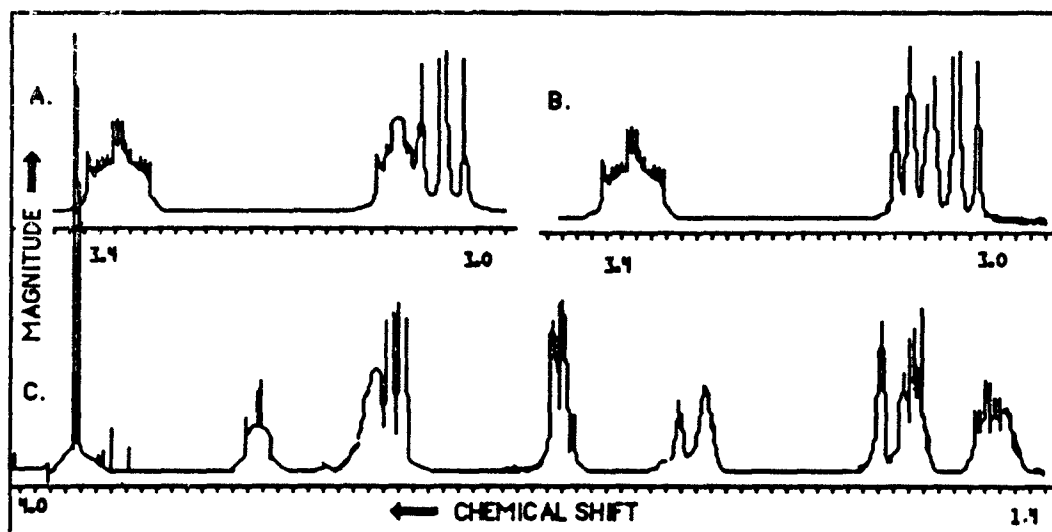


Figure 97. Proton coupled 500 MHz spectra of quinine. 1.3 to 4.0 spectrum with ^1H assignments. Upper inserts show resulting spectra before and after decoupling C10H.

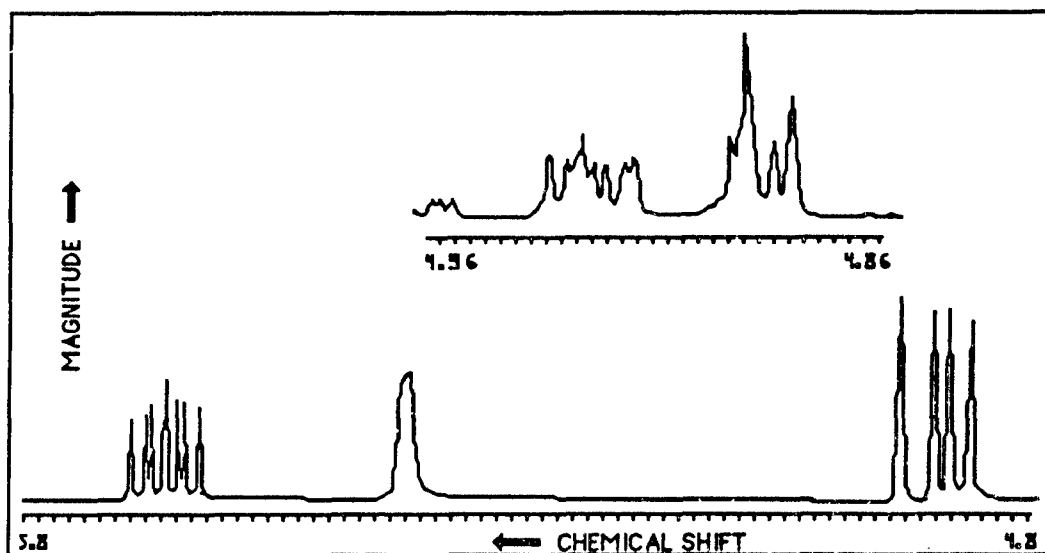


Figure 98. Proton coupled 500 MHz spectra of quinine. Upper insert shows resulting spectra with C18H decoupled.

TABLE 45.
¹H PROTON ASSIGNMENTS

C9H	C3H	C8H	C2H	C6H	C18H	C10H	C19H(trans)	C19(cis)	C20H	C10(OH)
8.60	7.92	7.48	7.28	7.20	5.71	5.50	4.93	4.88	3.88	3.68
										3.40
C11H	C16HA	C15HB	C16HB	C16H	C13H	C14HA	C12HA	C12HB	C14HB	
3.08	3.03	2.62	2.60	2.22	1.78	1.70	1.68	1.51	1.46	

¹H-¹H COUPLING CONSTANTS DETERMINED BY DOUBLE RESONANCE

J2,3	J2,6	J8,9	J10,11	J11,12A	J11,12B	J12A,12B	J17,16A	J16A,16B	
9.2	2.7	4.7	4.1	9.2	9.2	11.7	10.3	13.04	
J15A,15B	J14A,14B	J18,19t	J18,19c	J19t,19c	J13,18	J13,17	J17,18	J17,19c	
11.1	14.5	17.2	10.4	1.8	1.6	8.9	7.0	6.0	

Quinine, C₂₀H₂₄N₂O₂ has several interesting features; a fused benzene ring with a N containing ring, a rigid bridged structure containing N, and a terminal olefinic group. The NMR data for quinine are shown in Figures 94 to 100. The ¹H spectral assignments are shown as determined by double resonance with the

accompanying coupling constants. The large coupling constants of the saturated ring is characteristic of these rigid structures.

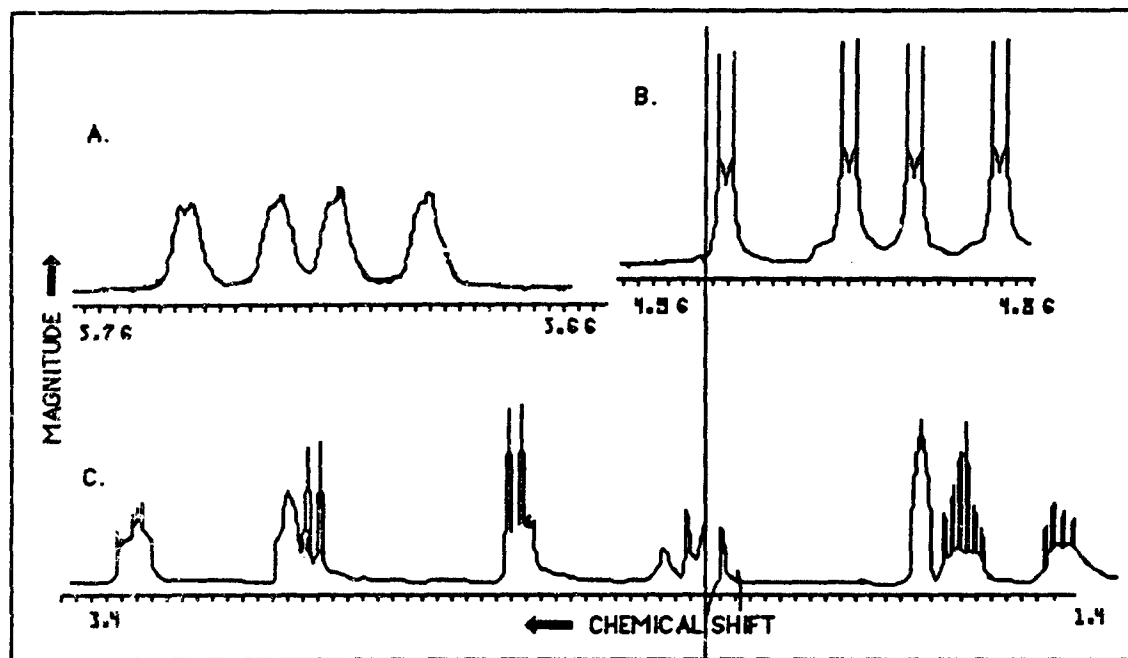


Figure 99. Proton coupled 500 MHz spectra of quinine. Inserts show resulting spectra with C17H decoupled.

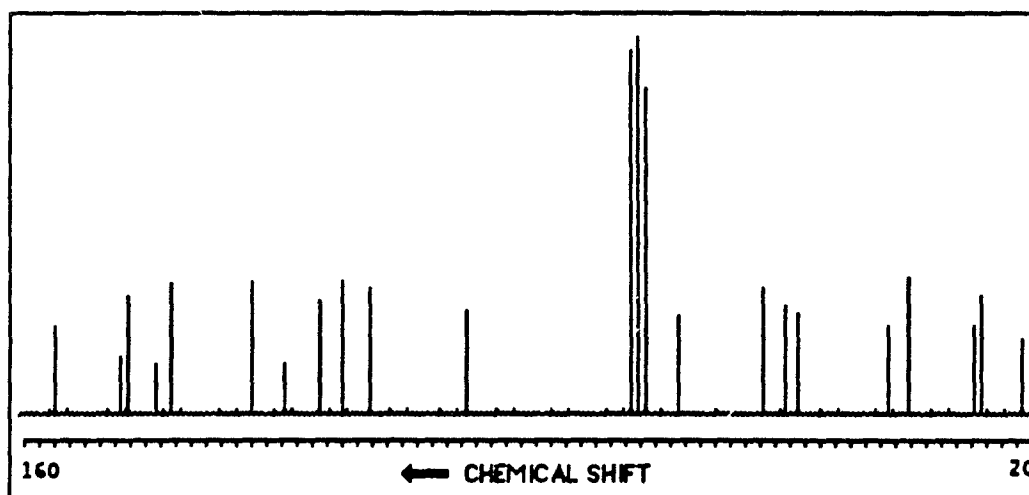


Figure 100. 300 MHz ^{13}C spectrum of quinine.

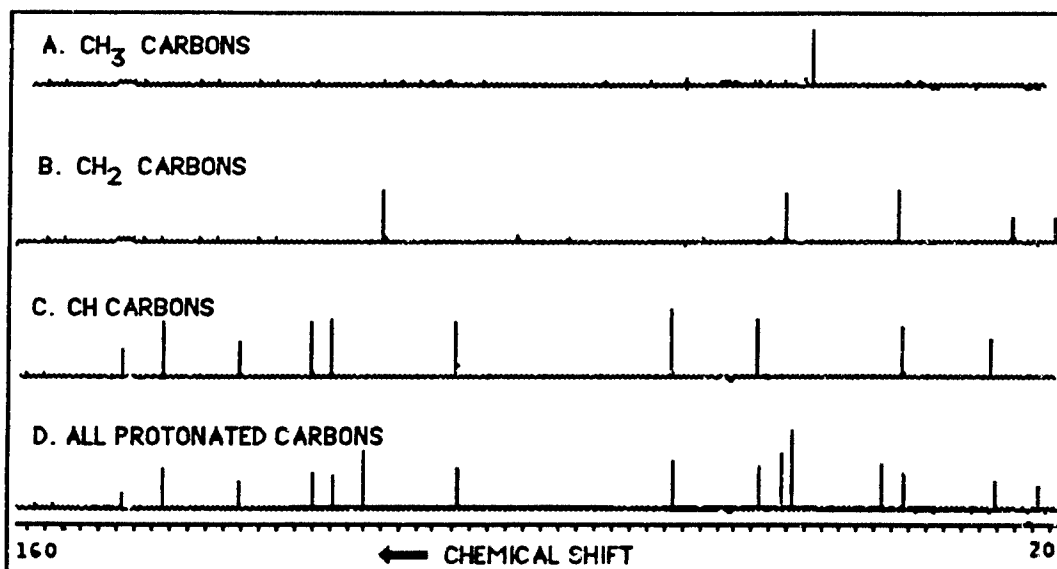


Figure 101. Distortionless, enhancement polarization transfer plot of quinine.

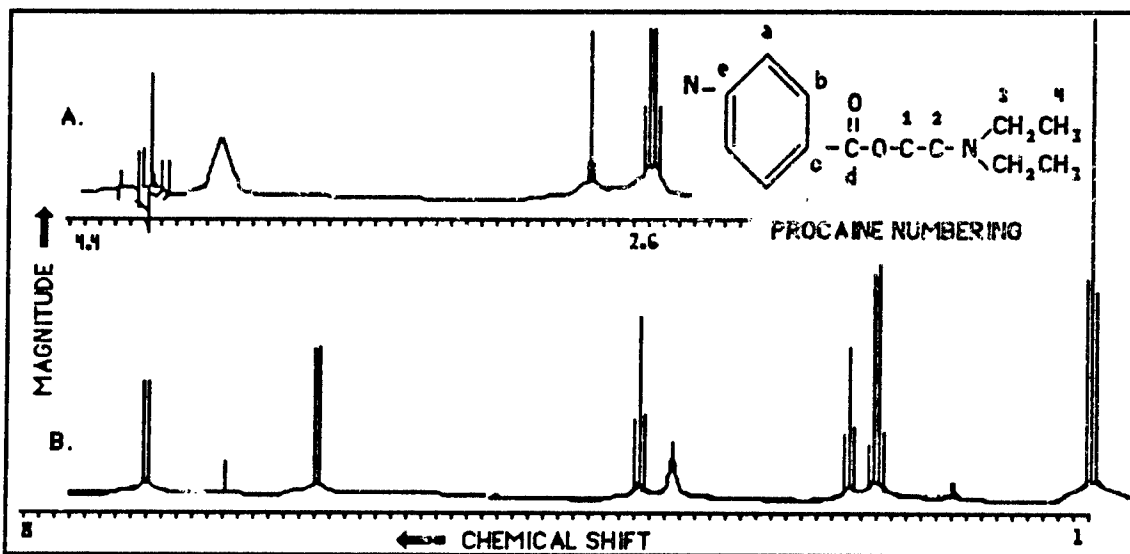


Figure 102. Proton coupled 500 MHz spectra of procaine.

Procaine

Procaine is a relatively simple molecule as analyzed by NMR but provides valuable information concerning the chemical shifts of protons on carbon bonded to nitrogen. As this molecule is not a rigid

structure like other molecules described in this report, its NMR analysis is particularly simple. As shown in the proton spectrum, Figure 101, the benzene ring is completely symmetrical with the two protons α to N resolving at lowest field, 7.8 PPM while the two protons β to N resolve at 6.6 PPM. Vicinal couplings of 8.7 Hz characterize the splitting. The geminal protons of the chain resolve together and show first order couplings. The upper insert in Figure 101 shows the decoupling of the C1H protons (4.30) from the C2H protons (2.8), where the 6.3 Hz triplet at 2.80 PPM collapses to a singlet.

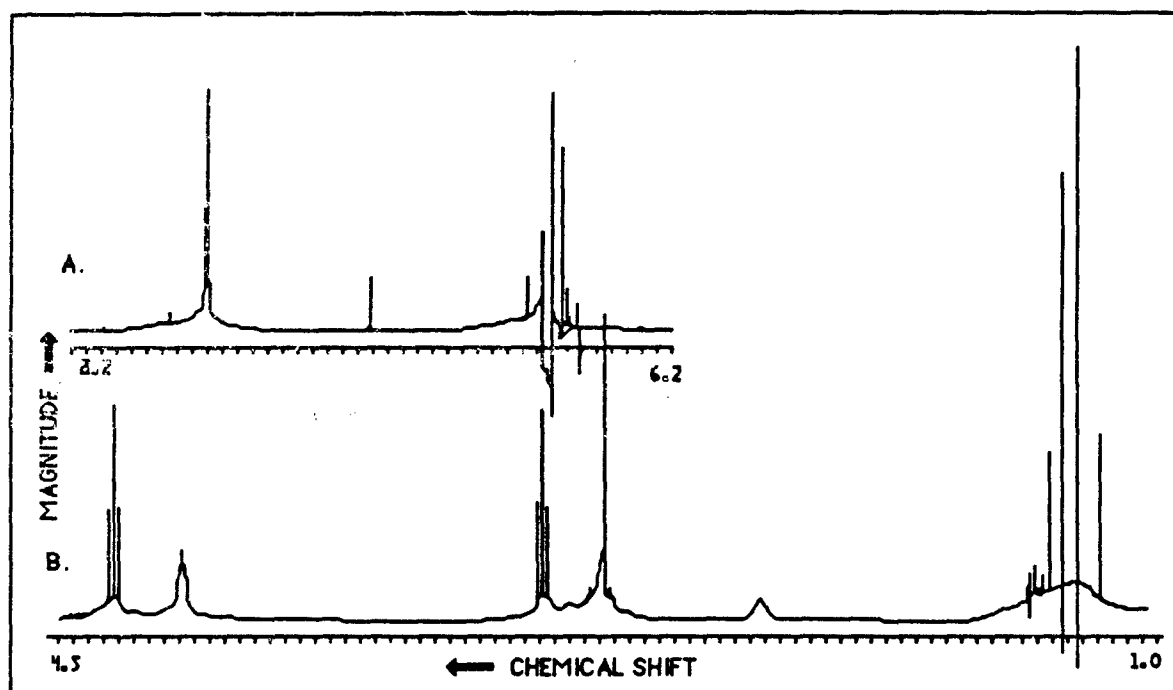


Figure 103. Proton coupled 500 MHz spectra of procaine with decoupling of terminal methyl carbon.

Figure 103 shows decoupling of the terminal methyl protons (1.0 PPM) with resulting collapse of the C3H methylene protons to a singlet at 2.60. The upper insert here shows the decoupling of the ring proton. The resonance at 4.05 PPM must be the NH protons, present in all sample observed and integrating fully to two protons.

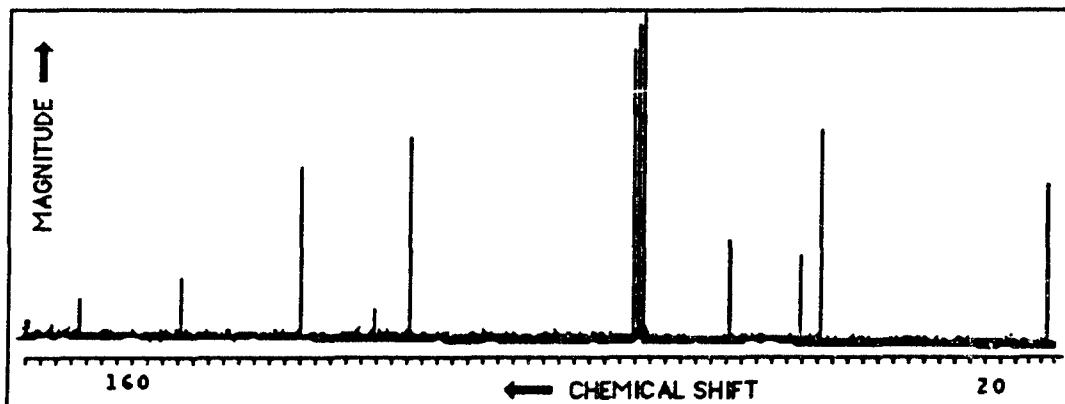
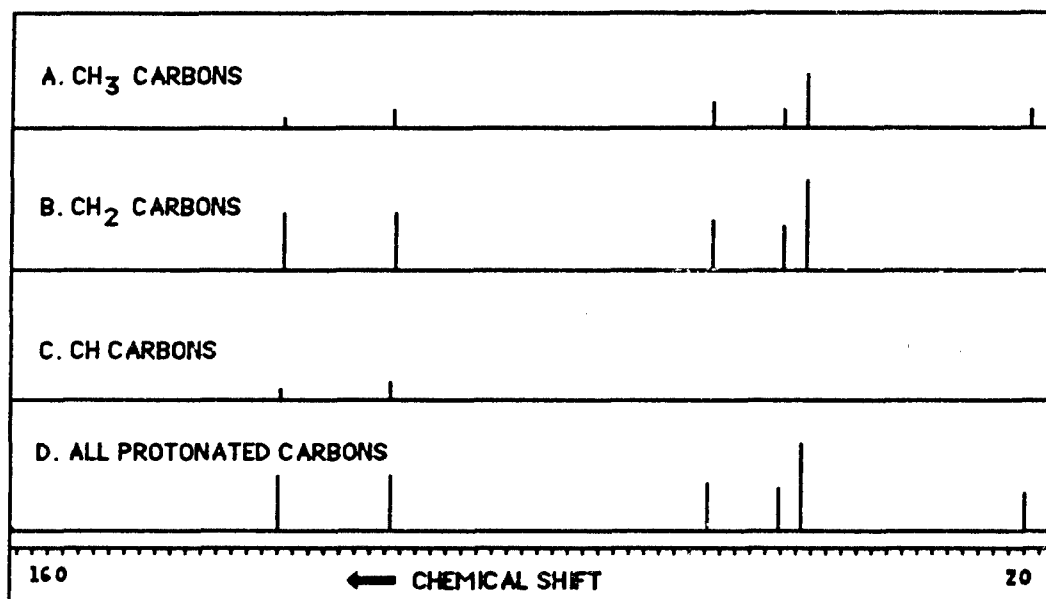
Figure 104. 300 MHz ^{13}C NMR spectrum of procaine.

Figure 105. Distortionless, enhancement polarization transfer plot of procaine.

The proton decoupled ^{13}C spectra is shown in Figure 104. Quarternary carbons are observed at 166P, C=O; 151 P, the ring carbon α to N, and 120 P, the ring carbon bonded to the carbonyl carbon. The height of the resonance lines at 132 P and 114 P indicate 2 carbons each, even in light of somewhat attenuated heights of quarternary carbon resonance lines. This 2 to 1 ratio is

also seen for the branched CH_2 and CH_3 resonances in the chain. A DEPT plot is also shown for completeness in Figure 105.

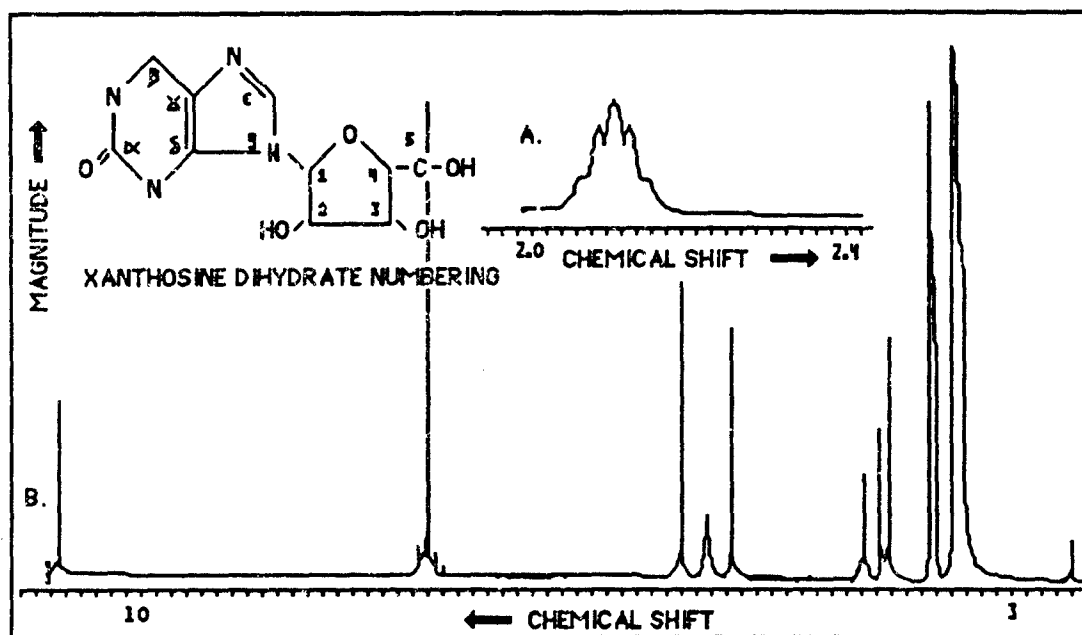


Figure 106. Proton coupled 500 MHz spectra of xanthosine dihydrate.

Xanthosine dihydrate.

Due to limited solubility of this compound in conventional solvents, CDCl_3 , CD_3OD , CD_3CN , D_2O , etc., we have examined xanthosine dihydrate in dimethylsulphoxide (DMSO). We were very pleased to find that the resonance due to hydroxal protons could be observed, a phenomena not normally seen when using proton donating solvents.

The full proton spectrum in DMSO is shown in Figure 106. The singlets at lowest field 10.85 and 7.85 must be ring N-H and C-H protons respectively and the lowest field midrange resonance at 5.72 must be the proton on the ribose ring carbon bonded to O and N, designated C1H. We then used selective decoupling to determine the remaining assignments.

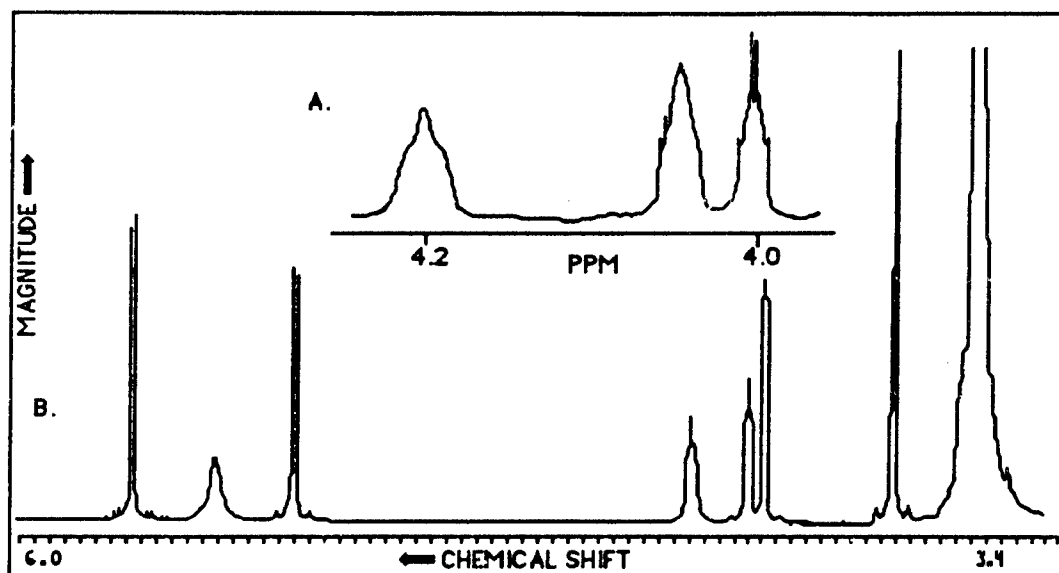


Figure 107. Proton coupled 500 MHz spectra of xanthosine dihydrate. 6.0 to 3.0 PPM region of proton spectra

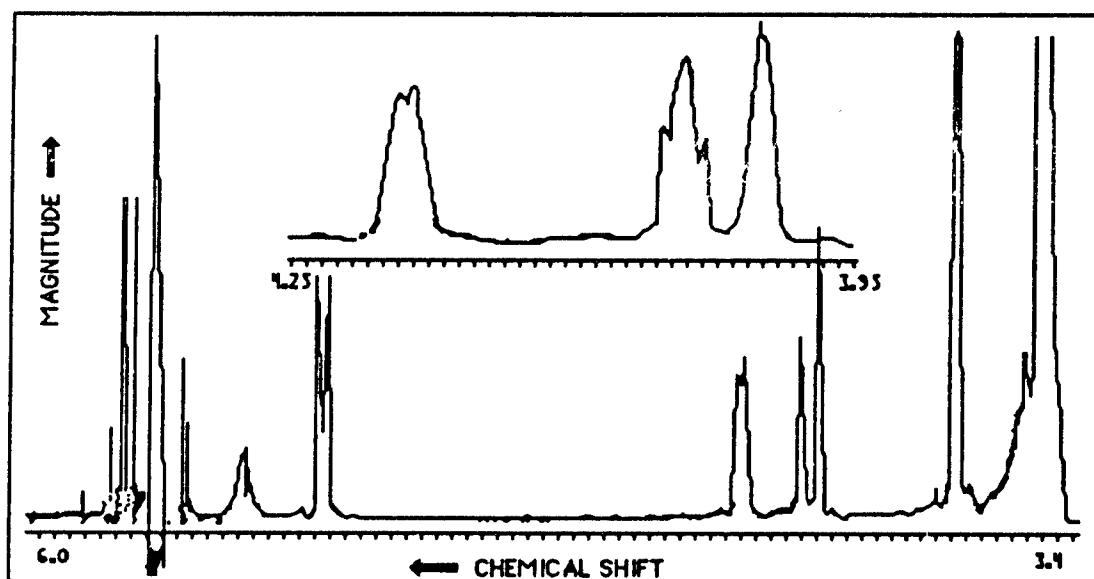


Figure 108. Proton decoupled 500 MHz spectra of xanthosine dihydrate. 3.0 to 6.0 region of spectrum with 5.72 (C1H) decoupled.

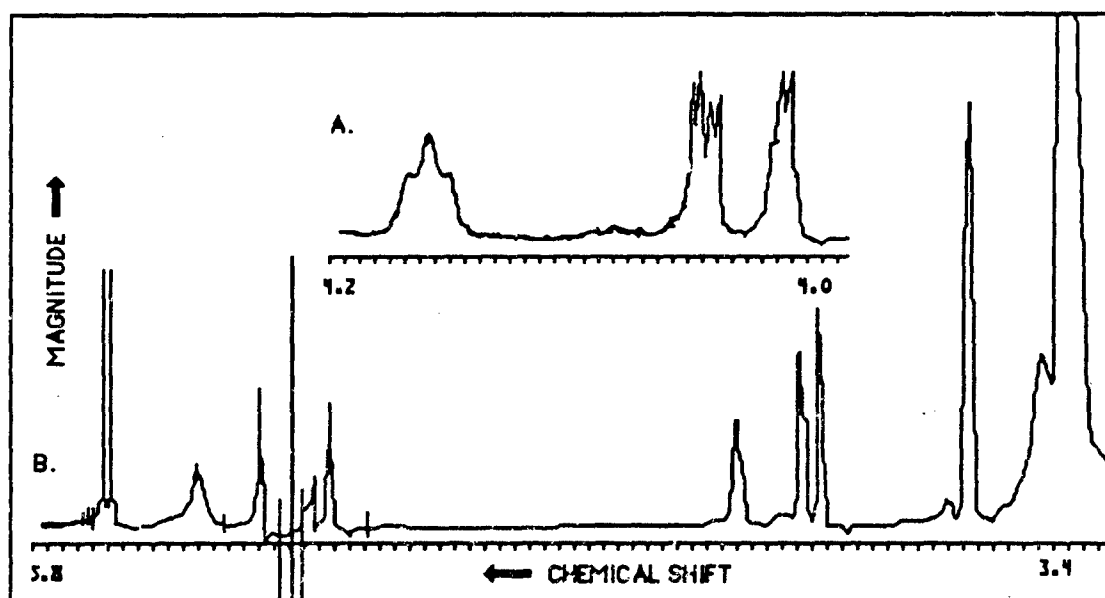


Figure 109. Proton decoupled 500 MHz spectra of xanthosine dihydrate.

In Figure 108 the proton of spectra from 6.0-3.0 PPM is shown revealing 7 peaks, excluding the large OH peak at 3.4 due to dihydrate and NaOH inherent in the compound. The upper insert, Figure 108 shows the fine structures of the 4.0 PPM peaks. Decoupling of 5.72 (C1H) and collapse of 4.20 (C2H) is shown in Figure 108, a 4.9 Hz doublet being observed at 4.20. Note that this is the only peak affected thereby assigning the 4.20 resonance as C2H. In Figure 109, the 5.29 resonance is decoupled, collapsing the 4.04 peak (C3H) into a split doublet, 5.0 and 2.1 Hz, thus establishing the coupling between 4.21 (C2H) and 4.05 (C3H) through the 4.9 coupling constant (Figure 109 and Figure 110).

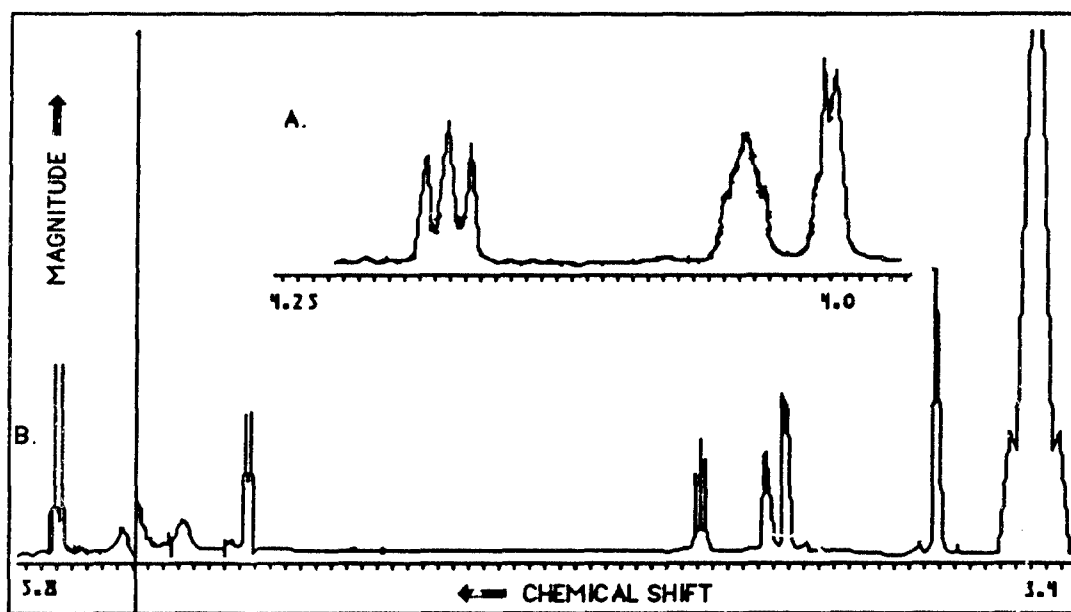


Figure 110. Proton decoupled 500 MHz spectra of xanthosine dehydrate with OH decoupled.

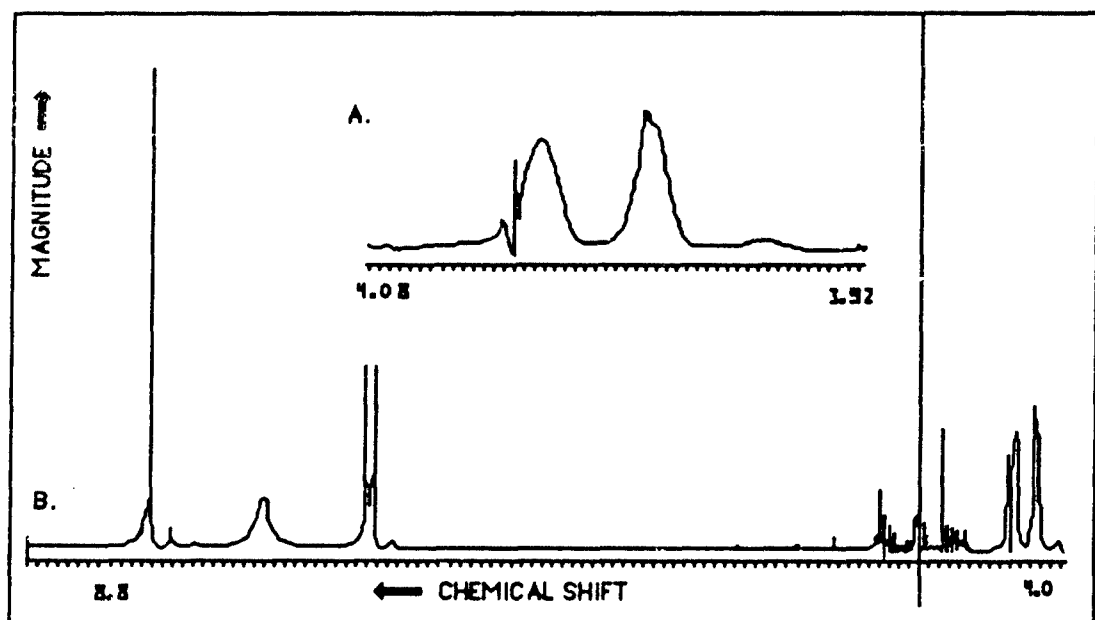


Figure 111. Proton decoupled 500 MHz spectra of xanthosine dihydrate.

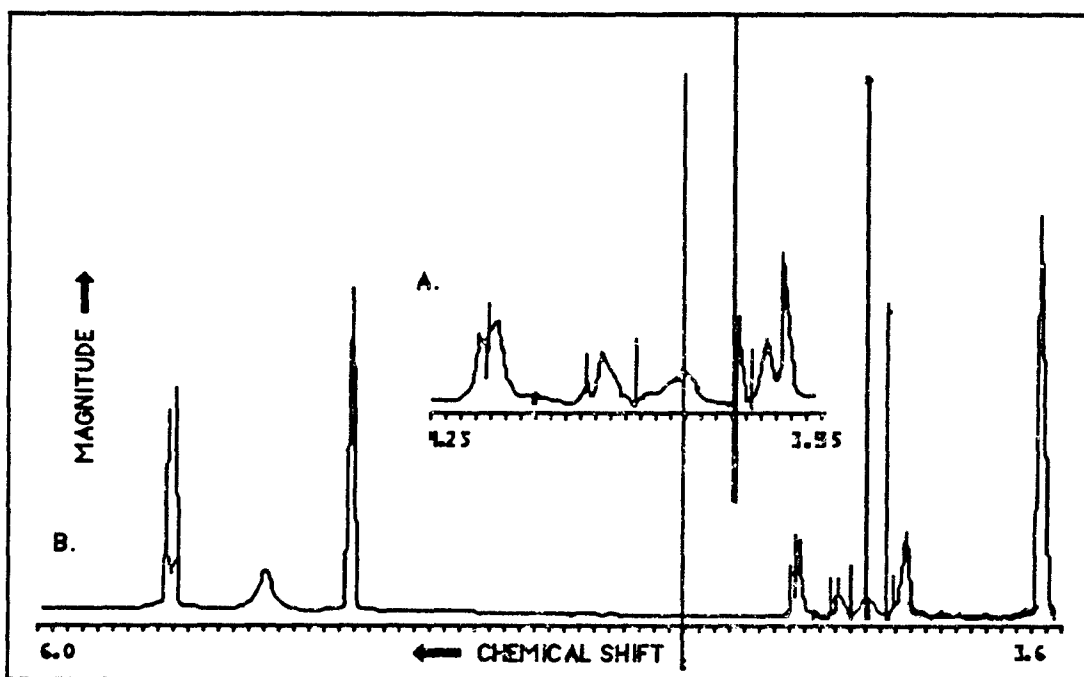


Figure 112. Proton decoupled 500 MHz spectra of xanthosine dihydrate.

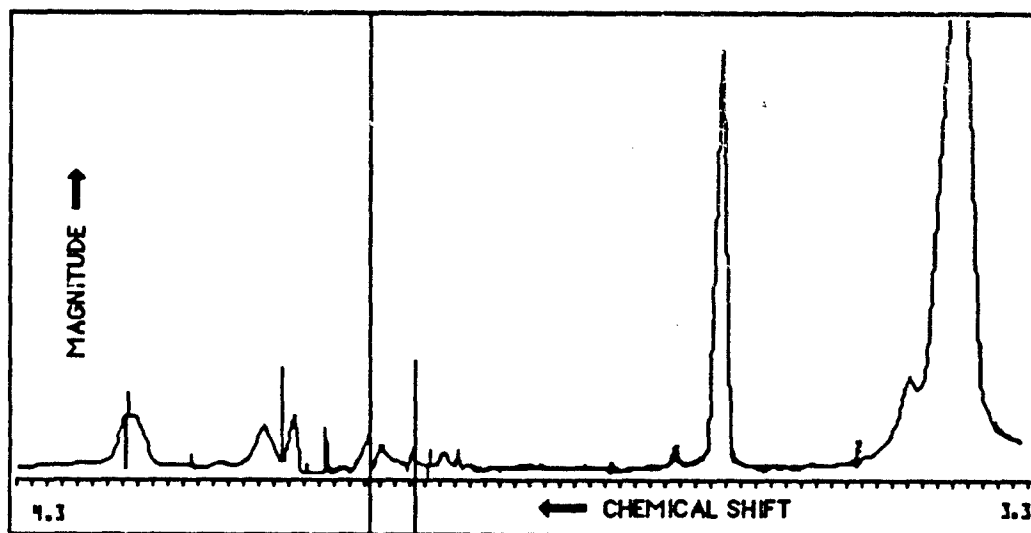


Figure 113. Proton decoupled 500 MHz spectra of xanthosine dihydrate. Decoupling at 3.98 PPM.

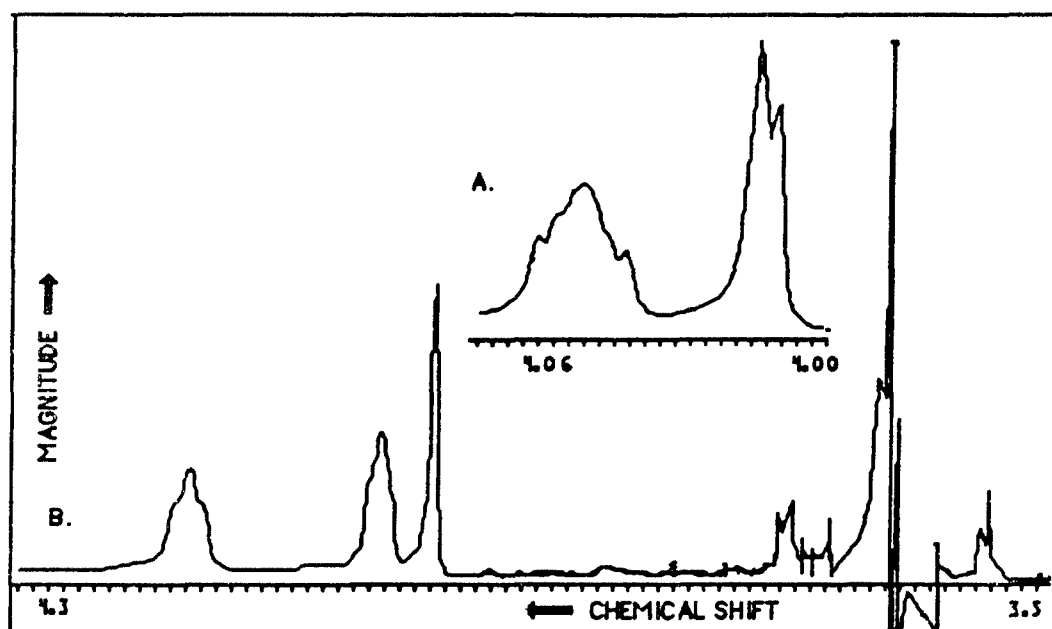


Figure 114. Proton decoupled 500 MHz spectrum of xanthosine dihydrate.

When the broad OH peak is decoupled as shown in Figure 114, the distinct splitting of 4.20 is seen as actually four lines of coupling constants 6.9 Hz and 4.9 Hz. These are the couplings of C2H with C1H and C3H respectively. In DMSO a small coupling of C2H and C2OH must therefore exist, thus blurring 4.20 in the uncoupled spectra. Figure 114 shows the decoupling of 4.20 (C2H) and the resulting singlet at 5.72 (C1H).

Figure 114 shows the decoupling of 4.05 (C3H) and resulting 7.0 doublet (C2H) at 4.20 and singlet at 5.29 (C4H). Decoupling the 3.98 resonance as shown in Figure 114 collapses 3.63 to a singlet. As this resonance integrated to 2 protons and is in the 3.6-3.8 range, the methylene of CH₂OH, it is assigned as C5H₂, and the 4.0 resonance as C3, C5OH, hydroxyl resonances. When 3.63 is decoupled as shown in Figure 115, the side bands of the 4.0 resonances are lost, with 2 Hz splitting remaining, indicating coupling between C3H and C3OH.

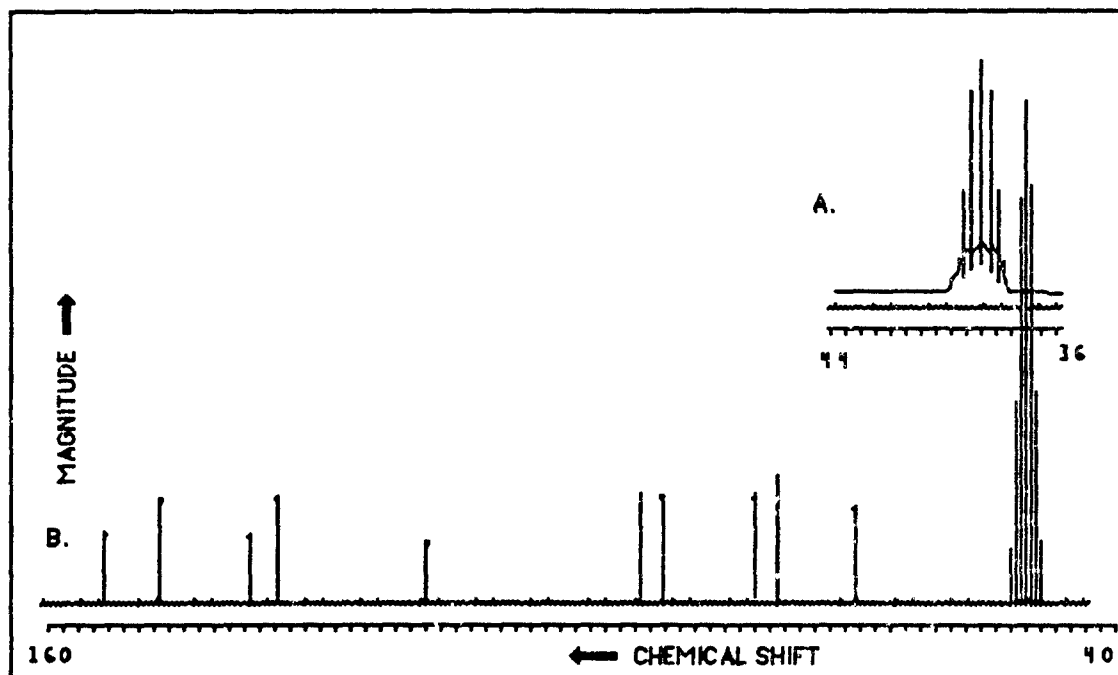


Figure 115. ^{13}C spectrum of xanthosine dihydrate.

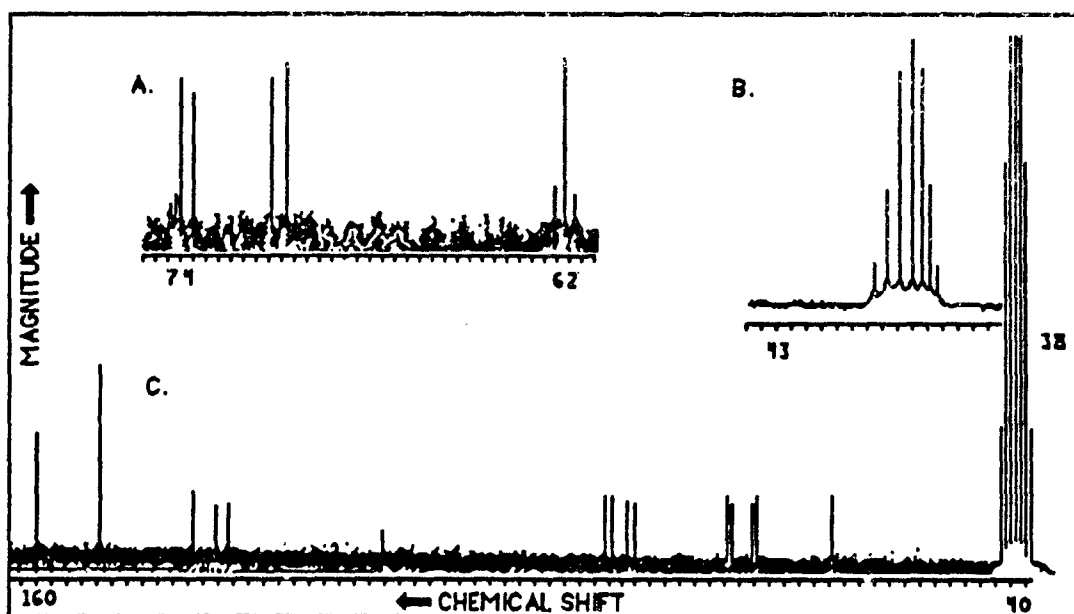


Figure 116. ^{13}C proton off-resonance decoupled spectrum of xanthosine dihydrate.

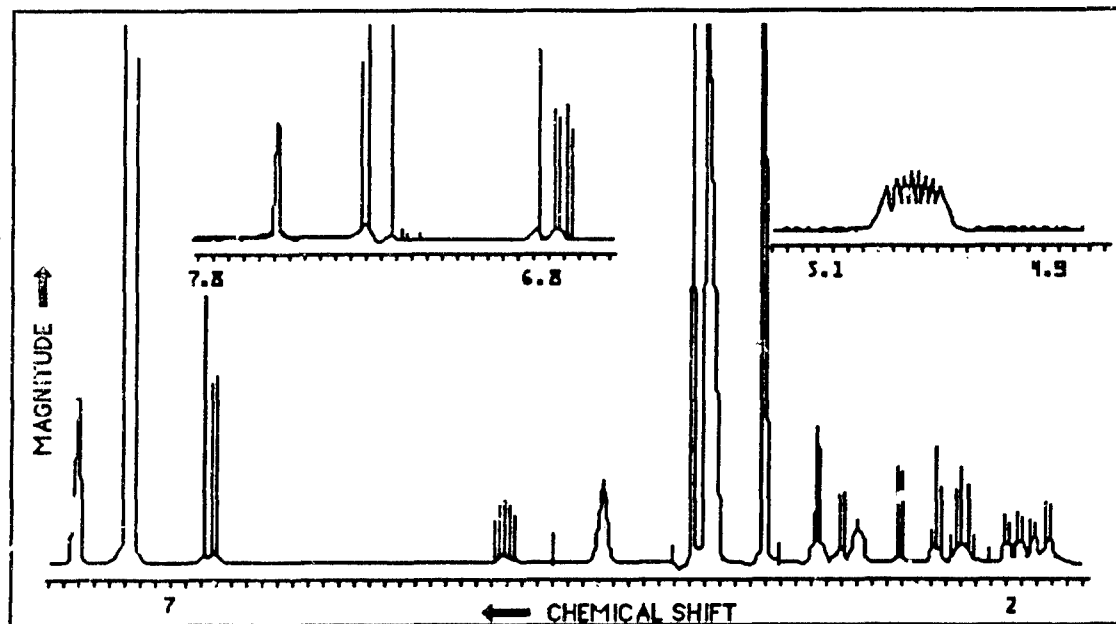


Figure 117. Proton coupled 500 MHz spectra of reserpine. Upper left insert shows low field region, the resonances are the two ring structures. Upper insert right shows the 8 lines of the C18H multiplet.

Reserpine

Reserpine, $C_{33}H_{39}N_2O_9$ was the last compound analyzed and reported upon. Having a molecular weight of about 600, it borders on the threshold of having a complete ¹H NMR spectra. Considerably more time was required to analyze this molecule in comparison to the others in this report. The most complicated region of spectra for molecules of this type, the methylene region for 2.7 to 1.0 PPM was completely resolved. All resonances could be analyzed and coupling constants measured, thus attesting to the high resolving power of the VXR-500 instrument.

The proton decoupled C13 spectra is shown in Figure 117, where all 10 carbon atoms resolve separately, a C13 proton off-resonance decoupled spectrum is shown in Figure 118, identifying quarternary carbons at 158, 150, 140, and 116 PPM. These resonances being singlets. The mid-field carbons resolve as doublets, thus identifying

themselves as CH carbons with the exception of C5 at 61 PPM which resolves as a triplet, more clearly seen in the upper insert.

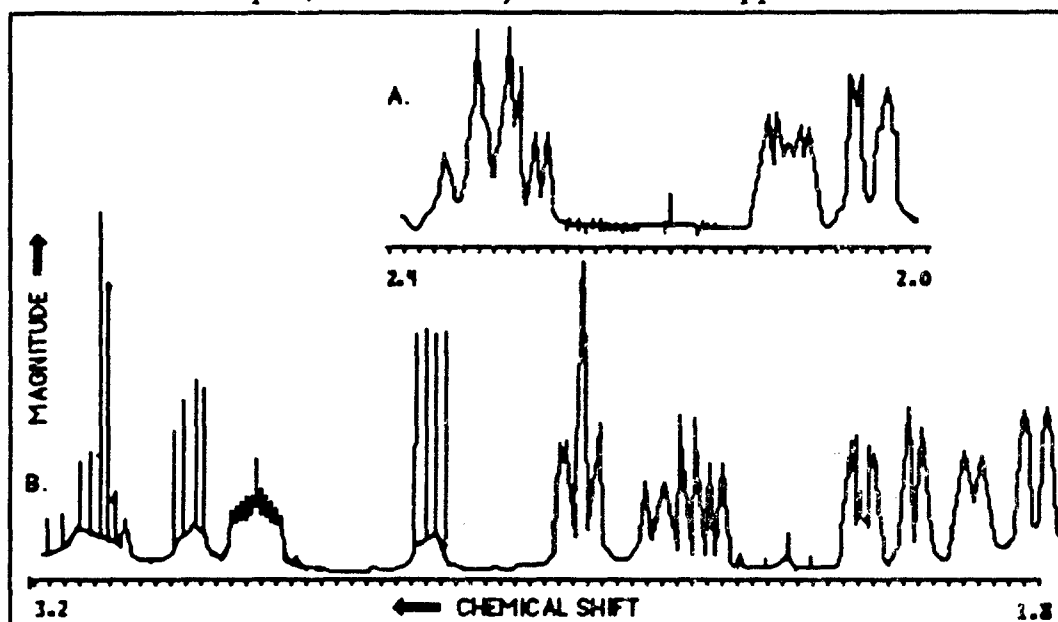


Figure 118. Proton 500 MHz spectra of reserpine. 1.8 to 3.2 PPM region with 5.02 (C18H) decoupled. Apparent changes are seen at 2.30 (C19AH) and 1.97 (C19BH) thus identifying each of the protons.

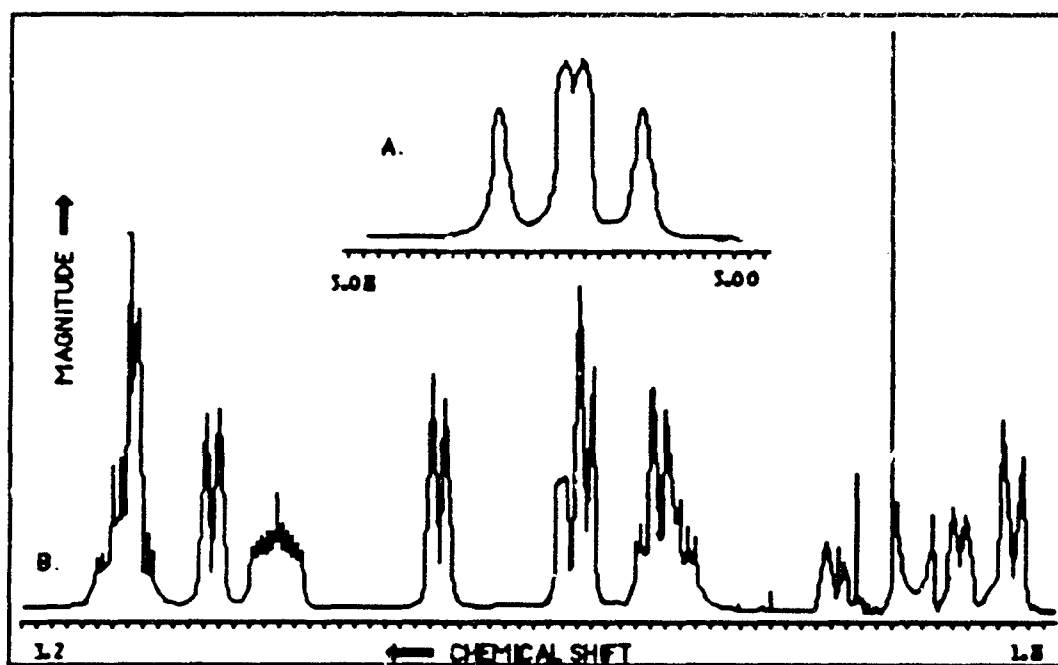


Figure 119. Proton 500 MHz spectra of reserpine. 1.8 to 3.2 region with 1.97 (C19BH) decoupled. Note change in 2.04 resonance (C14H).

Apparent partial saturation of 2.04 accounts for small change in 2.68 (C16H). Upper insert 5.02 (C18H) with coupling constants of 11.8 and 9.6 Hz. The 5.0 Hz coupling constant is due to C19BH.

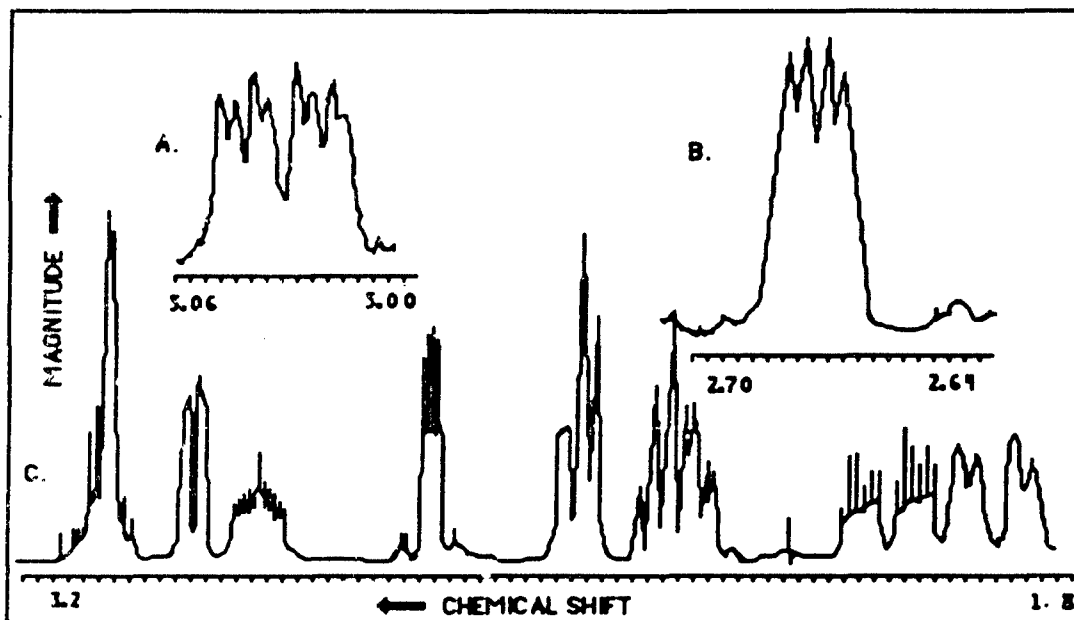


Figure 120. Proton decoupled 500 MHz spectra of reserpine. 1.8 to 3.32 spectral region with 3.89 (C17H) decoupled. Apparent changes in the spectrum are seen at 2.68 (C16H) and 5.03 PPM shown in upper left insert. Upper right insert shows 2.68 resonance having lost the large 11.2 Hz splitting due to C17H at 3.89.

One peak however, on first analysis, did escape detection. It turned out that one proton resonance was under the large methyl resonance at 3.90 PPM; undetected at first due to small artifacts normally found near the base of a large peak. This peak turned out to be C17H, coupled to both 5.02 and 2.68. When 3.90 was saturated, 5.02 and 2.68 both changed. This is shown in Figure 122. This was further confirmed by integration of the methyl peaks.

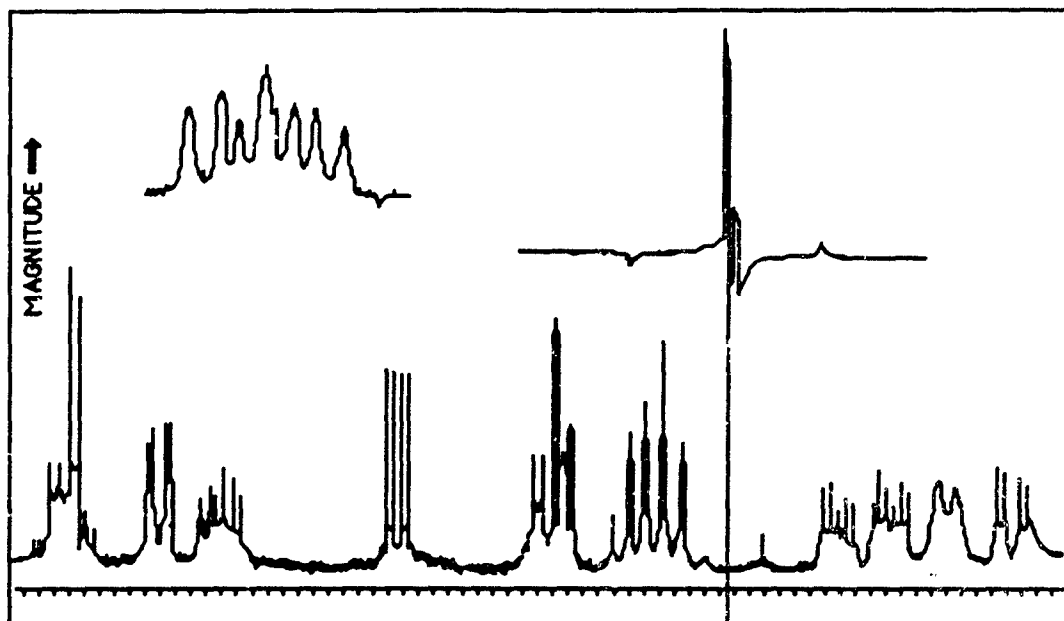


Figure 121. Proton decoupled 500 MHz spectra of reserpine. Decoupling C11H at 4.44 PPM, reveals changes in the spectrum at 2.29 (C12AH) and C12B (1.78). A small coupling is removed from C10B at 2.93 PPM. The upper left insert reveals no change in C18H at 5.02.

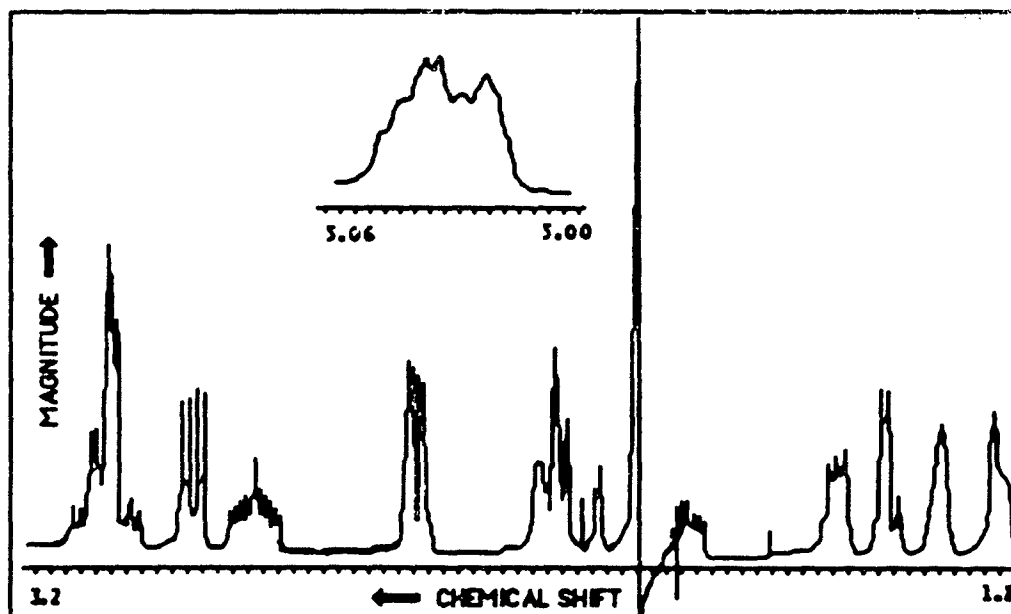


Figure 122. Proton decoupled 500 MHz spectra of reserpine. 1.8 to 3.32 spectral region with 2.34 decoupling.

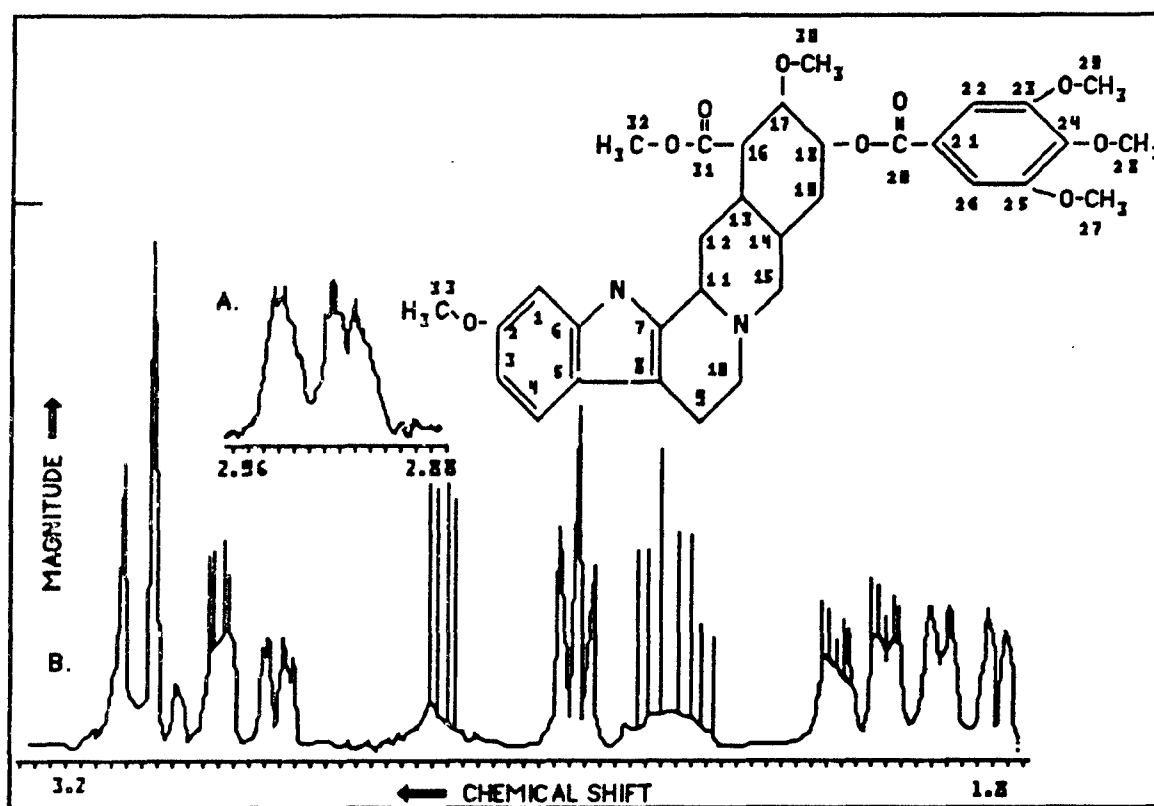


Figure 123. Proton decoupled 500 MHz spectra of reserpine. Decoupling at 3.14 (C10AH) produces change at 2.93 (C10BH).

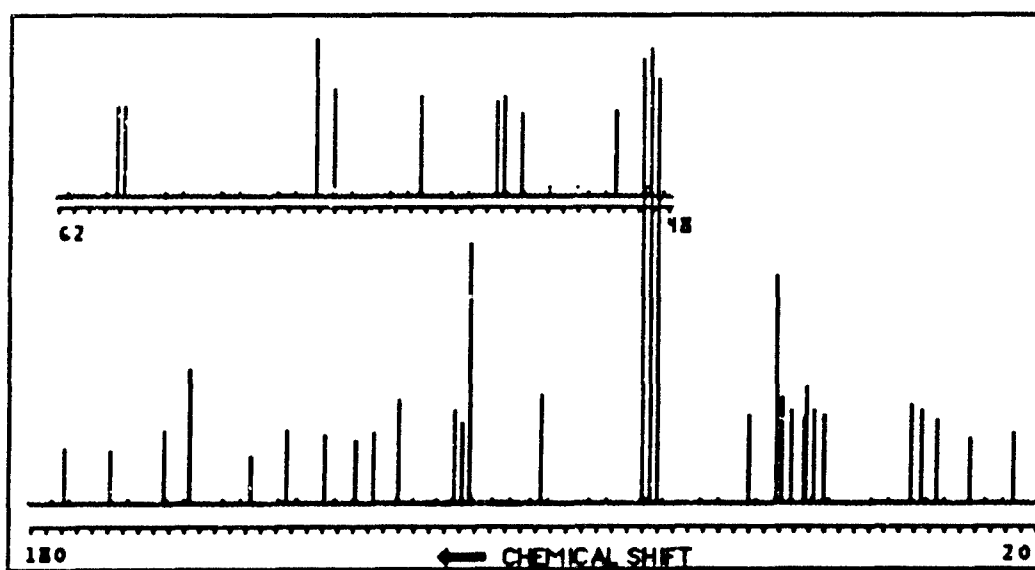


Figure 124. 300 MHz ^{13}C NMR spectrum of reserpine.

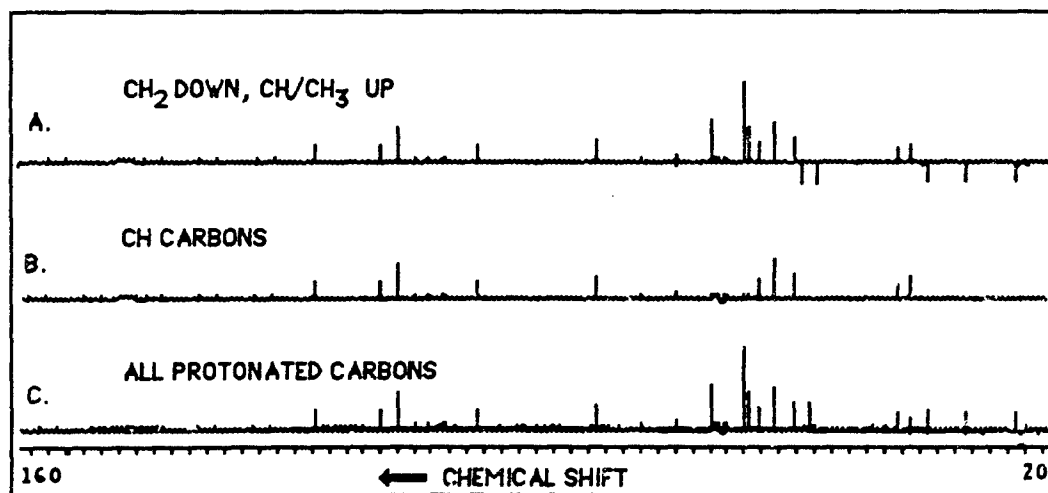


Figure 125. Distortionless, enhancement polarization transfer plot of reserpine.

The proton spectral assignments made for reserpine are as follows:

TABLE 46
ASSIGNMENTS

NH	C4H	C22,26H	C2H	C3H	C18H	C11H	C17H	C27,28,29H3	C33H3	C32H3
7.57	7.31	7.30	6.82	6.75	5.02	4.44	3.90	3.89	3.82	3.80
C30H3	C10AH	C9AH	C15AH	C10BH	C16H	C9BH	C15BH	C19AH	C12AH	
3.48	3.17	3.15	3.03	2.93	2.68	2.46	2.44	2.33	2.29	
C13H	C19BH	C14H	C12BH							
2.04	1.97	1.88	1.78							

TABLE 47.
¹H-¹H COUPLING CONSTANTS

J3,4	J1,3	J9A,9B	J9A,10A	J9A,10B	J9B,10B	J10A,10B	J11,10B	
8.5	2.1	3.9	11.2	6.5	15.8	10.8	2.2	
J11,12A	J11,12B	J12A,12B	J12A,13	J12B,13	J13,16	J16,17	J17,18	
6.0	1.0	14.4	13.5	3.8	4.7	11.0	9.6	
J18,19A	J18,19B	J19A,19B	J19A,14	J19B,14	J14,15A	J15A,15B	J22,26	
11.8	5.0	13.0	12.4	4.0	3.3	11.0	1.1	

The examination of model compounds was perhaps one of the most valuable things that we could have done to prepare for the examination of the toxin by NMR. Many of the same groups found in the toxin were also found in the model compounds. This experience made assignments much easier.

NMR Spectrum of GT-4 "Maitotoxin".

Spectra of intermediate extracts.

We obtained the 300 MHz proton spectrum of preparative HPLC purified maitotoxin (Fraction P4F3) in methanol as shown in Figure 126. The amount of sample used was minimal as indicated by the solvent to sample peak ratio, even though we used 99.95% deuteriomethanol.

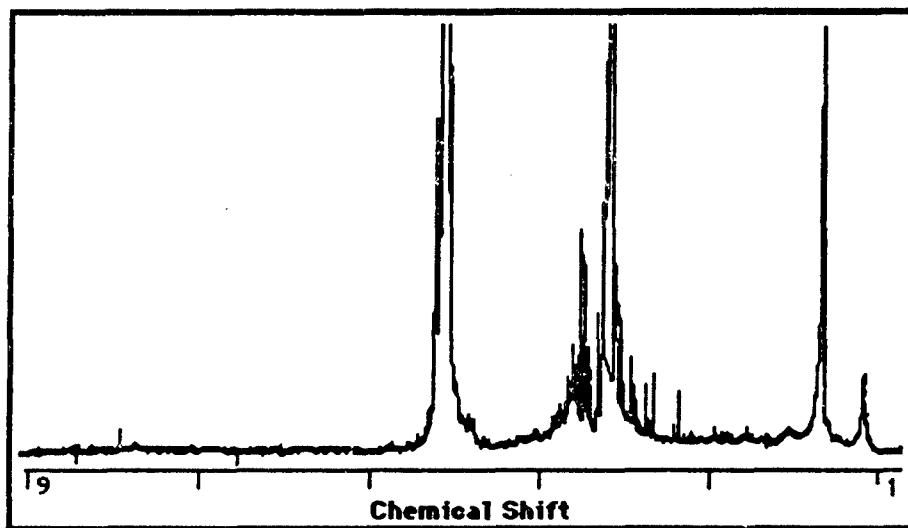


Figure 126. 300 MHz Spectrum of Preparative HPLC Purified Maitotoxin.

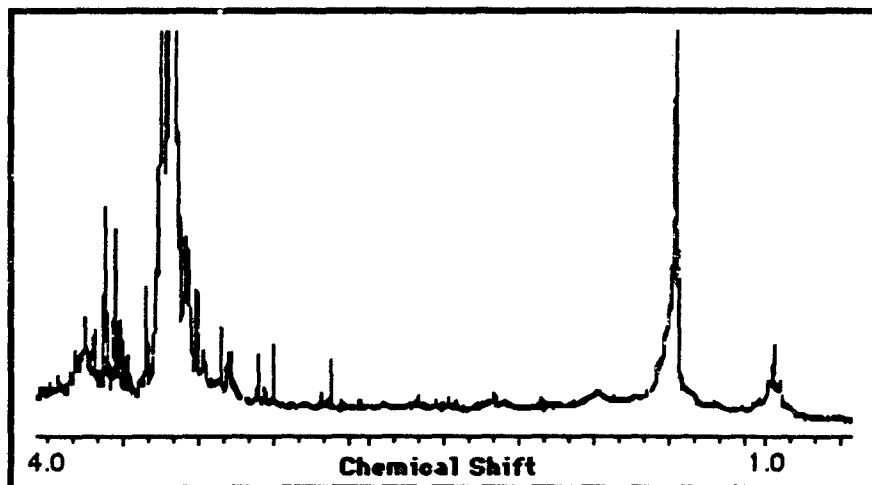


Figure 127. 300 MHz Spectrum of Preparative HPLC Purified Maitotoxin

Furthermore the OH peak at 4.8 PPM may have been enhanced by proton exchange with OH groups on the sample - it being out of proportion with the CH₃ peak at 3.30 PPM. Figure 126 is the enlarged right side of Figure 125.

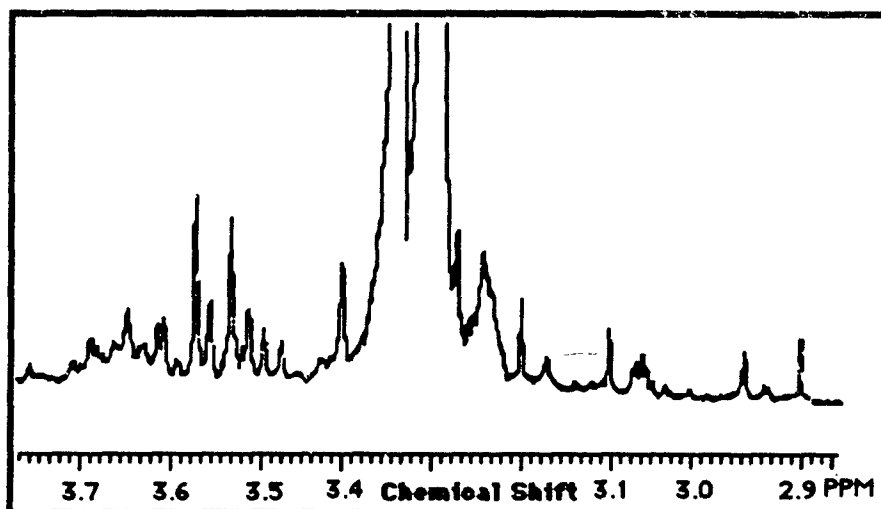


Figure 128. Enlarged Right Portion of Spectrum of Preparative HPLC Purified Maitotoxin.

The spectrum indicates that this sample exists as a two component system. One set of large peaks is seen in contrast to a set of smaller

peaks. The larger set of peaks may be an aliphatic type molecule closely associated with the toxin molecule, presumably the series of smaller peaks. Figure 128, reveals the contrasting larger and smaller peaks in even greater detail.

We believed that the toxin molecule is represented by the smaller peaks because it had been reported that maitotoxin contains highly polar OH, NH₂, and ether linkages. These resonances occur at lower field than 3.7 PPM, the lowest field resonance of the larger peaks in the spectrum. As seen in Figure 127, some resonances are seen at lower field although the signal to noise ratio here is questionable, even though the spectrum was accumulated for 16 hours over night. Resonances in the 5.5-9.0 PPM range would include NH, olefinic, and conjugated ring protons which maitotoxin could contain.

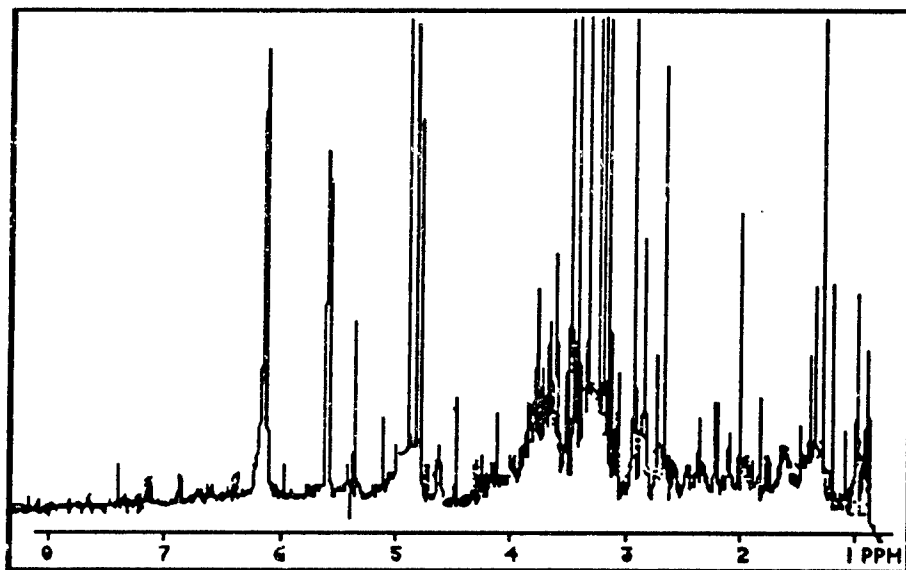


Figure 129. Complete proton spectrum (1-9 PPM) of rust brown fraction (P4F3-4) from color separation on HPLC unit of 10 ml of crude GT-combo. This sample contained 1,000,000 IEU.

Numerous attempts to obtain an NMR spectrum of the toxin from fractions extracted from the HPLC column of small amounts (1 or 2 ml) of crude toxin were unfruitful. Basically this revealed a pattern of large and small peaks but none could unequivocally be assigned to

the toxin. Moreover we were faced with the continued loss of total toxicity and lack of gain in purity of the sample.

However, when larger amounts of crude toxin were used, small peaks in the low field region, 5.7-8.8 PPM emerged which were not previously resolved. The spectrum from such a fraction containing 1,000,000 IEU of toxin and the major brown pigment is shown in Figure 128.

This fraction was obtained from color separation on the HPLC preparative unit from 10 ml of crude GT-combo. Another fraction from 10 ml of crude GT-combo containing 2,000,000 IEU was taken from the upside of the dominant 209 peak. This spectrum is shown in Figure 129. and reveals very distinctly small peaks in the 5.5-8.8 PPM region.

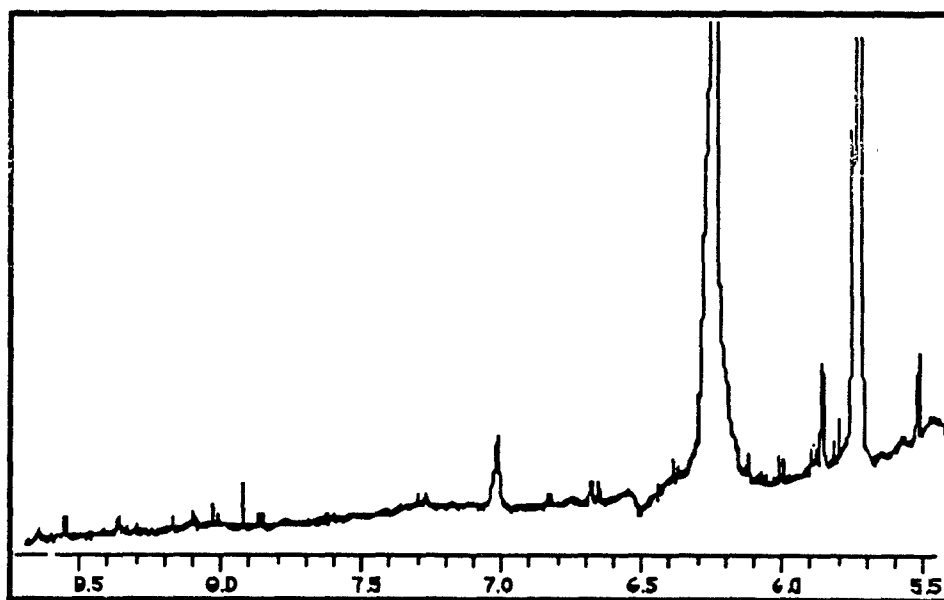


Figure 130. Lowfield region of ^1H spectrum (5.5-8.8 PPM) of upside of 209 peak off column P4F5 which was light green in color) separation on HPLC unit of 10 ml of crude GT-combo. This sample contained 2,000,000 IEU.

Another fraction containing 600,000 IEU obtained from color separation of the HPLC column is shown in Figure 130.

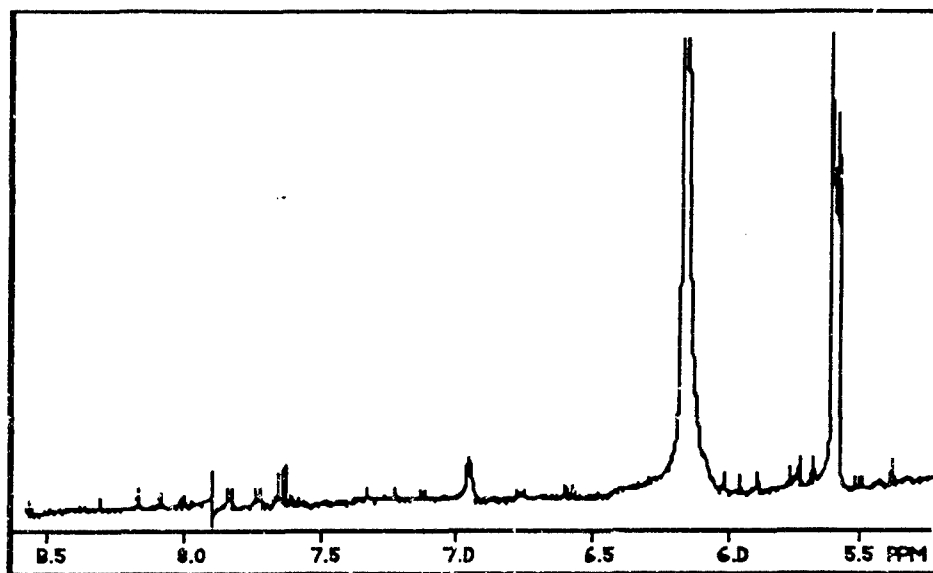


Figure 131. Lowfield region of ^1H spectrum (5.5-8.8 PPM) of downside of large 209 peak (P4F6 = brown in color) separation of 10 ml of crude GT-combo. This sample contained 600,000 IEU.

Thus the larger a sample we used, the more small emerging peaks we could see. We believed that these small emerging peaks are from the toxin and minor contaminants and are observable only when the toxin concentration exceeds several hundred MU. A listing of the peaks common to these spectra and their multiplicity was compiled as follows:

TABLE 48.
PARTIAL PEAK ASSIGNMENTS TO MAITOTOXIN NMR SPECTRA

Δ (PPM)		Multiplicity		Δ (PPM)	Multiplicity
	Δ (PPM)	Multiplicity			
8.68	s	8.02	d(9Hz)	6.04	d(7.02Hz)
8.58	d(6Hz)	7.83	d(4.5Hz)	5.90	d(4.5Hz)
8.38	s	7.23	s	5.78	d(7.0Hz)
8.31	s	7.12	d(8Hz)	5.70	d(8.0Hz)
8.17	s	6.75	d(9Hz)		
8.10	s	6.58	d(13.5Hz)		

We surmised that signals in the low field region of the proton NMR spectrum possibly arose from NH and OH groups in conjunction with other polar moieties. This implied that the toxin was very polar

and could explain many phenomena which we and others have observed. The splitting of the small doublets in the 5-9 Hz region is a strong indication that they do not arise from the protons on the long conjugated carbon chains of the pigment molecules. These couplings from cis and trans double bonds are commonly known in the 11-15 Hz range.

NMR of solvent extracts of Sep-Pak separations. However to further substantiate this we extracted the pigments with various solvents (Figure 131) and examined their NMR spectrum. From the area near the 210 peak on the HPLC column we found three pigments, a brown pigment and 2 green pigments. Chloroform extracts the brown pigment and one of the green pigments. DMSO extracts the other green pigment. The brown pigment can then be extracted from the first green pigment with ACN. The proton spectrum of the brown pigment is shown in Figure 131.

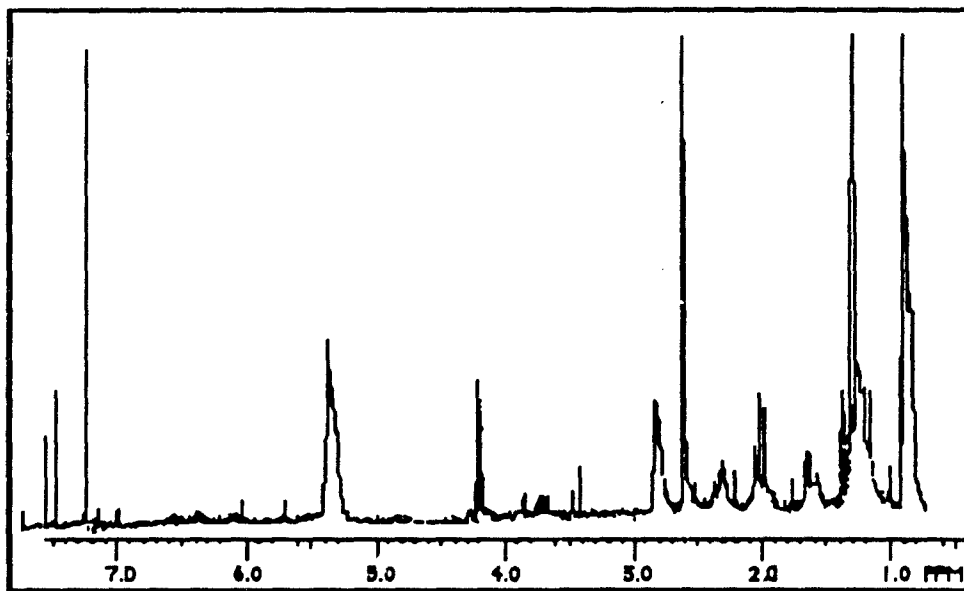


Figure 132. Complete ^1H spectrum (1.0-8.0 PPM) of brown ACN soluble pigment after chloroform extraction of 10 ml of crude GT-combo. This sample did not have any activity toward the ileum preparation.

While small degradation peaks are seen in the 5.5-7.5 region, these do not match those listed from the samples containing large

amounts of toxin. The spectrum of the second green pigment, the DMSO extract is shown in Figure 132.

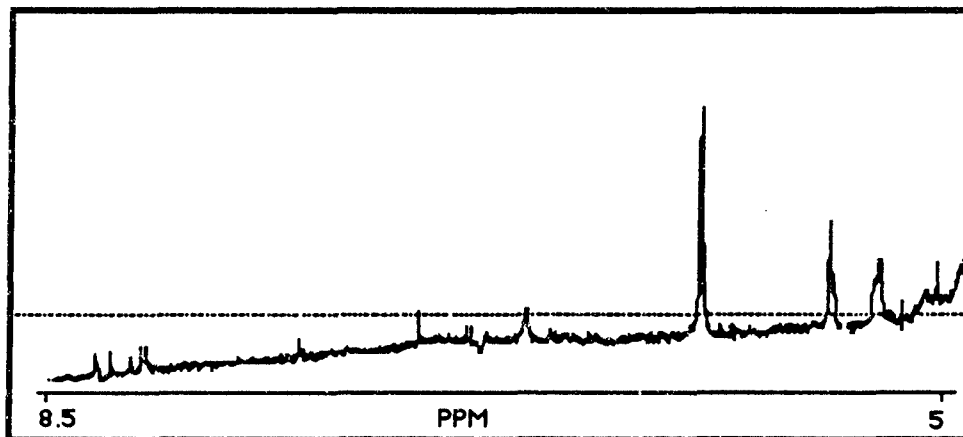


Figure 133. Lowfield ^1H spectrum of DMSO extraction 10 ml of crude GT-combo. This sample contained 200,000 IEU.

This sample contained 100 MU of toxin and a few of the signals which we are attributing to the toxin. The NMR spectrum of the first green pigment with no MTX is shown in Figure 133. and contained one of the toxin signals.

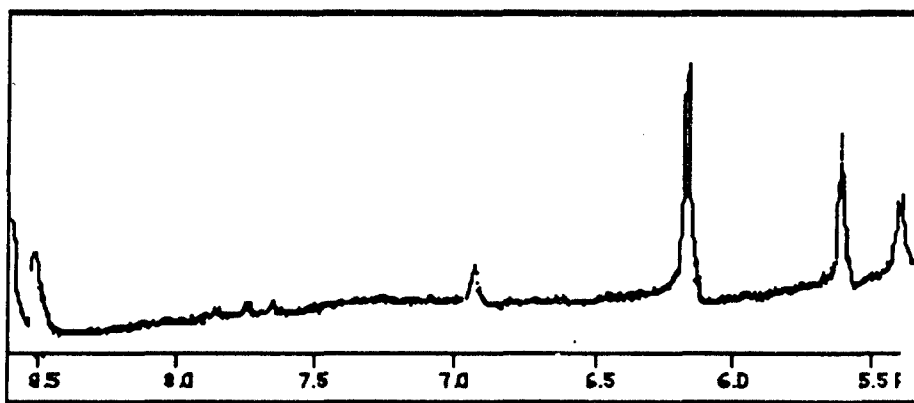


Figure 134 Lowfield region of ^1H spectrum (5.3-8.7 PPM) of green pigment from chloroform extract of 10 ml of crude GT-combo. This sample contained was not toxic to the ileum preparation.

We felt that the toxin was very closely associated with the pigments and as has been shown can be extracted with the pigment and further purified.

To date there has only been one published NMR spectrum for maitotoxin and this is the one published by Yasumoto.^[121] This spectrum is redrawn here as Figure 134.

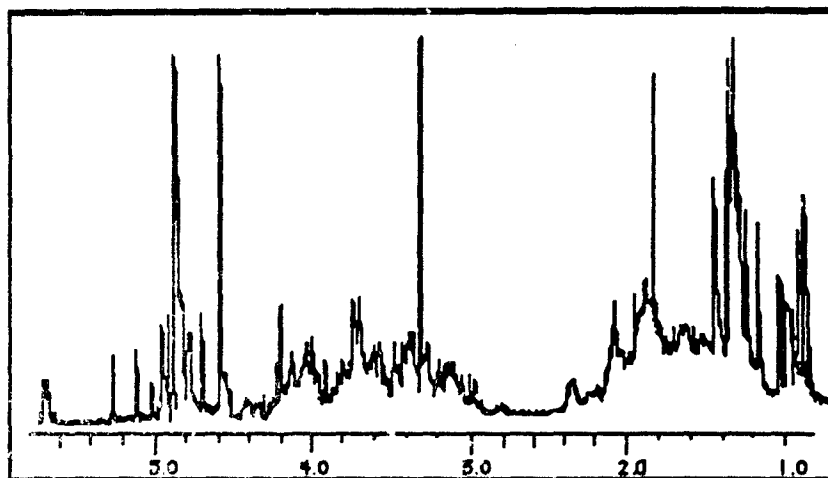


Figure 135. Spectrum for maitotoxin published by Yasumoto (1985). Solvent system was methanol- D_2O .

Comparing the spectrum obtained by Yasumoto and the one's we have obtained for crude maitotoxin, they appear to be very similar. However notice, (and this is our conclusion) that the majority of the peaks obtained in the crude scan are due to the associated pigments and or associated sulfolipids and the toxin signals are either too small to be seen or are obscured by the contaminants. Notice also, the similarity between Yasumoto's spectra and our spectra on small amounts of maitotoxin.

TABLE 49
TENTATIVE NMR SHIFT ASSIGNMENT AND PROBABLE STRUCTURES

No.	Shift	Descrip	Probable Structural Assignment
(1).	0.89	t(7.0 Hz)	terminal methyl
(2).	0.96	t(7.0 Hz)	terminal methyl
(3).	1.11	s	methyl on tertiary carbon
(4).	1.28	s	chain methylene
(5).	1.46	q(12,5Hz)	methylene on six membered ring
(6).	1.59	q(10, 4Hz)	methylene adjacent to carbon bearing oxygen
(7).	2.08	ddd(10, 8,5 Hz)	methylene adjacent to double bonded carbon
(8).	2.32	dd	methylene protons beta to alpha carbon
(9).	2.45	bs	methylene protons alpha to carbonyl carbon
(10).	2.58	dd	methylene protons adjacent to both carbonyl and oxygen bearing carbon
(11).	2.82	br d	methylene group between two double bonded carbons
(12).	3.48	s	methoxy group
(13).	4.00	dd (8, 3 Hz)	proton on secondary carbon bearing oxygen
(14).	4.13	br s	hydroxyl proton on secondary carbon bearing oxygen
(15).	4.32	d (6 Hz)	proton on secondary carbon bonded to carbon bearing oxygen
(16).	4.48	br d	proton on primary carbon bonded to carbon bearing oxygen
(17).	5.37	dd (14, 6 Hz)	olefinic proton on chain double bonded carbon
(18).	5.40	d(3 Hz)	proton on primary carbon bonded to two oxygens
(19).	5.62	d(14 Hz)	olefinic proton alpha to carbonyl carbon
(20).	5.70	d (8.0 Hz)	olefinic protons on 6 membered ether ring
(21).	5.75	s	OH (observed in DMSO)
(22).	5.78	d (7.0 Hz)	olefinic proton adjacent to double bonded carbon bearing terminal methylene
(23).	5.90	d (4.5 Hz)	NH adjacent to carbonyl
(24).	6.04	d (1.0 Hz)	proton on terminal methylene adjacent to aldehyde group
(25).	6.15	d (1.0 Hz)	proton on terminal methylene adjacent to aldehyde group
(26).	6.58	d (13.5 Hz)	proton on carbon adjacent to both acetyl ester and nitrogen
(27).	6.76	d (9.0 Hz)	olefinic proton on carbon bonded to a carbon with hydroxyl group
(28).	6.95	brs	three protons of a terminal guanidino group
(29).	7.12	d (8.0 Hz)	protons on terminal amino from carbonyl carbon
(30).	7.23	s	NH group bonded to guanidino group
(31).	7.83	d (4.5 Hz)	NH between double bonded carbon and carbonyl
(32).	8.02	d (9.0 Hz)	olefinic proton in resonating double bond adjacent to N and a carbonyl carbon
(33).	8.10	s	same as above; the second of two olefinic carbons
(34).	8.38	s	terminal nitroxyl group
(35).	8.58	d (6.0 Hz)	olefinic hydroxyl group
(36).	8.68	s	aldehyde proton

While the ^1H NMR spectra published by Yasumoto shows signals only in the 1.0 to 6.0 PPM, we believed that the signals which we observe in the 6.0 to 8.7 PPM arise from OH and NH groups which would exchange in a MeOH- D_2O solvent as was used by Yasumoto for his proton spectra. Our NMR runs have all been made in deuteriated methanol. Our sample shows other small peaks which do coincide with those from the Yasumoto's NMR spectra which we found highly encouraging. Our observations tended to support the hypothesis that MTX is a large polyether compound with numerous polar sites.

Notice that based on the NMR results so far (i.e. the size of the toxin peaks) the toxin concentration is not more than 100 μg and this was essentially from 11 mls of GT-combo which contained 101.2 mg of material. In order to achieve a separation of 1 mg for an excellent NMR spectrum we would need to process 110 mls of material. This, then was our next logical step.

Nevertheless, the experiment did provide data relating to the toxic peak. With the larger amount of material we subjected the samples to NMR and found several peaks which correlate with toxic activity. These peaks are described in the following Table 49 and probable structural assignments had been made for them. Both the assignments and their probable structures were tentative at the time.

We ran NMR spectra on two samples of high MTX content. NMR MTX #1 had 100,000 mu at a purity level of 300 ng/mu (1%) and was subsequently incorporated into a larger sample NMR MTX #2; 330,000 mu at a purity level of 30 ng/mu (10%).

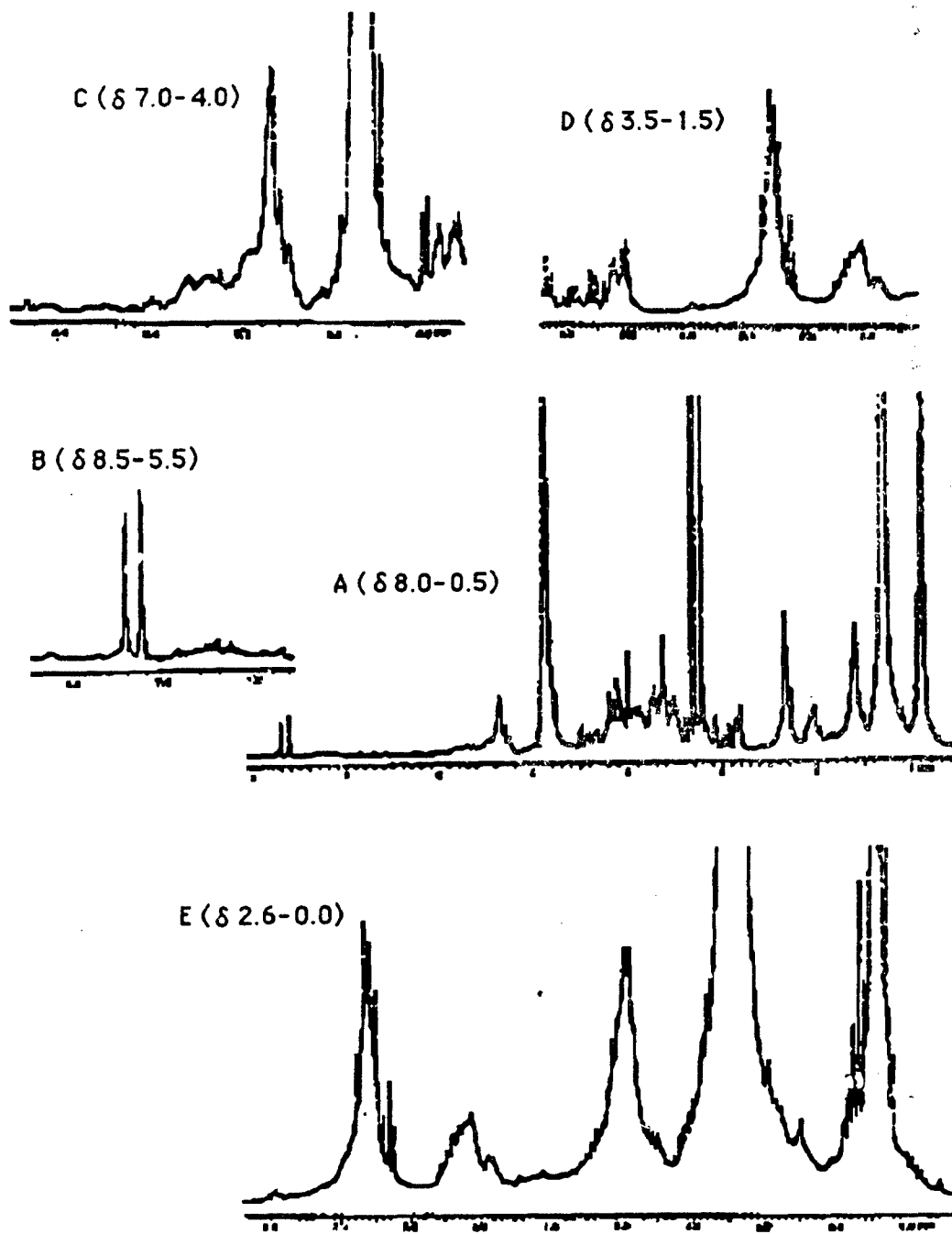


Figure 136. NMR spectra of fraction MTX #2.

This further purification was achieved by briefly washing the toxin with H₂O on a C-18 column.

Large low field peaks at δ 8.5, δ 8.12 and δ 6.92 were removed and the whole spectrum profile was much reduced. Certain peaks in the δ 7.5 to δ 6.0 range appeared enhanced, although characteristic long relaxation times of low field peaks made this assessment only tentative. In NMR MTX #2, the dominant peaks in the δ 4.2 to δ 3.4 range are greatly attenuated, unquestionably due to the removal of large sugar ring type compounds in the H₂O C-18 cleanup. Large C-18:3 lipid peaks at δ 5.35, 2.82, 2.05, 1.60, 1.30 and 0.95 visible in NMR MTX #2 may have been due to material picked up from the C-18 column as they were not present to this extent in NMR MTX #1. Increased concentration of a prenyl-lipid type compound (indicated by ring peaks at δ 7.7 and δ 7.6) are seen in NMR MTX #2. We have found this particular compound repeatedly in large concentration in pigment extractions and it appears light green at low concentrations. Finding this compound present at this stage of the cleaning procedure substantiated a partial lipid nature of the toxin.

The NMR spectrum of NMR MTX #2 is strikingly similar to the published ¹H spectrum of Yasumoto. The low field signals at δ 4.5 to δ 6.0 coincide and the δ 4.5 to δ 3.0 profile is very similar, while peaks in δ 2.4 to δ 2.8 range are completely eliminated. The small section of peak δ 4.6 to δ 4.2 are identical. The enhancement of high field peaks is undoubtedly due to lipid pickup from the column.

Structural correlates from NMR spectra of purified GT-4.

Thus far, we were faced with the prospect that purification past the 1 μ g/MU level resulted in a loss of toxic activity. Experiments with extraction past this level resulted in loss in toxicity (which could be mimicked by heating). Different solvents which were tried split the toxic activity, which we attributed to limited solubility. Preliminary experiments with the NMR had shown that scans of anything less than 5 mg would not produce productive spectra. We had identified presumptive peaks which tended to correlate with toxicity in more impure samples. Therefore we decided to follow these peaks in the NMR scans as our measure of purity past the 1 μ g/MU level.

A sample consisting of 200,000 MU from GT-350 was processed past the 1 μ g/MU level. Repetitions of the same step were utilized to help purify the sample. Toxicity tests indicated that mouse units were lost after each step of the purification process and even upon storage of the precipitate. Thus even though we lost most of the toxicity, we were still confident that we had the toxic moiety (albeit modified) in the purified sample. After the final purification step the sample weighed 1.4 mg. A proton spectrum was easily achieved in five minutes using the VXR-500 spectrometer. Running the same sample for 66 hours in the VXR-300 instrument produced a ^{13}C spectrum with 135 lines.

The proton spectrum showed 10 protons in the olefinic region, 5.0 to 6.0. Although protons on carbons bonded to a keto carbon also adsorb in this range, the couplings as provided by a 2-D COSY spectrum does distinguish between the two. The proton resonances and their coupled resonances indicate the following:

TABLE 50
TABLE OF PROJECTED GROUPS FROM SPECIFIC ^1H NMR PEAKS

δ	COUPLED TO	TYPE OF STRUCTURE	DIAGRAM
5.08	-	exomethylene	T
5.20	-	exomethylene	T
5.12	2.48, 1.6	trisubstituted olefinic bond	U
5.12	2.05	trisubstituted olefinic bond	V
5.25	4.15	proton on keto carbon bounded to carbon bearing oxygen on 6 membered hydroxylated ring	W
5.29, 5.30, 5.30,	2.78, 2.0,	chain segment of two	X
5.30	1.97	disubstituted olefinic bonds	
5.45	3.40	proton on keto carbon bounded to carbon bearing oxygen on 6 membered non-hydroxylated ring	Y

The data from the ^{13}C accumulated spectra revealed 55 carbons in the aliphatic range, forty two carbons sp^3 bonded to oxygen and nitrogen and 37 double bonded carbons. This distribution is quite different from any data published to date, especially in the double bond range. The MTX spectra published by Yasumoto only shows 8

double bonded carbons. The range in which the 134 signals appear is given along with the general structure types.

TABLE 51.
TABLE OF PROJECTED GROUPS FROM SPECIFIC ^{13}C NMR PEAKS

δ range	No. Carbons	Structure Type
24.96-9.76	25	Methyl
41.13-25.30	30	Methylene & methines
59.47-42.02	13	Carbons bonded to N
84.33-60.90	23	Carbons bonded to O
104.41-96.76	6	Keto carbons (possibly some high field C=C such as exomethylenes)
148.1-107.18	24	Double bonded carbons
170.79-151.50	13	Carbonyls and carboxylic carbons

In a very short period of time we assigned a terminal chromophore, $\text{C}_{11}\text{H}_{14}\text{N}_3\text{O}_3$, a close replica of calimycin, the calcium ionophore as the other terminal end; and fragments containing 5 isolated olefinic bonds, $\text{C}_{17}\text{H}_{24}\text{O}$ (total). The molecular weights and carbon types within these 3 groups are shown in the following table.

TABLE 52.
MTX FROM GT-350 STRUCTURE GROUPS ASSIGNED FROM ^1H AND ^{13}C SPECTRA

Group	Molecular Formula	MW	G	OCO	CO	CN	CH_2CH	CH_3
Terminal chromophore	$\text{C}_{11}\text{H}_{14}\text{N}_3\text{O}_3$	236	9	0	1	0	1	0
Calcium ionophore	$\text{C}_{30}\text{H}_{37}\text{N}_4\text{O}_5$	533	14	1	2	1	8	5
Olefinic fragments	$\text{C}_{17}\text{H}_{24}\text{O}$	244	10	0	1	0	4	2
Total Assig. to date		1013	33	1	4	1	13	7

The assigned groups constitute about 1,000 MW leaving 1,800-2,000 MW in the central chain section of the molecule. With only 4 low field carbons yet to be assigned, it does not appear that any more conjugated ring structures exist. The presence of proton resonances in the 3.4-2.8 ppm range also suggest a bridged ring structure as seen in atropine or quinine containing 1 or more nitrogen atoms. Ten additional carbon resonances in the 42-59 ppm region are to be assigned, which probably are some carbons bearing nitrogen. We further assume probably 40-50 oxygen atoms on

carbons and hydroxal groups, as 22-25 carbons in the 60-85 ppm region remained to be assigned. Analysis of the $^1\text{H}2\text{D}$ COSY spectrum is invaluable in this effort.

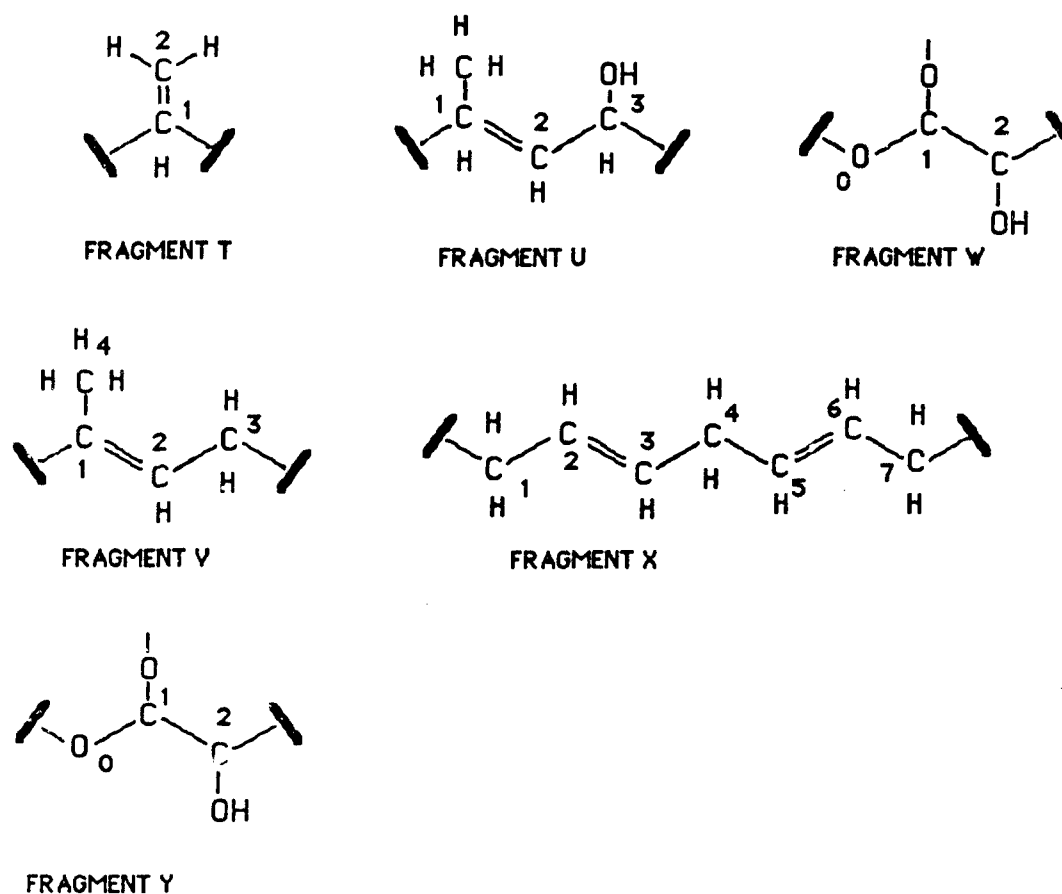


Figure 137. Fragments T through Y determined from ^1H NMR spectrum Projected from ^1H , ^{13}C , and ^1H COSY Spectrum.

Partial structures were assimilated from ^1H 1-D and $^1\text{H}2\text{D}$ COSY spectra. Carbon assignments are made using lines from the 66 Hz accumulated ^{13}C spectra and ^{13}C data on standard samples which we have acquired on the same instruments.

TABLE 53.
TENTATIVE ASSIGNMENTS OF ^{13}C AND ^1H SHIFTS FOR FRAGMENTS T
THROUGH Y.

	Carbon δ	Proton δ	Proton δ	Code	Functional Group
1	115.08			1T	-C- (=C)
2	107.18	5.08	5.20	2T	=C (H ₂)
3	107.68	1.6	1.6, 1.6	1U	-C-H ₃
4	125.45	5.12		2U	-C= (H)
5	73.47	3.48		3U	-C- (H, OH)
5	12.56	1.6	1.6, 1.6	4U	-C-H ₃
6	108.66	1.7		1V	-C= (H)
7	123.96	5.12		2V	-C= (H)
8	28.14	2.02	2.05	3V	-C- (2)
9	12.31	1.6	1.6	4V	-C(H ₃)
9				0W	-O-C
10	103.03	5.25		1W	-C- (H, -O-)
11	82.24	4.15	OH	2W	-C- (H, OH)
12	26.62	2.02	2.0	1X	-C- (H ₂)
13	129.48	5.30		2X	-C= (H)
14	129.84	5.29		3X	-C= (H)
15	25.30	2.75	2.75	4X	-C- (H ₂)
16	130.51	5.30		5X	-C= (H)
17	131.07	5.30		6X	-C= (H)
18	26.00			7X	-C- (H ₂)
19				0Y	-O-C
20	98.23	5.45		1Y	-C- (H, -O-)
21	64.64	3.40		2Y	-C- (H, OH)

Using both the ^{13}C , ^1H , and 2D-COSY spectra a preliminary assignment can be made for one of the terminal ends of the molecule.

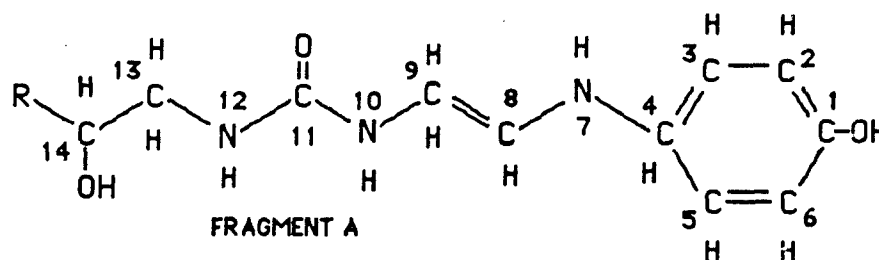


Figure 138. Projected Structure of Terminal Fragment A Determined from ^1H , ^{13}C , and ^1H COSY Spectrum

TABLE 54.
TENTATIVE ASSIGNMENTS OF ^{13}C AND ^1H SHIFTS FOR TERMINAL
FRAGMENT A

	Carbon δ	Proton δ	Proton δ	Proton δ	
1	151.50		OH	1A	=C- (OH)
2	128.16	7.61		2A	=C- (H)
3	125.32	7.71		3A	=C- (H)
4	148.1			4A	-C= (H)
5	125.32	7.71		5A	=C- (H)
6	128.16	7.61		6A	=C- (H) (H)
7					-N- (H)
8	147.9	7.40		7A	-C= (H)
9	153.78	7.95		8A	-C= (H)
10					-N- (H)
11	170.79			9A	-C- (=O)
13	44.79	4.26	4.26	10A	-C- (H ₂)
12					-N- (H)
14	67.26	3.85	OH	11A	-C- (H, OH)

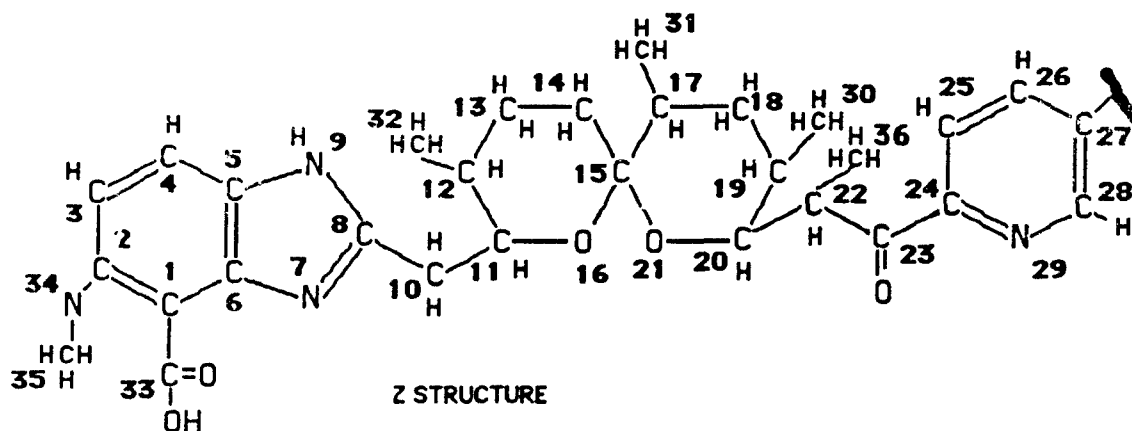


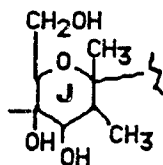
Figure 139. Projected Structure of Terminal Fragment Z Determined from ^1H , ^{13}C , and ^1H COSY Spectrum

TABLE 55.
TENTATIVE ASSIGNMENTS OF ^{13}C AND ^1H SHIFTS FOR TERMINAL
FRAGMENT Z

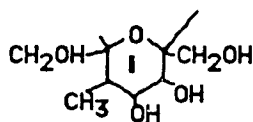
No.	Carbon δ	Proton δ	Proton δ	Proton δ
1	96.76			
2	126.96			
3	122.46	7.37		
4	142.1	7.45		
5	137.2			
6	139.24			
7				
8	160.8			
9		8.55		
10	32.45	2.48		
11	66.95	4.26		
12	29.46	1.25		
13				
14				
15	104.41			
16				
17				
18				
19		1.70		
20	64.40	4.30		
21				
22	34.88	2.48		
23	170.1			
24	142.1			
25	109.84	6.84		
26	103.41	7.22		
27	99.71			
28	133.39	7.73		
29				
30	10.82	0.85		
31	11.39			
32	14.01	0.80		
33	161.52			
34				
35	42.02			
36	16.56			

TABLE 56
STRUCTURE AND ASSIGNMENTS FOR PART J AND I

Fragment	¹ H	¹³ C
J1	-	Q
J2	3.80	73.47
J3	4.21	71.54
J4	1.38	34.49
J4Me	0.89	18.0
J5	-	Q
J6	1.41	19.3
J7	3.75 & 3.81	62.14



Fragment	¹ H	¹³ C
I1	-	Q
I2	4.30	62.27
I3	4.15	62.14
I4	1.61	34.67
I4Me	0.99	09.76
I5	-	Q
I6	3.65, 3.75	62.14
I7	3.67, 3.72	62.14



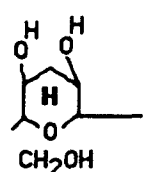
In this section we give the structural determination of another part of the isolated molecule from *G. toxicus* 350 utilizing our NMR data consisting of the ¹H proton spectrum, the 66 hr accumulated ¹³C spectrum and the COSY 2D ¹H spectrum. Again, we base our proposed structure on comparison of NMR data we obtained on our instruments with model compounds such as the antibiotics, monensin, sodium ionophore X-537A, calcium ionophore A-23187, novobiocin, etc; the saccharides such as galactose, trehalose, xylose and nitrogen containing receptor site deactivators such as reserpine, bepridil, diltiazem and others.

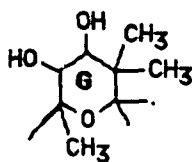
Immediately apparent in the ¹³C spectrum were six signals in the 105-96 ppm range indicating keto carbons of six-membered ether rings such as found in trehalose and some antibiotics.

Also approximately 30 signals between 60 & 85 ppm indicate the same. The COSY 2D ¹H spectrum further indicated that most of the proton signals in the 3.4-5.4 ppm were coupled to each other such as

in the saccharides with a minimum of coupling to high field methylene and methine carbons. Some coupling to signals in the 1.6-1.3 ppm range indicated a limited number of CH and CH₂'s in the ether rings.

TABLE 57
STRUCTURE AND ASSIGNMENTS FOR PART H AND G

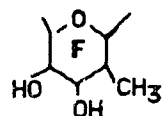
	Fragment	¹ H	¹³ C
	H1	3.64	63.33
	H2	3.83	69.10
	H3	4.06	70.74
	H4	4.0	64.64
	H5	-	Q
	H6	3.74, 3.77	62.14

	Fragment	¹ H	¹³ C
	G1	3.51	71.54
	G2	-	34.88
	G2Me	1.40, 1.39	10.31, 10.47
	G3	4.21	67.26
	G4	4.28	64.40
	G5	-	Q
	G6	1.38	16.56

The formulation of 9 such ether rings utilize all the carbons in the ¹³C spectrum between 60 and 85 ppm while it appears that some quaternary carbons in this range did not resolve. This is not uncommon and may be related to the limited solubility of the molecule. All of the protons arranged in the structure are indicated by the COSY 2D spectrum. Using the available data we have incorporated these ring structures B through J into a complex ring structure which we believe connects to the terminal end A.

TABLE 58.
STRUCTURE AND ASSIGNMENTS FOR PART F AND E

Fragment	¹ H	¹³ C
F1	5.38	96.76
F2	3.40	72.45
F3	4.70	69.10
F4	1.37	35.07
F4Me	0.88	10.68
F5	4.10	84.12



Fragment	¹ H	¹³ C
E1	4.27	69.32
E2	3.55	69.10
E3	3.90	66.71
E4	1.30	35.63
E4Me	0.85	14.01
E5	-	Q
E6	3.79, 3.84	62.14

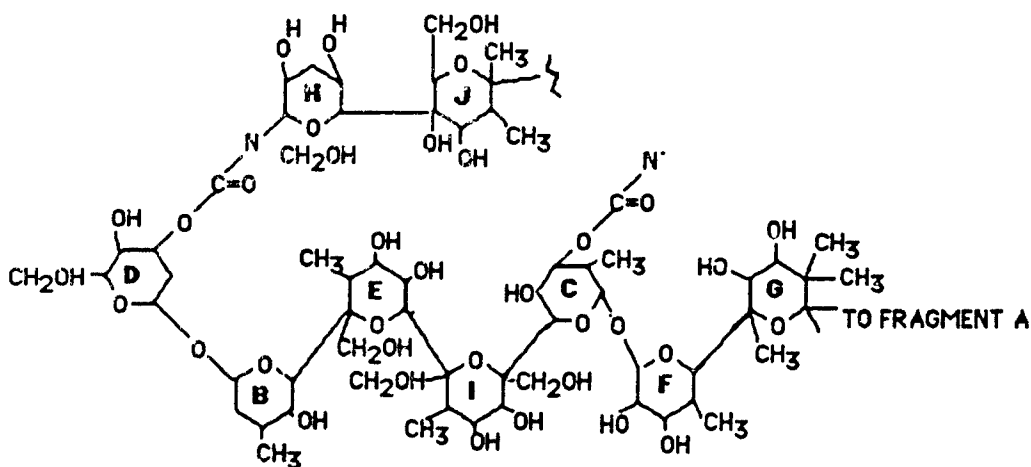
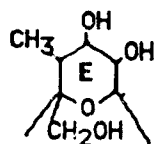


Figure 140. Coupling of Fragment A to Fragment B-J through ring G.

We recognize that coupling these structures together in a 1500 MW fragment is not totally specific, however the structure we have indicated does satisfy all of the COSY 2D data. If short chain segments coupled the ether rings, there would be more coupling with high field signals. The COSY 2D did not indicate this. In this

structure, 7 of the adjoining sites are made at a quarternary carbon, 2 through an oxygen and ring G is coupled to fragment A.

Discussion of NMR results. The partial structure of the suspected toxin as discerned from the ^{13}C and ^1H NMR spectra is quite different from anything that has been speculated or published thus far. Over one third of the molecule appears to be relative lipid like with very few charged groups and the remainder of the molecule contains numerous hydroxal groups clustered on a polyether segment finally terminated by a hydroxalated six carbon ring.

PERSONNEL SUPPORTED

TABLE 59
PERSONNEL EMPLOYED ON THE CONTRACT

Name	% Effort	Position	Dates
-----Faculty, Staff Positions -----			
Miller, Donald M	50%	Prin. Inv.	1Dec86-31Mar91
Tindall, Donald R.	20%	Co-Prin. Inv.	1Dec86-31Mar91
Bomber, Jeff	100%	PostDoc	15Jun87-30Jun90
Venable, Charles W	100%	PostDoc	16May87-30Nov90
Rakotoniaina	100%	Researcher	16May87-30Nov90
Kohler, Sue	50%	Tech.	1Jan87-30Jun90
Tindall, Pat	25%	Tech	1Jun87-31Mar91
-----Graduate Students-----			
Adamson, Robert	50%	Grad. Stu.	1Jun88-30Nov90
Aikman, Kevin E	50%	Grad. Stu.	1May88-28Feb91
Ghosh, Sarbani	50%	Grad. Stu.	1Aug90-30Nov90
Ghosh, Sushmita	50%	Grad. Stu.	1Aug90-30Nov90
Hassan, Faiqa	50%	Grad. Stu.	1Jun88-30Jan90
Jacyno, Mark	50%	Grad. Stu.	15Aug87-28Feb91
Morton, Steve	50%	Grad. Stu.	1Jul90-28Feb91
Tibbs, Brian	50%	Grad. Stu.	1Jan87-31Mar88
Vogt, Scott	50%	Grad. Stu.	15Jan90-31Sep90
-----Student Workers-----			
Checkley, Andrew	25%	Stu. Wk.	1Nov89-30Nov90
Cooper, Valerie	25%	Stu. Wk.	2Sep90-31Mar91
Corgiat, Dean A	25%	Stu. Wk.	15May89-31Mar91
Cunningham, Tracey	25%	Stu. Wk.	25Jan87-28Feb90
Dufner, Robert M.	25%	Stu. Wk.	19Jun90-31Aug90
Gofron, Ronald J	25%	Stu. Wk.	15May89-31Dec90
Hamra, Kent	25%	Stu. Wk.	14Dec87-31Apr89
Hassenstad, Deana	25%	Stu. Wk.	1Oct88-31Jul89
Jost, Joseph M	25%	Stu. Wk.	15May89-31Jul89
Lewin, Arien	25%	Stu. Wk.	1Aug90-31Aug90
Mallonee, Donald L	25%	Stu. Wk.	1Oct89-10Aug90
McVey, Dan	25%	Stu. Wk.	8Aug88-30Nov89
Mosley, Toi	25%	Stu. Wk.	9May90-28Feb91
Mullings, Franz R.	25%	Stu. Wk.	1Oct89-31Dec90
Pearce, Melody	25%	Stu. Wk.	1Oct88-30Jun89
Roman, Jeffrey G	25%	Stu. Wk.	25Feb88-30Dec89
Sikora, Linda	25%	Stu. Wk.	15May89-28Feb90
Stufflebeam, Mike	25%	Stu. Wk.	1Oct88-30Jun89
Vogt, Scott	25%	Stu. Wk.	12Sep88-15Jan90

TRAVEL DURING THE FOUR YEARS OF THE CONTRACT.

Travel to scientific meetings & contractor meetings.

The Federated American Societies for Experimental Biology meeting in Washington, D. C, 28 Mar-4 Apr 1987, was attended by Drs. Tindall and Miller. Subsequently Fort Detrick was visited for a contractors meeting and a report for the first year.

The Federated American Societies for Experimental Biology meeting in Las Vegas, Nevada, 18 to 27 Apr 1988, was attended by Drs. Tindall, Bomber and Miller. Three posters were presented.

The meeting of the Association of Marine Laboratories of the Caribbean meeting in Sarasota, Florida, 21-28 May 1988 was attended by Drs Tindall and Miller. Three posters were presented.

The International Congress of Toxinology in Stillwater, Oklahoma from 1 to 8 Aug. 1988 was attended by Drs Bomber, Tindall and Miller. Three papers were presented.

The Joint U.S.-Japan Conference on Toxic Materials in Foods in Washington, D. C. from 1-5 Nov 1988 was attended by Drs. Miller and Tindall. Subsequently Fort Detrick was visited for a contractors meeting and a report for the second year.

The FASEB meeting in New Orleans, La from 19-23 March was attended by D. M. Miller, Mark Jacyno and Faiqa Hasssan, 19-23 March 1989, Two papers were presented.

The Fourth International Conference on Toxic Dinoflagellates in Lund, Sweden was attended by Drs. D. R. Tindall, J. Bomber and D. M. Miller. Three posters were presented.

As a guest of the Australian Government the principal investigator visited Queensland Institute of Technology, Brisbane Australia during the month of October and the first two weeks of November, 1989. An attempt was made to acquire *G. toxicus*. Rough weather attended but a couple of the subcultures survived, including the Polynesian strain.

D. Miller attended a contractors meeting at Fort Detrick, 20-23 Jan 1990 and presented a report for the third year.

The Marine Toxins Session of the ACS Meeting, 26-29 Aug 1990 in Washington, D. C. was attended by D. M. Miller, and subsequently Ft Detrick was visited for the presentation of the Final Verbal Report for this contract.

According to pre-approved plans a field trip was conducted to collect dinoflagellates from the around the area of the coral sea. The trip was successful, due in part to the help of Dr. Michael Capra from the Queensland University of Technology (QUT). He arranged for vehicles, access to transport, and permits for both Australia and Fiji and coordinated all aspects of the trip. During the last part of the trip an outbreak of fish poisoning occurred. A seminar was presented at The University of the South Pacific.

Travel to Florida to obtain seawater.

Three trips were made to the Florida Institute of Technology, Melbourne, Fl. for loads of sea water. These trips were made on As promised, each time they lowered their price per gallon at the pump so that the last cost for us was \$0.69 per gallon. We were able to load approximately 1,444 gallons of water into a truck.

Publications resulting from the contract.

Abstracts of papers or posters given at meetings.

1. Miller, D.M. and Tindall, D.R., (1987) Factors interacting with the effects of the maitotoxin fraction from *Gambierdiscus toxicus*, *Conference on Natural Toxins from Aquatic and Marine Environments*.
2. Miller, D.M. and Tindall, D.R., (1987) Factors interacting with the effects of the maitotoxin fraction from *Gambierdiscus toxicus*, *Fed. Proc.*, 46, need.
3. Tindall, D.R. and Miller, D.M., (1987) Bioassay of a fast-acting low molecular weight toxin from a dinoflagellate, *Prorocentrum concavum*, *Conference on Natural Toxins from Aquatic and Marine Environments*.
4. Tindall, D.R. and Miller, D.M., (1987) Two potent toxins from *Ostreopsis lenticularis*, a dinoflagellate common to ciguatera-endemic regions of the Caribbean and tropical Atlantic, *Fed. Proc.*, 46, 3730.

5. Tindall, L. R., and Miller, D.M., (1988) A ciguatera-causing dinoflagellate *Gambierdiscus toxicus*, *FASEB J.*, ABST
6. Bomber, J.W. and Tindall, D.R., (1988) Genetic variability in acclimated cell toxicities among Atlantic and Pacific clones of the ciguatera-causing dinoflagellate *Gambierdiscus toxicus*, *FASEB J.*, ABST
7. Bomber, J.W., Tindall, D.R. and Miller, D.M., (1988) Intraspecific variability in acclimated cell toxicities among Atlantic and Pacific clones of the ciguatera-causing dinoflagellate, *Gambierdiscus toxicus*, *9th World Congress on Animal, Plant, and Microbial Toxins (IST)*.
8. Miller, D.M. and Tindall, D.R., (1988) An acetonitrile-soluble toxic fraction from the dinoflagellate, *Gambierdiscus toxicus*, *Annual Meeting of the Association of Island Marine Laboratories of the Caribbean*.
9. Miller, D.M. and Tindall, D.R., (1988) Identification of an acetonitrile-soluble toxic fraction from *Gambierdiscus toxicus*, *Fed. Proc.*, 47, Abst.
10. Miller, D.M. and Tindall, D.R., (1988) Preparative HPLC separation of maitotoxin from crude extracts of *Gambierdiscus toxicus*, *9th World Congress on Animal, Plant, and Microbial Toxins (IST)*.
11. Tindall, D.R. and Miller, D.M., (1988) Toxins from *Ostreopsis lenticularis*, a dinoflagellate common to ciguatera-endemic regions of the Caribbean and tropical Atlantic, *Annual Meeting of the Association of Island Marine Laboratories of the Caribbean*.
12. Tindall, D.R., Miller, D.M. and Bomber, J., (1988) Culture and toxicity of dinoflagellates from ciguatera endemic regions of the world, *9th World Congress on Animal, Plant and Microbial Toxins (IST)*.
13. Hassan, F., Miller, D.M. and Tindall, D.R., (1989) Effect of maitotoxin on morphology of chick embryo cells (primary cell cultures), *FASEB J.*, 3,
14. Jacyno, M., Miller, D.M. and Tindall, D.R., (1989) Preparative HPLC separation of two toxic fractions from extracts of *Gambierdiscus toxicus*, *FASEB J.*, 3, A1190.
15. Bomber, J.W., Tindall, D.R., Venable, C.W. and Miller, D.M., (1990) Pigment composition and low-light response of fourteen clones of *Gambierdiscus toxicus*, *Fourth International Conference on Toxic Marine Phytoplankton*.
16. Miller, D.M., Tindall, D.R. and Venable, C.W., (1990) NMR spectroscopy of components isolated from *Gambierdiscus toxicus*, *Fourth International Conference on Toxic Marine Phytoplankton*.
17. Tindall, D.M., Miller, D.M. and Tindall, P.M., (1990) Toxicity of *Ostreopsis lenticularis* from the British and United States Virgin Islands, *Fourth International Conference on Toxic Marine Phytoplankton*.

Papers in journal or book chapters.

1. Bomber, J.W., Tindall, D.R. and Miller, D.M., (1989) Genetic variability in toxin potencies among seventeen clones of *Gambierdiscus toxicus* (Dinophyceae), *J. Phycol.*, 25, 617-625.
2. Bomber, J., (1990) Genetic variability in toxic dinoflagellates, in *Ciguatera Seafood Toxins*, Miller, D.M., Eds., CRC Press Inc, Boca Raton, Fla, 135-170.
3. Bomber, J.W., Tindall, D.R., Venable, C.W. and Miller, D.M., (1990) Pigment composition and low-light response of fourteen clones of *Gambierdiscus toxicus*, in *Toxic Marine Phytoplankton Blooms*, Granéli, E., Sundström, B., Edler, L. and Anderson, D.M., Eds., Elsevier Press, New York, 263-268.
4. Miller, D.M., Tindall, D.R. and Venable, C.W., (1990) NMR spectroscopy of components isolated from *Gambierdiscus toxicus*, in *Toxic Marine Phytoplankton Blooms*, Granéli, E., Sundström, B., Edler, L. and Anderson, D.M., Eds., Elsevier Press, New York, 305-310.
5. Tindall, D.M., Miller, D.M. and Tindall, P.M., (1990) Toxicity of *Ostreopsis lenticularis* from the British and United States Virgin Islands, in *Toxic Marine Phytoplankton Blooms*, Granéli, E., Sundström, B., Edler, L. and Anderson, D.M., Eds., Elsevier Press, New York, 424-429.
6. Hassan, F., Miller, D.M. and Tindall, D.R., (1990) Morphologic effects of maitotoxin on liver and brain cells of chick embryos: light microscopy and electron microscopy studies, in *Ciguatera Seafood Toxins*, Miller, D.M., Eds., CRC Press, Boca Raton, FL, 117-134.
7. Jacyno, M. and Miller, D.M., (1990) Extraction methods for marine toxins, in *Ciguatera Sea Food Toxins*, Miller, D.M., Eds., CRC Press Inc, Boca Raton, Fla, 53-72.
8. Miller, D.M., (1991) The guinea pig ileum as an assay system, in *Ciguatera Sea Food Toxins*, Miller, D.M., Eds., CRC Press Inc, Boca Raton, Fla, 103-116.
9. Rakatoninina, C. and Miller, D.M., (1990) Biological assays for ciguatera type toxins, in *Ciguatera Sea Food Toxins*, Miller, D.M., Eds., CRC Press Inc, Boca Raton, Fla, 73-86.
10. Venable, C.W. and Miller, D.M., (1990) NMR of marine toxins, in *Ciguatera Sea Food Toxins*, Miller, D.M., Eds., CRC Press Inc, Boca Raton, Fla, 87-101.

Theses completed by students.

1. Hassan, F., (1989) Morphological effects of maitotoxin and ciguatoxin extracted from a dinoflagellate *Gambierdiscus toxicus* (SIU 350 and 175) on liver and brain cells of chick embryos, Doctoral Dissertation, Southern Illinois University, Carbondale, Illinois

2. Adamson, R. J. (1990) Extractions of a ciguatera-type toxin from *Lutjanus bohar*, the red snapper. Masters Research Report, Southern Illinois University, Carbondale, Illinois
3. Jacyno, M. (1990) Neurological effects of toxins extracted from the dinoflagellate *Gambierdiscus toxicus* on the sciatic nerve of *Rana pipens*. Masters Research Report, Southern Illinois University, Carbondale, Illinois

VISITATION TO THE LABORATORY

Dr Aaron Fox of the University of Chicago visited the laboratory 26 Feb 88. Dr. Fox is interested in the pharmacology and function of neuronal calcium channels and hence maitotoxin.

Dr J. Babinchack of the National Marine Fisheries Laboratory, Charleston, South Carolina visited our laboratories on 18 through 21 Apr 88. He presented a seminar for the group entitled ciguatera toxin research. While visiting he observed the ileum assay system, culturing techniques, and mouse bioassays.

Drs Michael F. Capra and John Cameron from the Faculty of Health Sciences, Queensland Institute of Technology, Brisbane, Queensland Australia visited the laboratory for three days prior to the start of the IST meeting in Stillwater, OK. They were taken through our entire procedures, including the ileum assay technique. They asked for and received samples of crude extract. They intend to see if the effects they see on nerve with extracts from the Australian material^[122-124] is the same as ours.

In April of 1990 the laboratory was visited by Dr. Richard C. Lewis from the Department of Fisheries of Queensland, Australia.

In July of 1990 the laboratory was visited by Dr. Christopher S. Lobban from the Marine Laboratory, University of Guam. Dr. Lobban, was seeking help on techniques since he has been awarded a Minority Grant from NIH to study *Gambierdiscus toxicus* around Guam.

DELIVERABLES

During the contract period we delivered shipments of toxin as follows:

TABLE 60.
DELIVERABLES MADE DURING THIS CONTRACT

Lot No	Mass (mg)	Contract Item	Amt	Date
Lot GT350/Crude		001 AL	13.8 mg	
Lot GT350/Crude		001 AM	10.38 mg	
Lot GT350-COMB	9.2	001AN	1 ml	15Mar88
Lot GT350-COMB	9.2	001AO	1 ml	15Mar88
Lot GT350-COMB	9.2	001AP	1 ml	15Mar88
Lot GT350-COMB	9.2	001AQ	1 ml	15Mar88
Lot GT350-COMB	9.2	001AR	1 ml	15Mar88
Lot GT350-COMB	9.2	001AS	1 ml	15Mar88
Lot GT350-COMB	9.2	001AT	1 ml	15Mar88
Lot GT350-COMB	9.2	001AU	1 ml	15Mar88
Lot GT350-COMB	9.2	001AV	1 ml	15Mar88
Lot GT350-COMB	9.2	001AW	1 ml	15Mar88
Lot GT350 2B87'u'	.116	001AA-1	.116 mg	22Apr88
Lot GT350 2B87'u'	.116	001AA-2	.116 mg	22Apr88
Lot GT350 2B87'u'	.116	001AA-3	.116 mg	22Apr88
Lot GT175	9.2	001AX	1 ml	15Aug88
Lot GT175	9.2	001AY	1 ml	15Aug88
Lot GT175	9.2	001AZ	1 ml	15Aug88
Lot GT175	9.2	001BA	1 ml	15Aug88
Lot GT175	9.2	001BB	1 ml	15Aug88
Lot GT175	1.5	001BC	1 ml	15Aug88
Lot GT175	1.5	001BD	1 ml	15Mar88
Lot GT175	1.5	001BE	1 ml	15Aug88
Lot GT175	1.5	001BF	1 ml	15Aug88
Lot GT175	1.5	001BG	1 ml	15Aug88
Lot GT175	23.2	001BF	1 ml	27Oct88
Lot GT175	23.2	001BG	1 ml	27Oct88
Lot GT350	23.2	001BH	4 ml	27Oct88
Lot GT350	23.2	001BI	4 ml	27Oct88
Lot GT350	23.2	001BJ	4 ml	27Oct88
Lot GT350	23.2	001BK	4 ml	27Oct88
Lot GT175	516.6	001BL	205 ml	11Nov88
Lot GT350/GT-1 Ext	0.0	001BM	1.0 ml	8Mar89
Lot GT350/GT-4 Ext	0.0	001BN	1.0 ml	8Mar89
Lot GT175/GT-1 Ext	0.0	001BO	0.1 ml	8Mar89
Lot GT175/GT-4 Ext	0.0	001BP	1.0 ml	8Mar89
Lot GT175/GT-4 Ext	0.0	001BQ	400 0ml	3Apr89
Lot GT175/GT-4(25%)	0.0	001BR	3.0 ml	27May89
Lot GT175/Crude		001BS-1	0.458 Kg	1Jan90
Lot GT175/Crude		001BS-2	0.458 Kg	1Jan90
Lot GT175/Crude		001BS-3	0.458 Kg	1Jan90
Lot GT175/Crude		001BS-4	0.458 Kg	1Jan90
Lot GT350/Crude		001BT		30Jan90

Lot GT350/GT-4		001BU		30Jan90
Lot GT350/GT-4		001BV		30Jan90
Lot GT175/Aust RB		001BW	0.5 Kg	30Jan90
Lot GT175/NB Spn Mk		001BX	1.0 Kg	27Feb90
Lot GT175/Crude		001BY	2.15 mg	27Feb90
Lot GT175/GT-4		001BZ	0.34 mg	27Feb90
Lot GT175/GT-1		001CA	0.71 mg	27Feb90
Lot GT175/Crude		001CB	0.458 Kg	13Jun90
Lot GT175/Crude	800	001CC-1	250.0 ml	16Jan91
Lot GT175/Crude	800	001CC-2	250.0 ml	16Jan91
Lot GT175/Crude	800	001CC-3	250.0 ml	16Jan91
Lot GT175/Crude	800	001CC-4	250.0 ml	16Jan91

LITERATURE CITED

1. Halstead, B.W., (1958) Fish poisonings - Their pharmacology, diagnosis, and treatment, *Clin. Pharmacol. Therap.*, 5, 615-627.
2. Halstead, B.W., (1967) Poisonous and Venomous Marine Animals of the World, U. S. Government Printing Office, Washington, D. C, 1967.
3. Randall, J.E., (1958) A review of ciguatera, tropical fish poisoning, with a tentative explanation of its cause, *Bull. Mar. Sci. Gulf. Caribb*, 8, 236-267.
4. Lawrence, D.N., Enriguez, M.B., Lumish, R.M. and Maceo, A., (1980) Ciguatera fish poisoning in Miami, *JAMA*, 244, 254-258.
5. Bagnis, R.A., Kuberski, T. and Laugier, S., (1979) Clinical observations on 3,009 cases of ciguatera (fish poisoning) in the South Pacific, *Am. J. Trop. Med. Hyg.*, 28, 1067-1073.
6. Tackett, C.O., (1982) Clinical and Epidemiologic Features of Ciguatera in the Caribbean, U. S. Department of Health and Human Services Pamphlet, PHS, CDC, Atlanta, Georgia, 1982.
7. Capra, M.F., Cameron, J. and Flowers, A.E., (1988) The effect of ciguatoxin on teleost nerves, *Proceedings, World Congress on Animal, Plant and Microbial Toxins (9th)*,
8. Capra, M.F., Cameron, J., Flowers, A.E., Coombe, I.F., Blanton, C.G. and Hahn, S.T., (1988) The effects of ciguatoxin on teleosts. in *Sixth International Coral Reef Congress*, Choat, J.H., Barnes, D., Borowitzka, M.A., Coll, J.C., Davies, P.J., Flood, P., Hatcher, B.G., Hopley, D., Hutchings, P.A., Kinsey, D., Orme, G.R., Pichon, M., Sale, P.F., Sammarco, P., Wallace, C.C., Wilkinson, C., Wolanski, E. and Bellwood, O., Eds., 6th International Coral Reef Symposium Executive Committee, Townsville, Australia, 8-12 Aug 1989, 37-41.
9. Capra, M., Cameron, J., Flowers, A.E., Coombes, I.F., Blanton, C.G. and Hahn, S.T., (1988) The effects of ciguatoxin on mammalian nerves, *Proceedings, Sixth International Coral Reef Congress*, 4, 457-462.
10. Cameron, J. and Capra, M.F., (1987) Interim report on clinical and symptomatological studies performed on the victims of ciguatera poisoning in Sydney on 26th and 27th May 1987,
11. Cameron, J., Flowers, A.E. and Capra, M.F., (1988) The effects of ciguatoxin on nerve conduction parameters in humans and the laboratory rat, *Proceedings, Ninth World Congress on Animal, Plant and Microbial Toxins, Stillwater, OK, ??, ??*
12. Sylva, D.P., de and Higman, J.B., (1980) A plan to reduce ciguatera in the tropical western Atlantic region, *Bull. Mar. Sci.*, 32, 139-153.

13. Lewis, N.D., (1984) Ciguatera in the Pacific: Incidence and implications for marine resource development, in *Seafood Toxins*, Ragelis, E.P., Eds., American Chemical Society, Washington, D. C., 289-306.
14. Baylet, R., Beccaria, C., Niauxsat, P.M., Boyer, F. and Guillaud, M., (1978) Food poisoning by ciguatoxin in France, *Pathol. Biol.*, 26, 95-97.
15. Bagnis, R.A., (1968) Clinical aspects of ciguatera (fish poisoning) in French Polynesia, *Hawaii Med. J.*, 28, 25-28.
16. Li, K.-m. and Au, A.T.C., (1968) Clinical diagnosis - Ciguatera poisoning, *Far East Med. J.*, 4, 313-315.
17. Banner, A.H., (1974) The biological origin and transmission of ciguatoxin, in *Marine Science. Bioactive Compounds from the Sea.*, Humm, H.J. and Lane, C.E., Eds., Marcel Dekker, New York, 15-36.
18. Li, K.-m., (1968) Action of ciguatera fish poison and multiple toxins in ciguatera fish species, in *Poisonous and Venomous Marine Animals*, Halstead, B., Eds., U. S. Government Printing Office, Washington, D. C.,
19. Hashimoto, Y. and Fusetani, N., (1968) A preliminary report on the toxicity of the amberjack *Seriola aureovittata*, *Bull. Jpn. Soc. Sci. Fish.*, 34, 618-626.
20. Yasumoto, T., Hashimoto, Y., Bagnis, R.A., Randall, J.E. and Banner, A.H., (1971) Toxicity of the surgeonfishes, *Bull. Jpn. Soc. Sci. Fish.*, 37, 724-734.
21. Yasumoto, T. and Kanno, K., (1976) Occurrence of toxins resembling ciguatoxin, scaritoxin, and maitotoxin in a turban shell, *Bull. Jpn. Soc. Sci. Fish.*, 42, 1399-1404.
22. Yasumoto, T., Nakajima, I., Bagnis, R.A. and Adachi, R., (1977) Finding of a dinoflagellate as a likely culprit of ciguatera, *Bull. Jpn. Soc. Sci. Fish.*, 43, 1021-1026.
23. Bagnis, R.A., Loussan, E. and Thevenin, S., (1974) Les intoxications par poissons perroquets aux Isles Gambier, *Méd. Trop.*, 34, 523-527.
24. Yasumoto, T., (1990) New results on marine dinoflagellate toxins, in *Toxic Marine Phytoplankton Blooms*, Graneli, E., Sundstrom, B., Edler, L. and Anderson, D.M., Eds., Elsevier Press, New York,
25. Kodama, A.M., Hokama, Y., Yasumoto, T., Fukui, M., Manea, S.J. and Sutherland, N., (1989) Clinical and laboratory findings implicating palytoxin as cause of ciguatera poisoning due to *Decopterus macrosoma* (Mackerel), *Toxicon*, 27, 1051-1053.
26. Yokoyama, A., Murata, M., Oshima, Y., Iwashita, T. and Yasumoto, T., (1988) Some chemical properties of maitotoxin, a putative calcium channel agonist isolated from a marine dinoflagellate, *J. Biochem.*, 104, 184-187.

27. Lombet, A., Bidard, J.-N. and Lazdunski, M., (1987) Ciguatoxin and brevetoxin share a common receptor site on the neuronal voltage-dependent Na^+ channel, *FEBS Let.*, 219, 355-359.
28. Poli, M., (1985) Characterization of the *Ptychodiscus brevis* polyether binding component in excitable membranes, in *Toxic Dinoflagellates*, Anderson, D.M., White, A.W. and Baden, D.G., Eds., Elsevier North-Holland Press, New York, 357-362.
29. Flowers, A.E., (1989) The effects of ciguatoxin on teleost nerves, Masters Thesis in Health Science, Queensland University of Technology, Brisbane, Australia, 1989.
30. Cameron, J. and Capra, M.F., (1990) Neurological studies on the effects of ciguatoxin on mammalian nerve, in *Ciguatera Sea Food Toxins*, Miller, D.M., Eds., CRC Press Inc, Boca Raton, Fla, 21-32.
31. Kobayashi, M., Miyakoda, G., Nakamura, T. and Ohizumi, Y., (1985) Ca^{2+} -dependent arrhythmogenic effects of maitotoxin, the most potent marine toxin known, on isolated rat cardiac muscle cells, *Eur. J. Pharmacol.*, 111, 121-123.
32. Kobayashi, M., Ohizumi, Y. and Yasumoto, T., (1985) The mechanism of action of maitotoxin in relation to Ca^{2+} movements in the guinea-pig and rat cardiac muscle, *Br. J. Pharmacol.*, 86, 385-391.
33. Miyahara, J.T., Akau, C.K. and Yasumoto, T., (1979) Effects of ciguatoxin and maitotoxin on the isolated guinea pig atria, *Res. Comm. Chem. Pathol. Pharmacol.*, 25, 177-180.
34. Ohizumi, Y. and Yasumoto, T., (1983) Contraction response of the rabbit aorta to MTX, the most potent marine toxin, *J. Physiol. (London)*, 337, 711-721.
35. Ohizumi, Y., Kajiwar, A. and Yasumoto, T., (1983) Excitatory effect of the most potent marine toxin, MTX, on the guinea pig vas deferens, *J. Pharmacol. Exp. Therap.*, 227, 199-204.
36. Kim, Y.I., Login, I. and Yasumoto, T., (1985) Maitotoxin activates quantal transmitter release at the neuromuscular junction: evidence for elevated intraterminal Ca^{2+} in the motor nerve terminal, *Brain Res.*, 346, 357-362.
37. Takahashi, M., Tatsumi, M., Ohizumi, Y. and Yasumoto, T., (1983) Ca^{2+} channel activating function of maitotoxin, the most potent marine toxin known, in clonal rat pheochromocytoma cells, *J. Biol. Chem.*, 258, 10944-10949.
38. Ueda, T., Tamura, S., Harada, H., Yasumoto, T. and Takai, H., (1986) The maitotoxin evoked Ca^{++} entry into synaptosomes is enhanced by cholera toxin, *Neurosci. Let.*, 67, 141-146.

39. Shalaby, I.A., Kongsamut, S. and Miller, R.J., (1986) Maitotoxin-induced release of g-[3H] aminobutyric acid from cultures of striatal neurons, *J. Neurochem.*, 46, 1161-1165.
40. Sladeczek, F., Schmidt, B.H., Alonso, R., Vian, L., Tip, A., Yasumoto, T., Cory, R.N. and Bockaert, J., (1988) New insights into maitotoxin action, *Eur. J. Biochem.*, 174, 663-670.
41. Freedman, S.B., Miller, R.J., Miller, D.M. and Tindall, D.R., (1984) Interactions of maitotoxin with voltage-sensitive calcium channels in cultured neuronal cells, *Proc. Nat. Acad. Sci.*, 81, 4582-4585.
42. Login, I.S., Judd, H.M., Cronin, M.J., Koike, K., Schettini, G., Yasumoto, T. and MacLeod, R.M., (1985) The effects of maitotoxin on $^{45}\text{Ca}^{2+}$ flux and hormone release in GH₃ rat pituitary cells, *Endocrinol.*, 116, 622-627.
43. Hassan, F., Miller, D.M. and Tindall, D.R., (1989) Effect of maitotoxin on morphology of chick embryo cells (primary cell cultures), *FASEB J.*, 3, A327.
44. Hassan, F., (1989) Effects of maitotoxin and ciguatoxin on primary cell cultures of chick brain and liver, Doctoral Dissertation, Southern Illinois University, Carbondale, Illinois, 1989.
45. Hassan, F., Miller, D.M. and Tindall, D.R., (1990) Morphologic effects of maitotoxin on liver and brain cells of chick embryos: light microscopy and electron microscopy studies, in *Ciguatera Seafood Toxins*, Miller, D.M., Eds., CRC Press, Boca Raton, FL, 117-134.
46. Terao, K., Ito, E., Kakinuma, Y., Igarashi, K., Kobayashi, M., Ohizumi, Y. and Yasumoto, T., (1989) Histopathological studies on experimental marine toxin poisoning -4. Pathogenesis of experimental maitotoxin poisoning, *Toxicon*, 27, 979-988.
47. Faivre, J.-F., Deroubaix, E., Coulombe, A., Legrand, A.-M. and Coraboeuf, E., (1990) Effect of maitotoxin on calcium current and background inward current in isolated ventricular rat myocytes, *Toxicon*, 28, 925-937.
48. Kutty, R.K., Singh, Y., Santostasi, G. and Krishna, G., (1989) Maitotoxin-induced liver cell death involving loss of cell ATP following influx of calcium, *Toxicol. Appl. Pharmacol.*, 101, 1.
49. Santostasi, G., Kutty, R.K., Bartorelli, A.L., Yasumoto, T. and Krishna, G., (1990) Maitotoxin-induced myocardial cell injury: calcium accumulation followed by ATP depletion preceded cell death, *Toxicol. Appl. Pharmacol.*, 102, 164.
50. Lee, C.Y., Lin, W.W. and Chuang, D.M., (1991) Effects of maitotoxin on phosphoinositide (PI) turnover in cerebellar granule cells (Abstract), *Toxicon*, 1991, 283.

51. Berta, P., Sladeczek, F., Derancourt, J., Durand, M., Travo, P. and Haiech, J., (1986) Maitotoxin stimulates the formation of inositol phosphates in rat aortic myocytes, *FEBS Lett.*, 197, 349-352.
52. Wellner, R.B., Patton, L.L., Holmes, M.J. and Lewis, R.L., (1991) Maitotoxin (MTX) stimulate K⁺ transport in a human salivary epithelial cell line (HSG-PA), *FASEB J.*, A821.
53. Yasumoto, T., Nakajima, I., Chungue, E. and Bagnis, R.A., (1977) Toxins in the gut contents of parrotfish, *Bull. Jpn. Soc. Sci. Fish.*, 43, 69-74.
54. Yasumoto, T., Bagnis, R.A., Thevenin, S. and Garcon, M., (1977) A survey of comparative toxicity in the food chain of ciguatera, *Bull. Jpn. Soc. Sci. Fish.*, 43, 1015-1019.
55. Adachi, R. and Fukuyo, Y., (1979) The thecal structure of a marine toxic dinoflagellate *Gambierdiscus toxicus* gen. et sp. nov collected in a ciguatera endemic area, *Bull. Jpn. Soc. Sci. Fish.*, 45, 67-71.
56. Yasumoto, T., Nakajima, I., Oshima, Y. and Bagnis, R.A., (1979) A new toxic dinoflagellate found in association with ciguatera, in *Toxic Dinoflagellate Blooms*, Taylor, D.L. and Seliger, H.H., Eds., Elsevier North-Holland, New York, 65-70.
57. Yasumoto, T., Oshima, Y., Murakami, Y., Nakajima, I., Bagnis, R.A. and Fukuyo, Y., (1980) Toxicity of benthic dinoflagellates found in coral reef, *Bull. Jpn. Soc. Sci. Fish.*, 46, 327-331.
58. Withers, N.W., (1931) Toxin production, nutrition, and distribution of *Gambierdiscus toxicus* (Hawaiian Strain). *Proceedings of the Fourth International Coral Reef Symposium*, 2, 449-451.
59. McFarren, E.F., Tanabe, H., Silva, F.J., Wilson, W.B., Campbell, J.E. and Lewis, K.H., (1965) The occurrence of a ciguatera-like poison in oyster, clams, and *Gynodinium breve* cultures, *Toxicon*, 3, 111-123.
60. Bergmann, J.S. and Alam, M., (1981) On the toxicity of the ciguatera producing dinoflagellate *Gambierdiscus toxicus* Adachi and Fukuyo isolated from the Florida Keys, *J. Environ. Sci. Health A1*, 6, 493-500.
61. Tindall, D.R., Dickey, R.W., Carlson, R.D. and Morey-Gaines, G., (1984) Ciguatoxicogenic dinoflagellates from the Caribbean, in *Seafood Toxins*, Ragelis, E.P., Eds., American Chemical Society Symposium Series 262, Washington, D. C., 225-240.
62. Tindall, D.M., Miller, D.M. and Tindall, P.M., (1990) Toxicity of *Ostreopsis lenticularis* from the British and United States Virgin Islands, in *Toxic Marine Phytoplankton Blooms*, Granéli, E., Sundström, B., Edler, L. and Anderson, D.M., Eds., Elsevier Press, New York, 424-429.
63. Yentsch, C.M. and Mague, F.C., (1980) Evidence for an apparent annual rhythm in the toxic red tide dinoflagellate *Gonyaulax excavata*, *Int. J. Chronobiol.*, 7, 77-84.

64. Schmidt, R.J., Loeblich, A.R. and Hastings, J.W., (1979) Comparative study of luminescent and non luminescent strains of *Gonyaulax excavata* (Pyrrhophyta), *J. Phycol.*, 14, 5-9.
65. Oshima, Y., Hayakawa, T., Hashimoto, H., Kotaki, Y. and Yasumoto, T., (1982) Classification of *Protogonyaulax tamarensis* from Northern Japan into three strains by toxin composition, *Bull. Jpn. Soc. Sci. Fish.*, 48, 851-854.
66. Bagnis, R.A., Chanteau, S., Chungue, E., Hurtel, J.-M., Yasumoto, T. and Inoue, A., (1980) Origins of ciguatera fish poisoning: a new dinoflagellate, *Gambierdiscus toxicus* Adachi and Fukuyo, definitively involved as a causal agent, *Toxicon*, 18, 199-208.
67. Dickey, R.W., Miller, D.M. and Tindall, D.R., (1984) Extraction of a water-soluble toxin from a dinoflagellate, *Gambierdiscus toxicus*, in *Seafood Toxins*, Ragelis, E.P., Eds., American Chemical Society Symposium Series 262, Washington, D. C., 257-269.
68. Carlson, R.D., Morey-Gaines, G., Tindall, D.R. and Dickey, R.W., (1984) Ecology of toxic dinoflagellates from the Caribbean Sea: Effect of macroalgal extracts on growth in culture, in *Seafood Toxins, Proceedings, American Chemical Society Conference on Toxins in Seafood*, Ragelis, R.P., Eds., 271-287.
69. Miller, D.M., Dickey, R.W. and Tindall, D.R., (1984) Lipid soluble toxins from a dinoflagellate, *Gambierdiscus toxicus*, in *Seafood Toxins*, Ragelis, R.P., Eds., American Chemical Society Symposium Series 262, Washington, D. C., 241-255.
70. Provosoli, L., (1968) Media and prospects for the cultivation of marine algae, in *Proceedings, Fourth International Seaweed Symposium*, DeVerville, D. and Feldman, J., Eds., Pergammon Press, Oxford, 9-17.
71. Steidiger, K.A., (1983) A re-evaluation of toxic dinoflagellate biology and ecology, in *Progress in Phycological Research*, Round, F.E. and Chapman, V.J., Eds., Elsevier Press, New York, 147-188.
72. Brand, L.W., Guillard, R.R.L. and Murphy, L.S., (1981) A method for the rapid and precise determination of acclimated phytoplankton reproduction rates, *J. Plankt. Res.*, 3, 192-201.
73. Bomber, J.W., Tindall, D.R. and Miller, D.M., (1989) Genetic variability in toxin potencies among seventeen clones of *Gambierdiscus toxicus* (Dinophyceae), *J. Phycol.*, 25, 617-625.
74. Kochert, G., (1978) Quantitation of the macromolecular components of microalgae, in *Handbook of Phycological Methods: Physiological and Biochemical Methods*, Hellebust, J.A. and Cragie, J.S., Eds., Cambridge University Press, Cambridge, 189-195.
75. Dubois, M., Gilles, K.A., Hamilton, J.K., Rebers, P.A. and Smith, F., (1956) Colorimetric method for determination of sugars and related substances, *Analyt. Chem.*, 28, 350-356.

76. Freeman, N.K., Lindren, F.T., Ng, Y.C. and Nichols, A.V., (1957) Infrared spectra of some lipoproteins and related lipids, *J. Biol. Chem.*, 203, 293-304.
77. Sperry, W.N. and Brand, F.C., (1955) The determination of total lipids in the blood serum, *J. Biol. Chem.*, 213, 69-76.
78. Jeffrey, S.W., Sielicki, M. and Haxo, F.T., (1975) Chloroplast pigment patterns in dinoflagellates, *J. Phycol.*, 11, 374-384.
79. Jensen, A., (1978) Chlorophylls and carotenoids, in *Handbook of Phycological Methods: Physiological and Biochemical Methods*, Hellebust, J.A. and Cragie, J.S., Eds., Cambridge University Press, Cambridge, 59-70.
80. Weil, C.S., (1952) Tables for convenient calculation of median effective dose (LD50 or ED50) and instructions for their use, *Biometrics*, 8, 249-63.
81. Strickland, J.D.H. and Parsons, T.R., (1972) A Practical Handbook of Seawater Analysis, *Fish Res. Bd. Canada Bull.*, 167, 310.
82. Bomber, J.W., (1987) Ecology, genetic variability and physiology fo the ciguatera-causing dinoflagellate *Gambierdiscus toxicus* Adachi and Fukuyo, PhD Dissertation, Florida Institute of Technology, Melbourne, FL, 1987.
83. Sokal, R.R. and Rohlf, F.J., (1981) Biometry. W. H. Freeman and Co., New York, NY, 1981.
84. Indelicato, S.R. and Watcon, D.A., (1986) Identification of the photosynthetic pigments of the tropical benthic dinoflagellate *Gambierdiscus toxicus*, *Mar. Fish. Rev.*, 48, 44-47.
85. Miller, D.M., Tindall, D.R. and Venable, C.W., (1990) NMR spectroscopy of components isolated from *Gambierdiscus toxicus*, in *Toxic Marine Phytoplankton Blooms*, Graneli, E., Sundstrom, B., Edler, L. and Anderson, D.M., Eds., Elsevier Press, New York, 305-310.
86. Anderson, H.J., Barrett, D. and Craver, R., (1949) *Arch. Intl. Pharmacol. Ther.*, Apr 1, 544-547.
87. Fogg, G.E., (1965) *Algal Cultures and Phytoplankton Ecology*, The University of Wisconsin Press, Madison, WI, 1965.
88. Myklestad, S., (1977) Production of carbohydrates by marine phytoplanktonic diatoms. II. Influence of the N/P ratio in the growth medium on the assimilation ratio, growth rate, and production of carbohydrates by *Chaetoceros affinis* var. *willei* (Gran) Hustedt and *Skeletonema costatum* (Grev.) Cleve, *J. Exp. Mar. Biol. and Ecol.*, 29, 161-179.

89. Dortch, Q., (1982) Effect of growth conditions on accumulation of internal nitrate, ammonia, amino acids and protein in three marine diatoms, *J. Exp. Mar. Biol. Ecol.*, 61, 243-264.
90. Ben Amontz, A., Tornabene, T.G. and Thomas, W.H., (1985) Chemical profiles of selected species of microalgae with emphasis on lipids, *J. Phycol.*, 21, 72-81.
91. Anderson, D.M., Kulis, D.M. and Binder, B.J., (1984) Sexuality and cyst formation in the dinoflagellate *Gonyaulax tamerensis*: Cyst yield in batch cultures, *J. Phycol.*, 20, 418-425.
92. Faust, M.A., Sager, J.C. and Meeson, B.W., (1982) Response of *Prorocentrum mariae-Lebouriae* (Dinophyceae) to light of different spectral qualities and irradiances: Growth and pigmentation, *J. Phycol.*, 18, 349-356.
93. Babinchak, J.A., Jollow, D.J., Voegtline, M.S. and Higerd, T.B., (1986) Toxin production by *Gambierdiscus toxicus* isolated from the Florida Keys, *Mar. Fish. Rev.*, 48, 53-56.
94. Ogata, T., Ishimaru, T. and Kodama, M., (1987) Effect of water temperature and light intensity on growth rate and toxin production in *Protogonyaulax tamarensis*, *Mar. Biol.*, 95, 217-220.
95. Durand, M., Squiban, A. and Pesado, D., (1985) Production and toxicity of *Gambierdiscus toxicus*, Adachi and Fukuyo (Dinophyceae), *Phycologia*, 24, 217-223.
96. Durand, M., (1987) A study of toxin production by *Gambierdiscus toxicus* in culture, *Toxicon*, 24, 1153-1157.
97. Laurie-Ahlberg, C.C., (1985) Genetic variation affecting the expression of enzyme-coding genes in *Drosophilla* an evolutionary perspective, in *Isozymes. Current Topics In Biology and Medical Research*, 33-88.
98. Salzman, A., (1986) Analysis of natural selection on a quantitative physiological trait: Salt tolerance in Western Ragweed (*Ambrosia pfilostachya*), PhD Dissertation, University of Chicago, Chicago, IL, 1986.
99. Wood, A.M., Lande, R. and Fryxell, G.A., (1987) Quantitative genetic analysis of morphological variation in an Antarctic diatom grown at two light intensities, *J. Phycol.*, 23, 42-54.
100. Martin, J.F. and Demain, A.L., (1980) Control of antibiotic synthesis, *Microbiol. Rev.*, 44, 230-251.
101. Meeson, B.W. and Faust, M.A., (1985) Response of *Prorocentrum minimum* (Dinophyceae) to different spectral qualities and irradiances: Growth and photosynthesis, in *Marine Biology of Polar Regions and Effects of Stress on Marine Organisms*, Gray, J.I. and Christiansen, M.E., Eds., John Wiley and Sons Ltd., London, 445-461.

102. Maranda, L., Anderson, D.M. and Shimizu, Y., (1985) Comparison of toxicity between populations of *Gonyaulax tamarensis* of Eastern North American Waters, *Estuar. Coast Shelf Sci.*, 21, 401-410.
103. Watson, D.A. and Loeblich, A.R., III, (1983) The application of electrophoresis to the systematics of the marine dinoflagellate genus *Heterocapsa*, *Biochem. Syst. Ecol.*, 11, 67-71.
104. Hayhome, B.A. and Pfeister, L., A, (1983) Electrophoretic analysis of soluble enzymes in five freshwater dinoflagellate species, *Am. J. Bot.*, 8, 1165-1172.
105. Brand, L.E., Murphy, L.S., Guillard, R.R.L. and Lee, H.-T., (1981) Genetic variability and differentiation in the temperature niche component of the diatom *Thalassiosira pseudonana*, *Mar. Biol.*, 62, 103-110.
106. Brand, L.W., (1981) Genetic variability in reproduction rates in marine phytoplankton populations, *Evolution*, 35, 1117-1127.
107. Testeson, R.R., Ballantine, D.L., Testeson, C.G., Bardales, A.T., Durst, H.D. and Higerd, T.B., (1986) Comparative toxicity of *Gambierdiscus toxicus*, *Obstreopsis cf. lenticularis*, and associated microflora, *Mar. Fish. Rev.*, 48, 57-59.
108. Lewontin, R.C., (1985) Population genetics, in *Annual Reviews of Genetics*, 81-102.
109. Bomber, J.W., Guillard, R.R.L. and Nelson, W.G., (1988) Roles of temperature, salinity and light in seasonality, growth and toxicity of ciguatera-causing *Gambierdiscus toxicus* Adachi et Fukuyo (Dinophyceae), *J. Exp. Mar. Biol. Ecol.*, 115, 53-65.
110. Liu, C.M., Hermann, T.E., Prosser, B.L.T., Palleroni, N.J., Westley, J.W. and Miller, P.A., (1981) X-14766A, a halogen containing polyether antibiotic produced by *Streptomyces malachitofuscus* subsp. *downeyi*. Discovery, fermentation, biological properties and taxonomy of the producing culture, *J. Antibiot.*, 34, 133-138.
111. Liu, C.-M., (1982) Microbial aspects of polyether antibiotics: activity, production and biosynthesis, in *Polyether antibiotics: Naturally occurring acid ionophores*, Westley, J.W., Eds., Marcel Dekker, Inc., New York, 43-102.
112. Durand-Clement, M., (1987) Study of production and toxicity of cultured *Gambierdiscus toxicus*, *Biol. Bull.*, 172, 108-121.
113. Aikman, K. and Tindall, D.R., (1989) Physiology and potency of a dinoflagellate, *Prorocentrum concavum* through one complete growth cycle, *Phycol. Soc. Amer. Mtg.*, Toronto, Canada,
114. Shimizu, (1990) Biosynthesis of Dinoflagellate Toxins, in *Toxic Marine Phytoplankton Blooms*, Graneli, E., Sundstrom, B., Edler, L. and Anderson, D.M., Eds., Elsevier Press, New York, 305-310.

115. Dickey, R.W., Bobzin, S.C., Faulkner, D.J., Bencsath, F.A. and Adrzejewski, D., (1990) The identification of okadiac acid from a Caribbean dinoflagellate, *Prorocentrum concavum*, *Toxicon*, 28, 371-377.
116. Miller, D.M. and Tindall, D.R., (1988) Identification of an acetonitrile-soluble toxic fraction from *Gambierdiscus toxicus*, *Fed. Proc.*, 47, need.
117. Miller, D.M. and Tindall, D.R., (1988) An acetonitrile-soluble toxic fraction from the dinoflagellate, *Gambierdiscus toxicus*, *Annual Meeting of the Association of Island Marine Laboratories of the Caribbean*,
118. Tindall, D.R. and Miller, D.M., (1985) Purification of maitotoxin from the dinoflagellate, *Gambierdiscus toxicus*, using high pressure liquid chromatography, in *Toxic Dinoflagellates*, Anderson, D.M., White, A.W. and Baden, D.G., Eds., Elsevier Science Publishing Co., New York, Amsterdam and Oxford, 321-326.
119. Herman, P., Hladfk, J. and Sofrová, D., (1989) Effect of detergents on thylakoid membranes of chloroplasts, *Photosynthetica*, 22, 411-422.
120. Miller, D.M., Tindall, D.R. and Venable, C.W., (1990) NMR spectroscopy of components isolated from *Gambierdiscus toxicus*, in *Toxic Marine Phytoplankton Blooms*, Graneli, E., Sundstrom, B., Edler, L. and Anderson, D.M., Eds., Elsevier Press, New York, 305-310.
121. Yasumoto, T., (1985) Recent progress in the chemistry of dinoflagellate toxins, in *Toxic Dinoflagellates*, Anderson, D.M., White, A.W. and Baden, D.G., Eds., Elsevier Science Publishing Co., New York, Amsterdam and Oxford, 259-270.
122. Capra, M.F., Flowers, A.E. and Cameron, J., (1987) The effect of ciguatoxin on the rate of Na^+ efflux in unmyelinated olfactory nerves of teleosts, *First Asia-Pacific Congress on Animal, Plant and Microbial Toxins*,
123. Capra, M.F. and Cameron, J., (1987) Ciguatera poisoning: Pharmacology and Pathology, *Report to the Fishing Industries Research Committee, Department of Primary Industries, Canberra, Australia*,
124. Capra, M.F., Flowers, A.E. and Cameron, J., (1987) The effect of ciguatoxin on the rate of Na^+ efflux in unmyelinated olfactory nerves of teleosts, *First Asia-Pacific Congress on Animal, Plant and Microbial Toxins*,

GLOSSARY

ACN	Acetonitrile
ACN-insoluble	Acetonitrile insoluble fraction
ACN-soluble	Acetonitrile soluble fraction
ANOVA	Analysis of variance
CTX	Ciguatoxin
DEPT	Distortionless Enhancement Polarization Transfer Plot
DMSO	Dimethyl sulfoxide
ESAF	Ether soluble acetone filtrate
ESAP	Ether soluble acetone precipitate
GT-1	One of two toxins found in CTX group from <i>G. toxicus</i> .
GT-2	One of two toxins found in CTX group from <i>G. toxicus</i> .
GT-3	One of two toxins found in MTX group from <i>G. toxicus</i> .
GT-4	One of two toxins found in MTX group from <i>G. toxicus</i> .
HPLC	High Pressure Liquid Chromatography
IEU	Ileum Equivalent Units
MTX	Maitotoxin
MU	Mouse units
NMR	Nuclear Magnetic Resonance
P-	Abbreviation for Preparative
PPM	Parts per million
PSS	Physiological Saline Solution
SK	Acronym for Sep Pak separation of toxins
SP-	Abbreviation for Semipreparative
TEA	Tetraethylammonium
TLC	Thin layer chromatography
WSAF	Water soluble acetone filtrate
WSAP	Water soluble acetone precipitate
XTL	Acronym for crystalization step

DISTRIBUTION

5 copies	Commander US Army Medical Research Institute of Infectious Diseases ATTN: SGRD-UIZ-M Fort Detrick, Frederick MD 21702-5011
1 copy	Commander US Army Medical Research and Development Command ATTN: SGRD-RMI-S Fort Detrick, Frederick, MD 21702-5012
2 copies	Defense Technical Information Center (DTIC) ATTN: DTIC-DDAC Cameron Station Alexandria, VA 22304-6145
1 copy	Dean School of Medicine Uniformed Services University of the Health Sciences 4301 Jones Bridge Road Bethesda, MD 20814-4799
1 copy	Commandant Academy of Health Sciences, US Army ATTN: AHS-CDM Fort Sam Houston, TX 78234-6100

THIS REPORT HAS BEEN DELIMITED
AND CLEARED FOR PUBLIC RELEASE
UNDER DOD DIRECTIVE 5200.20 AND
NO RESTRICTIONS ARE IMPOSED UPON
ITS USE AND DISCLOSURE.

DISTRIBUTION STATEMENT A

APPROVED FOR PUBLIC RELEASE,
DISTRIBUTION UNLIMITED.
